INFORMATION TO USERS

This manuscript has been reproduced from the microfilm master. UMI films the text directly from the original or copy submitted. Thus, some thesis and dissertation copies are in typewriter face, while others may be from any type of computer printer.

The quality of this reproduction is dependent upon the quality of the copy submitted. Broken or indistinct print, colored or poor quality illustrations and photographs, print bleedthrough, substandard margins, and improper alignment can adversely affect reproduction.

In the unlikely event that the author did not send UMI a complete manuscript and there are missing pages, these will be noted. Also, if unauthorized copyright material had to be removed, a note will indicate the deletion.

Oversize materials (e.g., maps, drawings, charts) are reproduced by sectioning the original, beginning at the upper left-hand corner and continuing from left to right in equal sections with small overlaps.

Photographs included in the original manuscript have been reproduced xerographically in this copy. Higher quality 6" x 9" black and white photographic prints are available for any photographs or illustrations appearing in this copy for an additional charge. Contact UMI directly to order.

ProQuest Information and Learning
300 North Zeeb Road, Ann Arbor, MI 48106-1346 USA
800-521-0600

SPINA ACCRESCO MECHANICUS:
ON THE DEVELOPMENTAL BIOMECHANICS OF THE SPINE

by

David John Nuckley

A dissertation submitted in partial fulfillment of the
requirements for the degree of

Doctor of Philosophy

University of Washington

2002

Program Authorized to Offer Degree: Department of Bioengineering

UMI Number: 3041048

ProQuest Information and Learning Company
300 North Zeeb Road
P.O. Box 1346
Ann Arbor, MI 48106-1346

In presenting this dissertation in partial fulfillment of the requirements for the Doctoral degree at the University of Washington, I agree that the Library shall make its copies freely available for inspection. I further agree that extensive copying of the dissertation is allowable only for scholarly purposes, consistent with "fair use" as prescribed in the U.S. Copyright Law. Requests for copying or reproduction of this dissertation may be referred to Bell and Howell Information and Learning, 300 North Zeeb Road, Ann Arbor, MI 48106-1346, to whom the author has granted "the right to reproduce and sell (a) copies of the manuscript in microform and/or (b) printed copies of the manuscript made from microform."

Signature 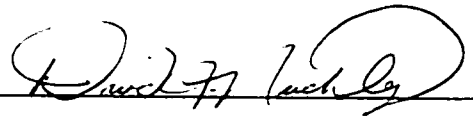

Date 15 March 2002

University of Washington
Graduate School

This is to certify that I have examined this copy of a doctoral dissertation by

David John Nuckley

and have found that it is complete and satisfactory in all respects,
and that any and all revisions required by the final
examining committee have been made.

Chair of Supervisory Committee:

Randal Ching

Reading Committee:

Francis Spelman

Sohail Mirza 3/14/02

Randal Ching

Date: 14 March 2002

University of Washington

Abstract

SPINA ACCRESCO MECHANICUS:
ON THE DEVELOPMENTAL BIOMECHANICS OF THE SPINE

David John Nuckley

Chairperson of the Supervisory Committee: Associate Professor Randal P. Ching
Department of Orthopaedics and Sports Medicine

Epidemiological data and clinical indicia reveal devastating consequences associated with pediatric neck injuries. Neither injury prevention nor clinical management strategies will be able to effectively reduce these effects on children, without an understanding of cervical spine developmental biomechanics. This investigation examines the biomechanical characteristics (functional biomechanics and tolerance) and morphological patho-mechanics of injury (tissue failure) in the maturing cervical spine. The cadaveric baboon *(Papio anubis)* spine, an anatomic and kinematic analog to the human cadaveric spine, served as the model to investigate these issues across the developmental spectrum. Significant relationships were discovered between both structural and material properties and developmental age. Further, significant gender, spinal level and loading rate effects were found to be associated with the mechanical development of the spine. Structural properties were strongly correlated with maturation indicating that tissue size may be a positive predictive tool. Unfortunately, size alone cannot predict pediatric spinal mechanics since its material properties also increased with development. The complex maturation process involves concomitant increases in both intrinsic material properties and structure giving rise to an age-specific mechanical response of the spine. These functional and tolerance data were employed in computational modeling efforts, which may facilitate the generation of enhanced pediatric injury prevention schema. The functional biomechanics data were used to generate maturation-specific constituent relationships and the tolerance data provide injury criteria for this computational model as well as physical (anthropomorphic test dummy) models. Another facet of this research evaluated clinically relevant injuries to identify the patho-

mechanical response of the developing spine. Every injury created in the pediatric spine involved the failure of the growth plate (physis) regardless of mechanism. In compression the compromised growth plate was associated with vertebral fractures or disc herniations. Tensile mechanisms involved the growth plate zone of calcification separating from the vertebral body, yet this severe injury did not affect the developing intervertebral disc. These patterns support a physis focused assessment and management of pediatric injuries. The sum of this research fills a dearth in the developmental biomechanics literature concerning the spinal mechanical characteristics motivating injury prevention and the spinal patho-mechanical patterns aiding clinical management techniques.

TABLE OF CONTENTS

LIST OF FIGURES

Number *Page*

LIST OF TABLES

Number *Page*

ACKNOWLEDGMENTS

There are a number of individuals that I would like to thank for their contributions to my dissertation research as well as my graduate education. My formal education in the Department of Bioengineering was very meaningful in shaping my research and education perspectives; for that I am thankful to the faculty and staff in the department. The most significant portion of my graduate learning involved my education, research, and teaching in the Applied Biomechanics Laboratory in the Department of Orthopaedics. There have been many faculty, residents, students, and staff that I have learned from in the laboratory and to all of them, I am grateful. Specifically though, I would like to thank Randy for his academic integrity and zeal for performing high quality engineering analyses. Further, Randy has afforded me the flexibility and freedom to explore my research interests, examine my teaching abilities, and grow into a more complete scientist and engineer. Randy's mentoring and friendship has promoted my graduate education in innumerable ways. Also, to all of the other students and faculty that I have worked with in the laboratory: Jarrod Carter, Suzanne Hertsted, Dr. Fredrick Mann, Richard Harrington, Mike Eck, Grace Ku, Joe Van Nausdle, Patrick Medley, Geoffrey Raynak, Chimba Mkandawire, and Ruth Ochia. I offer my sincere gratitude. Finally, to my supervisory committee: Drs. Francis Spelman, Sohail Mirza, Joan Sanders, David Eyre, and Eric Feigl, thank you for your service to my education, your wisdom and your support.

The agencies that invested in our laboratory and my education have been generous in funding this research and I am very thankful for their support throughout my education. The Centers for Disease Control and Prevention, National Highway Traffic Safety Administration, Cervical Spine Research Society, and Orthopaedic Research and Education Foundation have supported the Applied Biomechanics Laboratory and research presented herein.

Finally, I would like to thank specific individuals for their support throughout my education. I would like to begin by thanking all of my high school science teachers who inspired and believed in me. Next, Dr. Steven Chamberlain of Syracuse University

deserves my gratitude for his mentoring, example, and the opportunity to perform original research. At the University of Washington, Dr. Francis Spelman has provided me with an excellent example of scholarship and an integration of life and scientific pursuits. I believe that becoming an engineer and scientist requires a strong support group and often this group is your best friends. I thank everyone who I have been blessed to call my friend throughout this endeavor. For all of his support, advice, listening, and overall friendship, I thank Jarrod Carter. I could not have accomplished this without such a good friend with whom to work side-by-side, and I am eternally grateful. I would also like to thank my mom and sister for their personal support throughout the years. Even though they don't fully understand what it is that I am doing, their love and support has been constant. I thank you both from the bottom of my heart for your examples, comfort, wisdom, and love throughout the years. And finally, I wish thank my wife, Nicole. Your undying support and love throughout my graduate career have been essential to my completion. You have been my sounding board, my voice of wisdom, my teacher, and my best friend. From serious discussions to Simpson's banter, you have aided and shared in my graduate education and personal growth. My most sincere and heartfelt gratitude go out to you and I only hope that I can be as supportive throughout your graduate career. I only hope that this research can make all of you proud and I thank you.

DEDICATION

I would like to dedicate this dissertation to my first engineering teacher, my father.

CHAPTER 1:
INTRODUCTION

Despite the often-devastating consequences associated with pediatric neck injuries, few experimental data exist characterizing cervical spine developmental morphology or mechanics. This paucity of basic age-related properties of the neck make it impossible to fully understand the mechanical function of the developing cervical spine and subsequently develop models to expose injury prevention and management schemes that may mitigate the catastrophic effects of pediatric neck injuries.

1.1 SIGNIFICANCE

Pediatric cervical spine injury is a devastating trauma outcome with fatal or life-long debilitating consequences. Although spinal column injuries to the pediatric populace account for less than 15% of all spine injuries, their subsequent spinal cord injury and fatality rates eclipse those of the adult population.[4, 27, 31, 73, 94, 157, 173, 192] Each year in the United States, over 8,000 children under the age of 20 are killed by automotive related accidents,[1] representing 27% of all automotive related fatalities. More alarming though, is that children account for approximately 56% of all incapacitating injuries due to automobile accidents.[1] Of those incapacitated, most sustain varying degrees of irreversible neurological deficit due to spinal cord or nerve root injuries.[94] In children, spinal injuries most often occur in the cervical region (80%);[73, 75, 76, 124, 157] and, mechanistically predominate from compression or tension to the spinal column as a result of automotive, sport, or fall incidents.[42, 43, 50, 73, 75, 76] Further, compared to all other pediatric injuries, cervical spine traumas result in the most severe trauma (average AIS of 3.5), highest mortality (15%), and longest hospital stays (15-days).[19] Hence, the long-

term financial, psychological, and quality-of-life costs associated with pediatric cervical spine injury —for the child, his or her family, and society— are catastrophic.

Efforts to understand, manage, and reduce these injuries have recently turned to modeling the developing cervical spine via computational models (rigid body and finite element) and physical models (anthropomorphic crash test dummies). Unfortunately, very little data exist for injury thresholds or even tissue constituent properties for the developing neck to make these models biofidelic. Epidemiologically, the spinal physis (growth plate) has been implicated in most injuries to the cervical spine, although the spinal growth plate morphology and developmental course are not well understood.[4, 15, 23] Since efforts to manage these injuries currently result in spinal fusion which halts growth and limits range of motion, the identification of a less deleterious surgery would be advantageous. Examination of the patho-mechanics of physis tissue may help identify an enhanced alternative surgical approach. Therefore, this dissertation is focused on improving child injury prevention and management strategies by: determining spinal tissue functional mechanics, measuring the tolerance of these spinal tissues, evaluating tissue failures histologically, and developing modeling parameters for the developing cervical spine.

1.2 SPECIFIC AIMS AND HYPOTHESES

To achieve the above-stated goal, this research effort documents developing spine functional mechanics (constituent properties) and injury-tolerance levels (failure properties) in tension and compression as well as characterizes the resulting injuries to understand the patho-mechanics. These age-dependent functional and tolerance characteristics have not been previously described in the spine literature. The cadaveric baboon (*Papio anubis*) spine, an anatomic and kinematic analog to the human cadaveric spine, was used to investigate these questions across the developmental spectrum. This human surrogate provided the most comprehensive set of biomechanics data to date for the pediatric spine given limited supplies of pediatric human tissues. The following are the specific objectives of this project.

Measure the functional biomechanical characteristics of the developing functional spinal unit and vertebrae. The compressive and tensile viscoelastic mechanics are measured examining differences by developmental age, gender, and spinal level.

Quantify the compressive and tensile failure biomechanics of the developing spine. The tolerances of maturing spinal tissues (from isolated vertebra to full spinal segments) are recorded and evaluated by skeletal maturity, gender, spinal level, and loading rate.

Analyze failure patterns of the developing physis and establish a relationship between the zone or tissue of failure and developmental maturity. Histological examination of the physis (growth plate) throughout development elucidates the patho-mechanics of the tissues which constitute the physis for tension and compression.

Develop the compressive and tensile constitutive equations and failure criteria for the maturing cervical spine. Model parameters are established for a constitutive model explaining the properties of the cervical spine throughout the stages of development.

The general hypotheses for this research effort are listed below. They govern the rationale behind the proposal and are expanded upon and specifically tested as a part of the research methods.

i. *The mechanical constituent properties of spinal tissues in compression and tension vary with developmental age and by gender and spinal level.*

ii. *Spinal injury tolerance for compression and tension varies with advanced development and by gender, cervical spine level, and loading rate.*

iii. *The morphological patho-mechanics (tissue failure within and around the physis) is altered by the mechanism of failure (tension or compression) and by developmental changes in the tissue.*

The following chapter will detail contemporary insight on the developing spine anatomy and biomechanics. Following this background, each of the four specific aims is addressed in a subsequent chapter providing thorough coverage of the methods, results, and discussion of that specific aim. Within these chapters, specific hypotheses are tested, examined, and discussed. A general discussion of the results of this research project follows these four chapters. This general discussion chapter, "New Insight on the Developing Spine" examines the potential impact of this research effort in the context of its ability to fill the voids ascertained in the review of the contemporary literature.

CHAPTER 2:
CONTEMPORARY INSIGHT ON THE DEVELOPING SPINE

The objectives of this proposal are motivated by a critical examination of the cervical spine developmental morphology, biomechanics, and epidemiology literature. This review of the literature provides the rationale for this research plan and demonstrates the necessity for investigation. An examination of the developmental morphology of the human cervical spine reveals a highly dynamic and interdependent system. The growth of the cervical spine tissues in concert not only affects the biomechanics of each specific tissue, but also influences the functional biomechanics of the entire cervical spine. Little data exist pertaining to the mechanical constituent properties of the developing neck. Further, in spite of the prevalence of injuries to the pediatric neck, there has not been a significant experimental biomechanics investigation of injuries to the child cervical spine. An analysis of injury prevention strategies confirms the need for both cervical spine mechanical constituent properties and neck injury thresholds for use in modeling computationally (rigid body and finite element models) and physically (anthropomorphic crash test dummies). This review of the literature demonstrates the current status of developmental biomechanics experimental research and modeling.

2.1. DEVELOPING SPINE ANATOMY

Development of the cervical spine involves integrated molecular, cellular, and systemic maturation and remodeling events, which maintain the functional and neuro-protective roles of the spine throughout latitudinal and longitudinal growth. The osteoligamentous spinal column develops largely via the processes of chondrification (cartilage formation), endochondral ossification (bone formation), and tissue differentiation (disc and ligament

formation). As these changes take place, spinal morphology and mechanics is altered in a complex optimization of function and maturation. This efficient spinogenesis relationship is particularly evident in the physis or growth plate. The physis is a cartilaginous tissue responsible for longitudinal growth in the spine and implicated epidemiologically in most mechanical failures of the developing spine. This examination of the anatomy of the maturing spine begins by outlining the basic development of the spine and concludes with a thorough review of the developing physis.

2.1.1. BASIC SPINAL DEVELOPMENT

Axial spinal column formation and growth occurs through stages of tissue differentiation, chondrification, and endochondral ossification. Embryonic mesenchymal cells differentiate, condense, and transform into chondrocytes which form cartilage at the primary centers of chondrification. This creates a cartilaginous model of the future spine by the eighth week of development in utero.[187] Chondrification begins at the centrum of the body and at each neural arch; the chondrifying centers then spread and fuse with one another anteriorly at the body and posteriorly forming a cartilaginous spinous process.[155] Intervertebral disc development involves perichordal tissue condensation forming the annulus fibrosus around the differentiating nucleus pulposus as endochondral ossification begins. At about the ninth fetal week, a primary ossification nucleus develops in the body centrum initiating vertebral body bone formation. Two other primary ossification centers form in each neural arch.[74, 108] These primary ossific nuclei increase in size creating the bony vertebra (***Figure 1***). The bones forming the neural arches fuse to one another posteriorly between years two and three. These bony arches form the posterior of the spinal canal. The anterior margin of the spinal canal is formed by the vertebral body, and the spinal canal reaches its full adult dimensions around eight-years of age. Posterior bone growth continues until the spinous process is fully formed. Anteriorly, the neural arch nuclei, which form the pedicle and lateral margins of the vertebral body, extend to fuse with the vertebral body between years four and six.[55, 90]

The first (atlas) and second (axis) cervical vertebrae have different patterns of ossification from the lower cervical spine described above. The first cervical vertebra is formed by

three primary ossification centers similar to the lower cervical vertebrae; the anterior ossific nucleus, however, may not appear until several months postnatally. Posterior fusion of the neural arches occurs near the third year of life and these fuse with the body at about the seventh year.[55, 153] The second cervical vertebra has five primary ossification nuclei: two in the odontoid process, one in the body centrum and one in each neural arch. The odontoid process fuses in utero, except for the apex which fuses between three and six years. The odontoid fuses with the body between three to six years and this fusion line is present until about 11-years. The second cervical vertebra neural arches are formed at the seventh fetal month, and fuse posteriorly by two to three years and anteriorly to the body at three to six years.[55, 154, 155]

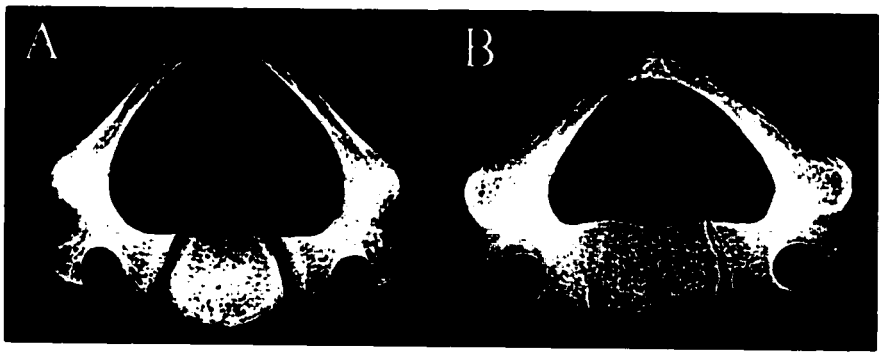

Figure 1. *Maturation of the Third Cervical Vertebrae. Radiographs of tissue sections for* ***(A)*** *a 2-year old demonstrating posterior and lateral synchrondroses and* ***(B)*** *an 8-year old showing the fusion of the primary ossification centers.*[155]

Around the 7th fetal month, physes begin to form on the superior and inferior aspects of each vertebral body. These cartilage plates demarcate the boundary between the intervertebral disc and the vertebral body. The intervertebral disc material becomes progressively defined, forming clear disc structure at birth. This intervertebral disc is densely connected by matriceal and collagen fiber continuities into the superior and inferior epiphyses.[109]

Secondary ossification centers develop in late childhood (6 to 12-years) circumferentially at the superior and inferior surfaces of the vertebral body and at the tip of the spinous process.[55, 155] These secondary ossification centers (epiphyses) aid the physis in longitudinal growth and fuse to the primary vertebral centrum between ages 16 to 20.

The uncinate processes form laterally from these ossification nuclei and leave the cartilaginous endplate in the central portion. Completion of this development occurs around age 18 to 22, and results in the mature osteoligamentous spinal column.[55, 90, 155]

2.1.2. PHYSIS MORPHOLOGY AND DEVELOPMENT

Axial skeletogenesis is principally driven by the cartilaginous physis. The physis synchronizes longitudinal and lateral chondrogenesis with osteogenesis (interstitial cartilage growth with appositional bone growth) while bearing load and responding to local and systemic forces and factors. Topographically, the physes of the spine are located on the superior and inferior ends of the vertebral bodies. They intercede structurally between the epiphysis (distally) and the metaphysis to enable the longitudinal growth of vertebral bodies.[11, 17, 44, 109] This growth involves the synthesis and subsequent replacement of cartilage in the growth plate by bony tissue through temporally and spatially chondrocyte-coordinated differentiation, growth, and remodeling events. This functionally ubiquitous tissue has not been specifically characterized in the spine, although it is known to support longitudinal growth and circumferential expansion of the vertebral body from its superior and inferior surfaces.[155]

Anatomically, there are three tissue layers which interact to promote bone growth: the epiphysis, physis, and metaphysis. Vertebral anatomy, although different in appearance, contains genetically equivalent tissues in the same orientation compared with long bones.[44, 109] This review will discuss each of these tissue layers with emphasis on the physis morphology and development (***Figure 2***).

The epiphyses of the cervical vertebrae are thin cartilaginous structures representing the secondary ossification centers and are in direct contact with the intervertebral disc. This cartilaginous structure develops a thicker ring shape on the periphery called a ring apophysis, which is unique to tissues experiencing localized tension across the physis.[109] In the spine this tension is developed by branching fibers of the long intervertebral ligaments which insert into the ring apophysis.[11, 109] The epiphysis provides vascular support to the physis and serves as the constant distal end of vertebral body growth.[44]

Upon growth cessation, the epiphysis ossifies into the uncinate processes superior laterally and the vertebral endplate inferiorly and superior medially.[85, 109]

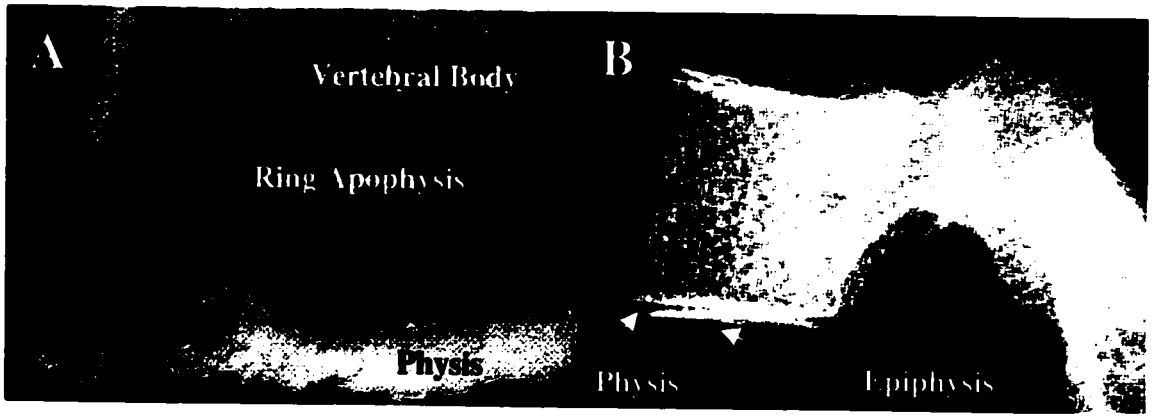

Figure 2. *Vertebral Physis Anatomy.* ***(A)*** *The vertebral ring apophysis and the physis inferior to a human (16-y.o.) lumbar vertebra.* ***(B)*** *Radiograph of human 12-year old vertebra demonstrating the epiphyseal plates and physis boundaries.*

Morphologically, the physis contains distinct cellular and matrix organization throughout its development.[17, 84, 85] The role of the physis is the chondrocyte production of an extracellular matrix and the subsequent calcification of that matrix in a balanced function.[16] Collagen types I, II, IX, X, and XI have been implicated as primary matrix components within the physis.[106, 114] Type X collagen is unique to the physis and may ensure the normal distribution of matrix vesicles and proteoglycans within the physis matrix, impacting the supporting properties of the physis and the mineralization process.[106] The remaining collagen types develop into the extracellular matrix.

The purpose of the physis is supported by a complex cellular organization, which is subdivided into zones that are morphologically distinct and functionally identified (***Figure 3***). At the border between the epiphysis and the physis lies a reserve zone of cartilaginous tissue; this is followed by the proliferative zone and hypertrophic zone which finally give rise to the metaphysis. The reserve zone contains spherically shaped cells which are actively synthesizing protein and an extracellular matrix rich in hydroxyproline but with randomly distributed and oriented collagen fibrils. This zone is

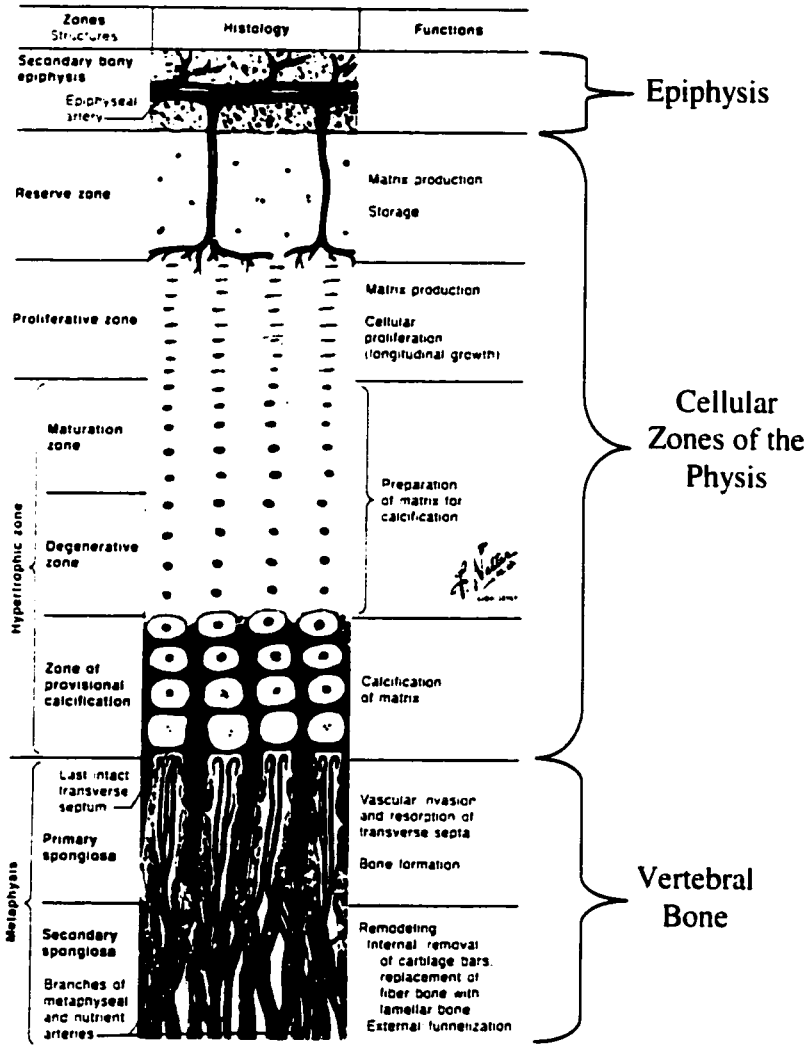

Figure 3. *Morphology of the Physis. The zones and functions accompany each morphological tissue representation. Reprinted from CIBA Collection of Medical Illus., Frank H. Netter, MD.*

thought to be responsible for matrix production and storage of nutritional elements required for use in subsequent zones. The next proximal zone is the proliferative zone which contains flattened chondrocytes aligned in vertical columns perpendicular to the vertebral superior surface.[17, 85] The rate of longitudinal bone growth is equal to the rate of production of new chondrocytes at the top of the proliferative zone (e.g. 5-cells/day) multiplied by the size of exiting chondrocytes (e.g. 30-μ giving a growth rate of 150-μ/day).[17] Each column of chondrocytes has been discovered to produce 5-cells per day

giving daily growth of approximately 150-μm (30-μm cell diameter). This long bone growth is much faster than would be expected in the spine. Each spinal growth plate grows slowly, adding only a small amount to the height, although the sum of each of the 48 spinal growth plates does equate to significant spinal height growth.[13] Thus, the function of the proliferative zone is the production of extracellular matrix components coupled with cellular proliferation. The hypertrophic zone is morphologically distinct because the chondrocyte size increases as the matrix is prepared for calcification. It is also in this zone that provisional calcification takes place and cellular apoptosis occurs.[17, 85]

The metaphysis is morphologically new bone prepared for remodeling at the physeal border. Metaphyseal functions include the resorption of the transverse septa (cellular columns) through vascular ingrowth, bone formation, and bone remodeling. The calcified matrix created in the hypertrophic zone is replaced by primary spongiosa and then is subsequently remodeled by osteoblast/osteoclast function into secondary spongiosa in the metaphysis.[17, 85] At the end of development, the vertebral epiphysis and physis flatten into a hyaline cartilage layer between the vertebra and disc called the vertebral end plate.[44] This full cascade of growth events thus results in the bony vertebral body.

This review of the developmental anatomy of the physis and maturing cervical spine is incomplete, as the vertebral physis has not been specifically characterized. It is clear, however, that the concerted dynamic of cellular, tissue, and systemic development of the cervical spine dictates its functionality; therefore comprehension of the anatomy and morphology of the developing cervical spine are paramount to understanding its biomechanics. In fact, an examination of growth patterns provides a basis for understanding and modeling the biomechanical response of spinal tissues. For example, in the human population, height, weight, inverse pulse rate, and even metacarpal cortical bone area demonstrate second order polynomial functions with development. These second order polynomials fit growth characteristics by age (through 30-years) and may help elucidate the relationship between spine biomechanical parameters and

development. Since the second order polynomial has biological basis in development, the maturation patterns of the biomechanical response of the spine will likely follow a similar pattern.

2.2. BIOMECHANICS OF THE DEVELOPING SPINE

Biomechanical evaluation of the developing cervical spine may occur on a tissue, segmental, or systemic level. Regardless of investigatory domain, the cervical spine's mechanical complexity is directly related to its anatomical development. This biomechanics review will examine the literature for spine tissue mechanics as a function of age, segmental mechanics as a function of age, full cervical spine injury mechanics from an epidemiological perspective, and biomechanically derived injury thresholds.

2.2.1. SPINAL TISSUE BIOMECHANICS

Vertebral body, ligament, intervertebral disc, and physeal plate (physis) tissue properties all dictate the functional mechanics of the cervical spine. As these individual tissues develop, their changing mechanical properties affect the mechanics of the surrounding tissues as well as the whole functional spine. Although very little data exists for the properties of these tissues as they develop, this review indicates trends in tissue mechanical performance.

A number of studies have examined vertebral body mechanical properties as they change with age; however, these vertebral body experiments included but a few data points younger than 20-years, so it is difficult to draw meaningful conclusions.[8, 9, 138, 139, 177, 200] Throughout its chondrification and ossification, the vertebra, which is the primary structural unit of the spine, has differing mechanical and physical characteristics. Vertebral cortical bone density increases with maturation until adulthood while cancellous bone density increases only through the later stages of puberty and appears more dependent on mechanical stresses in the spine.[135] Pediatric cortical bone exhibits a lower bending strength and modulus of elasticity compared with adult cortical bone. Further, developing cortical bone absorbs more energy and has greater deformation at failure than its adult counterpart.[32, 33]

General ligament mechanical properties have been evaluated as a function of development indicating ligament stiffness and modulus of elasticity increase with skeletal maturity. Further, the ligament tensile failure mechanism is bony avulsion in younger ligaments and mid-substance failure in skeletally mature ligaments.[197] Clinically, it is commonly regarded that pediatric ligaments are stronger than their bony insertion. Other experiments have evaluated the changes in ligament mechanics from maturity to a degenerative state and have found that the modulus, ultimate stress, and strain energy decrease with age and there is a reversal in the failure mechanism where older ligaments tend to avulse bone at failure.[150, 197] Spinal ligaments demonstrated similar trends with respect to mechanical properties and aging;[143-146] however, no complete examination of developing spinal ligament properties exists.

Intervertebral disc mechanical properties have been primarily evaluated from the degeneration perspective.[100, 118, 194, 200] Consequently little data exist on the biomechanics of intervertebral disc development. Intervertebral disc development involves tissue changes such as nucleus pulposus collagen fiber formation leading to annulus fibrosus maturation and physis maturation through collagen matrix organization.[188, 212] Collagen content in the annulus fibrosis and nucleus pulposus has been demonstrated to increase with age, indicating an ability to carry greater load as adults.[181] Further, the degree of collagen cross-linking in the annulus affects the tissues' resilience and this cross-linking has also been shown to be age related.[172] Unfortunately, most of these tissue level changes have not been well quantified in spite of their imminent consequence on the mechanical performance of the complete intervertebral disc.

The cartilaginous physis is an anisotropic tissue with unique biomechanical responses related to its morphology which vary with development and applied load.[23] The stresses that develop with the application of load to the physis are dependent upon both the strain and the strain rate, clearly defining the physis as a viscoelastic material.[15] This viscoelastic tissue maintains the lowest elastic modulus and hardness measurements compared with its surrounding tissues, the primary spongiosa and the epiphyseal trabecular bone and cartilage.[110] Not surprising, there is greater collagen content in regions of the physis that have been found to be the stiffest and strongest, indicating

regional variations in the growth plate mechanics.[30] Further, the failure mechanics of the physis has been shown to be positively correlated with the number of contours on the plate surface.[71] These undulations are seen on the physis-metaphysis boundary and they dictate local and gross mechanical properties (shear resistance) to the growth plate complex.[30]. Low levels of tension increase the synthetic activity of physeal cartilage and small compressive forces tend to decrease its osteogenic activity.[117] As the physis develops, its tensile mechanical properties (modulus and ultimate failure load) increase and not merely due to size changes in the tissue.[72] Further, the tensile load required to fail the physis increases with age while the displacement decreases. This suggests a reduced ductility of the developing physis with increasing age.[15] All of the aforementioned research was performed on long bone specimens leaving open speculation regarding the mechanics of the spinal physes especially when considering their anatomical dissimilarity.

2.2.2. FUNCTIONAL SPINAL UNIT BIOMECHANICS

The interdependence of bone, ligament, intervertebral disc, and physis properties in spinal development is extremely complex. A few studies have attempted to understand parts of this system;[92, 93, 144, 169] to my knowledge, however, the role of systemic growth on mechanics has not been investigated. In the absence of experimental biomechanics data, clinical evaluation of the developing spine has provided an understanding of its basic mechanics.

Anatomical changes in the developing spine are associated with specific functional mechanical property changes and define the spine's functional kinematics. Some specific pediatric spine properties which may dictate mechanical performance and kinematics include: ligament laxity, weakness of the paraspinal musculature, unossified vertebrae, the horizontal orientation of the facet joints, and the cartilaginous physes.[6, 26, 73, 94, 102, 126, 157, 173, 182, 186, 192] These properties have been implicated in various injuries to children; however, the causal role of these specific properties has not been experimentally validated.

A seminal study performed by Pintar et al.[169] used a goat cadaver model to examine the developmental biomechanics of cervical functional spinal units. They determined scaling parameters for the developing cervical spine (***Table 1***) which enable the estimation of pediatric properties and tolerances from adult data. This study examined goat FSU specimens of adult and one, three, six, and twelve-year old human equivalent ages in bending and tension. They found that both the stiffness and failure load increase with increasing age. While their study provides an excellent view into the developmental biomechanics of cervical spine FSUs, it is limited by their use of female and male specimens and use of a goat (quadruped) model.[169] Therefore, in spite of its injury predominance, further data are needed to understand the basic functional biomechanics of the developing cervical spine to generate either direct criteria or scaling relationships for modeling.

Table 1. *Scaling Parameters for the Developing Cervical FSU. These values represent the most significant effort to understand the developing cervical spine in spite the use of a caprine (goat) model.*

Age (HE Years)	Bending Stiffness	Tensile Stiffness	Tensile Failure Load
1.0	0.11	0.17	0.12
3.0	0.15	0.23	0.20
6.0	0.57	0.54	0.38
12.0	0.62	0.85	0.78
Adult	1.0	1.0	1.0

2.2.3. SPINAL SYSTEMIC INJURY BIOMECHANICS

Our lack of understanding of developing cervical spine mechanics is revealed in the prevalence and types of injuries sustained by children. These injuries to the cervical spine may affect the mechanical stability or the neuroprotective ability (the ability of the spine to protect the neurologic tissues) of the spinal column. Mechanical instability of the developing cervical spine may arise from fractures, dislocations, ligament tears, and disc failures. However, most of these injuries originate at the physis between the calcification zone and the primary spongiosa.[15, 23, 30, 109, 110, 115] Further, where

mechanical instability exists, neural and vascular tissues may also be affected. All of these tissue injuries may result from a number of mechanisms and modes of injury. This review will examine injuries affecting both mechanical instability and neuroprotective ability of the spine by presenting epidemiological reports of pediatric injury mechanisms.

Motor vehicle related accidents cause the majority of pediatric spinal fractures; and of those, approximately 80% occur to the cervical spine.[73, 75, 76, 124, 157] Younger children (≤ 11-years) tend to have fractures of the upper three cervical vertebrae while older children follow the adult pattern of lower cervical injuries (***Figure 4***).[73, 123, 149] Fractures of the pediatric vertebrae occur approximately 50% of the time in C5 and C6, and most fractures are wedge compression, with teardrop and burst fractures occurring infrequently.[94] Fractures that occur in the pediatric vertebrae are often through the physis

Figure 4. *Cervical Level of Injury vs. Age. Injury markers correspond to Δ=Fractures, •=Dislocations, and *=Fractures and Dislocations. Distribution of age and cervical level of injury for a series of 222 children under the age of 16 at hospital admission. Synthesis of data from McGrory et al. [123], Henrys et al.[81], Evans et al.[54], and Dietrich et al.[43].*

and complex in nature.[4, 109] A zone of weakness exists between the epiphyseal cartilage and the vertebral body ossification. This weak zone travels primarily through the hypertrophic zone where the matrix/cell volume ratio is the lowest.[15, 23, 30, 109, 110, 115] Fracture mechanics of the pediatric cervical spine, while not the same as in adults, includes a host of impact loading and inertial loading mechanisms.[54, 76, 81]

In addition to vertebral fracture, another injury resulting in mechanical instability is vertebral body subluxation or dislocation. Increased laxity of the ligaments and near horizontal facet orientation in the developing cervical spine are believed to be responsible for the increased number of subluxation injuries in the normal pediatric spine with bending.[65, 82] Further, even the normal pediatric anatomy may allow an anterior subluxation of up to 3-mm of C2 with respect to C3.[182] Similarly, Miller et al.[134] found that the adolescent spine is 1 to 10 times more flexible than the adult spine depending upon the applied load. Excessive distraction of the pediatric spinal column most commonly results in an avulsion of the growth plate from the vertebral body at the zone of calcification.[31]

These changes in the spinal column's mechanical stability (fracture, dislocation, or both) may result in neurologic tissue damage via a number of mechanisms. Spinal cord and nerve root injury may occur primarily by a tension or compression mechanism,[193] and secondarily by complications from edema, ischemia, or hematoma.[2] Primary neural integrity may be compromised by a mechanical crushing of the spinal cord and/or nerve roots, or by neural tissue elongation in a tension mechanism. These mechanisms of neural injury result from changes in the boundary conditions of these delicate tissues. Thus, dynamic changes in the spinal canal and intervertebral foramen which house the neural tissue in the spine may result in neural tissue injury.

When loaded in tension, the infant spine may be elongated up to 5.1-cm compared to the adult elongation of 2.0-cm over its entire length.[14, 112, 180] This tension experiment using cadaveric spines did not examine the effects on the neural tissues; thus, the compliance of the pediatric spine might not match that of the spinal cord resulting in a spinal cord injury at full tension. Flexion of the neck may result in an elongation injury of the spinal cord,

while extension of the neck can produce spinal canal longitudinal compression.[14, 180, 192] Since the nerve roots tether the spinal cord in place, excessive elongation or longitudinal compression of the spine may result in damage to the spinal cord.[192] Further, the spinal cord and meninges do not share the same elasticity as the spinal column; therefore, contusion, transection, infarction, and stretch injuries may also result.[173] Disc and ligamentum flavum bulging have been suggested to occlude the spinal cord predisposing the spine to an extension type injury.[14, 192] The pediatric disc has the ability to withstand quite high compressive loads and maintain its integrity so as to preserve the intervertebral foraminal space and the nerve roots.[124] Finally, vascular injury mechanisms have been proposed based on a number of cases noting hemorrhage in the spinal cord and craniocervical junction without evidence, post-injury, of complete subluxation.[28, 174]

Many cases of neurologic tissue damage demonstrate spinal cord injury without radiographic abnormality (SCIWORA). This neurologic injury without fracture occurs more frequently in the younger ages of 0 to 10-years while the older pediatrics ages 11 to 18-years present with fractures associated with the neurologic injury (***Figure 5***).[43, 203] A number of clinical studies have suggested possible factors which may predispose children to these neurologic tissue injuries in the cervical spine. The horizontal orientation of the facet joints in the upper pediatric cervical spine may permit increased translational motion in response to antero-posterior shear.[26, 186] Also, wedge-shaped vertebral bodies and incompletely developed uncinate processes in children may predispose them to vertebral subluxation.[6, 26, 126] Perhaps the most widely cited explanation has been that ligament laxity contributes to hypermobility of the spine which may place the spinal cord at risk for compressive or tensile injury.[73, 94, 102, 126, 157-159, 173, 182, 186, 192] This hypermobility coupled with the weak physeal boundary condition could be responsible for excessive displacement of the spinal cord. Further, physis fractures are very difficult to image and thus may not be apparent in a number of these SCIWORA cases. Spinal cord and nerve root injuries can have devastating consequences especially in children, therefore injury prevention and treatment strategies must understand both frank injuries (fractures, dislocations, etc.) and neural injuries.

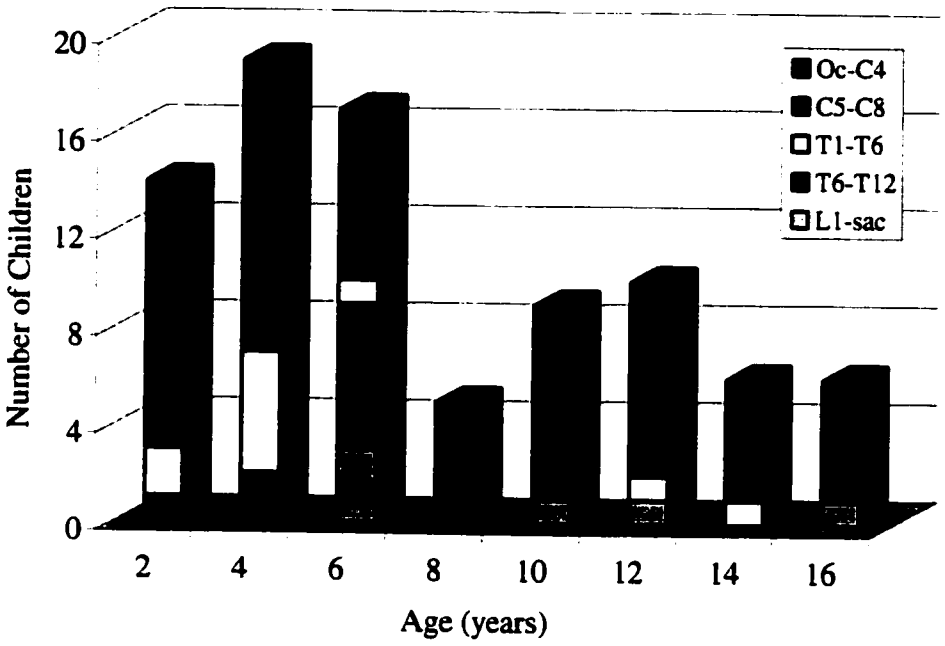

Figure 5. *Distribution of SCIWORA by Age. These 86 children presented without frank injuries, yet sustained a spinal cord injury. Synthesis from Cheshire et al.*[27]*, Kewalramani et al.*[94]*, Yngve et al.*[203]*, and Pang et al.*[158]

2.2.4. BIOMECHANICALLY DERIVED INJURY THRESHOLDS

The threshold of injury in the cervical spine will likely vary for structural injuries and neural injuries. Thus, examination of both injuries will elucidate the most sensitive tissues and consequently provide a systemically accurate threshold value. Biomechanical thresholds for the adult cervical spine have been determined for specific cervical tissues,[18, 32, 33, 91, 93, 138, 146] segments,[92, 93, 146, 211] and the full systemic osteoligamentous cervical spine.[70, 89, 98, 111, 129, 142, 148, 209, 211] While this three-level approach has been successful in defining adult neck injury criteria, very little data exist for these three investigatory levels in the pediatric age range. Therefore, this review of pediatric neck injury tolerances should, in its brevity, express the need for an assault on understanding the injury thresholds of the developing cervical spine.

Current adult neck injury thresholds, established using a few experimental biomechanics studies, include: 3,300-N in tension,[152, 211] 4,000-N in compression,[127, 142, 148, 152, 211] a 57-Nm extension moment and a 190-Nm flexion moment.[98, 130] These data have been scaled

and used with a few experimental (non-biologic) investigations to estimate pediatric neck injury thresholds. A current neck injury reference value program for evaluating anthropomorphic test dummies uses as its thresholds 3,000-N in tension, 3,000-N in compression, 70-Nm of flexion moment, and 35-Nm of extension moment for the 6-year old dummy.[40, 95] These thresholds were established based upon the measured dummy parameters acquired from tests conducted at 48-kph for each of the 6-year old, 3-year old, and 12-month old dummies. While these limits may represent a first approximation, they are not based upon tissue failure or experimental injury data (***Table 2***). Planath and Nilsson[171] used a 3-year old child dummy and a scaling algorithm to suggest the following thresholds for child neck protection: axial tensile force = 1000-N, shear force = 300-N, and a forward bending moment = 30-Nm. Prasad and Daniel[174] and Mertz and Weber[129, 131] attempted to assess neck injury thresholds by exposing 10-week old piglets and a 3-year old dummy to air bag deployment and torso deceleration inputs. They published tensile thresholds for a 1% risk of injury (1060-N), 10% risk of injury (1125-N), and 25% risk of injury (1160-N). Further, Mertz et al.[133] defined injury risk curves which would provide a threshold for a 1% probability of AIS $\geq$ 3 injury for neck tension, extension, and combined tension extension. These data were then scaled by subject size to include other ages in the threshold analysis. This size-wise scaling of properties across ages appears to be a large limitation of this work, as well as its use of the porcine model (discussed below) for a human surrogate. Further, their air bag loading lacked reproducibility.[129] A study which determined tensile neck injury criteria for four stillborn infants reported an average failure of 507-N for quasi-static tensile neck loading.[125]

Table 2. *Neck Injury Thresholds. Pediatric and adult injury assessment values are listed. Gray cells represent the only experimental tissue failure biomechanics data.* †[152, 211], ▲[127, 142, 148, 152, 211], ◉[98, 130], ✶[40, 95], *and* ☾[129, 131, 171, 174].

	Tension	Compression	Extension	Flexion
Adult	**3,300-N†**	**4,000-N▲**	**57-Nm◆**	**190-Nm◆**
6-y.o. Child	3,000-N✶	3,000-N✶	35-Nm✶	70-Nm✶
3-y.o. Child	1000-N☾			30-Nm☾

Cervical spine tissue tolerance and its developmental anatomy play integral roles in injury progression and occurrence. The generation of threshold criteria for use in child injury protection requires experimental injury threshold testing of an appropriate human surrogate.

2.2.5. OTHER FACTORS AFFECTING SPINAL BIOMECHANICS

Evaluation of the functional and tolerance mechanics of the developing spine involves many facets other than those directly related to maturation. The secondary effects of gender, spinal level, and loading rate play an important role in understanding the entire biomechanical response of the spine. This short review will address these factors as they affect the mechanics of the developing spine.

Gender-related differences in the spinal anatomy and mechanics may play an important role in understanding the developmental biomechanics of the spine. An investigation into child and adolescent vertebral cross-sectional areas as measured by quantitative CT found that female vertebral bodies were significantly smaller throughout development compared with males.[68] Unfortunately, biomechanical data are unavailable to compare the effect of size difference between the genders. A number of studies on adults have examined gender disparity both anatomically and biomechanically. The density and size of lumbar vertebrae were measured in healthy young adults resulting in insignificant differences in bone density between genders. They did, however, determine that the cross-sectional areas of women were 25% smaller than men.[67] The functional bending mechanics of the cervical spine exhibited differences between male and female ranges of motion at various ages of adulthood.[45] The tolerance or thresholds of male and female spinal tissues has not been widely examined aside from vertebral body crush experiments. A vertebral body crush experiment on L2 vertebrae of adult males and females (mean age of 29-years) exhibited a significant 16% decrease in the female ultimate failure load and an insignificant 2% decrease in the female strength.[137] Further, their vertebral ash-densities were nearly identical; however male vertebral body cross-sectional areas were significantly larger. This work suggests that size dictates the

ultimate failure load of these adult tissues.[137] Finally, a number of osteoporosis studies have evaluated gender differences leading them to equate bone density with ultimate failure load.[12, 103, 120] Osteoporotic changes in women lead to a 50% reduction in bone density compared with a 30% loss in men by the fourth decade of life.[120] Gender distinctions in adult spinal anatomy and biomechanics reinforce the evaluation of the maturing spine with a secondary emphasis on gender variations.

The various levels of the spine have differing geometries and mechanics easily seen in comparisons of the cervical, thoracic, and lumbar segments. However, within each of these spinal segments, the anatomy and mechanics may also be different from one functional spinal unit to the next. The geometry of the cervical spine vertebrae are different by spinal level,[161] suggesting that spinal mechanics may also be level dependent. A number of experimental studies have quantified the bending mechanics of the adult cervical spine demonstrating level specific measurements. Both the range of motion[46, 113, 116, 166, 194] and bending stiffness[160] have been shown to be level dependent. While bending mechanics has been well investigated, few experimental studies have evaluated different functional spinal units for unique compressive or tensile mechanics. One study by Yoganandan et al.[211] examined the tensile stiffness of adult individual cervical functional spinal units by level. This work revealed that the various cervical levels had different stiffness characteristics with the C3-4 level having the highest cervical stiffness. Although they did not perform statistical tests to establish level differences a qualitative look at the individual level means and standard deviations suggest valid differences.[211] These biomechanical studies on adult spinal level differences support the investigation into how these level differences arrive throughout development.

Loading rate has been suggested by many to dictate the biomechanical response of biologic tissues. The response of various ligamentous preparations have been shown to increase in elastic modulus and stiffness with increased strain rates. Danto et al.[35] demonstrated a 94% increase in the elastic modulus of the anterior cruciate ligament from slow (0.02-%/sec) to fast (380-%/sec) strain rates. Neumann et al.[146] examined the anterior longitudinal ligament at various loading rates (0.1-to-230-mm/sec) and found

that the ultimate load and stiffness increased by 50%. Along with mechanical properties, the mode of failure (ligamentous vs. bony) of bone-ligament-bone preparations has been shown to be influenced by loading rate with low rates resulting in mid-substance failures and high rates giving rise to bony avulsions.[151] In a study examining both loading rate and development, Peterson et al.[167, 168] examined the medial collateral ligament of mature and immature rabbits at different rates (0.01%/sec to 200%/sec). They discovered that the immature tissues demonstrated a strong dependence on extension rate while the mature tissues exhibited differences between strain rates to a lesser degree. In a comprehensive study on cervical spine ligaments, Yoganandan et al.[210] demonstrated increases in ultimate tensile failure load, stiffness, and energy–absorbing capacity at failure for loading rates of 8.89-to-2,500-mm/sec. These properties exhibited up to 3-fold increases from the slowest to fastest loading rate. Further, they discovered that the failure displacements in these tissues did not increase with loading rate. Another spinal study evaluated the compressive strength of lumbar motion segments and found the strength increased significantly between loading rates of 0.1 to 200mm/sec.[78] This review clearly suggests that loading rate is a significant factor to evaluate to correctly understand the biomechanical response of the developing spine.

This review was meant to highlight the most prominent factors that affect the biomechanical response of the maturing spine. While most of this work details adult experiments, these factors will likely play important roles throughout development as well. Further, accurate modeling of the developing spine will include all of the factors affecting its biomechanical response. Thus, the major influences of gender, spinal level, and loading rate will need to be considered along with the developmental effects on the biomechanical response of the spine.

2.3. MODELING THE DEVELOPING SPINE

Experimental and theoretical modeling of the human cervical spine has been approached using human subjects, anthropomorphic test dummies, cadavers, and computational (rigid body and finite element) models. Examination of injuries to the developing neck can be accomplished via these surrogates, with the exception of human subject testing. This

section reviews modeling efforts for the developing cervical spine and elucidates an optimal course of action in modeling the developing cervical spine.

2.3.1. ANTHROPOMORPHIC TEST DUMMIES

Since the early 1970's, anthropomorphic test dummies have been used in automotive crash simulations to determine protection reference values in an effort to minimize human injuries. These test dummies currently include biofidelic structure, mass, stiffness, and energy dissipation as well as transducers for the measurement of the environment 'seen' by the dummy. The Hybrid III dummy, the current industry standard, contains a viscoelastic neck structure which is intended to respond in a manner similar to the 'tensed' human neck exposed to a 35-mph crash.[130] This neck contains a 6-axis load cell at the interface between the neck and the head, and another 6-axis load cell between the neck and the torso. Full torso and head acceleration environments can be determined for this adult surrogate.[5] Mertz and Patrick developed corridors for safety including occipital condyle moment plotted against head rotation for flexion and extension.[129-132] These corridors for safety are based upon human volunteer and cadaver experimental testing and are applied to anthropomorphic test dummy load cell and accelerometer measurements. Further, they documented injury assessment values for Hybrid III neck measurements: 190-Nm for flexion, 57-Nm for extension, and plots for tension, compression and shear loading.[5] While this work represents the current protection reference values used in adult neck injury determination for the Hybrid III, it does not include data for the pediatric neck.

Child anthropomorphic test dummies have recently been developed based upon the 50th percentile male Hybrid III. A 6-year old, 3-year old, and a 12-month old dummy exist with scaled biofidelic properties and measurement instrumentation. The 3-year old 'air bag' dummy is designed to investigate the response of a 3-year old to a deploying cushion. This dummy's instrumentation is specialized for measurement of tension and extension injuries of the neck.[128] The 12-month old and 6-year old dummies have the same neck instrumentation as the adult Hybrid III. While each of these dummies contains a full complement of instrumentation, all three derive their biofidelic responses

from a scaling of the Hybrid III 50th percentile 'tensed' adult male.[5, 40] Validation of these dummies and enhancement of their biofidelity will result only when experimental kinematic and mechanical data for children exists. Further and most importantly, few experimental injury criteria exist to assess injury to the pediatric cervical spine given the dummy responses.

2.3.2. COMPUTATIONAL MODELING

Within the past decade, computational models have been utilized increasingly to understand cervical spine biomechanics. Computational models have the potential to overcome many of the limitations of cadaveric experimentation, including limited availability of donor tissue, interspecimen tissue variability, and experimentation that is both technically difficult and expensive. Once validated, the same model can be exercised in a variety of configurations; and parametric studies of numerous variables can be executed more efficiently. However, a computational model's ability to provide useful biomechanical insights into cervical spine behavior depends entirely on the availability of cadaveric experimental data. These data must define the material properties, tissue failure levels, and then validate the model responses.

In the lumped parameter approach to cervical spine modeling, each vertebra is represented by a rigid body; each motion segment's disk, ligaments, and facet joints are modeled by arrays of discrete springs and dashpots. Lumped parameter models have been used to describe aircraft ejections, whiplash injuries, and more recently, cervical spine responses to dynamic compressive loading.[10, 22, 37, 39, 175, 176, 191, 195] However, given the incomplete experimental data describing cervical motion segment mechanical properties, many of the models assume linear elastic, extrapolated (from physical models), or arbitrarily assigned properties. For dynamic analyses, material property characterization is particularly challenging. Through sensitivity analyses of the model parameters, Camacho et al.[22] and de Jager et al.[38] demonstrated that dynamic model responses are highly sensitive to changes in damping coefficients. Yet, experimental data characterizing the multi-axial dynamic responses of individual cervical motion segments are nonexistent, and thus selection of damping coefficients in most previous modeling

efforts have been somewhat arbitrary. In the Camacho et al.[22] model, motion segment linear damping coefficients were estimated from the hysteresis energy demonstrated in constant velocity testing of whole cadaveric spines at a single representative loading rate. They acknowledged that given the assumption of linear damping constants, the model might only be valid over a limited time domain.

Recently, the finite element method has been employed to study cervical spine mechanics. The complex geometry of the cervical anatomy can be accurately reproduced with this approach, including distinct representations of ligaments, intervertebral disc subcomponents, and facet joints. Motion segment and whole cervical spine finite element models have been used to understand the specific load-bearing roles of various motion segment substructures,[29, 69, 119] and to investigate responses to surgical procedures,[104, 105, 179, 190] small strain vertical compression,[96] frontal impact,[36, 96] and lateral impact.[36] In the models of Kumaresan et al.[104] and Goel et al.[69], the ligaments are modeled as nonlinear elastic cable elements and the nucleus pulposus is modeled as an incompressible fluid. The remaining material properties in these models and all the other models were linear elastic. Like the lumped parameter models, many of the properties in the finite element models are extrapolated from thoracolumbar data or arbitrarily assigned due to the lack of comprehensive experimental material property data for the tissues of the cervical region. Since viscoelastic effects are not incorporated into the material property definitions, these models may be of limited utility for dynamic analyses. Unlike the lumped parameter models, the detailed finite element models are capable of predicting stresses and strains within individual motion segment tissues. However, tolerance criteria and validation data do not exist for comparison with most of these predictions making these models irrelevant for injury prevention.

Modeling the pediatric cervical spine presents even greater challenges. Given the limited availability of human pediatric cadaveric tissue, and the ethical inability to perform pediatric volunteer experiments, biofidelic models of the human pediatric cervical spine are clearly needed for prediction of injury risk. However, the development of such physical or computational models is severely limited by the complete absence of material property data for pediatric cervical spine tissues, and the absence of experimentally

proven rules for scaling material properties from adult to pediatric age groups. Kumaresan et al.[105] investigated age-specific pediatric cervical spine responses by modifying their adult C4-C5-C6 finite element model. They investigated three approaches to approximating the pediatric cervical spine – structural scaling of the adult model, incorporating local age-specific geometrical and material property changes, and finally a combination of the two above approaches. They found that the pediatric models demonstrated increased flexibility compared to the adult models, with most of the increases resulting from the age-specific geometry and material property changes rather than from structural scaling. The rationale for determination of the age-specific material property scaling factors used was not detailed. No other computational models of the pediatric cervical spine have been reported in the literature.

The reliability of any of these computational model predictions relies critically on adequate representation of the motion segment mechanical properties. Thus, the tissue and functional spinal unit governing mechanics equations are of the utmost importance when considering any computational modeling endeavor. Experimental data has been used to fit a number of different theories explaining these governing functions of tissue mechanics. These theories have included description of tissue viscoelasticity using Voigt, Maxwell, and Kelvin solid models which employ linear springs and dashpots to approximate viscoelastic tissues mechanics.[61] The theory of linear viscoelasticity as applied by these models assumes that the stress in a tissue is unaffected by the strain history. This is, in fact, untrue, as a considerable difference can be seen between the loading and unloading stress response of a biologic tissue.[61] To overcome this limitation, a number of non-linear methods have been utilized to explain the mechanical response of biologic tissues. For example, Fung[61] developed a quasi-linear viscoelastic (QLV) theory which utilizes five or six material coefficients to describe the elastic response (a non-linear function of strain) and the relaxation response (a non-linear function at constant strain) of a soft tissue. Various soft tissues have been successfully modeled using this QLV theory in its general form.[62, 87, 107, 198] Each of these investigators has implemented variations to obtain better fits, to ease calculations, and to facilitate the use of these equations in subsequent modeling efforts. In all, these non-linear viscoelastic modeling

efforts appear to best model the mechanical response of biologic soft tissues. Utilization of non-linear formulations for the functional spinal unit mechanical properties and then importing these governing equations into a computational head-neck model would provide a powerful and significant tool in pediatric injury prevention.

2.3.3. CADAVER MODELS

Cadaver models are the current standard for biomechanical tissue testing and injury response. These models, although lacking muscular reaction, have the same anatomical geometry, tissue morphology and material properties giving strong credence to their mechanical and kinematic responses. Examination at the segmental and tissue levels of the osteoligamentous cervical spine diminishes the kinematic effects of musculature. Thus, cadaveric experimentation using functional spinal units provides the most optimal vehicle to obtaining developing cervical spine material properties and injury thresholds.

Human pediatric cadaveric specimens are difficult to obtain for cervical spine research, so many researchers have opted to use animal models. Sheep, canine, and pig models have been the most commonly used to model the pediatric human cervical spine.[101] The canine model is similar in size and has analogous anatomy to that of humans except for its horizontally positioned spine which undoubtedly affects its mechanics. The bone quality in the sheep model is closer to that of humans; however, it has larger pedicles,[101] and its canal space is more circular instead of kidney-shaped as in the human.[20] The vertebral end plates are also absent in the sheep, and here again the quadruped anatomy and subsequent mechanics make the sheep model sub-optimal.[20] Studies have used fetal and young pigs to model both the pediatric and adult human spine. Similar cervical spine developmental anatomy make the fetal pig a reasonable choice for pediatric cervical spine modeling, but it again has a horizontal orientation in normal posture.[129, 174] While the human vertebral body to intervertebral disc ratio is approximately 3:1, quadruped ratios are 4:1 and larger.[20, 66, 155] No histological evidence is available distinguishing human and animal (quadruped) models aside from these morphological differences. Mechanical testing of the spine requires that the structures in the model are similar in function as well as geometry. Thus, quadruped models with a horizontally directed

cervical spine may not be sufficient because the cervical spine tissues may develop differently in response to fundamentally different physiologic loads.

Due to its quasi-upright posture and genetic similarity, the anatomy and functional biomechanics of a primate will resemble that of humans more than any other animal model. The chimpanzee and baboon are very reasonable primate cadaver models. Tominaga et al.[185] compared the anatomy of baboons (*Papio anubis*) to that of humans and found that the architectural composition and geometry of the individual cervical vertebrae are similar at each level. The mechanics of the baboon upper cervical spine have been demonstrated to be similar to that of human cervical spine tissues; they have proportional neutral zones and elastic zones.[41] Further, the two species share a proportional relationship between bone and ligament structures. The baboon is about three quarters the size of the human, its uncovertebral joints are more concave, its pedicles are thinner, and its spinous processes are nonbifid and more horizontal.[111, 183, 185] However, these are small differences when the geometry, anatomy and mechanical properties of the baboon model compare so well with humans; and thus this model is well suited for use in cadaveric pediatric cervical spine research.[41, 111, 183, 185]

Establishment of the developmental age of cadaveric specimens (human and baboon) is particularly important for this study. Tominaga et al.[185] has suggested that the baboon develops approximately 2.9-times faster than a human. However, scaling of the baboons to estimate human-equivalent ages based upon this factor may sacrifice important accuracy in my data set. Therefore, I will review techniques for the assessment of skeletal maturity.

Developmental age is based upon the degree of skeletal maturation (bone ossification) of an individual, and does not necessarily depend upon chronological age. The current standard in assessment of skeletal maturation was developed by Fishman[57-59] and involves the use of hand-wrist radiographs. Skeletal maturation indicators, developed based on the four stages of bone maturation at six anatomic sites in the hand-wrist, offer a sensitive approach to appraising skeletal maturity.[79] A cervical vertebrae maturation index has recently been developed based upon the work by Fishman.[79] This cervical

vertebrae maturation index evaluates the first, second, and third cervical vertebra for radiographic characteristics that would place it in one of eighteen stages of maturation. This methodology has been validated and compared well with other indicators of skeletal maturity.[64, 79] Therefore, this methodology utilizing skeletal maturity provides an accurate and meaningful way to assess the developmental age of tissues.

2.4. SUMMARY AND DIRECTION

Examination of the developmental morphology of the human cervical spine reveals a highly dynamic and interdependent system within which the tissue morphology and mechanics are coupled. The paucity of data pertaining to the basic functional morphology and biomechanics of the developing neck has been manifest in numerous spinal injuries to the pediatric populace with catastrophic outcomes. Prevention of these injuries has been attempted using unvalidated models with neck injury thresholds established in the absence of experimental data. Further, a lack of understanding of the progression of these injuries and the tissues at risk necessitates the development of clinical management procedures. Therefore, this review of the literature directs an experimental and computational investigation into the morphology and biomechanics of the developing spine. Measurement of its biomechanical characteristics enables computational modeling and physical modeling to provide realistic predictions for injury prevention while analysis of the maturing spinal physis enables the review and modification of clinical management schemes for these injuries.

This review of the contemporary insight on the developing cervical spine motivated the generation of the following specific aims, which are investigated in this dissertation. Each of these specific aims is addressed in a subsequent chapter providing thorough coverage of the methods, results, and discussion of that specific aim. Specific hypotheses are tested, examined, and discussed as a part of each of these chapters. Following these four chapters corresponding to each specific aim, the sum of the results of this project are discussed. This chapter, "New Insight on the Developing Spine" examines the potential impact of this research effort in the context of its ability to fill the voids ascertained in the review of the contemporary literature.

Chapter 3: Measure the functional biomechanical characteristics of the developing functional spinal unit and vertebrae. The compressive and tensile viscoelastic mechanics are measured examining differences by developmental age, gender, and spinal level.

Chapter 4: Quantify the compressive and tensile failure biomechanics of the developing spine. The tolerances of maturing spinal tissues (from isolated vertebra to full spinal segments) are recorded and evaluated by skeletal maturity, gender, spinal level, and loading rate.

Chapter 5: Analyze failure patterns of the developing physis and establish a relationship between the zone or tissue of failure and developmental maturity. Histological examination of the physis (growth plate) throughout development elucidates the patho-mechanics of the tissues which constitute the physis for tension and compression.

Chapter 6: Develop the compressive and tensile constitutive equations and failure criteria for the maturing cervical spine. Model parameters are established for a constitutive model explaining the properties of the cervical spine throughout the stages of development.

CHAPTER 3:
FUNCTIONAL BIOMECHANICS OF THE DEVELOPING SPINE

3.1. INTRODUCTION

The functional biomechanics of the developing spine was evaluated in compression and tension for functional spinal units and individual tissues. This chapter details from conception to discussion, research aimed at understanding the physiologic compression and tension of functional spinal units as well as the compressive response of individual vertebrae throughout development. The main effect evaluated in each of these studies is development (or age), however, in an effort to more fully characterize the pediatric spine, the secondary effects of gender, size, and spinal level were examined. Comprehending the functional biomechanics of the spine will enable the accurate modeling and understanding of the mechanical response of a child's neck to inputs below the threshold for injury and within the range of normal everyday activity.

3.1.1. COMPRESSIVE BIOMECHANICS

These experiments evaluated the compressive mechanics of both maturing hard (vertebrae) and soft (intervertebral) tissues in an effort to understand the functional biomechanics of the developing spine in compression. Cadaveric baboon tissues were used due to the limited availability of human tissues in the pediatric age range. First, isolated thoracic vertebrae (T9) were subjected to compressive loading to document the compressive mechanical properties (stiffness and elastic modulus) of the developing vertebrae (bone). Next, cervical functional spinal units (Oc-C2, C3-4, C5-6, and C7-T1) were examined in non-destructive compression in an effort to understand the mechanical

characteristics (stiffness, elastic modulus, and viscoelastic relaxation) of the intervertebral soft tissues. This introduction will present specific research on both vertebrae and soft tissues in compression and detail experiments which have motivated and enabled the research performed herein.

Numerous experiments have been performed measuring the compressive mechanics of the adult vertebral body.[8, 48, 91, 138, 139, 147] However, to my knowledge, no study has investigated the mechanics of the immature (developing) vertebral body. Currey, et al.[33] compared pediatric and adult femoral cortical bone and found that the modulus of elasticity and the strength were lower for children, while the energy absorption and deformations prior to failure were greater. A vertebral body's compressive strength has been shown to be primarily (90%) due to its trabecular bone architecture.[91] Thus, an evaluation of the developmental mechanics of a single vertebral body, serves not only to uncover developmental changes in vertebrae, but also to take a unique first look at trabecular bone developmental mechanics.

Similarly, while a number of research studies have examined the adult functional spinal unit in compression,[100, 118, 122, 142, 148, 164] to my knowledge, no study has examined the compressive mechanics of the developing FSU. In fact, while the biochemistry of the developing intervertebral disc has been modestly characterized,[7, 172, 181, 189] the resulting biomechanical consequences of these biochemical changes have not. Scott et al.[181] suggested that the intervertebral disc would have greater load carrying ability with the increasing collagen content accompanying development. Unfortunately, no quantitative data exist linking development with the compressive mechanics of spinal soft tissues; therefore, this examination will engender clear relationships between the maturation of a functional unit and its response to compression.

3.1.2. TENSILE BIOMECHANICS

Subsequent to understanding the compressive mechanics of the spine, we evaluated the cervical spine soft tissues (FSUs) in tension across the developmental spectrum. Again, cadaveric baboon tissues were utilized due to the limited availability of human pediatric tissues. Cervical functional spinal units (Oc-C2, C3-4, C5-6, and C7-T1) were examined

in non-destructive (physiologic) tension in an effort to understand the mechanical characteristics (stiffness, elastic modulus, and viscoelastic relaxation) of the intervertebral soft tissues. A presentation of the research encouraging and facilitating this evaluation of the tensile mechanics of the developing cervical spine will follow in this short introduction.

Tensile mechanics of the adult spine has been evaluated in a number of studies.[34, 142-144, 165, 211] Only one group has previously examined the mechanics associated with tensile loading of the pediatric neck. Using a caprine (goat) model, Pintar et al.[169] documented the non-destructive tensile stiffness of individual functional spinal units. Based on these data, scaling factors were derived as a percentage of the adult properties.[169] While their work provided a first glimpse of the developmental pattern of tensile cervical spine mechanics, they acknowledged the limitations of their animal model (quadruped) and combined male and female sample group and suggested that "additional experimental evaluation [be] conducted using another animal model...". Therefore, this research effort sharpens our understanding of the tensile mechanics of the developing cervical spine by using a larger sample size, eliminating gender bias, and using a primate model.

3.2. METHODS

3.2.1. EXPERIMENTAL DESIGN

The primary goal of these studies was to explore the relationship between mechanics and spinal development, by documenting and correlating the compressive and tensile mechanical properties of isolated thoracic vertebrae and cervical functional spinal units across a range of ages from young pediatric to adult. Secondarily, the effects of gender and spinal level on the mechanics of the developing spine were examined.

Since human pediatric tissues are not readily available, these experiments utilized the baboon cadaver to model the human developing cervical spine. As discussed in Chapter 2, the upright posture, genetic and anatomic similarity, and the functional biomechanical loading of the baboon cervical spine make it a very attractive model. Further, adequate supplies of baboon cadaver tissues are available in the developing age ranges. Our tissues were obtained from the Washington Regional Primate Research Center where the

specimens were euthanized for unrelated research projects (vascular) that were short-term (6 to 8-weeks) having negligible effect on tissue quality. Thus, given the unavailability of human pediatric tissues, we identified the best model to understand the developing spine–the baboon cadaver.

Using this model, a series of non-destructive (functional range), tests were performed on each specimen to establish age-related properties and scaling relationships. The specific mechanical properties that were documented experimentally include compressive and tensile elastic modulus, stiffness, and viscoelastic relaxation. These measures enable the mechanical characterization of the spine in a given loading direction.[61] Further, these experiments on the functional biomechanics of the developing cervical spine will examine the following hypotheses:

1. *As the spine develops, the vertebral (hard tissue) compressive mechanical properties (stiffness and elastic modulus) increase.*
2. *The intervertebral (soft tissue) compressive mechanical properties (stiffness, relaxation time constant, and elastic modulus) increase with tissue maturation.*
3. *The viscoelastic response of the cervical spine in tension demonstrates increasing stiffness, relaxation time constant, and elastic modulus as a function of development.*
4. *Compressive mechanical properties of vertebral bone vary by gender in the developing spine.*
5. *The compressive mechanical properties of the intervertebral soft tissues are different for each cervical spine level.*
6. *The tensile mechanics of the developing cervical spine is unique to the cervical spine level investigated.*

3.2.2. SPECIMEN PREPARATION

Thirty-one fresh cadaver baboon spines (harvested at autopsy) were obtained through the Washington Regional Primate Research Center. Handling of all biologic tissues was in conformance with the University of Washington guidelines for bio-hazardous materials. The spinal musculature, nerve roots and associated tissue, and spinal cord and dura were removed from each specimen taking care not to damage the discs and ligaments. These

osteoligamentous specimens were visually and radiographically inspected and selected for testing based on lack of significant degenerative changes, deformity, or injury. The visual inspection was done to verify that the disc and ligaments were intact and each functional spinal unit was mobile. Following the visual inspection, lateral and anterior/posterior radiographs of each specimen were taken using an HP Faxitron (43855A, Hewlett Packard, McMinnville, OR) at 80-kVp for 20-seconds. The radiographs were used to examine the specimens for pre-existing pathology or degeneration and also to make measurements on the vertebral column. Each specimen was evaluated for normal vertebrae and intervertebral disc spaces as inclusion criteria; and only two specimens were rejected from the study due to radiographic anomaly.

Once accepted into the study, the developmental age of each specimen was determined via a skeletal maturation index developed in our laboratory and based upon skeletal maturation indicators.[64, 79] Our cervical vertebrae maturation index evaluates the first, second, and third cervical vertebra for radiographic characteristics indicative of human child spinal maturation (Appendix A). Computed tomography scans of each specimen were evaluated using this index and each specimen was given a skeletal age or human equivalent age. This procedure was used to age the specimens up to age 18-years and then a 2.9 scaling factor was applied to the skeletally mature (baboon age) to provide human equivalent ages above 18-years.[185] This aging process was performed prior to testing and the human equivalent ages were not linked with the specimen until the data was analyzed. The tissues in this study were from nine females and twenty-two males ranging in age from 1-to-30-human equivalent years. Immediately after dissection, each specimen was bathed in saline, wrapped in towels, sealed in a plastic bag, and fresh frozen at –20°F to preserve their mechanical properties.[163]

A sub-set of these specimens (13-males and 9-females) was selected for the vertebral compression study. The ninth thoracic vertebral body (T9) was examined because of its parallel growth / end plates and ease of dissection from each specimen. The T9 vertebral body was dissected from each spine and all of the intervertebral disc material was removed while preserving the vertebral physis and approximately 5-mm of the pedicle.

The intact (nominal) cross-sectional area of each vertebral body was determined by performing digital image analysis (NIH Image, NIH, Bethesda, MD) on scanned transverse-plane radiographs of the isolated specimens. The average intact height of each specimen was obtained through direct caliper measurements. In preparation for testing, each T9 vertebral body was embedded approximately 1-mm deep in dental plaster (Labstone Buff, Bayer Corp., South Bend, IN) on its superior and inferior surfaces (***Figure 6***). This potting procedure helped to secure the specimen within the loading apparatus while providing an even load distribution to the vertebral endplate surfaces.[201]

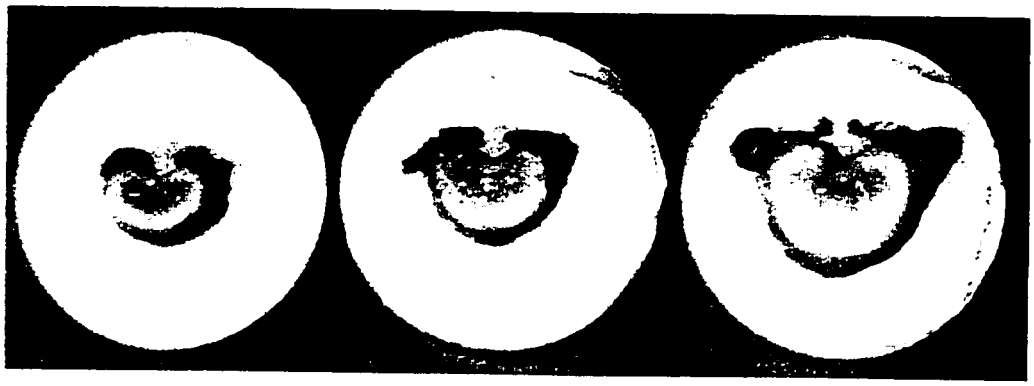

Figure 6. *Photograph of Vertebral Preparations of Varying Skeletal Maturity. These test specimens are human equivalent age 3, 9, and 12-years (left to right) and are shown with their inferior physis embedded in dental plaster cups beneath.*

Another subset of the specimen population was prepared for the cervical spine functional spinal unit testing (compression and tension). This set of specimens included only males to eliminate gender effects and the eighteen (18) specimens ranged in age from 1-to-26-human equivalent years. The compression and tension FSU tests used the same specimens tested non-destructively in each mode of loading; therefore, specimen preparation for these studies is identical. Each specimen was dissected into the following functional spinal units: Occiput-C2, C3-4, C5-6, and C7-T1. Following dissection, each FSU specimen was cross-pinned and potted in poly-methylmethacrylate (PMMA) through its superior and inferior vertebrae (***Figure 7***). This procedure enabled the rigid fixation of each vertebra for testing and facilitated spinal alignment consistency. The

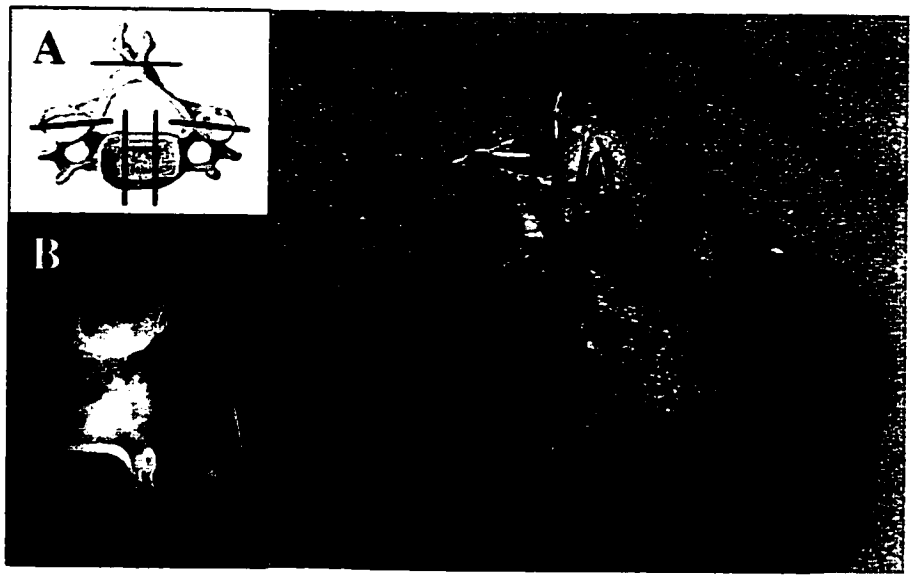

Figure 7. *Wiring and Potting of FSUs for Rigid Fixation During Mechanical Testing. (A) Schematic diagram of the wiring procedure (transverse plane) with the black lines indicating where wires are passed through the bone of the vertebra. (B) X-ray of the wired 1-FSU specimen (sagittal plane) demonstrating the looping of the wires for fixation into PMMA. (C) Potted superior section of a functional spinal unit in PMMA cup with the inferior vertebra (wires shown) upward.*

wiring procedure involved the use of 1.0-mm, 0.75-mm, and 0.5-mm diameter wire applied through the vertebral body anteriorly/posteriorly, the facet/lateral mass laterally and the spinous process laterally for stability. Each wire passing through the vertebrae was crimped outward and bent to make a complete wire loop within the potting. These wired specimens were then imbedded in poly-methylmethacrylate (Jet Acrylic – Lang Dental, Wheeler, IL) within cups made from 3" ID X 3.5" OD PVC tubing. Natural spinal alignment was achieved using the Frankfurt plane for the occiput and each vertebral bodies' growth plate / end plate surface. These landmarks were potted parallel to the cup surface ensuring the functional spinal unit was fixed in a natural position for testing. This fixation technique provided rigid boundaries at each vertebra, which facilitated the direct loading of the soft tissues between the vertebrae. Thus, the mounting and fixation were extremely rigid such that at physiologic (low) loads, the

mechanical response of this FSU system could be attributed to the naturally oriented soft tissues alone.

In summation, we assembled twenty-two vertebral body preparations of males and females throughout development, and twenty cervical functional spinal unit preparations of males across the developmental spectrum. These tissues will come to define the functional biomechanics of the developing cervical spine and provide insight into gender and spinal level variability. Once these specimens were all prepared for their respective experiments, they were bathed in saline, wrapped in towels, sealed in a plastic bag, and fresh frozen at –20°F to preserve their mechanical properties.[163]

3.2.3. EQUIPMENT AND INSTRUMENTATION

The input to our system (developing tissues) was applied using a servohydraulic test frame and the subsequent response of the system was measured with linear displacement transducers, video analysis (two-dimensional displacements), and a six-axis load cell. These input and output devices are discussed along with specifics on their control and acquisition as they were used for this experimental investigation (***Figure 8***).

A servohydraulic test frame by MTS (Model 858 Bionix, MTS Systems Corporation, Eden Prairie, MN) was used to apply both the tensile and compressive loads to the specimens. This frame was digitally controlled using TestStar™ II hardware and software (MTS Systems Corporation, Eden Prairie, MN) providing full PIDF feedback closed loop control. This system has a maximum displacement rate of 0.6-m/sec and was tuned to provide accurate and repeatable displacement profiles. The tuning parameters for the system were set to P = 1.000, I = 0.074, D = 0, and F = 0 for these tests to ensure a faithful dynamic response of the system (up to 10-mm/sec) as well as a steady-state displacement response with a maximum error of 0.01%.

A Linear Variable Differential Transformer (LVDT) was used to measure the linear displacement of the MTS hydraulic ram. The LVDT (Model 490.01 LVDT, S/N 036117, MTS, Eden Prairie, MN) built into the crosshead of the MTS frame was calibrated based on the National Institute for Standards and Technology (#114093-11D). This device has

Figure 8. *MTS Loading Frame (Input) and Measurement Devices (Output). (A) MTS Bionix 858 loading frame shown with instrumentation and tension fixturing. This frame is digitally controlled by the computer at right or via the pod between the frame and computer. (B) Linear compression-tension MTS load cell. (C) Six-axis load cell capable of measuring the forces and moments about the top plate.*

infinite resolution which upon analog-to-digital conversion becomes a resolution of 0.02-mm and is statically accurate to 0.001% FSO (0.001-mm).

The sagittal plane displacements of the cervical spine were measured using markers on each potting cup, which were tracked and analyzed. A digital video camera (GL1 NTSC Digital Video Camcorder, Cannon Inc., Jamesburg, NJ) captured images at 30-frames/sec and these were digitized and analyzed using WINanalyze motion analysis software (Mikromak GmbH, Erlangen, Germany). Even though the field of view (512 x 384) pixel resolution was 0.20-mm/pixel, this software offers sub-pixel resolution via its

digitizing algorithm.[60] Since only normalized linear and angular displacements are analyzed, the resolution of the WINanalyze motion analysis system dictates its error. Therefore, the resolution and measurement error of the WINanalyze motion analysis was ±0.08-mm and ±0.02-degrees, providing us with excellent measurement capabilities.

The uniaxial (tension and compression) load profiles were measured using an MTS Load Cell (Model 662.10A-04 Load Cell, S/N 35205, MTS, Eden Prairie, MN). This load cell was used as the primary load feedback sensor for the MTS load frame and has a functional range of ±1,500-N. Calibration of this device was accordance with the National Institute for Standards and Technology (#130058). The resolution of this uniaxial load cell was ±0.74-N and its total maximum uncertainty was 0.03% or ±0.45-N.

A more thorough measurement of the loads transmitted through the specimen was made using a custom-designed six-axis load cell (Model 4386, Robert A. Denton, Inc., Rochester Hills, MI). The design of this load cell was based on characteristics necessary and proven to provide static and dynamic fidelity for crash test dummies. The measurement capacity (range) of this load cell was specifically designed for low load events such as physiologic loading of biologic tissues. The following are each channels' measurement range: F_x = ±889.6-N, F_y = ±889.6-N, F_z = ±2,224.1-N, M_x = ±56.5-N-m, M_y = ±56.5-N-m, and M_z = ±33.9-N-m. These load channels correspond to specific spinal loading directions and are defined in ***Figure 9***. The calibration of this load cell was performed by the Morehouse Instrument Company (Report Number H607172LG0199) based upon the National Institute of Standards and Technology. According to the calibration, the total uncertainty for any channel at maximum capacity was 0.02% (F_x = ±0.178-N, F_y = ±0.178-N, F_z = ±0.445-N, M_x = ±0.011-N-m, M_y = ±0.011-N-m, and M_z = ±0.007-N-m).

This strain gauge load cell (6-axis) is excited with a stable 10-V input and the output is conditioned by a six channel strain gauge conditioner (SC-2043-SG, National Instruments™, Austin, TX). This accessory amplifier applies a 10X gain and a single-pole low-pass (1.6-kHz) buffered RC anti-aliasing filter prior to acquisition. This analog

filter meets the SAE J211-1 standard criteria for a channel frequency class (CFC) 1000 filter. Therefore, this accessory unit conditions each channel to a high-level signal with an appropriate dynamic content for biologic tissue mechanical testing.

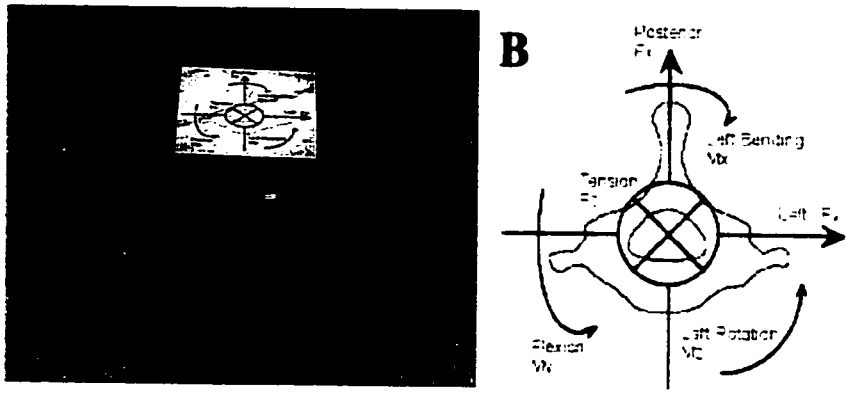

Figure 9. *Six-Axis Load Cell (Model 4386, Robert A. Denton, Inc.). (A) Photograph of the load cell where forces and moments applied to the top surface of the load cell (with the lower plate fixed) are converted into corresponding voltage outputs. (B) Schematic of the force and moment transformations into vertebral coordinates. The arrows indicate directions of positive voltage output (e.g. a positive M_y load cell output conveys a spinal flexion moment).*

Each of the above sensors were acquired with a high-speed multifunction data acquisition board (PCI-6071-E) with 12-bit resolution DACs and 32 differential channels (PCI-6071-E, National Instruments™, Austin, TX). This PCI bus card interfaces with an E-5200 Gateway personal computer with a 600 MHz Pentium® III processor and 256 MB of RAM running Windows NT 4.0 (E-5200, Gateway™, Sioux Falls, ND). Data acquisition was controlled by a custom designed LabVIEW™ virtual instrument (VI) (LabVIEW™, National Instruments™, Austin, TX). This system allowed for the software configuration of analog input channels such that each device may be optimally tuned (resolution and gain) prior to the analog to digital conversion and collection in LabVIEW. Thus, the data acquisition system and instrumentation function to provide the highest quality measurement outputs.

A detailed error analysis of the data acquisition, instrumentation, and specimen fixation techniques demonstrate a high level of confidence the experimental results. The tension

and compression fixtures were evaluated for their compliance using an aluminum block 1-billion times more stiff than the highest tissue stiffness measured herein. These tests revealed the compliance errors in both compression and tension to be less than 0.001%FSO. Propagation of error analysis was performed utilizing these compliance figures, the equations for stiffness and elastic modulus, and the resolution of each measurement device. The product of the partial derivative with respect to each factor (measurement device) and its resolution are summed for all factors of the stiffness and modulus equations. This method provides an error term E_a (worst case) or a root-mean squared error term E_{arms} (most probable) for stiffness and modulus measurements. The propagation of error through specimen fixation, instrumentation, and data acquisition imparts maximal uncertainty (E_a) of 1.22% for stiffness and 4.55% for elastic modulus and the most probable uncertainty (E_{arms}) of 1.07% for stiffness and 3.49% for elastic modulus.

3.2.4. PROTOCOL

Two distinct protocols were used to test the vertebral body specimens and the functional spinal unit specimens. However, every specimen had anterior/posterior and lateral radiographs taken for measurement purposes (HP Faxitron - 43855A, Hewlett Packard, McMinnville, OR). A stainless-steel hose clamp was attached to the inferior potting such that the bottom edge of the clamp was coplanar with the bottom surface of the cup. This hose clamp provided a known dimension on the radiograph as well as a landmark for transforming vertebral geometries on the radiograph. Therefore, measurements on these radiographs provided the vertebral body and disc dimensions of each specimen as well as the position of each specimens disc centroid (FSU testing only) for use in transforming the load cell data (Appendix B). The measurements made from radiographs in ImageJ (Research Services Branch, National Institute of Mental Health, Bethesda, Maryland) contained an uncertainty of 0.5-mm^2. Once all of the measurements were made, each specimen was designated for testing. Prior to testing every specimen was completely thawed for two hours in room temperature water[88], then warmed and hydrated for testing.

The specimens were kept near body temperature (37°C) in a hot water bath to ensure near physiologic temperature and hydration conditions just before testing.

The vertebral body preparations were placed in the MTS loading frame with the MTS Load Cell and MTS LVDT measuring the resulting uniaxial loads and deformations (***Figure 10***). The loading protocol included five loading cycles up to 100-N in compression followed by a final loading cycle up to 300-N. The compression testing was performed in displacement control at a rate of 1-mm/sec. This protocol mimics classical vertebral body crush experiments with a short preconditioning cycle and subsequent quasi-static loading to failure.[47, 139] Both the load and displacement across the vertebral body were recorded during each test at a sampling rate of 200-Hz.

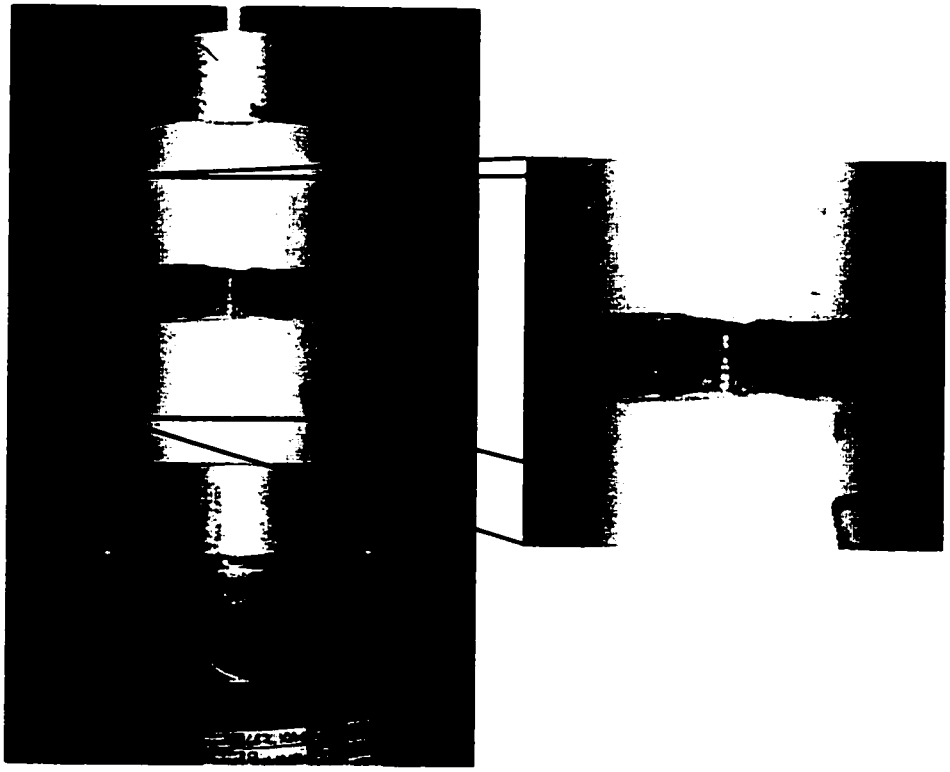

Figure 10. *Vertebral Body Compression Experimental Setup. Shown are the MTS ram compressing down onto the specimen and the MTS load cell measuring the event from beneath. A 10-year old human equivalent male specimen is shown facing anteriorly.*

Each functional spinal unit specimen underwent both tensile and compression non-destructive testing. Haversine and triangular wave displacement profiles and stress relaxations tests enable the characterization of the viscoelastic response of each tissue in each loading direction. The haversine displacement profiles facilitate the calculation of stiffness and elastic modulus while the triangular waves of differing loading rate (1.0-mm/sec, 10-mm/sec, and 100-mm/sec) enable the evaluation of the damping characteristics of the tissue through calculation of the hysteresis energy. Compression and tension were applied to each specimen via the MTS and specifically machined fixturing (***Figure 11***).

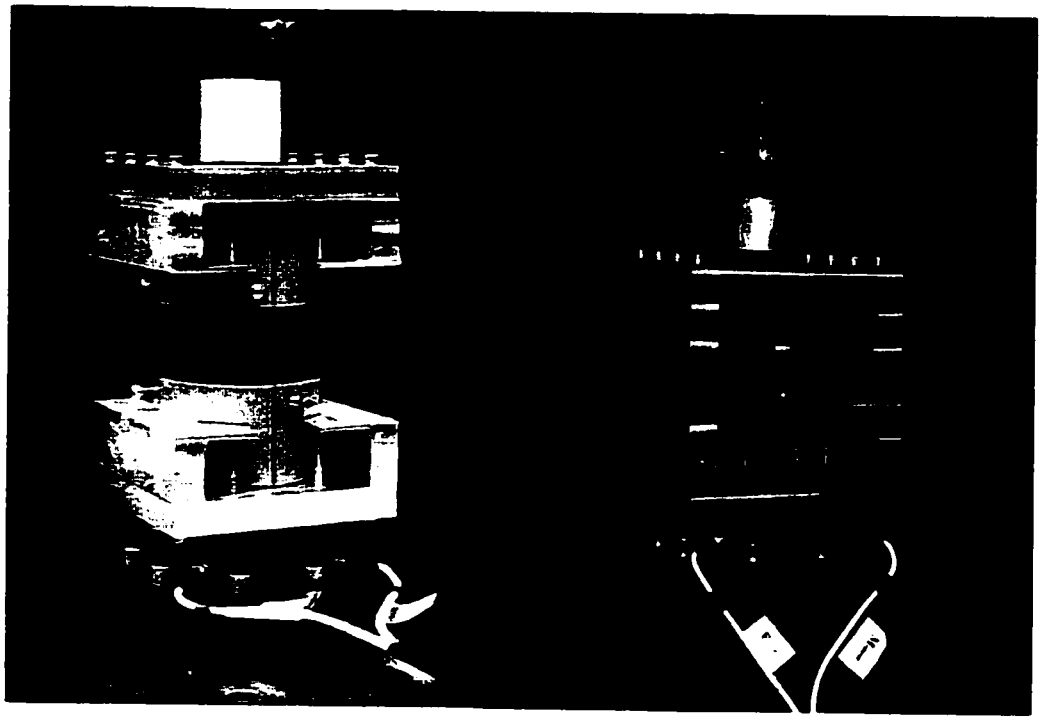

Figure 11. *Compression and Tension Experimental Apparatuses. (A) Compression fixturing enabling the application of pure compressive loads and displacements from the MTS ram (above) and measuring the resulting forces using the six-axis load cell (blue) below. (B) Tension fixturing consisting of aluminum chambers for the specimen potting cups to be held and pulled apart using the MTS ram. A universal joint between the ram and the superior chamber allows the application of pure tensile loads and the load cells beneath the specimen measure the resulting forces.*

Each functional spinal unit specimen was first tested in compression and then tested in tension. The specimens were positioned and oriented such that the center of the six-axis load cell was directly beneath the posterior longitudinal ligament. This positioning was extremely important as the compressive testing used a fixed–fixed end condition so that the six-axis load cell measured the resultant loads from a compressive input. Once in place, the MTS ram applied a non-destructive axial compressive load to the specimen of approximately 40% body weight. This load was applied in a displacement control protocol with a profile similar to that seen in ***Figure 12***. This profile loaded each specimen 5 cycles of haversine displacement quasi-static loading (1.0-mm/sec) followed by dynamic loading of three triangular displacement waveforms (constant velocity) for each of 1.0-mm/sec, 10.0-mm/sec, and 100.0-mm/s. The compression testing completed with a step displacement and hold for 180-seconds to measure the stress-relaxation response of the functional spinal unit.[164] The displacement of the MTS ram and force response (six-axis load cell) was recorded at 1.0-kHz and allows for the complete viscoelastic characterization of the tissue.

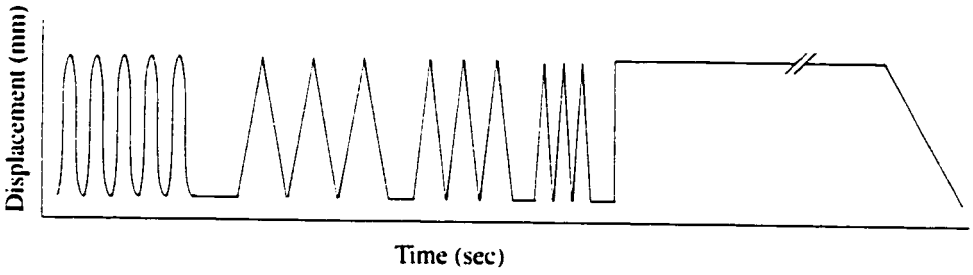

Figure 12. *Displacement Profile for the Compression and Tension Non-Destructive Testing. This profile enables the calculation of the stiffness, modulus of elasticity, hysteresis energy, and time constant.*

Following this non-destructive compression battery of tests, the specimen was held for no less than 10-minutes in the warm bath prior to tensile testing. Tensile displacements were applied to each specimen through a universal joint attached to the MTS ram. The MTS LVDT measured the axial displacement and video analysis was performed to understand the sagittal plane (2-D) displacements of the pined end condition superiorly.

These tension forces were transmitted through the specimen, and were measured with the six-axis load cell inferiorly with a fixed end condition. The specimen was again centered over the load cell and fixed in place. Then a sub-injury tensile force was applied to each specimen (40% body weight) employing the same displacement profile (***Figure 12***) used for compression and the same measurements were made. Following this non-destructive (physiologic range) testing regime, each specimen was again hydrated, wrapped in a towel, placed in a plastic bag, and frozen (-20°) for further testing on the tolerance of these tissues (next chapter).

3.2.5. DATA REDUCTION

For accurate understanding of the load environment in each FSU specimen, the forces measured at the load cell must be transformed up to the specimen. Therefore, the load cell measurements were geometrically transformed up to the centroid of the intervertebral disc. This transformation utilizes the radiograph measurements of each specimen and the static equilibrium equations. This transform assumes that this centroid point is rigidly attached to the load cell and remains stationary. Free body diagrams (***Figure 13***) guided the generation of the transform equations (***Equation 1***) which lead to load data for the response of the specimen at the centroid of the intervertebral disc of each specimen.

$$\sum F = 0 \qquad \sum M = 0$$

$$F_x = -F_{xlc} \qquad M_x = M_{xlc} - (F_{ylc} * z_{AVE}) + (F_{zlc} * x_{AP})$$

$$F_y = -F_{ylc} \qquad M_y = M_{ylc} + (F_{xlc} * z_{AVE}) - (F_{zlc} * x_{LAT})$$

$$F_z = -F_{zlc} \qquad M_z = M_{zlc} - (F_{xlc} * x_{AP}) + (F_{ylc} * x_{LAT})$$

Equation 1. *Set of Equations for Load Transform to the Disc Centroid. This set of equations is based upon the equilibrium equations and use the following conventions:* $_{x, y, z}$ *denote centroid values,* $_{xlc, ylc, zlc}$ *denote load cell values,* $_{LAT, AP, AVE}$ *denote from lateral radiograph, anterior/posterior radiograph, or the average of the two.*

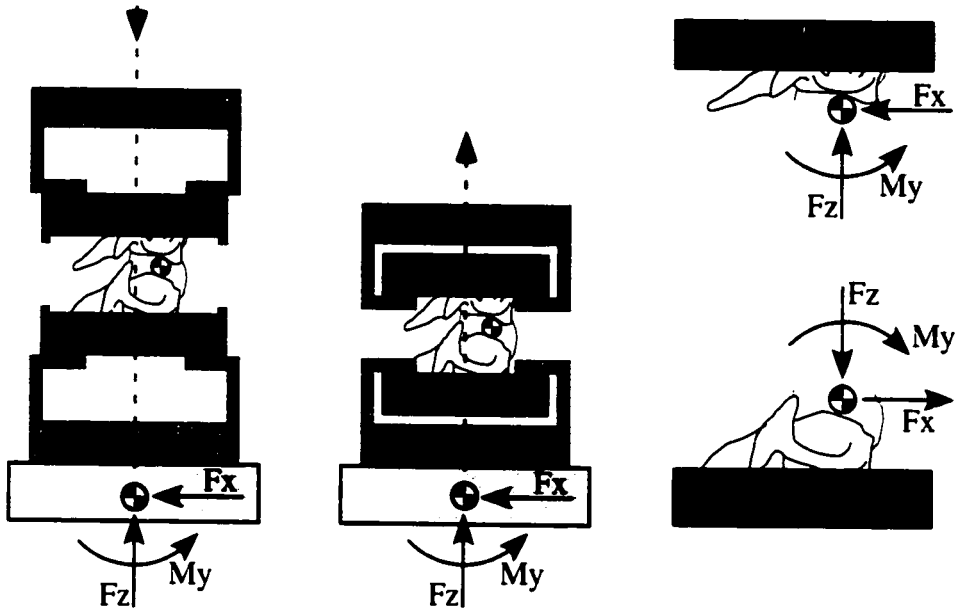

Figure 13. *Free Body Diagrams of the Experimental Apparatuses. These diagrams depict the relationship between the position of the load cell and the centroid of the disc. Utilizing the radiographs of each specimen, the six-axis load cell response is transformed giving the load profile at the centroid of the disc for each experiment.*

Both the vertebral body and functional spinal unit experiments produced load-displacement data, which was further manipulated to examine the experimental hypotheses. Each load-displacement data set was transformed into a stress-strain relationship (***Equation 2***). The specialized stress is defined as each time point of load divided by the original cross-sectional area of the vertebral body (vertebral body experiment) and the intervertebral disc at its centroid (functional spinal unit tests). This stress 'normalization' is not true engineering stress since the functional spinal unit load path includes structures other than those utilized in the stress calculation. The strain is defined as each time point change in displacement divided by the original unloaded height of the vertebral body (vertebral body test) and intervertebral disc (FSU experiments). In this way each specimen is normalized via a size based algorithm to provide a constituent property measure of the tissues without deference to the size of the individual. After completing this normalization, specimen structural properties (stiffness)

and tissue material properties (elastic modulus) were calculated. Stiffness and elastic modulus were computed as the slope of the linear portion of the load-displacement and stress-strain curves respectively.

$$\sigma_{(t)} = {Load(t)}/{Area(t_0)} \qquad \varepsilon_{(t)} = {\Delta Height(t)}/{Height(t_0)}$$

Equation 2. *Stress (σ) and Strain (ε) Relationships Normalizing the Load-Displacement Data. These equations provide constituent tissue mechanics independent of the size of the specimen. They reflect a specialized bulk stress and strain since they are normalized to a generalized size characteristic for each vertebrae and FSU specimen.*

The time constant (τ_ε) of relaxation at constant strain for the functional spinal unit experiments was calculated using the stress relaxation data sets.[61] The normalized load data was fit to a relaxation exponential (***Equation 3***) and the resulting coefficients from each tissue were calculated. Therefore, each vertebral body specimen will have compressive load-displacement, stress-strain, stiffness, and elastic modulus data and each functional spinal unit will have both compressive and tensile load-displacement, stress-strain, stiffness, elastic modulus, and relaxation time constant data.

$$F_z = A(Be^{-t/\tau_\varepsilon} + C)$$

Equation 3. *Equation Relating the Stress Relaxation Data to a Meaningful Exponential (decay) Fit Providing an Excellent Approximation of τ*[61]

3.2.6. STATISTICAL DESIGN

Utilizing the data sets of load-displacement (F-x), stress-strain (σ-ε), stiffness (k), elastic modulus (E), and relaxation time constant (τ), the stated hypotheses were statistically evaluated. Each hypothesis was examined independently below.

Hypothesis 1. As the spine develops, the vertebral (hard tissue) compressive mechanical properties (stiffness and elastic modulus) increase. The null hypothesis is that there is no change in the compressive stiffness or elastic modulus of vertebral specimens for different developmental ages (H_0: $\beta = 0$, H_1: $\beta > 0$, where β is the slope of the stiffness or elastic modulus regressed by age). The stiffness and elastic modulus were regressed by skeletal maturity (grouped and blocked by gender) and fit with a least-squares line to approximate the relationship. A statistical F-test for regression analysis was performed to determine if the slope of the regression was statistically significant.[178]

Hypothesis 2. The intervertebral (soft tissue) compressive mechanical properties (stiffness, relaxation time constant, and elastic modulus) increase with tissue maturation. The null hypotheses are that there are no changes in the compressive stiffness, elastic modulus, or relaxation time constant of the intervertebral tissues for different developmental ages (H_0: $\beta = 0$, H_1: $\beta > 0$, where β is the slope of the stiffness, relaxation time constant, or elastic modulus regressed by age). The stiffness, elastic modulus, and relaxation time constant were regressed by skeletal maturity (blocking by spinal level) and fit with a least-squares line to first approximate the relationship. A statistical F-test for regression analysis was performed to determine if the slope of the regression was statistically significant.[178]

Hypothesis 3. The viscoelastic response of the cervical spine in tension demonstrates increasing stiffness, relaxation time constant, and elastic modulus as a function of development. This hypothesis was tested using the same techniques described for Hypothesis 2.; however, the functional spinal unit tension data sets were evaluated.

Hypothesis 4. Compressive mechanical properties of vertebral bone vary by gender in the developing spine. The null hypothesis is that there are no differences in the compressive stiffness, elastic modulus, or vertebral body size between maturing males and females (H_0: $\zeta_m = \zeta_f$, H_1: $\zeta_m \neq \zeta_f$, where ζ_m (male) and ζ_f (female) are the slope of the stiffness, elastic modulus, and vertebral cross-sectional area regressed by age). A factorial analysis of variance (ANOVA) was used to examine each measure with and without gender

separation to establish if significant gender differences existed using development as a cofactor.

Hypothesis 5. The compressive mechanical properties of the intervertebral soft tissues are different for different cervical spine levels. The null hypotheses are that there are no differences in the compressive stiffness, elastic modulus, or relaxation time constant of the intervertebral tissues between each of the spinal levels (H_0: $\vartheta_{OC2} = \vartheta_{C34} = \vartheta_{C56} = \vartheta_{C7T1}$, H_1: $\vartheta_{OC2} \neq \vartheta_{C34} \neq \vartheta_{C56} \neq \vartheta_{C7T1}$ where $\vartheta_{(level)}$ denotes the slope of the stiffness, elastic modulus, or relaxation constant regressed by age). A factorial ANOVA was utilized to examine differences between levels within each specimen and the interaction of development and spinal level to determine if specific spinal levels develop their functional biomechanical characteristics at different rates. Individual contrasts were performed using the Tukey method to more clearly evaluate each spinal level. The Tukey honest significant difference test uses the Studentized range statistic making all pairwise comparisons such that the experiment-wise error rate is set at the error rate for the collection of comparisons. Thus, this method for pairwise analysis decreases the probability of a Type I error resulting in favorable statistical power characteristics.[56]

Hypothesis 6. The tensile mechanics of the developing cervical spine is unique to the cervical spine level investigated. This final hypothesis was tested in the same manner as Hypothesis 5. using the results of the tensile FSU experimentation.

Significance for all of the above analyses was established at an alpha level of 0.05.

3.3. RESULTS

The experimental results for this examination of the functional response of developing tissues to compression and tension demonstrate a clear relationship between mechanical properties and maturation. Specific results on the compressive and tensile mechanical responses are presented below. A discussion of specimen demographics and mechanical inputs should provide perspective for the compression and tension results. The specimen pool consisted of maturing baboon cervical and thoracic specimens which were given

"human equivalent ages" by assessing their skeletal maturity (***Figure 14***). The relationship between skeletal maturity and actual baboon chronological age suggests that human equivalent age may be approximated by a 2.7-scaling factor applied to the baboon age. These specimens had spinal geometries which were shown to increase in size with

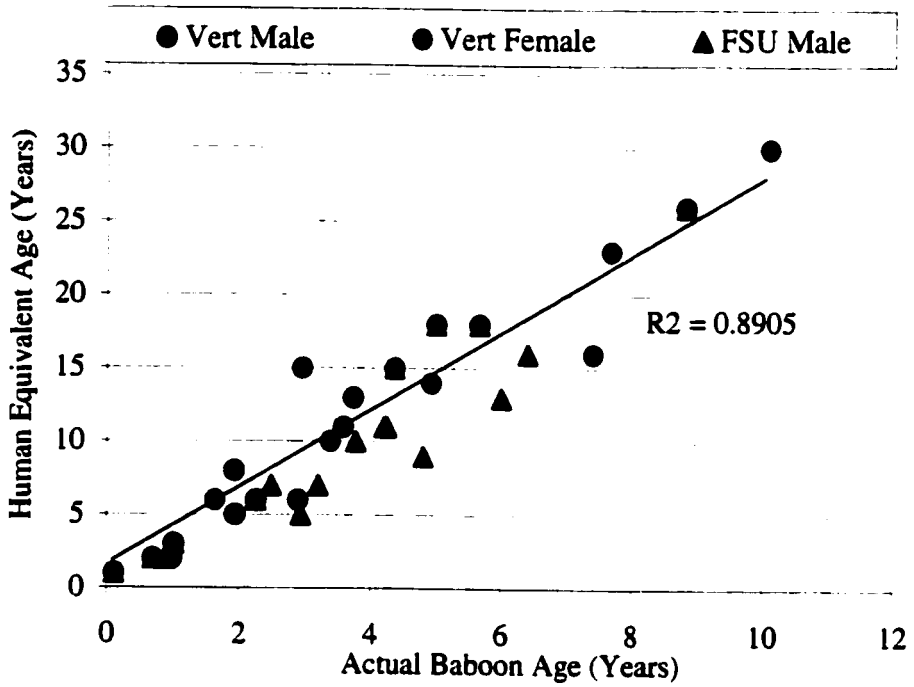

Figure 14. *Specimen Human Equivalent Age by Actual Baboon Age. Thirty-one specimens were tested in the functional biomechanical experiments and given human equivalent ages based upon a skeletal maturity index (regression slope = 2.7).*

Table 3. *Cross-Sectional Area of the Intervertebral Disc and Vertebral Body Increase with Maturity. This table demonstrates the goodness of fit (R^2) and significance of a linear regression of the area by developmental age.*

		R	R^2	F	Sig.
Intervertebral Disc Area	C3-C4	.961	.923	192.48	<0.0001 *
Vertebral Body Area	Grouped	.646	.418	14.34	0.001 *

development. The vertebral body and intervertebral disc cross-sectional areas significantly increased with skeletal maturation (***Table 3***). Further, gender and spinal level differences can be observed in the structural growth of spinal tissues (***Figure 15***).

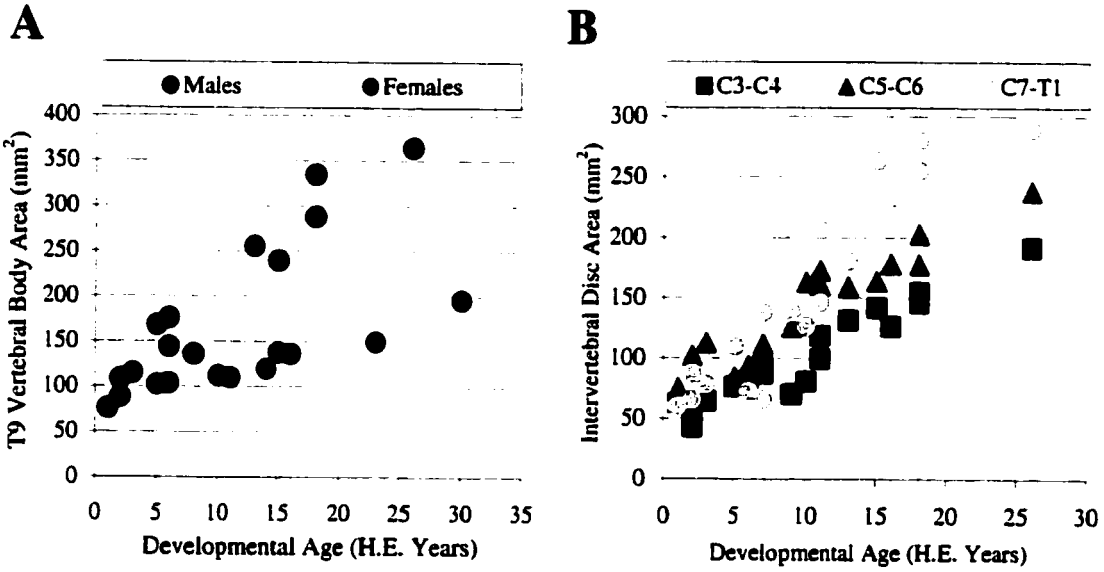

Figure 15. *Cross-Sectional Areas of Developing Vertebral Body and Intervertebral Disc Tissues. (A) T9 vertebral body areas for the male and female specimens. Note the size differences between males and females (p = 0.0012). (B) FSU intervertebral disc areas for different spinal levels. The intervertebral disc areas for the lower cervical spine are larger than those superior.*

Before delving into the mechanical responses of these tissues, sample load-displacement and stress-strain curves are shown explaining visually the stiffness and modulus of elasticity measurements for each sample (***Figure 16***). Each of the stiffness and modulus of elasticity measurements was taken as the slope of their respective curves and the linear portion was limited to that region of linearity above 0.1% strain and containing a linear fit, $r^2 > 0.900$. All of the stiffness and modulus of elasticity measurements met these criteria. The stress relaxation data was fit to an exponential and this resulted in the coefficient, τ_ε for each specimen. Relaxation data fits had an inverse-τ 95% confidence interval no greater than ±0.0001-sec (***Figure 17***).

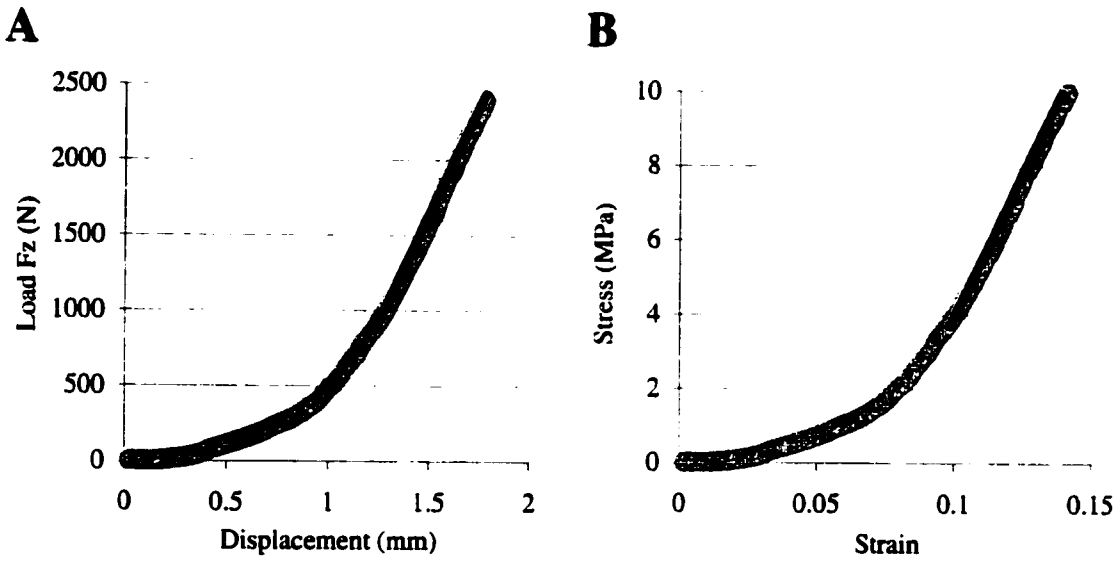

Figure 16. *Experimental Data Reduction from Load-Displacement and Stress-Strain Relationships. (A) Load-displacement curve of a 15-year old male T9 vertebral specimen in compression with stiffness calculated as the slope of the linear portion (2640-N/mm). (B) Stress-strain relationship for the same test showing the modulus of elasticity as the slope of this normalized data (139.2-MPa).*

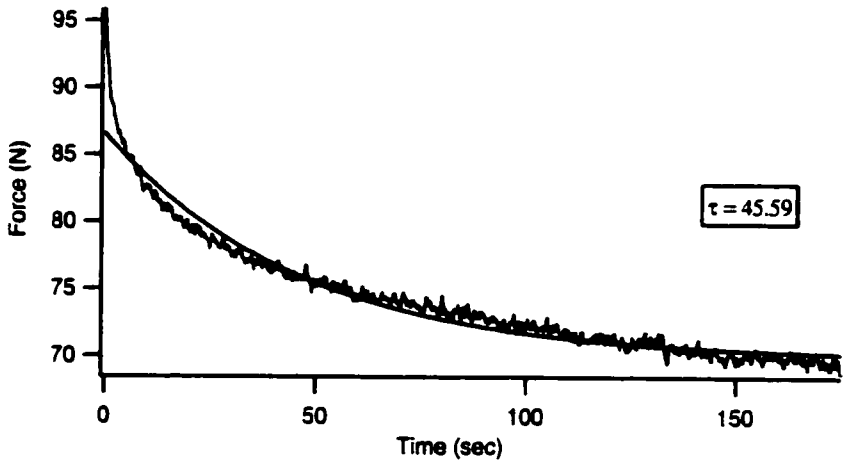

Figure 17. *Experimental Data Reduction from Stress-Relaxation Data. This plot represents the experimental data and fit of the relaxation data providing the time constant,* τ.

3.3.1. MECHANICAL RESPONSE TO COMPRESSION

The results of the vertebral body compressive mechanics and functional spinal unit compressive mechanics are presented here. These results demonstrate that statistically significant changes in structural properties (stiffness) and material properties (modulus of elasticity and relaxation time constant) occur in the developmental process. Further, gender and spinal level differences were observed. Vertebral body compressive stiffness ($r = 0.622$, $p = 0.002$) and modulus of elasticity ($r = 0.605$, $p = 0.040$) were found to be statistically correlated with development (***Figure 18*** and ***Figure 19***). Compensation for vertebral geometry (i.e., stress-strain versus load-displacement) demonstrates a weaker yet significant correlation between vertebral body mechanical development and skeletal maturity.

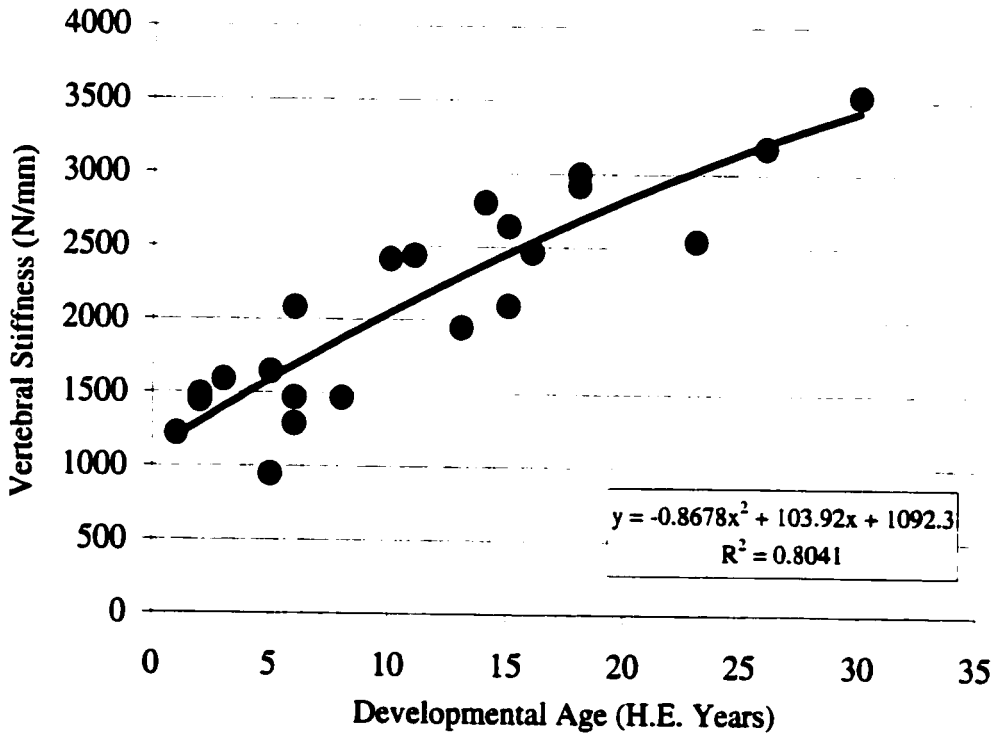

Figure 18. *Vertebral Body Compressive Stiffness as a Function of Developmental Age. A second order polynomial fit describes the change in this structural property with maturation.*

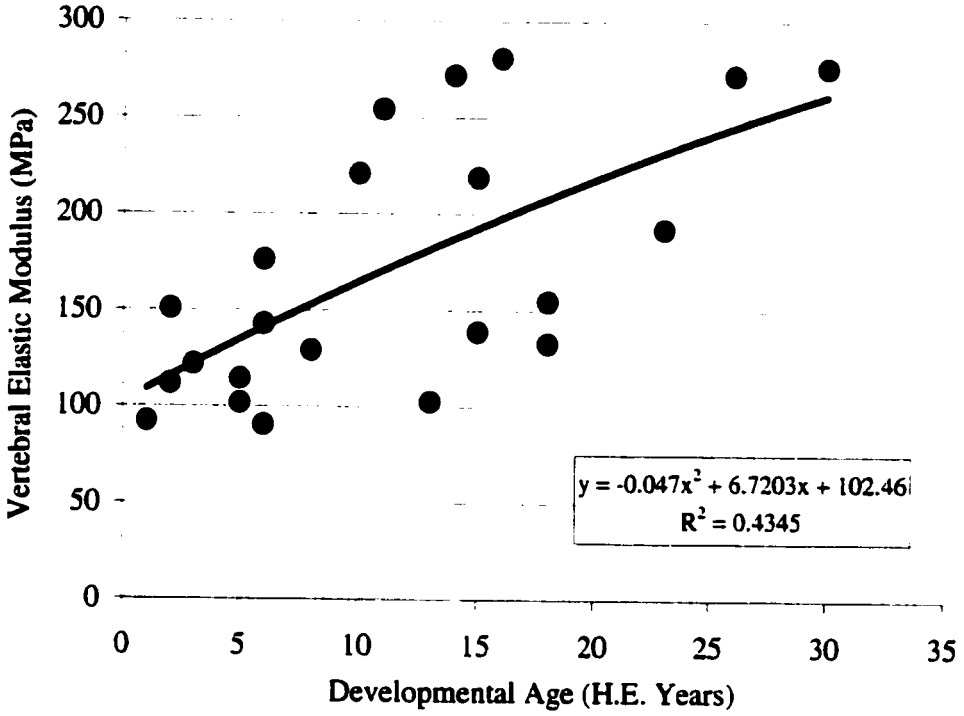

Figure 19. *Vertebral Body Modulus of Elasticity as a Function of Age. This relationship is shown as a 2nd order polynomial fit of a material (bone) property as a function of age.*

The compressive mechanics of developing functional spinal unit (soft tissues) follow similar patterns. Stiffness ($r = 0.994$, $p < 0.0001$), modulus of elasticity ($r = 0.847$, $p < 0.0001$), and relaxation time constant ($r = 0.256$, $p = 0.030$) when averaged across all cervical spine levels show clear relationships with skeletal maturity (***Figure 20***, ***Figure 21*** and ***Figure 22***).

These data demonstrate not only structural property dependence on development; they also demonstrate material property changes with maturation. Therefore, while size changes with development (***Figure 15***) it does not convey the whole story; there are intrinsic material property changes that affect the mechanics of the cervical spine FSUs.

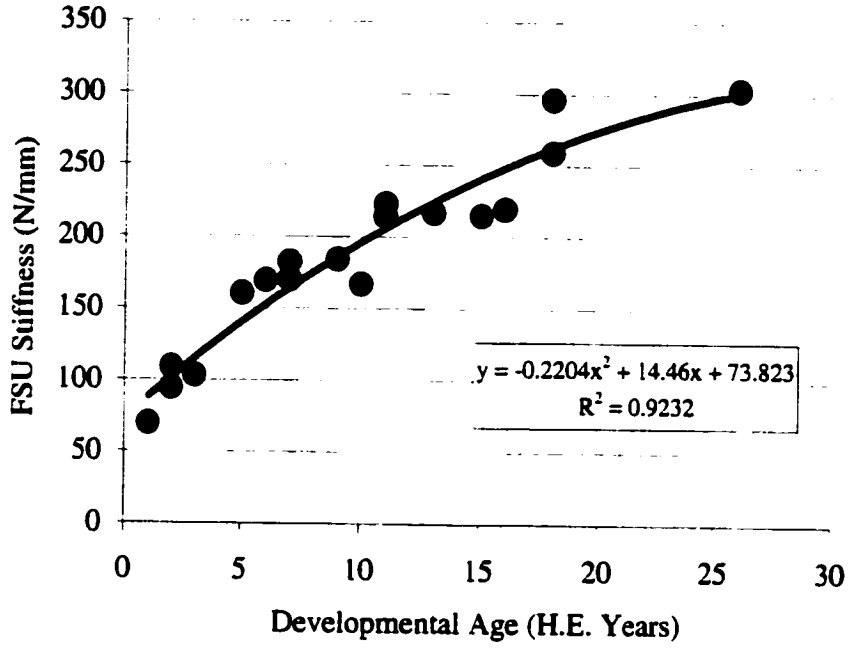

Figure 20. *Functional Spinal Unit Compressive Stiffness as a Function of Developmental Age. This plot illustrates the mean of four functional spinal units (Oc-C2, C3-4, C5-6, and C7-T1) for each specimen. A 2nd order polynomial fit very closely approximates this stiffness data.*

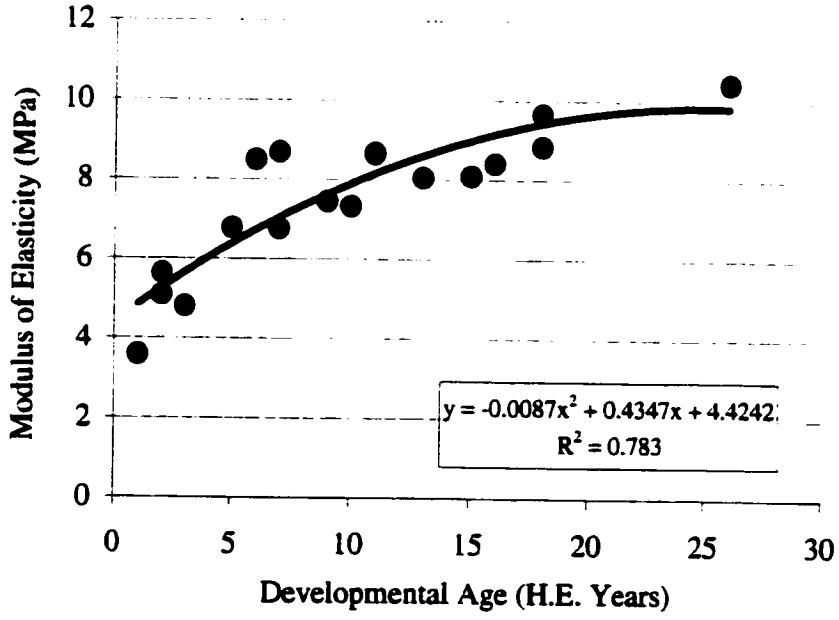

Figure 21. *Compressive Elastic Modulus as a Function of FSU Development. These data demonstrate age related changes in the compressive material properties of the cervical spine. Each point represents the mean of the three spinal units of that specimen.*

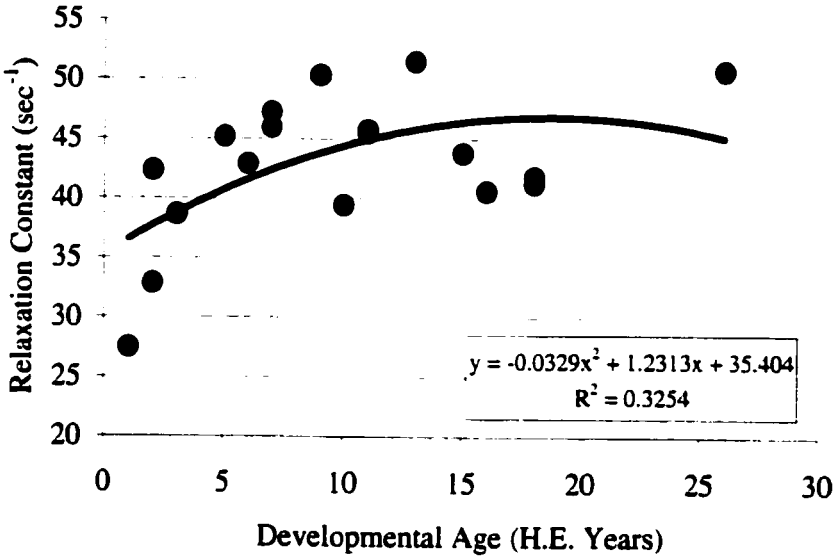

Figure 22. *Compressive Stress Relaxation Time Constant (τ) as a Function of Age. The mean FSU compressive relaxation constant demonstrates a weak dependence on development. Each point represents the mean of four cervical spine levels of each specimen.*

Separation by gender in the vertebral body compression mechanics study revealed stronger correlations with development than the grouped data. The relationship between age and stiffness was significant for both the males and females although the modulus of elasticity was significant for the males but not for the females (p = 0.095) (***Table 4*** and ***Figure 23***). Further, analysis of variance between genders revealed a significant difference in modulus of elasticity (p = 0.003) but not for stiffness (p = 0.337). This can be seen graphically in ***Figure 23***.

Table 4. *Vertebral Compression Stiffness and Elastic Modulus Correlation with Age Statistics. These data demonstrate grouped (gray) and separated by gender results of linear regression analyses to examine if a relationship exists between structural / material properties and development. Blue denoted male (N = 13) and red indicates female (N = 9) separation.*

	R	R^2	F	Sig.
Stiffness	.622	.387	12.65	0.002 *
by Gender				
Modulus	.605	.366	4.967	0.040 *
by Gender				

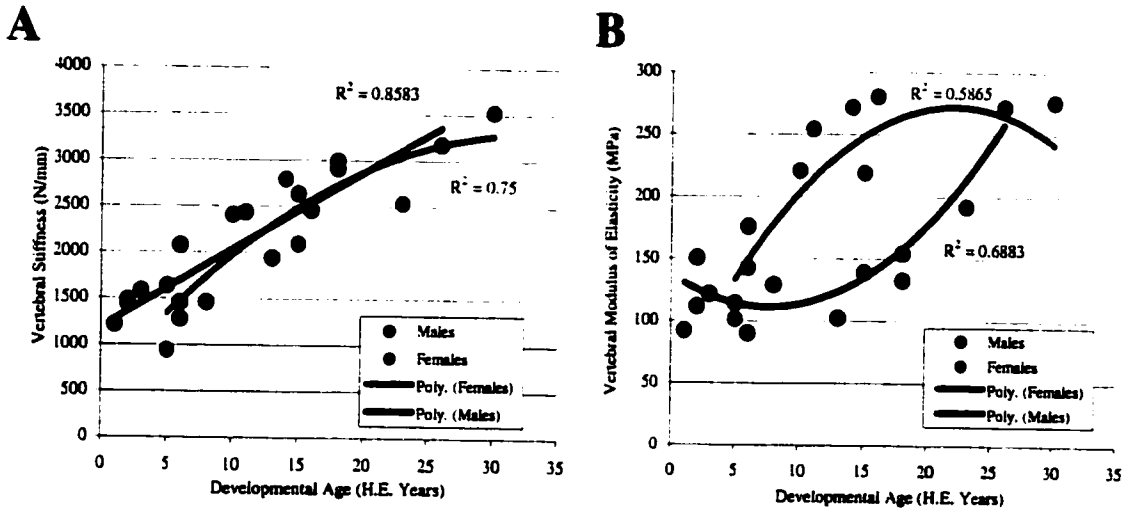

Figure 23. *Gender Differences in Developing Vertebrae Structural Properties and Material Properties. (A) Vertebral compressive stiffness as a function of age denoting gender differences. Note that these plots are very similar. (B) Vertebral elastic modulus in compression by age shows very different gender curves. This suggests that male and female bone material properties develop differently. All polynomial fits are 2nd order.*

Finally, the functional spinal unit data is examined by cervical spinal level. These data reveal distinct relationships between developmental compressive stiffness ($p < 0.0001$), modulus ($p = 0.007$), and constant strain relaxation time ($p = 0.0001$) and the various cervical spine levels (***Table 5***, ***Figure 24***, ***Figure 26***, and ***Figure 26***). Specifically, significant compressive stiffness differences exist between the Oc-C2 level and all other levels ($p < 0.0001$) and between C5-C6 and C7-T1 ($p = 0.013$). An examination of the compressive modulus reveals differences between all of the levels except the C5-C6 and C7-T1 ($p < 0.008$). The constant strain relaxation time constant demonstrates level-specific differences for each cervical spine FSU ($p < 0.018$). While these are all statistically different from one another, they do not all demonstrate developmental dependence.

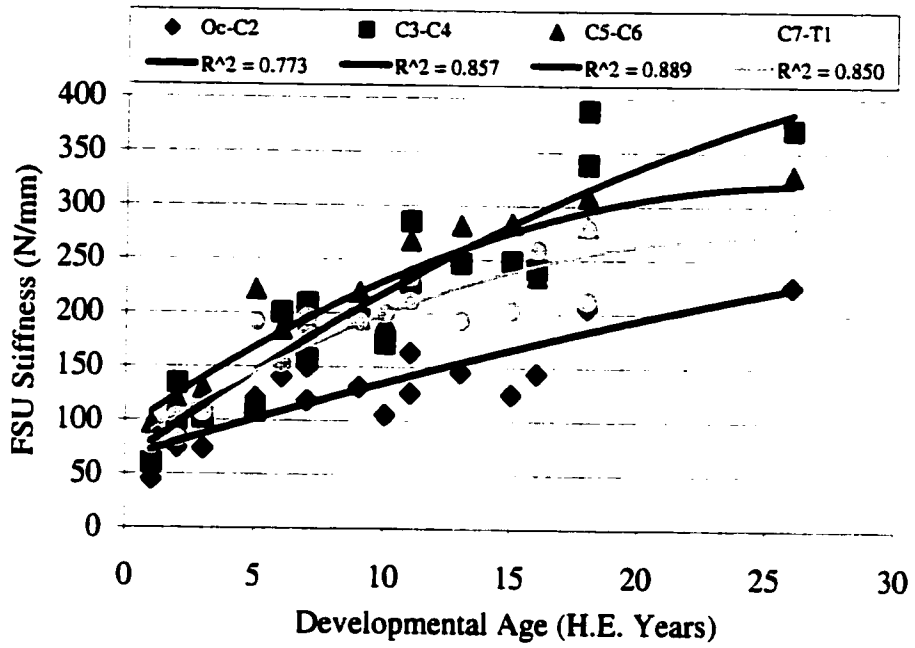

Figure 24. *Functional Spinal Unit Compressive Stiffness by Age. Each line represents a second order polynomial fit to one spinal level's stiffness data. Therefore, these lines represent the pattern of stiffness generation in the cervical spine for each level.*

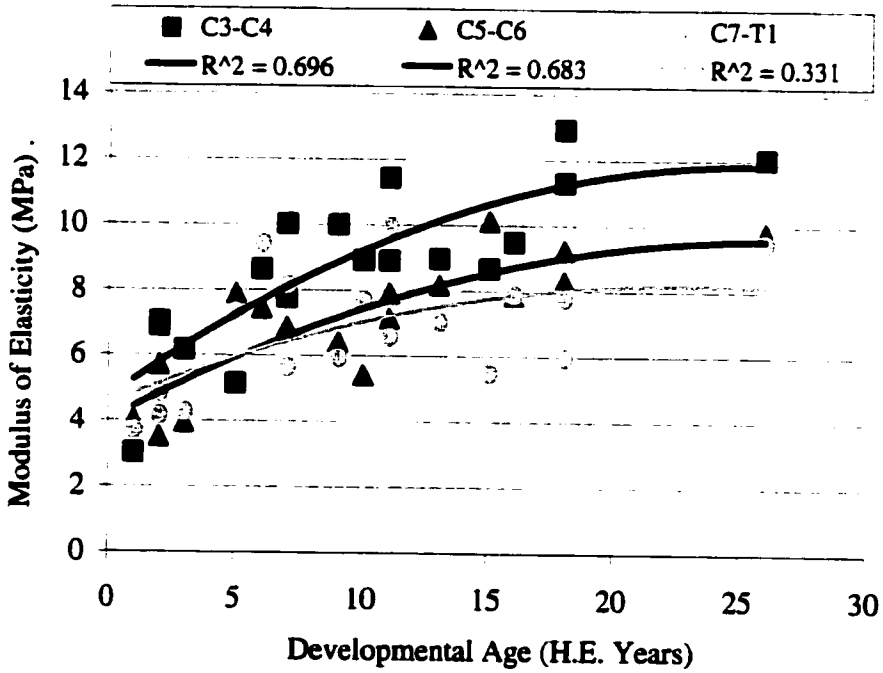

Figure 25. *Compressive Modulus of Elasticity of Developing Functional Spinal Units. Second order polynomial fits explain each FSUs elastic modulus development.*

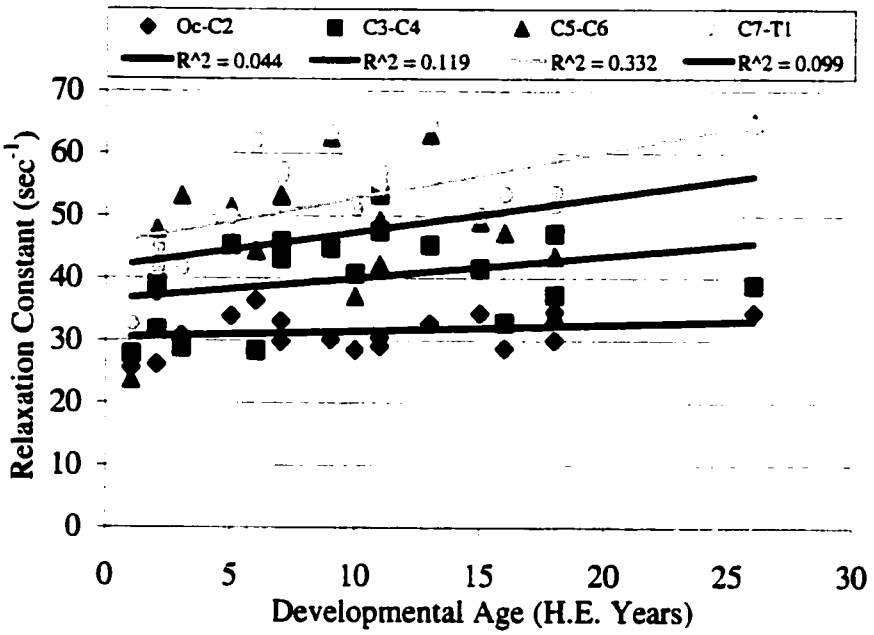

Figure 26. *Compression Relaxation Time Constant (τ) by Age and Level. These data demonstrate different spinal level relaxation time constants, but not necessarily an age dependence.*

Table 5. *FSU Compressive Stiffness and Elastic Modulus Correlation with Age Statistics. These data demonstrate individual functional spinal unit linear regression analyses examining the relationship between structural / material properties and development. (N = 18 per row)*

		R	R^2	F	Sig.
Stiffness	Oc-C2	.877	.769	53.15	<0.0001 *
	C3-C4	.919	.844	86.80	<0.0001 *
Time Constant	Oc-C2	.209	.044	.73	0.405
	C3-C4	.315	.099	1.76	0.203
Modulus	C3-C4	.800	.641	28.51	0.0005 *

3.3.2. MECHANICAL RESPONSE TO TENSION

The response of cervical functional spinal units to tensile inputs demonstrates a distinct relationship with age. The tensile stiffness ($r = 0.712$, $p < 0.0001$), modulus of elasticity ($r = 0.604$, $p < 0.0001$), and relaxation time constant ($r = 0.353$, $p = 0.002$) for all of the data were significantly correlated with developmental age (***Figure 27***, ***Figure 28***, and ***Figure 29***). Examining each functional spinal unit independently revealed tensile stiffness to be significant for all levels, tensile relaxation time constant as significant for C3-C4 only, and tensile modulus to be significant for all levels aside from the C7-T1 FSU (***Table 6***).

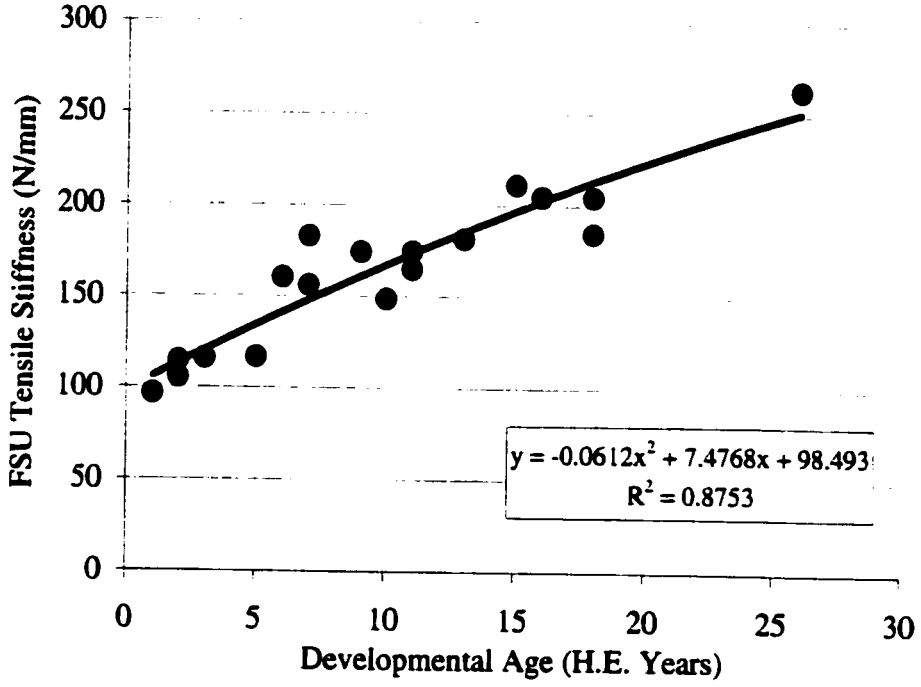

Figure 27. *Mean Tensile Stiffness of Developing Functional Spinal Units. These data represent the mean of four levels (Oc-C2, C3-C4, C5-C6, C7-T1) at each point and demonstrate the change in tensile stiffness as a function of age (2^{nd} order fit).*

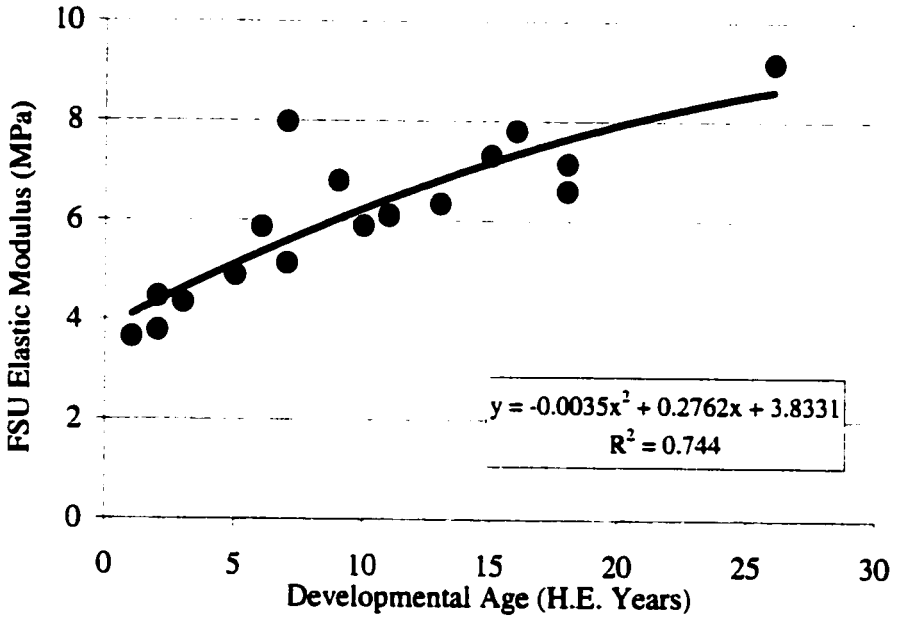

Figure 28. *FSU Tensile Elastic Modulus as a Function of Age. The average of three functional spinal units are displayed here (C3-C4, C5-C6, C7-T1) and shown with a second order fit.*

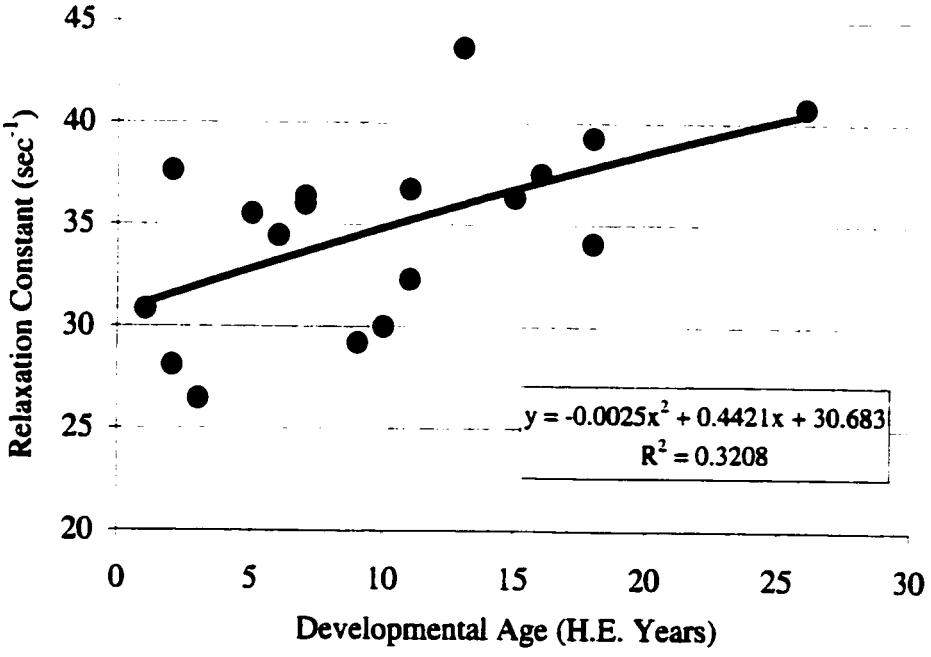

Figure 29. *Stress Relaxation Time Constant (τ) as a Function of Age. The mean FSU tensile relaxation constant demonstrates a weak association with development. Each point represents the mean of four cervical spine levels of each specimen.*

Table 6. *Statistical Evaluation of FSU Tensile Stiffness, Time Constant, and Elastic Modulus Correlation with Age. These data demonstrate individual functional spinal unit linear regression analyses examining structural/material properties throughout development. (N=18 per row)*

		R	R^2	F	Sig.
Stiffness	Oc-C2	.817	.668	32.14	<0.0001 *
	C3-C4	.829	.687	35.12	<0.0001 *
	C5-C6	.881	.776	53.41	<0.0001 *
Time Constant	Oc-C2	.238	.057	0.96	0.342
	C3-C4	.665	.442	12.68	0.003 *
	C5-C6	.488	.238	5.29	0.035 *
Modulus	C3-C4	.761	.579	22.02	<0.0001 *
	C5-C6	.774	.599	24.86	<0.0001 *

Comparison between cervical spinal levels reveals significantly different stiffnesses as a function of age (ANOVA stiffness by level $p < 0.0001$) (***Figure 30***). Tukey HSD contrasts revealed individual differences between each of the spinal levels except for the Oc-C2 to C7-T1 and C3-C4 to C5-C6 comparisons ($p < 0.001$). The relaxation time constant for these viscoelastic tissues is not spinal level dependent ($p = 0.082$) even though the various spinal levels appear to have differing patterns of maturation (***Figure 31***). An examination of the FSU tensile modulus of elasticity by spinal level reveals significant level effects ($p = 0.001$) (***Figure 32***). Contrasts of the C3-C4, C5-C6, and C7-T1 levels reveal each has significantly different elastic moduli compared with one another aside from the C5-C6 to C7-T1 comparison ($p < 0.033$).

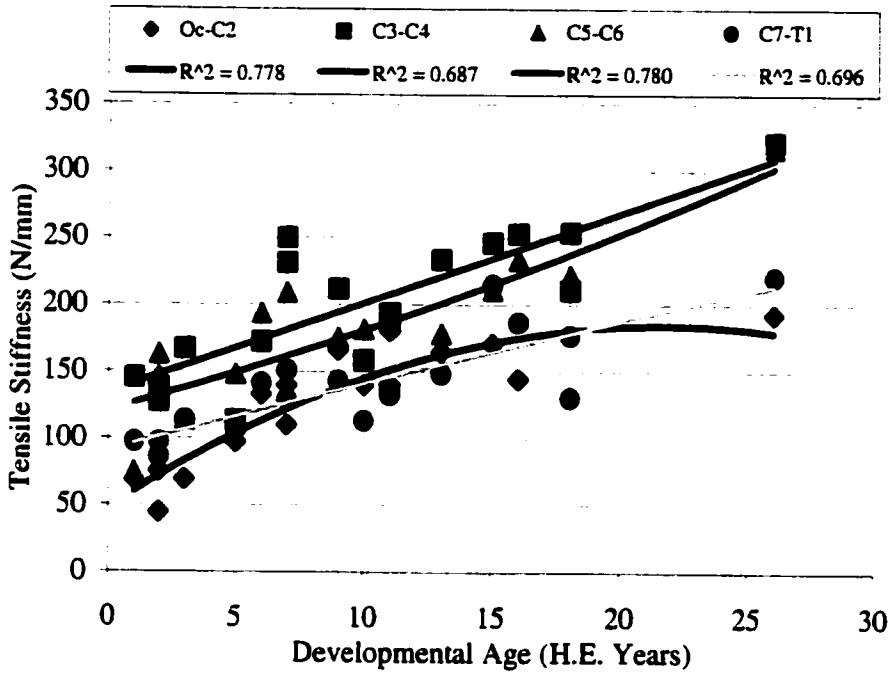

Figure 30. *Tensile Stiffness as a Function of Developmental Age and Spinal Level. Second order polynomial fits approximate each spinal levels development of tensile stiffness.*

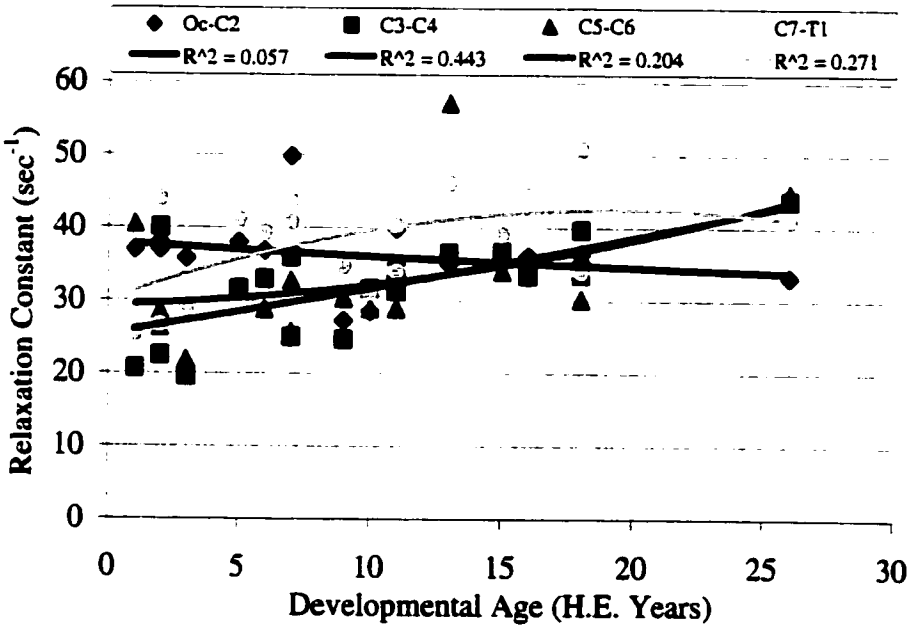

Figure 31. *Tensile Relaxation Time Constants (τ) by Age and Level. These data demonstrate very different patterns of spinal level τ development. The only level demonstrating a positive correlation with development is the C3-C4 level.*

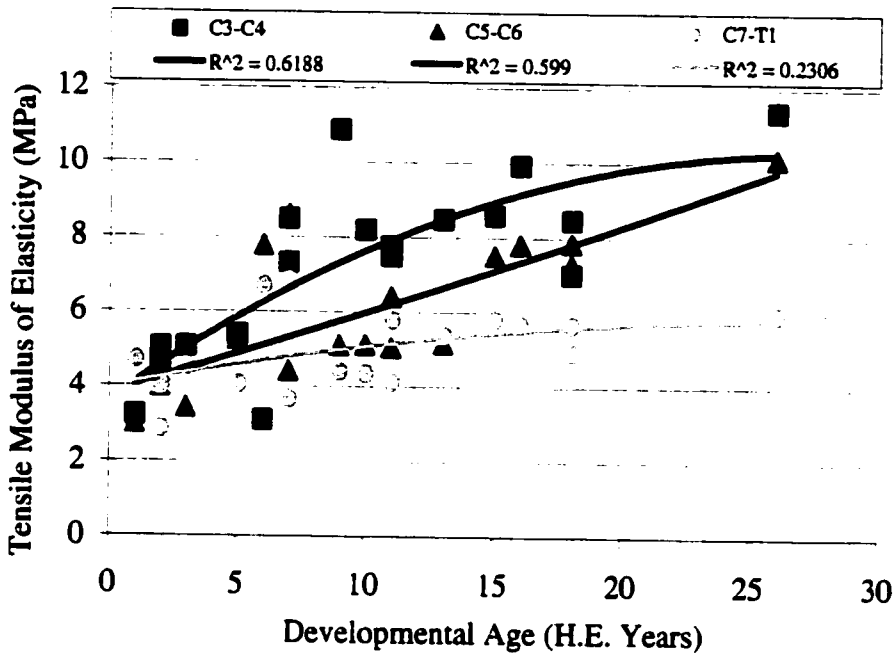

Figure 32. *Level Specific Changes in the Tensile Modulus Throughout Development. These data were fit to a second order polynomial for each spinal level.*

3.4. DISCUSSION

The functional biomechanics of the developing spine are important to understand in modeling its natural physiologic mechanics and in explaining skeletal developmental processes. This research defined the structural properties (stiffness) and material properties (modulus of elasticity and relaxation time constant) of spinal tissues as a function of developmental age. Significant relationships were discovered between these mechanical characteristics and skeletal maturity. This discussion will first examine each of the tested hypotheses and then delve into nuances and other interesting discoveries regarding the functional mechanics of the developing cervical spine.

Hypothesis 1. As the spine develops, the vertebral (hard tissue) compressive mechanical properties (stiffness and elastic modulus) increase. The null hypothesis is rejected since both the stiffness ($p = 0.002$) and elastic modulus ($p = 0.040$) were significantly correlated with development. Further, the alternative hypothesis is accepted which states that the compressive modulus and stiffness increase with vertebral development.

Hypothesis 2. The intervertebral (soft tissue) compressive mechanical properties (stiffness, relaxation time constant, and elastic modulus) increase with tissue maturation. Since the compressive stiffness ($p < 0.0001$), modulus of elasticity ($p < 0.0001$), and relaxation time constant ($p = 0.030$) were positively related to cervical FSU spinal development, the null hypothesis is rejected. Therefore, the alternate hypotheses that stiffness, relaxation time constant, and modulus of elasticity increase with development are accepted.

Hypothesis 3. The viscoelastic response of the cervical spine in tension demonstrates increasing stiffness, relaxation time constant, and elastic modulus as a function of development. Likewise for tension, the stiffness ($p < 0.0001$), relaxation time constant ($p = 0.002$), and modulus of elasticity ($p < 0.0001$) increased with development. Thus, the null hypothesis is rejected and the alternative hypotheses are accepted.

Hypothesis 4. Compressive mechanical properties of vertebral bone vary by gender in the developing spine. While vertebral cross-sectional area ($p = 0.0007$) and modulus of elasticity ($p < 0.0001$) throughout development were significantly different by gender, the stiffness ($p = 0.221$) demonstrated insignificant gender effects. Therefore, the null hypothesis is accepted that there are no gender-based differences in stiffness. However, the null hypothesis for the vertebral size and modulus of elasticity is rejected since those data demonstrated significant increases with maturation.

Hypothesis 5. The compressive mechanical properties of the intervertebral soft tissues are different for each cervical spine level. Analysis of variance techniques revealed the developmental compressive stiffness ($p < 0.0001$), time constant ($p = 0.0001$), and modulus ($p = 0.007$) to be significantly different by spinal level. Thus, the null hypothesis is rejected and the alternate hypothesis that spinal level differences exist is accepted. Contrasts elucidated that specific levels are different from one another but not all are different from each other.

Hypothesis 6. The tensile mechanics of the developing cervical spine is unique to the cervical spine level investigated. The null hypothesis is rejected and the alternate

hypothesis is accepted for the stiffness ($p < 0.001$) and elastic modulus ($p = 0.001$) which were shown to vary by spinal level. However, the null hypothesis is accepted for the time constant property, since no spinal level effects were present ($p = 0.082$). Finally, contrasts demonstrated that not every level is different from each other, but rather found particular level differences for each mechanical property.

These hypotheses summarize the main findings in this experimental endeavor. However, as in most experimental efforts, the results ask more questions than they answer. Therefore, this discussion will turn to review interesting findings that were not specifically tested.

Of extreme import to the applicability of this research is the assessment of skeletal maturity. The slope of the comparison between human equivalent age and actual age is 2.7, which closely approximates the 2.9-scaling factor by Tominaga et al.[185] This provides validation for the skeletal maturity assessment method and supports its use in the 'aging' of tissues of unknown chronology throughout maturation.

The differences between spinal hard and soft tissues were not specifically tested, but they revealed very similar developmental functions (***Figure 33***). The cervical functional spinal unit in compression is approximately 10-times less stiff compared with the T9 vertebral body. The second order function by which these data change with age are extremely similar in spite of the vast differences in the two tissues tested.

The vertebral body and functional spinal unit experiments all demonstrated significant increases in stiffness, a non-normalized measure based in part on the size of the specimen. Analysis of the areas of these tissues revealed that they too increase with developmental age. This might suggest that the developmental mechanics of the spine can be approximated using the size of the vertebral body / intervertebral disc. Size, however, does not tell the entire story since the intrinsic material properties of these tissues (elastic modulus) also increase with developmental age. A weaker modulus correlation coefficient (versus stiffness) indicates that differences in specimen size may

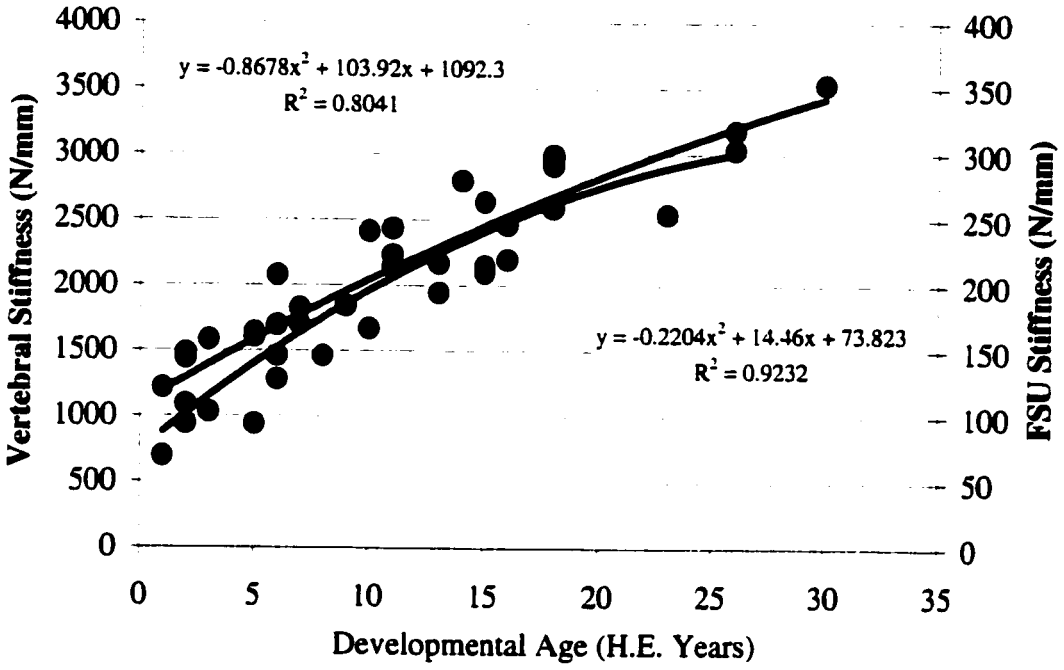

Figure 33. *Compressive Vertebral Stiffness and FSU Stiffness as a Function of Development. These data are the mean (grouped levels) of the FSU data and each vertebral specimen. Second order polynomials were fit to each data set and appear very similar in nature.*

outweigh differences in the inherent material properties as a function of age. However, it is clear that a combination of changes in the tissues themselves and the sheer volume of these tissues confer the overall mechanical function to the spine.

Gender differences in vertebral body development demonstrate significantly different cross-sectional areas and modulus of elasticity although their stiffnesses are indistinguishable. This suggests that males and females have different ways of achieving functional stiffness; increasing size faster in males and increasing the intrinsic material properties faster in females. It is extremely interesting though that males and females approximate very similar functional stiffnesses in spite of their different developmental courses. Previous studies on adults have identified gender differences resulting from primarily size discrepancies alone.[67, 137] Thus, this may be a developmental phenomenon.

Functional spinal unit differences are not completely unexpected since the adult cervical spine has differing material properties by level.[161, 205] Both the work by Yoganandan et al.[205] and this study uncover the C3-4 functional spinal unit as the most stiff and the Occiput-C2 level as the most ductile in both compression and tension. The developmental course to these properties appears to be constant for each spinal level with the starting mechanics dictating the adult functional mechanics of the spinal unit. This work by Yoganandan et al. supports the spinal level differences uncovered herein as well as encourages the use of baboon tissues to understand human developmental biomechanics.

Validation of the baboon model in the adult age range supports its use in understanding the developmental course of the child spine. Thus, a comparison with adult vertebral functional mechanical data found similar modulus of elasticity values. Hayes et al.[80] identified an adult range of compressive moduli from 75-to-350-MPa for specimens with varying density. The highest bone density has been correlated with the youngest specimens (20-to-30-years),[177] and should this hold for the Hayes et al. data set, the 20-to-30-year old average compressive modulus was 310-MPa which compares very well with the 290-MPa adult modulus discovered in the present study. These material property similarities support the use of baboon tissues to understand the human spine developmental biomechanics.

3.4.1. COMPRESSION AND TENSION SCALING RELATIONSHIPS

Since the data generated herein are for baboon tissues (smaller than human tissues), the absolute utility of the structural mechanics (stiffness) values remains at question. Therefore, these data have been used to develop scaling algorithms which might be applied to adult human data providing child mechanical characteristics (***Figure 34***). These scaling relationships are different for modulus of elasticity and stiffness in each direction of loading and for each tissue (***Table 7***). The scaling factors are based upon the second order fit equations for each mechanical property and represent the first effort in understanding the functional development of the spine. Previous studies have used geometric scaling methods or scaled material properties from non-spinal tissues (e.g.,

calcaneal tendon) to obtain first-order estimates of pediatric spinal mechanics.[51, 125, 131] These approximations generated scaling values of 0.34 (3-y.o.) and 0.45 (6-y.o.) that are used for every property and tissue. These values are not based on spinal tissues and therefore were not expected to compare well with the specific values calculated herein.

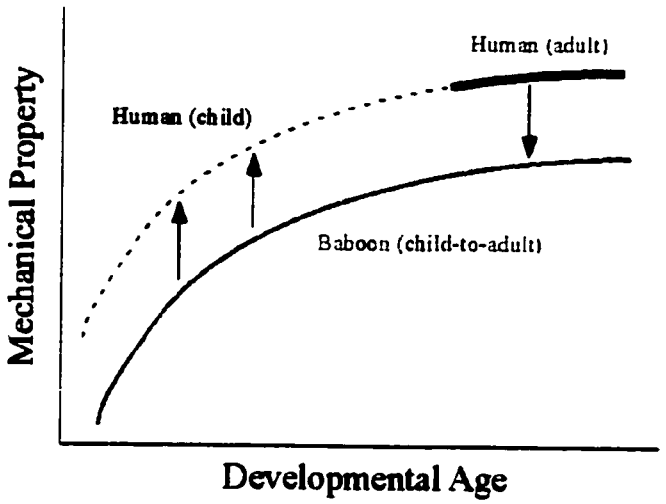

Figure 34. *Scaling of Baboon Pediatric Data to the Human Child. This figure depicts the use of human adult data and scaling algorithms for baboon data to generate human child properties.*

Table 7. *Scaling Values for the Functional Biomechanics of the Spine. These data were generated using the 2nd order fit of experimental data and represent the factor by which human adult data should be scaled to provide child mechanical properties.*

	Vertebral Compression		FSU Compression		FSU Tension	
Age	Stiffness	Modulus	Stiffness	Modulus	Stiffness	Modulus
1	[illegible]	.44	[illegible]	.49	[illegible]	.47
3	[illegible]	.50	[illegible]	.57	[illegible]	.54
6	[illegible]	.57	[illegible]	.68	[illegible]	.62
9	[illegible]	.65	[illegible]	.77	[illegible]	.70
12	[illegible]	.72	[illegible]	.85	[illegible]	.77
15	[illegible]	.79	[illegible]	.91	[illegible]	.83
Adult	[illegible]	1.00	[illegible]	1.00	[illegible]	1.00

The scaling values found by Pintar et al.[169] for spinal tissues are very comparable with the above scaling values for the 6 and 12-year olds, but a bit lower for the 1 and 3-year olds. The differences in the values presented here and those of Pintar et al. may arise from the animal model selected or the mixed gender specimen pool.

The scaling factors will enable the modeling of cervical spine tissues in the developing age range in the absence of human pediatric experimental data. While these relationships may not be exact, they represent the most comprehensive effort to understand the functional mechanics of the developing spine.

3.4.2. SUMMARY

The data generated herein clearly demonstrate that changes in the material properties and structural properties occur with spinal development. Further, these data provide a basic understanding of the maturation changes in the structure (size) and material properties of both vertebral and intervertebral tissues. Modeling of the developing spine will now be possible using the scaling factors generated and also functional spinal unit and gender relationships. These data exist as the first complete set of compression-tension functional biomechanical criteria for the developing spine. Finally, the basic science appreciation of developmental biomechanics empowers efforts to model, minimize, and manage pediatric spinal column injuries.

CHAPTER 4:
TOLERANCE OF THE DEVELOPING CERVICAL SPINE

4.1. INTRODUCTION

The tolerance of the developing spine is evaluated in compression and tension for two functional spinal unit segments, single functional spinal units and individual tissues. This chapter details, from conception to discussion, research aimed at understanding the compressive failure of individual vertebrae and two functional spinal unit segments as well as the tensile failure of functional spinal units throughout the developmental spectrum. The main effect evaluated in each of these studies was development (age), however, in an effort to more fully characterize the pediatric spine, the secondary effects of gender, spinal level, and loading rate were examined. A thorough understanding of the tolerance of the developing spine will provide physiologic end-points for computational modeling and physical modeling (anthropomorphic test dummies). These data will be seminal in the creation of injury thresholds for children in automotive crashes, falls, or sporting incidents to enable the development of injury prevention strategies.

4.1.1. COMPRESSIVE TOLERANCE OF THE SPINE

The compressive tolerance of the spine was examined for both maturing vertebrae and spinal segments (2-FSUs) in an effort to understand the failure mechanics of the developing spine in compression. Cadaveric baboon tissues were again used due to the limited availability of human pediatric tissues. Isolated T9 vertebral bodies (their functional biomechanics previously characterized) were subjected to compressive loading in displacement control to failure. The failure characteristics (ultimate failure load and ultimate strength) were documented for each of the maturing vertebral bodies.

Subsequent to this study, cervical spine 2-FSU segments (Oc-C2, C3-C5, C6-T1) were loaded dynamically to failure and the ultimate failure load and strength were measured. In this way, the compressive tolerance of spinal segments and individual vertebral bodies will be elucidated.

The compressive mechanics of isolated vertebral bodies was previously discussed (3.1.1) for both the functional and failure mechanics of vertebral bone. This current study represents the first of its kind evaluating the tolerance characteristics of developing vertebrae and also provides a clearer picture of gender related differences throughout development. Gender differences have been observed by others in the adult population, most often relating bone density to ultimate failure load and strength.[12, 103, 120, 137] Thus, precedence exists to investigate gender distinctions in the maturing vertebral body.

The second compressive investigation involves the study of 2-FSU (cervical) constructs to determine their compressive tolerance characteristics. It has been suggested that the adult spine is most often injured in compression;[3, 208] therefore, a number of research studies have examined the adult cervical spine in compression.[25, 122, 142, 148, 162, 170, 202, 213] To my knowledge though, no examination of the compressive mechanics of developing tissues has been performed.

Previous studies have used 2-FSU segments to examine the compressive mechanics of the adult spine because they allow the spinal tissues to fail either in soft or hard tissues without buckling.[25, 162, 170, 202, 213] These efforts used quasi-static loading or drop-weight apparatus to examine the compressive mechanics of 2-FSU specimens. Since these 2-FSU constructs have proven useful in understanding the adult spine, they were utilized in this effort to comprehend the developing spine. An experimental study by Nightingale et al.[148] developed full head and cervical spine responses to compressive impacts. The results of this research were modeled by Camacho et al.[21] and this model exposed haversine displacement impulses occurring across 2-FSU constructs.[24] Therefore, an accurate compressive input to a 2-FSU construct involves a haversine displacement impulse.

Dynamic compressive loading of these spinal constructs has proven successful in generating clinically relevant adult injuries.[25, 142, 148] Unfortunately, these dynamic investigations used varying loading rates; however, McElhaney et al.[121] determined that the whole cervical spine has a 'real world' compressive velocity threshold of 3.1-m/sec. Unfortunately, the velocity across a 2-FSU specimen is uncertain, but methods suggested by Edwards[49] enable the scaling of velocity to segments shorter than the full spine. Edwards's approximation assumes the spine is comprised of equivalent springs and so that the full cervical spine velocity can be multiplied by 2/7 to get the velocity across a 2-FSU segment. Therefore, to approximate real world velocity events, 2-FSU constructs will be investigated at 0.9-m/sec. These methods previously shown to be successful in measuring adult compressive tolerance were utilized in this study. Unique to this research effort is the attempt to understand the compressive failure mechanics of the developing cervical spine.

The secondary factor of spinal level will be investigated in these tolerance experiments as well. While bending and single FSU level distinctions have been identified, no tolerance data has been recorded comparing different spinal levels for 2-FSU compressive failures.[160, 211] These data will examine the susceptibility to injury of different spinal levels throughout development.

4.1.2. TENSILE TOLERANCE OF THE SPINE

This research will document the tolerance of the developing functional spinal unit in tension both quasi-statically and dynamically. In this way, the tensile failure characteristics (ultimate failure load, strain, and strength) of developing tissues will be determined to aid modeling efforts by providing thresholds for tissue failure. Like those before it, this study utilized developing spinal tissues from the baboon (*papio anubis*). Cervical functional spinal units (Oc-C2, C3-C4, C5-C6, and C7-T1) were quasi-statically loaded to failure in tension so as to understand how ultimate failure load, strain, and strength change with maturation. Further, tissues of a similar age were subjected to differing degrees of dynamic tensile loading in an effort to understand the rate-effects on

tolerance characteristics. This research is motivated by epidemiological and experimental studies on the tensile failure mechanics of the spine.

While air bags save thousands of lives each year, their effectiveness in protecting the pediatric passenger appears critically deficient and may actually be harmful. From 1990 to 1999, 58% of all air bag related fatalities were children (1-to-16-years).[1] These 87 child deaths, when compared with adult fatalities, suggest unique mechanisms of injury and tissue failure tolerances based upon injury patterns. Neck injury patterns associated with air bag related fatalities in children suggest that tension may be one of the causal mechanisms for these injuries.[97] Only one other group has previously examined the mechanics associated with tensile loading of the pediatric neck.[169] Using a caprine (goat) model, Pintar and associates documented the failure mechanics of these specimens in tension. Based on these data, scaling factors were derived as a percentage of the adult properties. In their conclusion, Pintar et al. suggested an experimental effort using another animal model would aid the understanding of cervical spine tensile tolerance. Therefore, this cadaver baboon tensile tolerance experimentation fulfills this appeal and aids in advancement of injury criteria to determine safe limits of air bag inflation.

The application of quasi-statically collected experimental tolerance data to real-world events hinges on understanding the rate dependence of this tolerance data. Thus, a secondary investigation into the effects of various loading rates was performed. Many have investigated the effects of rate in ligaments and have found up to 3-fold increases in structural properties between 8-mm/sec and 2,500-mm/sec loading rates.[35, 167, 168, 210] Therefore, in an effort to most clearly understand the tolerance of the developing spine, a companion study was performed to elucidate the rate dependence exhibited by the spine.

4.2. METHODS

4.2.1. EXPERIMENTAL DESIGN

The objective of these experiments was to document the relationship between tissue tolerance and spinal development by measuring the compressive and tensile ultimate failure load, strain, and strength of maturing vertebral bodies, FSUs and spinal segments.

A secondary goal of this experimental effort was to document the effects of gender, spinal level, and loading rate during these failure experiments. Using the cadaver baboon model, destructive tests were performed on various tissues and their tolerance responses were measured. These experiments addressed the following research hypotheses:

1. *As the spine develops, the vertebral body compressive tolerance (ultimate failure load and strength) increases.*
2. *The compressive tolerance (ultimate failure load and strength) of spinal segments increases with maturity.*
3. *The failure response (tolerance) of the cervical spine in tension demonstrates increasing ultimate failure load and strength with development.*
4. *Compressive tolerance of vertebral bone varies by gender in the developing spine.*
5. *The compressive tolerance of the maturing cervical spine (2-FSU constructs) is different for different cervical spine levels.*
6. *The tensile tolerance of the developing cervical spine (1-FSU) is unique to the cervical spine level investigated.*
7. *The tensile tolerance of single functional spinal units of a similar age increases with increasing loading rate.*
8. *The ultimate tensile strain of developing cervical FSUs does not vary as a function of developmental age.*

4.2.2. SPECIMEN PREPARATION

Fifty-nine, fresh frozen cadaver baboon spines were obtained through the Washington Regional Primate Research Center. These tissues were handled, screened, aged, and prepared similarly to those in the previous chapter (3.2.2). The two sub-sets of these specimens for the vertebral body experiments (N=22) and the single functional spinal unit tests (N=18) remained the same from the previous functional characteristics testing. Their preparation for experimentation was also the same. A sub-set of twenty, 20 male specimens across the developmental spectrum was prepared for 2-FSU compression experiments. The complete experimental matrix is presented for each specimen in Appendix C. These specimens ranged in age from 1-to-25-human equivalent years. Each specimen was dissected into the following 2-functional spinal unit segments: Oc-C2, C3-C5, C6-T1. Following dissection each of these specimens was cross-pinned and

potted in poly-methylmethacrylate as was performed on the single FSU preparations. The same potting cups were used and alignment was set such that the middle vertebra's endplates were parallel to the potting cup surface. This fixation procedure facilitated the direct loading of the two intervertebral discs and the middle vertebra in compression.

A final sub-set (N=8) of these specimens was selected to be all male aged 10 ±0.6-human equivalent years. This group of specimens was selected to evaluate the effects of loading rate on the tensile mechanics of the spine. Thus, these specimens were dissected into single functional spinal units (Oc-C2, C3-C4, C5-C6, and C7-T1) and prepared exactly as the other 1-FSU test specimens. Again, upon complete preparation of each spinal sample, they were bathed in saline, wrapped in towels, sealed in a plastic bag, and fresh frozen at -20° until testing.

4.2.3. EQUIPMENT AND INSTRUMENTATION

The inputs to our developing tissues are applied using a high-rate or low-rate servohydraulic test frame. The responses of these tissues are measured using a linear displacement transducer, video analysis (two-dimensional displacements) and a six-axis load cell. Some of these devices have been previously discussed (3.2.3); however, those that have not will be presented here to give complete descriptions of all tools utilized in these tissue tolerance tests.

A custom-built high-rate servohydraulic test frame was used to generate the high-rate compressive loading and high-rate tensile loading (***Figure 35***). This 15-kip capacity test frame was manufactured by MTS (MTS Systems Corporation, Eden Prairie, MN) and given the custom model number 318.10S. The frame was based on an MTS 810 single-axis test frame with the hydraulic ram mounted in the crosshead. This ram's 12-m/sec maximum velocity is achieved using a 10-gallon accumulator pack, high-rate manifold, and high-rate valve. This system was digitally controlled using TestStar™ II software and hardware (MTS Systems Corporation, Eden Prairie, MN). The frame maintains PIDF feedback closed-loop control for stroke rates up to 3-m/sec but can perform open-loop 'one shot' tests up to 12-m/sec. The tuning parameters for this system were set

specifically for each loading rate. The compression testing (closed loop) utilized the following parameters: P = 0.5635, I = 0.0550, D = 0, and F = 0. These optimized the displacement to little overshoot with good velocity characteristics. The tensile tests were performed open loop and needed only to have a fast dynamic response getting up to constant velocity. These tensile tests thus used the following tuning parameters: 0.5, 5 and 50-mm/sec (P = 1.000, I = 0.074, D = 0, and F = 0), 500-mm/sec (P = 0.61, I = 0.74, D = 0, and F = 0), and 5000-mm/sec (P = 0.61, I = 0.74, D = 0.001, and F = 0).

Figure 35. *High-Speed MTS (318.10S) and Control Computer. This picture shows the high rate MTS (input) and the instrumentation tower (output measurement) with the personal computer controlling the event in between.*

This high-rate MTS contains a linear displacement transducer mounted on the hydraulic ram in the frame's crosshead (model 244.11 LVDT, S/N 1028919, MTS, Eden Prairie, MN). This LVDT was calibrated based on a National Institute for Standards and Technology traceable standard (Part # 115682-01A) and has a resolution of 0.0074-mm.

Experiments performed on the high-rate frame were documented using a high-speed video camera, Kodak Ektapro RO-1000 (Eastman Kodak Company, Motion Analysis Systems Division, San Diego, CA). This camera records at 1000-frames/sec in 24-bit color with a resolution of 512 x 384. Markers placed on each specimen can be tracked using WINanalyze software and the 2-dimensional displacements resolved.

A low-range six-axis load cell was described in the earlier instrumentation section; however, the failure tests in this experiment exceed that cell's range. Thus, a high-range six-axis load cell was used for the dynamic experimental testing. This six-axis load cell (Model 4526, Robert A. Denton, Inc., Rochester Hills, MI) is based on the same design as the low-range version. Since this cell is designed for use in dynamic simulations of automobile crashes (Hybrid III neck load cell), its design has been proven to have adequate dynamic fidelity in years of use in automotive crash testing. Thus, this load cell design was deemed to be more than adequate for the purposes of this project's testing.

This high-range load cell has the following ranges: F_x = ±4,448-N, F_y = ±4,448-N, F_z = ±11,120-N, M_x = ±338.9-N-m, M_y = ±338.9-N-m, and M_z = ±203.4-N-m. Calibration of this sensor is traceable to the National Institute of Standards and Technology (#F538145KJ2799) and has a maximum total uncertainty for any channel of 0.02% (F_x = ±0.9-N, F_y = ±0.9-N, F_z = ±2.2-N, M_x = ±0.07-N-m, M_y = ±0.07-N-m, and M_z = ±0.04-N-m). The schematic of the force and moment transformations into vertebral coordinates for the low-range six-axis load cell applies for this cell as well (***Figure 9***). Further, this load cell is conditioned using the same strain gauge conditioner with amplification and CFC-1000 filtering. Thus, this load cell meets current standards for dynamic testing of biologic tissues in high-rate injury events.

All of these sensors were sampled using the previously described LabVIEW data acquisition hardware and software on personal computers. The dynamic events of the 2-FSU compression and single FSU high-rate tension tests required sampling at 40-kHz to fulfill the Nyquist criteria. The quasi-static vertebral body and FSU tension tests had their sensors sampled at 200-Hz. These instrumentation and data acquisition methods

generated data sets with excellent dynamic content for the accurate characterization of the tolerance of the tissues measured.

4.2.4. PROTOCOL

Four distinct experimental protocols were utilized to evaluate the tolerance of the developing spine. As before, every specimen is radiographed anterior/posterior and lateral to make spinal measurements. Once all of the preliminary measurements and preparations were made the specimens were ready for testing. Prior to testing each specimen was completely thawed for two hours and kept hydrated at room temperature until testing.

The twenty-two specimens allocated for vertebral body compressive failure testing received the following protocol. Once placed into the MTS loading frame, the ram was lowered to create contact with the specimen. Then, a compressive ramp displacement at 1-mm/sec was applied to 75% strain (greater than the mean failure strain of bone).[91, 139, 147] The load (MTS load cell) and displacement (MTS LVDT) across the vertebral body were recorded during each failure test at a sampling rate of 200-Hz.

The single FSU tensile experiments were performed on the MTS using the fixturing shown in ***Figure 11***. Each specimen was loaded to failure by a tensile ramp displacement at 1.0-mm/sec. This displacement profile left each end of the specimen in one chamber of the tensile loading apparatus and the soft tissues between severed. The resulting load-displacement profile was recorded at 200-Hz enabling the full characterization of the failure mechanics.

Single functional spinal unit tensile tests were performed at varying loading rates to examine the rate-effects on the tensile tolerance of the tissues. Eight specimens of similar age were divided into their functional spinal units and then each FSU was randomized to a loading rate group. The loading rates investigated were 5-mm/sec, 50-mm/sec, 500-mm/sec, and 5,000-mm/sec. This examination of loading rate spanning four orders of magnitude covers the range of loading rates that might be expected from static activities to highly dynamic airbag interactions. Since each specimen was

randomly assigned a loading rate, inter-specimen variability should be diminished and the effect of loading rate alone should be able to be distinguished.

This experimental protocol involved the use of a custom yolk assembly (designed by Jarrod Carter, Ph.D.) for the application of dynamic tensile loads to the cervical FSUs (***Figure 36***).[24] This setup enabled the MTS ram to ramp up to speed prior to loading the

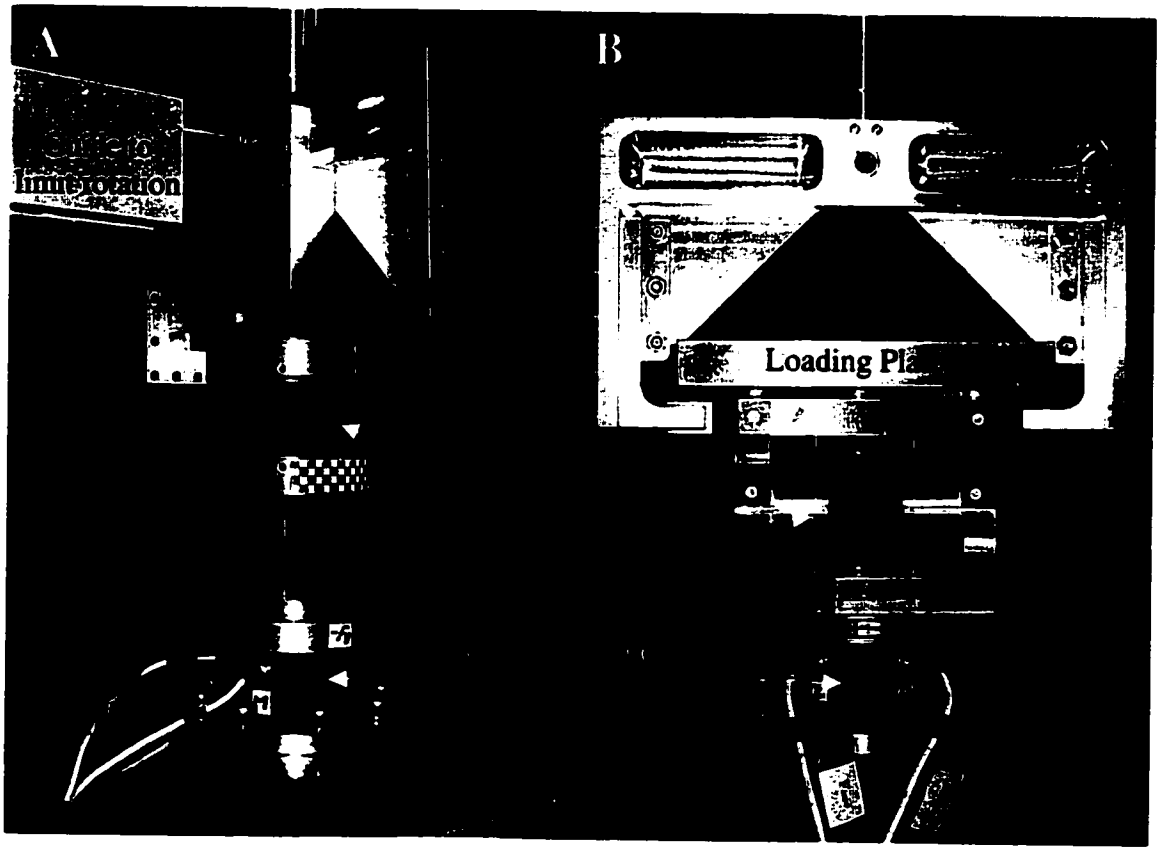

Figure 36. *Experimental Test Set-Ups for Dynamic Testing in Compression and Tension. (A) Compressive assembly demonstrates the ram attached a to yolk assembly supplying compressive displacements to the specimen within the circular cups. The high-range six-axis load cell is shown beneath the specimen rigidly attached to the MTS table. (B) Tensile testing apparatus with a specimen shown in the tensile chambers prior to testing. The upper yolk assembly ramps up to constant velocity and then contacts the loading plate attached to the superior specimen chamber. The constant loading rate event is monitored by the six-axis load cell mounted beneath the specimen.*

specimen. In this way, each specimen was loaded at a constant velocity to failure. The six-axes of load and linear displacement were measured for these experiments at the following frequencies: 5-mm/sec (500-Hz), 50-mm/sec (1.0-kHz), 500-mm/sec (50.0-kHz), and 5000-mm/sec (100.0-kHz). High-speed video documented the test for visualization of the tissue failures.

Following the vertebral body and 1-FSU experiments, an examination of 2-FSU constructs was performed to elucidate the compressive mechanics of the developing spine. These experiments were performed using the high-rate servohydraulic MTS providing a controlled dynamic axial compressive displacement to each specimen. This setup contained a fixed-fixed end-condition where the axial load vector was approximately aligned (±3-mm) with the posterior longitudinal ligament of each specimen (***Figure 36***). After the specimen was loaded into the inferior cup of the testing apparatus, the MTS ram was lowered to contact the superior potting cup. With the specimen now coupled to the MTS ram, the axial displacement haversine profile was imparted to the specimen to produce displacements between 8 and 16-mm (60% strain) with a 15-msec pulse duration. These experimental tests loaded the 2-FSU constructs to failure at approximately 0.9-m/sec and the resulting six-axis loads and linear displacements were recorded at 40-kHz. Again, this event was documented on high-speed video at 1000-frames/sec.

4.2.5. DATA REDUCTION

The dynamic events investigated herein required filtering to remove high frequency noise. A forward-backward 4-pole Butterworth low-pass digital filter was applied to all of the data with a cutoff frequency of 1-kHz. This filtering provides a data set which is unaltered in its time domain (phaseless) and has excellent response. This filtering method meets the SAE J211-1 specifications for a CFC 600.

After filtering, the load data were transformed in the same way as described in the previous chapter (3.2.5.) so that the loads correspond to the centroid of the disc (1-FSU) and the centroid of the inferior disc (2-FSU) of each specimen. Once the load data were

transformed, load-displacement plots were made and these data normalized to provide a stress-strain curve as well. The ultimate failure load and ultimate strength were computed from the load-displacement and stress-strain curves respectively. For the tensile data, these measures were the maximal force and stress carried by the specimen. The vertebral compression ultimate failure load and strength were then established using a 2-percent offset method (based on the original specimen height) from the load-displacement and stress-strain relationships respectively. Finally, the 2-FSU compression data was evaluated for the first significant reversal in load and stress where the peaks prior to these reversals denote the ultimate failure load and strength.

4.2.6. DATA ANALYSIS

Utilizing the data sets of load-displacement (F-x), stress-strain (σ-ε), stiffness (k), elastic modulus (E), and relaxation time constant (τ), the stated hypotheses were statistically evaluated. Each hypothesis was examined independently below.

Hypothesis 1. As the spine develops, the vertebral body compressive tolerance (ultimate failure load and strength) increases. The null hypothesis is that there is no change in the compressive failure load or strength of vertebral body specimens for different developmental ages (H0: $\beta = 0$, H1: $\beta > 0$, where β is the slope of the failure load or strength regressed by age). The ultimate load and strength were regressed by skeletal maturity (grouped and blocked by gender) and fit with a least-squares line to approximate the relationship. A statistical F-test for regression analysis was performed to determine if the slope of the regression was statistically significant.[178]

Hypothesis 2. The compressive tolerance (ultimate failure load and strength) of spinal segments increases with maturity. The null hypotheses are that there are no changes in the compressive ultimate failure load or strength of 2-FSU spinal segments of different developmental ages (H_0: $\beta = 0$, H_1: $\beta > 0$, where β is the slope of the ultimate load or strength regressed by age). The ultimate failure load and strength were regressed by skeletal maturity (blocking by spinal level) and fit with a least-squares line to

approximate the relationship. A statistical F-test for regression analysis was performed to determine if the slope of the regression was statistically significant.

Hypothesis 3. The failure response (tolerance) of the cervical spine in tension demonstrates increasing ultimate failure load and strength with development. This hypothesis was tested using the same techniques described for Hypothesis 2.; however, the 2-FSU compression data was replaced with the single FSU tension failure data.

Hypothesis 4. Compressive tolerance of vertebral bone varies by gender in the developing spine. The null hypothesis is that there are no differences in the compressive failure load carried or strength between maturing males and females (H_0: $\zeta_m = \zeta_f$, H_1: $\zeta_m \neq \zeta_f$, where ζ_m (male) and ζ_f (female) are the slope of the ultimate force and strength regressed by age). A factorial analysis of variance (ANOVA) was used to examine each measure with and without gender separation to establish if significant gender differences existed using development as a cofactor.

Hypothesis 5. The compressive tolerance of the maturing cervical spine (2-FSU constructs) is different for different cervical spine levels. The null hypotheses are that there are no differences in the failure load carried or strength of the 2-FSU constructs between each of the spinal levels (H_0: $\vartheta_{OC2} = \vartheta_{C35} = \vartheta_{C6T1}$, H_1: $\vartheta_{OC2} \neq \vartheta_{C35} \neq \vartheta_{C6T1}$ where $\vartheta_{(level)}$ denotes the slope of the ultimate force and strength regressed by age). A factorial ANOVA was utilized to examine differences between levels within each specimen and the interaction of development and spinal level to determine if specific spinal levels develop their functional biomechanical characteristics at different rates. Individual contrasts were performed using the Tukey method to more clearly evaluate each spinal level. The Tukey honest significant difference test uses the Studentized range statistic making all pairwise comparisons such that the experiment-wise error rate is set at the error rate for the collection of comparisons. Thus, this method for pairwise analysis decreases the probability of a Type I error resulting in favorable statistical power characteristics.[56]

Hypothesis 6. The tensile tolerance of the developing cervical spine (1-FSU) is unique to the cervical spine level investigated. This hypothesis was tested using the same statistical methods as those performed for Hypothesis 5. The only difference was the single FSU data in tension was used instead of the 2-FSU compressive data.

Hypothesis 7. The tensile tolerance of single functional spinal units of a similar age increases with increasing loading rate. The null hypothesis is that there is no change in the tensile failure load or strength of intervertebral tissues for different rates of loading (H0: $\beta = 0$, H1: $\beta > 0$, where β is the slope of the failure load or strength regressed by loading rate). Analysis of variance techniques will elucidate if a loading rate effect exists and post hoc analyses will reveal specific differences between loading rates. The sample size of this data set limits the number of statistical tests able to be performed with confidence. The ANOVA contains only 20 residual degrees of freedom after rate and spinal level main effects and the interaction were investigated.

Hypothesis 8. The ultimate tensile strain of developing cervical FSUs does not vary as a function of developmental age. The null hypothesis is that there is a relationship between failure strain for single functional spinal units in tension and developmental age(H0: $\beta = 0$, H1: $\beta > 0$, where β is the slope of the failure strain regressed by age). A statistical F-test for regression analysis was performed to determine if the slope of the regression was statistically significant.

Significance for all of the above analyses was established at an alpha level of 0.05.

4.3. RESULTS

The experimental results for vertebral body, 1-FSU, and 2-FSU failure tests reveal clear relationships between spinal development and tolerance. Each of the plots comparing a structural or material property by developmental age was generated from individual load-displacement and stress-strain curves for each tissue tested. The failure characteristics were determined from these curves in a similar fashion for ultimate failure load and ultimate strength (***Figure 37***).

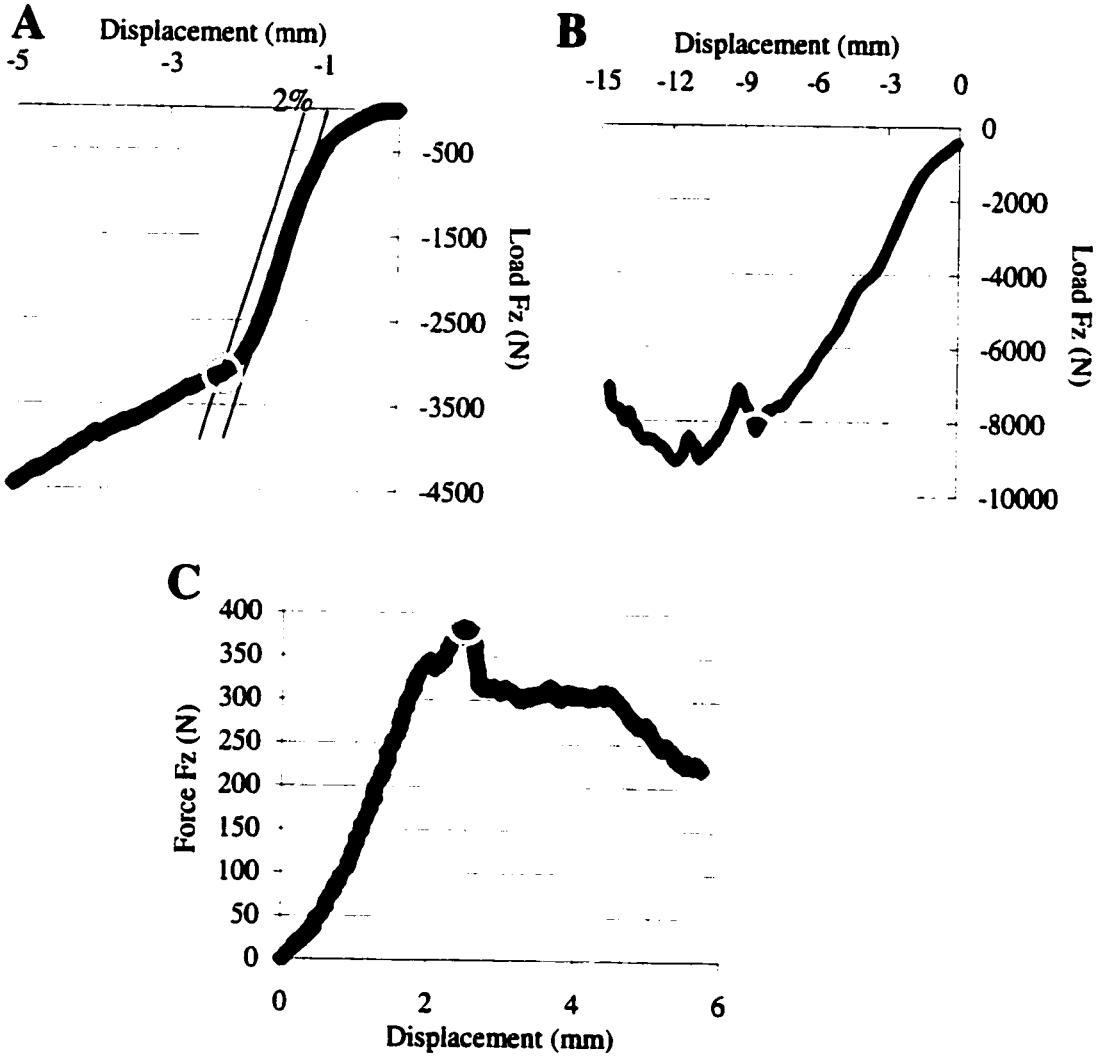

Figure 37. *Sample Failure Load-Displacement Curves Demonstrating the Ultimate Failure Load. (A) T9 vertebral body compression test utilized a 2% offset method to determine the failure load. (B) The failure load for the 2-FSU tests was determined as the peak before an inflection point (drop in load). (C) Single FSU tensile tests utilized the largest load carried by the specimen as the ultimate failure load.*

4.3.1. COMPRESSION TOLERANCE

This section presents the data from the T9 vertebral body compression tests and the 2-FSU cervical spine compression tests. The results of the vertebral body compression experiments demonstrate significant changes in the ultimate failure load with development ($p = 0.0001$) (***Figure 38***). Also, the normalized data for the ultimate strength

of the vertebral body specimens increases with spinal maturation ($p = 0.017$) (***Figure 39***). The strength (ultimate stress) of these vertebrae is not as strongly correlated with age as the non-normalized failure load data. This suggests that the cross-sectional area (normalizing factor) plays an important role in the ability of the isolated vertebrae to carry load.

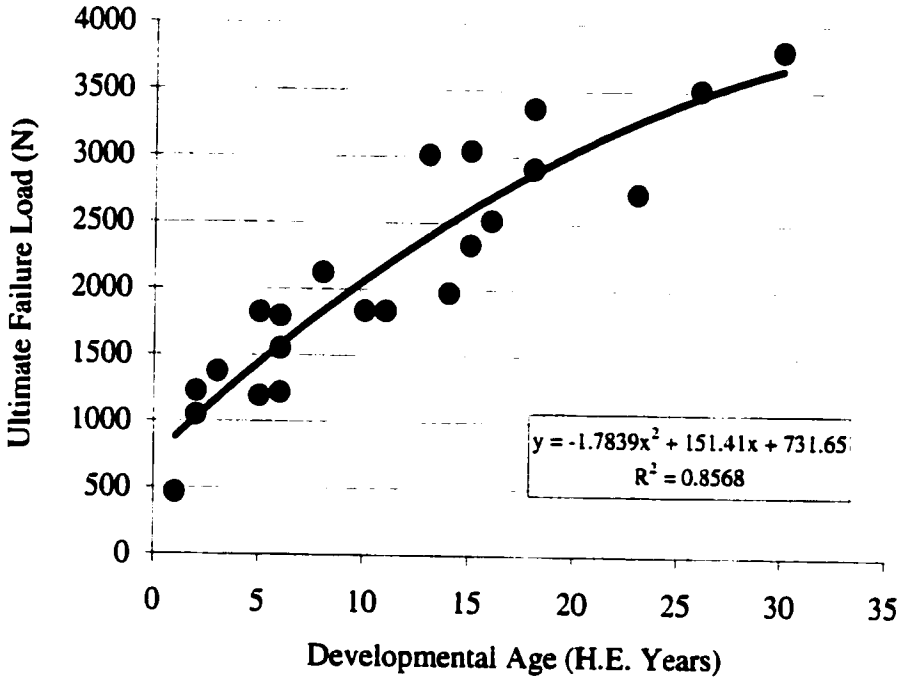

Figure 38. *Ultimate Compressive Failure Load of the Vertebral Body as a Function of Age. This plot demonstrates the 2nd order polynomial relationship between a structural failure characteristic and maturation.*

Separation of these vertebral body compression data by gender yields very interesting results. First, ***Figure 40*** depicts the same data as in ***Figure 38***; however, the genders are broken out. Vertebral body ultimate failure load is significantly different between genders ($p = 0.041$) and the data become much tighter with gender separation. Next, this same vertebral body failure load data is plotted against each specimen's cross-sectional area to see if the relationship between failure load and size was similar between the genders. ***Figure 41*** clearly demonstrates that females can carry much larger loads for the same vertebral body size compared with males. This plot suggests that the intrinsic

material properties differ by gender such that females achieve greater load carrying ability with the same volume of tissue (***Figure 42***). In fact, the compressive strength of the T9 vertebra is significantly related to development and also shows a weak distinction between males and females ($p = 0.040$) (***Figure 42***). An individual look at the tolerance of the T9 vertebra with and without gender separation provides a clear picture of the fit to a linear model and significance of development on vertebral tolerance (***Table 8***).

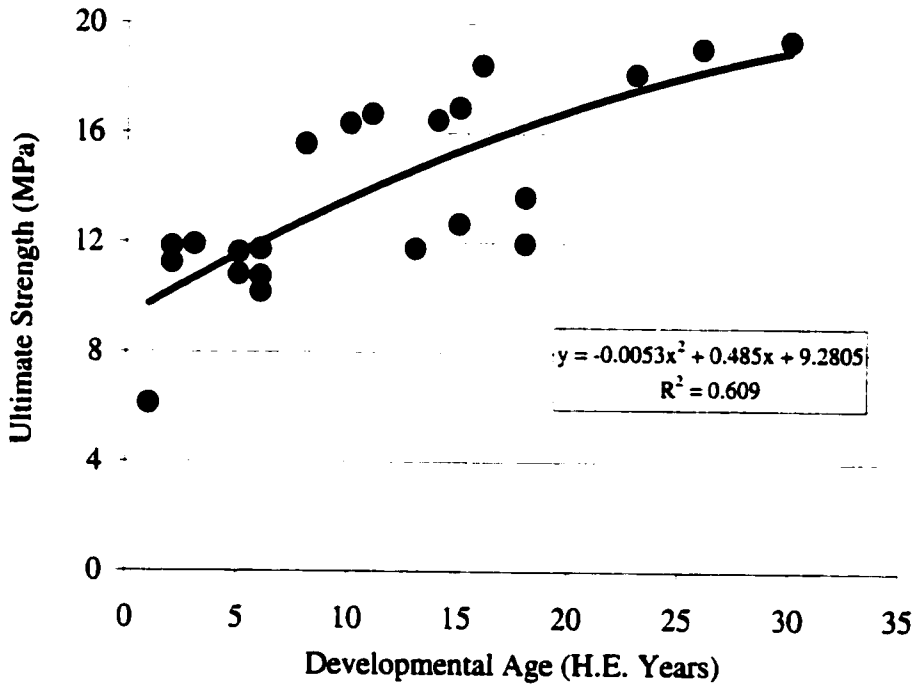

Figure 39. *Ultimate Strength of Developing T9 Vertebrae in Compression. While this fit is not as strong as for ultimate load, a dependence on maturation exists for material failure properties.*

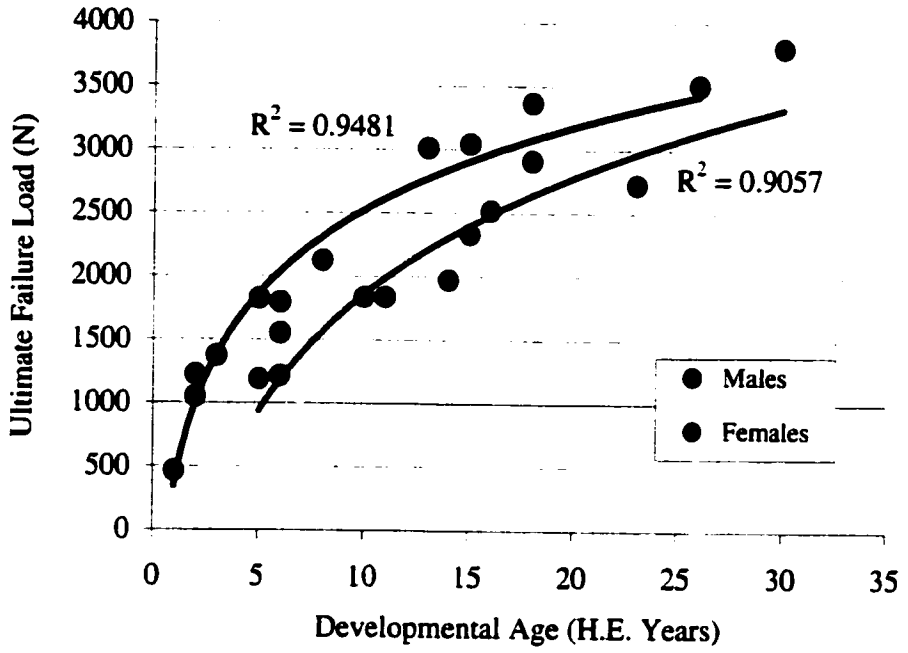

Figure 40. *Compressive Ultimate Failure Load of T9 Vertebrae as a Function of Age and Gender. Note that the r^2 values increase for both the males and females from the grouped data.*

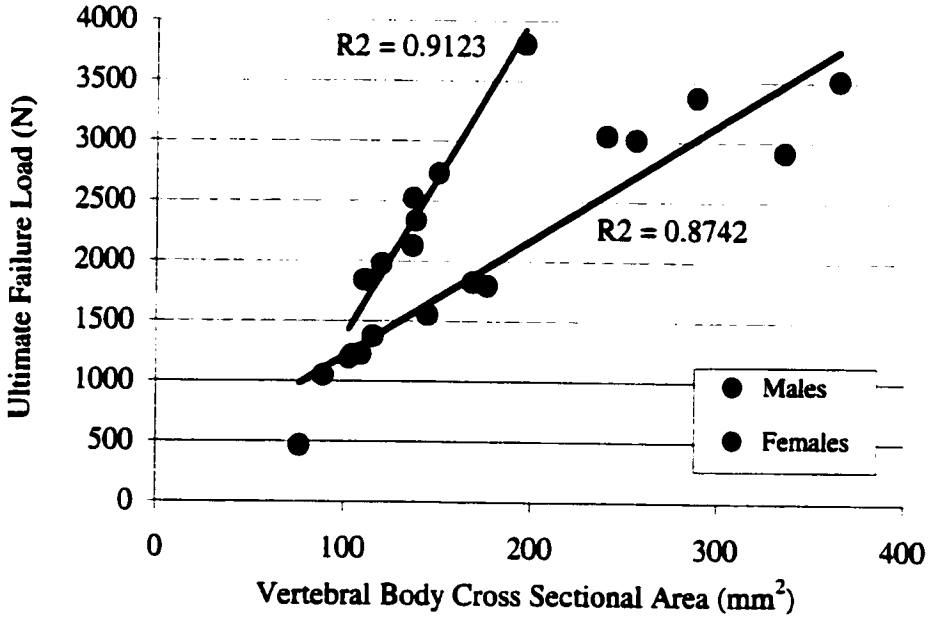

Figure 41. *Relationship Between Ultimate Failure Load and Vertebral Body Size. Females demonstrate a greater load carrying ability for the same size vertebra which suggests that their material properties are different.*

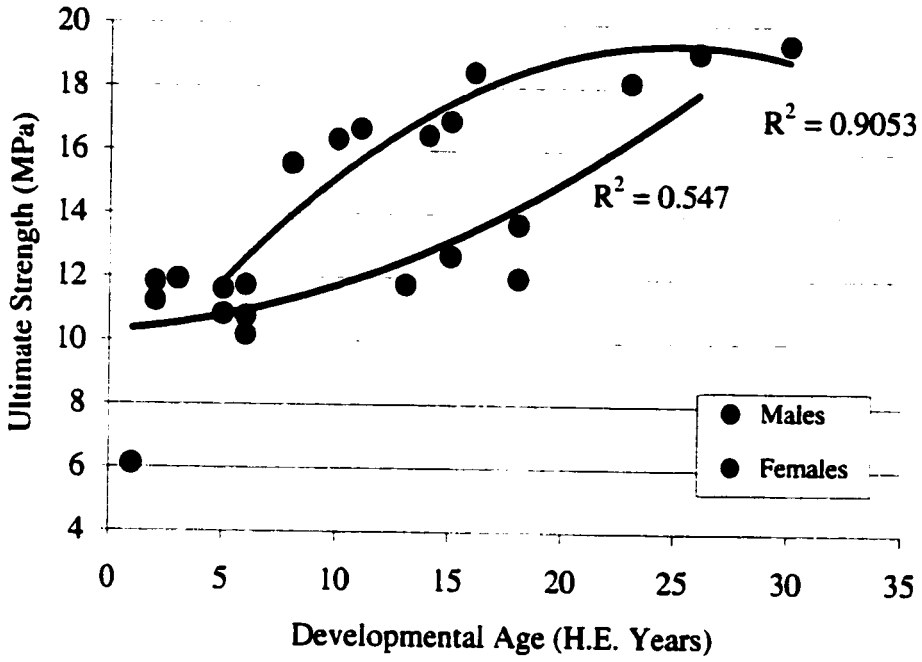

Figure 42. *Vertebral Ultimate Strength Throughout Development. These data also suggest that the female tissues develop larger material properties at a quicker rate than males.*

Table 8. *Linear Regression Fit and F-Statistic for Vertebral Body Compression Failure Data. All of the values are significantly correlated with developmental age, but not all are tremendously strong.*

	R	R^2	F	Sig.
Load Ult	.802	.643	36.07	0.0001 *
by Gender				
Strength	.541	.293	4.98	0.041 *
by Gender				

Next, the results for the compression testing on the 2-FSU test specimens will be presented. The input to each specimen varied in its amount of strain input, but the loading rate was within 0.75 to 1.00-m/sec. The displacement protocol included a haversine input and the specimen was to fail within the target velocities above. illustrates the displacement input to each specimen and a filtered differentiation of that data to provide the velocity profile.

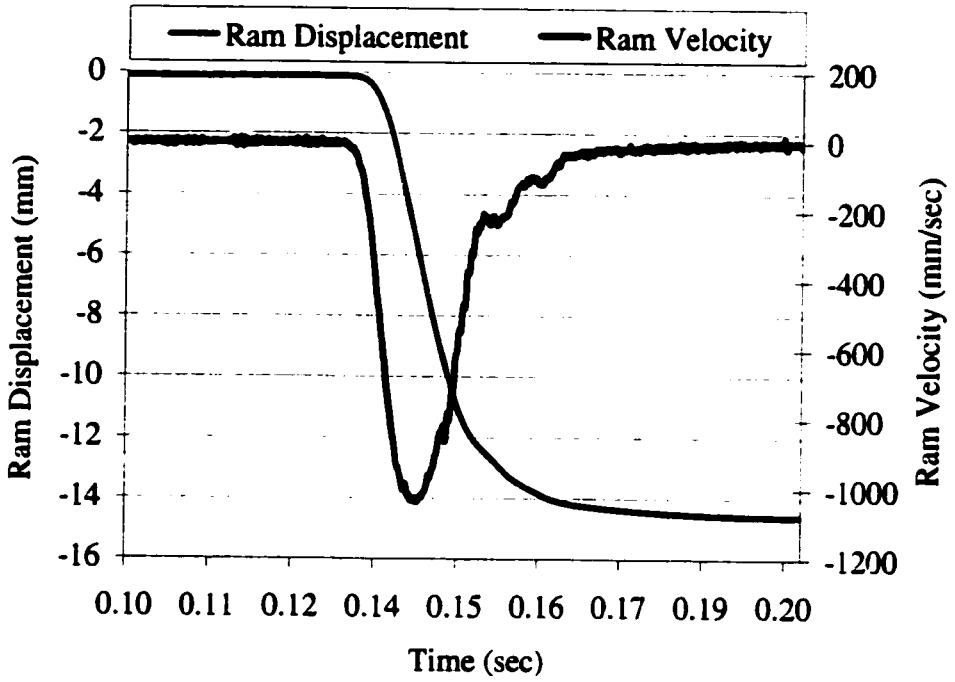

Figure 43. *2-FSU Compression Input Displacement and Velocity Profiles. This plot demonstrates the input to the system from which the tolerance of the developing cervical spine will be determined.*

The compressive mechanics of two functional spinal unit segments was found to have a distinct relationship with development and differing patterns between the levels of the cervical spine. Specifically, the compressive ultimate failure load ($r = 0.966$, $p < 0.0001$) and strength ($r = 0.916$, $p < 0.0001$) were significantly correlated with spinal development (***Figure 44*** and ***Figure 45***). Separation of the data by spinal level reveals further significant differences by level for both ultimate failure load ($p < 0.0001$) and strength ($p < 0.0001$). These data separated by spinal level (***Figure 46*** and ***Figure 47***) illustrate similar developmental growth functions in spite of their different magnitudes. Post-hoc comparisons between each of the spinal levels demonstrated each level to be significantly different from one another in both structural and material properties (***Table 9***).

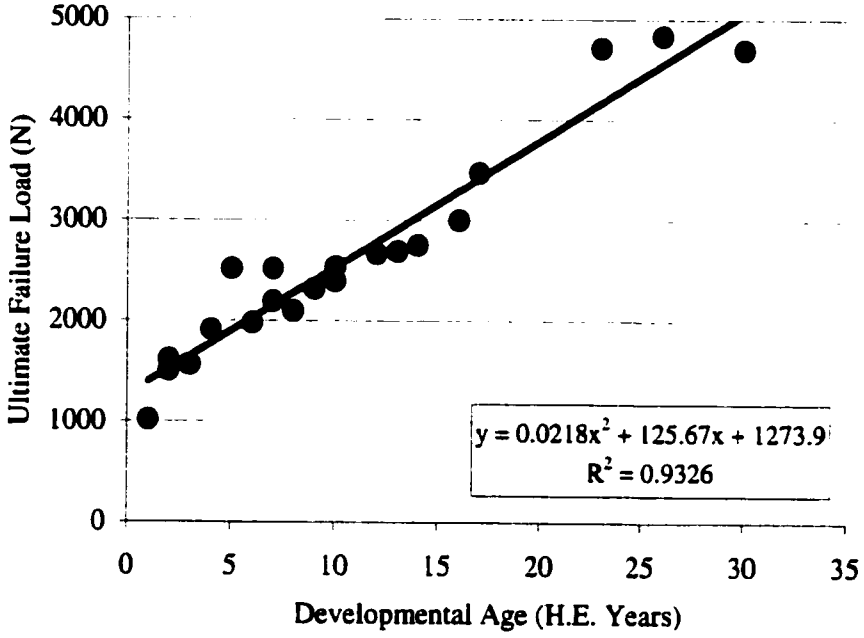

Figure 44. *Mean Ultimate Compressive Failure Load for Developing Two Functional Spinal Unit Segments. The relationship between ultimate load (average of all spinal levels for each specimen) and maturation is significant and shown fitting a 2nd order polynomial.*

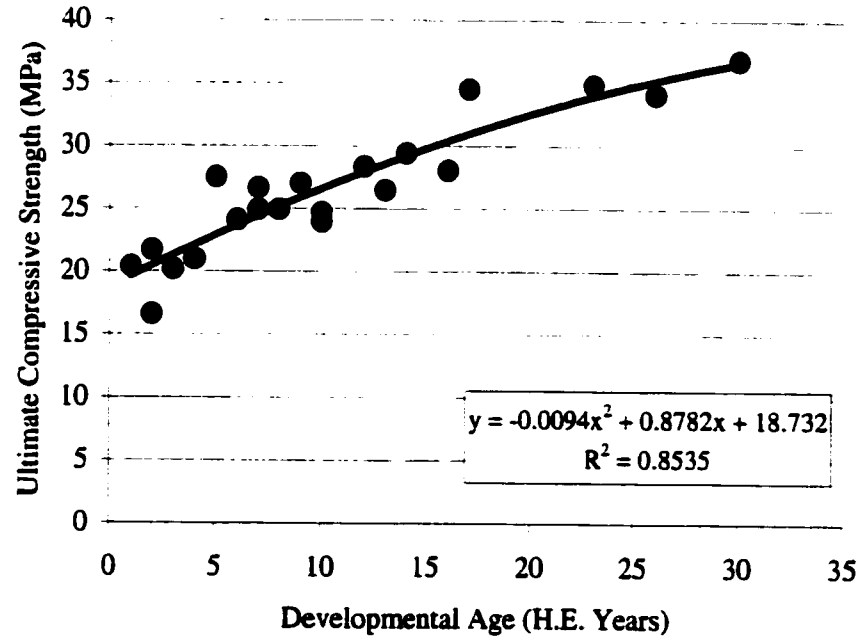

Figure 45. *Compressive Strength of Maturing Cervical 2-FSU Segments. These data depict the failure stress (strength) across development (2nd order polynomial fit).*

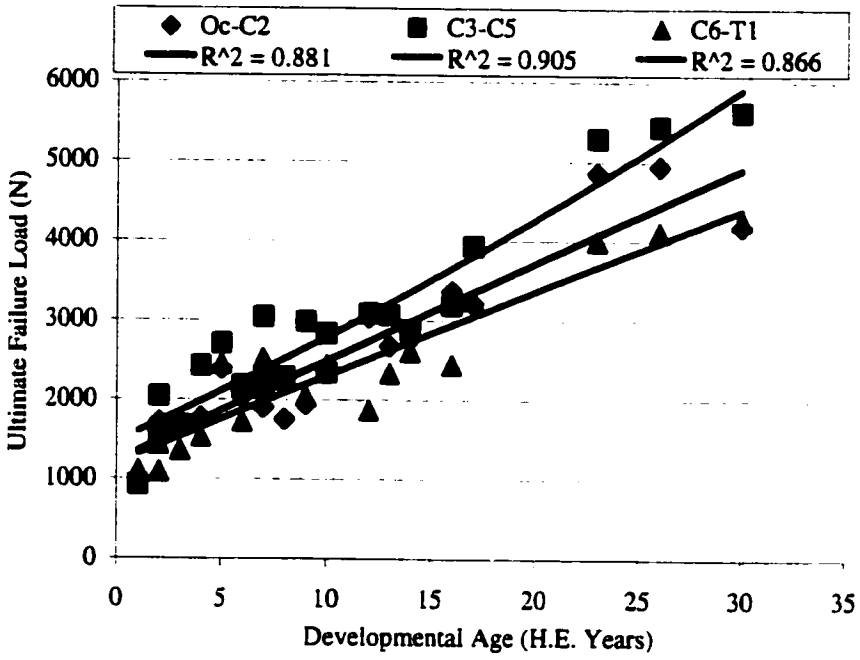

Figure 46. *Ultimate Compressive Failure Load of 2-FSU Constructs by Development with Level Separation. Each level was significantly different from each other and correlated with maturation (2nd order polynomial fits).*

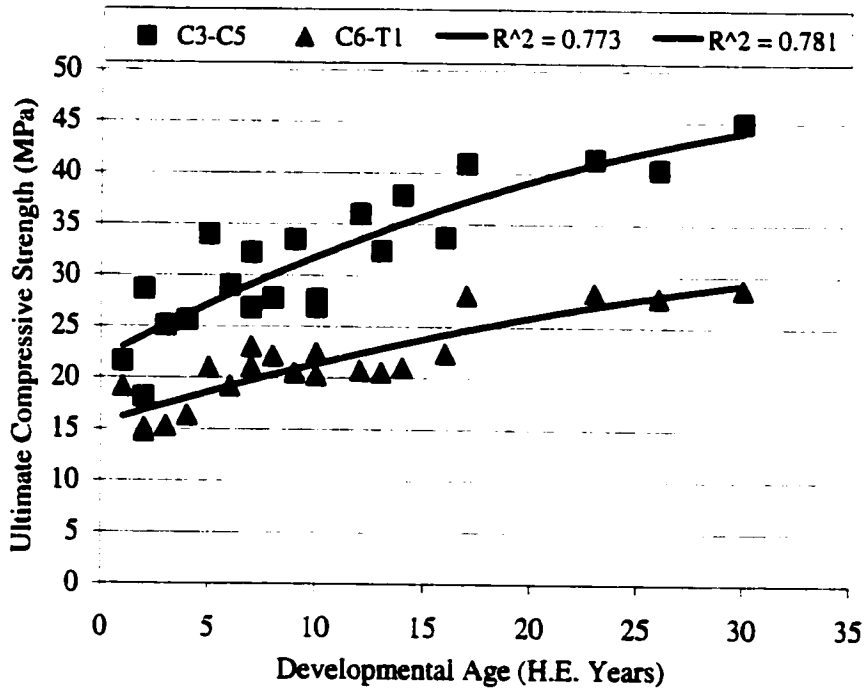

Figure 47. *Ultimate Compressive Strength of 2-FSU Segments Throughout Maturation. Significant spinal level differences are exhibited and each level is fit with a second order polynomial illustrating strength changes with skeletal development.*

Table 9. *Cervical Spine Compressive Tolerance Relationship with Skeletal Maturation. Linear regression statistical analyses depict the strength and significance of this relationship.*

		R	R^2	F	Sig.
Ultimate Failure Load	Oc-C2	.939	.881	133.3	<0.0001 *
	C3-C5	.950	.903	176.9	<0.0001 *
Strength	C3-C5	.870	.757	59.3	<0.0001 *

4.3.2. TENSION TOLERANCE

Cervical spine functional spinal units subjected to tensile displacement to failure demonstrate distinct relationships with development. The tensile ultimate failure load ($r = 0.805$, $p < 0.0001$) and strength ($r = 0.596$, $p = 0.001$) were statistically correlated with spinal maturation (***Figure 48*** and ***Figure 49***). An examination of the tensile strain at which each specimen failed revealed no significant correlation with spinal development ($r = 0.261$ $p = 0.119$) or by spinal level ($p = 0.277$). There appears to be a strain range which dictates failure throughout development, while the strength varies with age. Therefore, perhaps these tissues fail because of a strain-based tissue limitation rather than a stress-based limitation (***Figure 50***). An examination of the level related differences in cervical spine tolerance reveals that significant developmental differences exist for both ultimate carrying load ($p < 0.0001$) and strength ($p < 0.0001$) (***Figure 51***). Specifically, the ultimate failure load is different between the Oc-C2 and all other levels ($p < 0.006$), but no other differences exist. Contrasts on the strength of the C3-C4, and C5-C6, and C7-T1 levels reveal that every level is significantly different from each other ($p < 0.0001$). Finally, each level has been investigated independently for their correlation with skeletal maturation (***Table 10***).

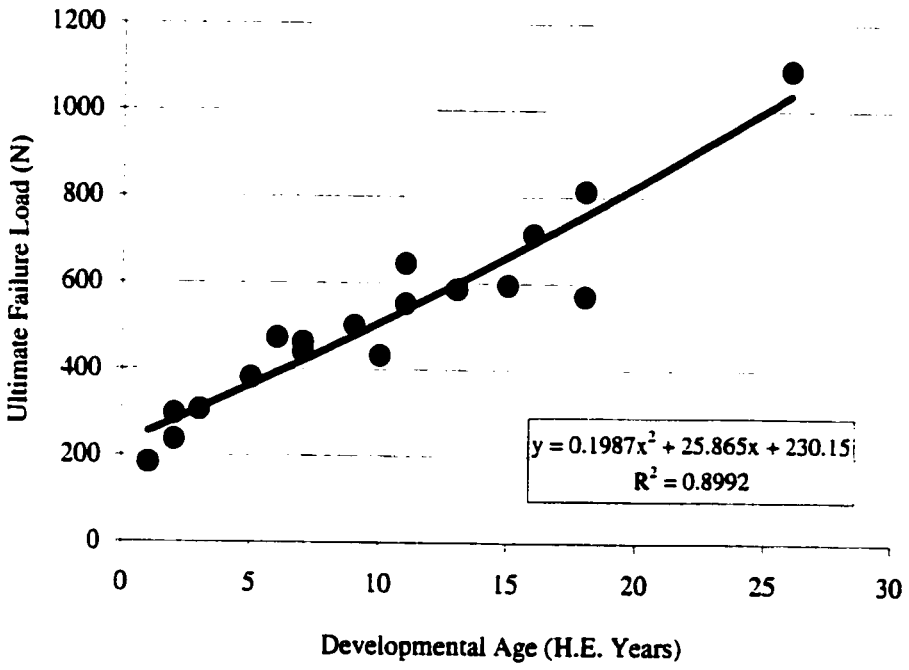

Figure 48. *Mean Ultimate Tensile Failure Load for Developing Functional Spinal Units. The relationship between ultimate load (average of all spinal levels for each specimen) and maturation is significant and shown here fitting a second order polynomial.*

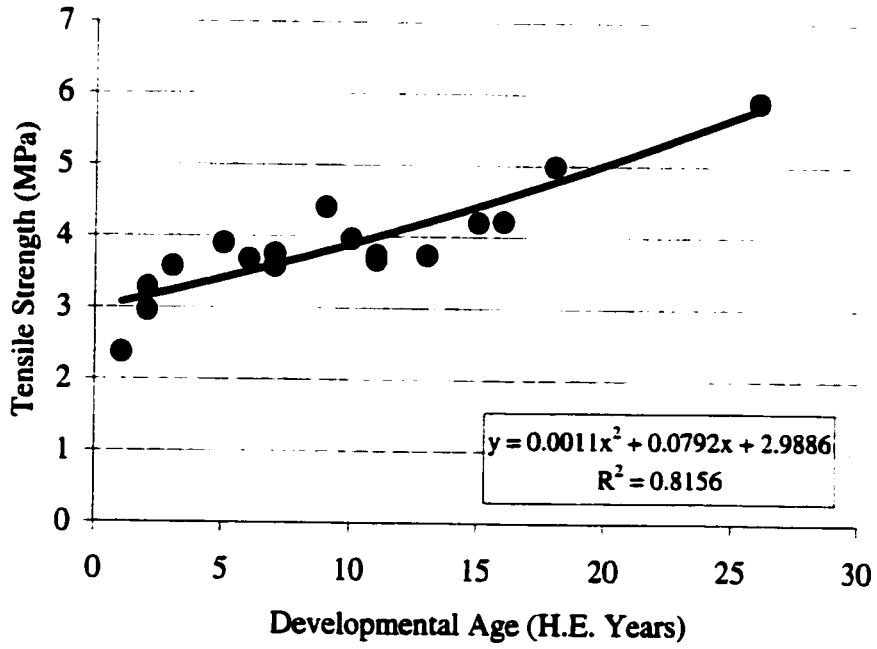

Figure 49. *Tensile Strength of Developing Cervical FSUs. These data depict the failure stress (strength) across development and are fit with a 2nd order polynomial.*

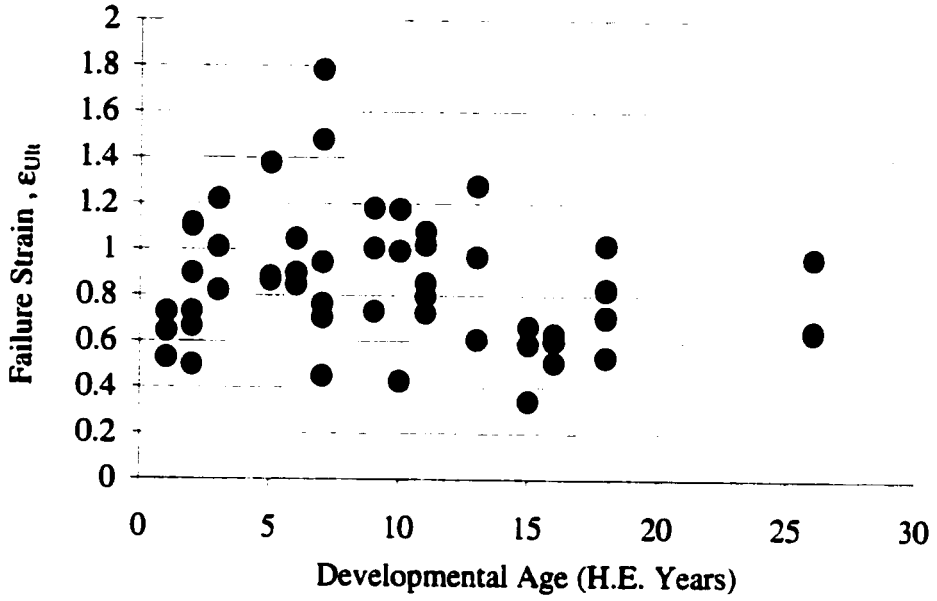

Figure 50. *Tensile Failure Strains as a Function of Developmental Age. The failure strains were determined as the strain at which the maximal load occurred. Strain at failure does not demonstrate any significant relationship with skeletal maturity.*

Table 10. *Linear Regression Analysis of Ultimate Failure Load and Strength by Age. Each cervical spinal level demonstrates a significant correlation with spinal development.*

		R	R^2	F	Sig.
Ultimate Failure Load	Oc-C2	.893	.797	62.92	<0.0001 *
	C3-C4	.857	.734	44.25	<0.0001 *
Strength	C3-C4	.789	.622	16.37	0.0002*

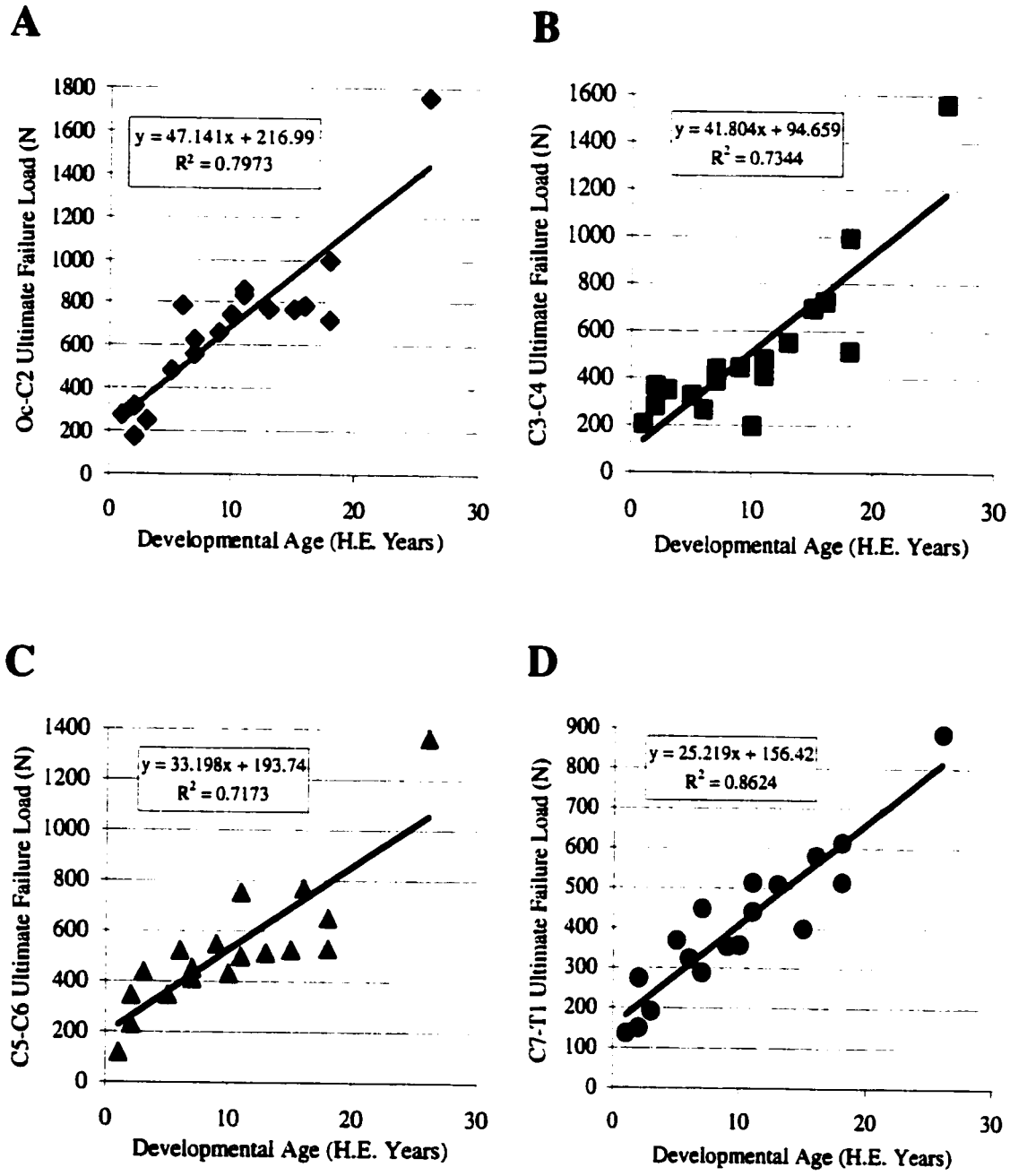

Figure 51. *Individual Cervical Functional Spinal Unit Ultimate Failure Loads of Developing Tissues. The cervical functional spinal units (A) Oc-C2, (B) C3-C4, (C) C5-C6, and (D) C7-T1 are regressed linearly with skeletal development.*

The results of the functional spinal unit testing across differing loading rates demonstrate clear rate effects. The tensile failure load ($p < 0.0001$) was significantly increased with

an increased loading rate (***Figure 52***). Within two orders of magnitude for loading rate there does not appear to be a difference in failure loads; however moving beyond two orders of magnitude does change the tolerance (***Figure 53***). The box plots (***Figure 53***) depict the 95% confidence interval around each loading rate mean failure load. Thus, examining the overlap of these boxes provides a way of testing differences between loading rates. Thus, tolerance of the cervical spine is dependant upon the loading rate as well as the maturity of the tissues. Finally, an investigation into the failure strain (mean = 1.072, standard deviation = 0.311) reveals no significant relationship with loading rate (ANOVA, p = 0.214). This suggests that functional spinal unit tissues fail due to a similar excessive strain rather than an excessive stress (***Figure 54***).

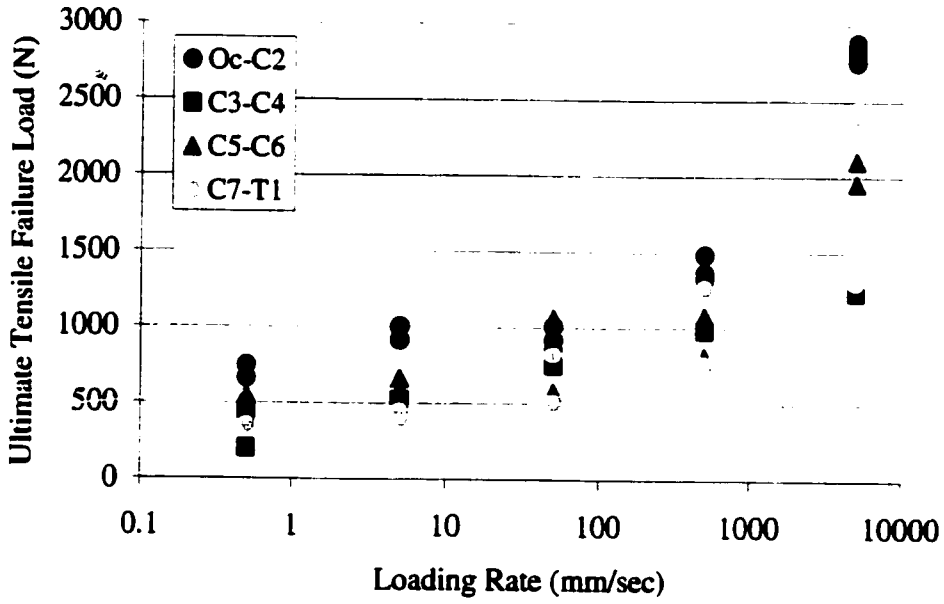

Figure 52. *Ultimate Tensile Failure Load by Loading Rate for 10-Year Old Male Cervical FSUs. Each specimen was randomized to a specific loading rate to remove inter-specimen variability. These data demonstrate significant loading rate effects ($p < 0.0001$) as well as suggests that different cervical spine levels behave differently at higher loading rates.*

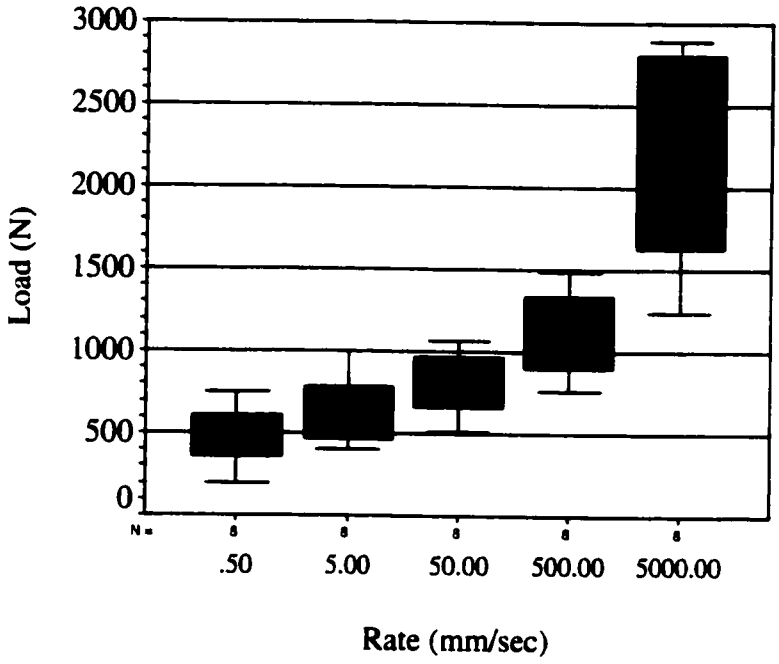

Figure 53. *Box Plot Demonstrating the Effects of Loading Rate on the Ultimate Tensile Failure Load. This box plot demonstrates all of the data between the brackets and 95% confidence intervals in red can be compared between loading rates for significant differences.*

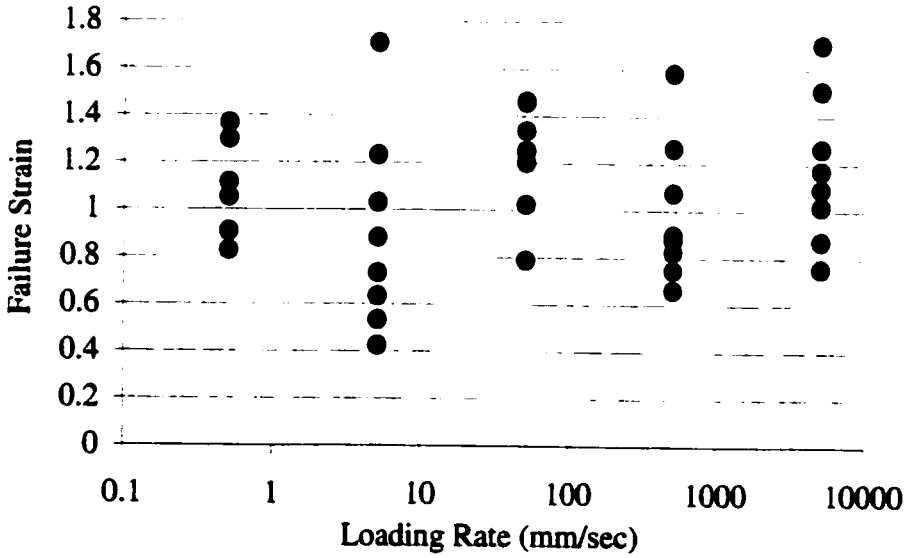

Figure 54. *Ultimate Failure Strains by Loading Rate. The ultimate failure strain was determined at the ultimate failure stress (strength) and demonstrates no correlation with loading rate.*

4.4. DISCUSSION

Understanding the tolerance of the developing spine is tantamount to modeling and preventing injuries to children and this data provides a glimpse, albeit with limitations, into these thresholds. This research defined the structural tolerance (ultimate failure load) and material tolerance (strength) of spinal tissues as a function of developmental age. Significant relationships were discovered between these mechanical characteristics and skeletal maturity. Further, secondary effects of gender, spinal level, and loading rate were also demonstrated by these results. This discussion will first examine each of the tested hypotheses and then explore the scaling of spinal injury thresholds and other interesting results uncovered in these spinal tolerance experiments.

Hypothesis 1. As the spine develops, the vertebral compressive tolerance (ultimate failure load and strength) increases. The null hypothesis is rejected since both the ultimate failure load ($p = 0.0001$) and strength ($p = 0.017$) with significantly positively correlated with development. The alternative hypothesis that the compressive ultimate load and strength increase with vertebral maturation is accepted.

Hypothesis 2. The compressive tolerance (ultimate failure load and strength) of spinal segments increases with maturity. Both the ultimate failure load ($p < 0.0001$) and the strength ($p < 0.0001$) were significantly correlated with spinal maturation through regression analysis. Thus, the null hypothesis is rejected and the alternate hypothesis that compressive failure tolerance is dependent upon age is accepted.

Hypothesis 3. The failure response of the cervical spine in tension demonstrates increasing ultimate failure load and strength with development. Since the ultimate tensile carrying load ($p < 0.0001$) and strength ($p = 0.001$) were significantly related to cervical FSU development, the null hypothesis is rejected. Therefore, the alternate hypothesis as stated above is accepted.

Hypothesis 4. Compressive tolerance of vertebral bone varies by gender in the developing spine. The null hypothesis is rejected. Thus, the alternative hypothesis is

accepted since both the ultimate load ($p < 0.0001$) and strength ($p = 0.041$) throughout maturation are different by gender.

Hypothesis 5. The compressive tolerance of the maturing cervical spine (2-FSU constructs) is different for different cervical spine levels. The analysis of variance tests and post-hoc contrasts revealed that every spinal level tested was significantly different from each other ($p < 0.038$). Thus, the null hypothesis is rejected and the alternative hypothesis is accepted, concluding that spinal level differences exist when comparing the compressive tolerance of 2-FSU constructs.

Hypothesis 6. The tensile tolerance of the developing cervical spine (1-FSU) is unique to the cervical spine level investigated. Analysis of variance techniques identified the developmental ultimate carrying load ($p < 0.0001$) and strength ($p < 0.0001$) to be significantly different by spinal level. Therefore, the null hypothesis is rejected and the alternative hypothesis is accepted. The contrasts identified specific levels which were unique, but not all were significantly different from one another.

Hypothesis 7. The tensile tolerance of single functional spinal units of a similar age increases with increasing loading rate. The null hypothesis is rejected since a loading rate effect was determined when measuring the ultimate failure load ($p < 0.0001$). Therefore, the alternative hypothesis is accepted; an increase in loading rate will increase the resulting tensile failure load of a functional spinal unit specimen. Descriptive statistics elucidate differences between specific loading rates as well.

Hypothesis 8. The ultimate tensile strain of developing cervical FSUs does not vary as a function of developmental age. Without a statistically significant relationship between the tensile failure strain and maturity, ($p = 0.119$) the null hypothesis is rejected. Thus, the alternative hypothesis that ultimate strain does not vary significantly by age is accepted and implicated strain as the means by which a tissue fails.

These hypotheses summarize the main findings of this research project, however, the tolerance of the developing spine is more complex than these basic hypotheses. The

vertebral body compressive ultimate load and strength were both significantly associated with spinal maturation. However, with gender separation the fit of these data was enhanced. Pictorially, ***Figure 40*** demonstrates the gender effect on vertebral compressive failure load. Gender appears to play an integral role in both the structural and material property generation throughout development. While the female vertebral bodies are smaller for similar age specimen, their constituent strength is larger for those same age specimens. This enhanced strength of female vertebrae earlier in development may be something to investigate as an indication or cause of earlier osteoporotic onset in females. The ultimate failure load for maturing male vertebrae is larger than that for females even though their functional biomechanics (stiffness) are indistinguishable. This suggests that male and female vertebrae respond mechanically very similarly until failure where the male has a higher injury tolerance. The adult vertebral compressive strength data collected here compares very well with the work by Mosekilde et al.[137] Further, the gender distinctions discovered have also been shown by others in the adult populace.[12, 45, 103, 120, 137] What has not been previously understood is the developmental course of tissue maturation and resulting biomechanics which lead to this gender disparity.

The 2-FSU compression tolerances demonstrated significant correlations with development as well as level specific differences. Spinal column maturation resulted in increasing ultimate failure load and to a lesser degree increasing strength. This again supports size (structural properties) over material properties as a predictor of spinal mechanics. The level distinctions observed show the lower cervical spine with smaller ultimate failure loads and strength compared with the middle and upper cervical spine. At the very young ages, however, the lowest load at failure is indistinguishable by level. This supports the epidemiological indicia that younger children sustain upper cervical spine injuries while older children and adolescents incur middle to lower cervical spine injuries. Finally, the 2-FSU compression tolerance data for the adult baboon demonstrate similar failure tolerances in the adult human.[24] While the failure load data should be slightly smaller for the baboons compared with the humans, that may be explained by the mixed male and female sample of humans throughout adulthood. Isolation of the youngest males in the research by Carter illustrates higher failure loads by as much as

26% compared with the baboon failure loads of this research. This adult comparison aids in the validation of the baboon model and supports the resulting pediatric tolerance criteria.

The tensile failure load tolerance was shown to be significantly associated with spinal maturation; however the failure strain was not altered by development or loading rate. This result suggests that intervertebral tissues fail as a result of excessive displacements or strains and not because of excessive loads of stresses. A number of studies have examined whether loads or displacements lead to tissue failure.[63, 170, 204] Tissue-specific results were found; however, ligamentous tissues demonstrated a strain dependence similar to that discovered in the experiments herein. In fact, a study of adult functional spinal units exhibited similar strain based results around 100% strain at failure.[211] Further, comparison of adult tensile failure loads discovered in these experiments with human adult tensile failure loads reveal similar yet slightly smaller failure loads for the adult baboon.[140, 211] Since the adult baboon is smaller than the adult human, these results support the baboon model as a predictor of pediatric tensile tolerance.

An examination of the developing cervical spine by level reveals very different failure characteristics from the upper to lower cervical spine. ***Figure 55*** demonstrates age and level differences in the ultimate failure load for single functional spinal units in tension. These data depict from a tolerance perspective that which was seen epidemiologically (***Figure 4***). If a similar load were applied to each functional spinal unit in the spine until one failed, the FSU having the lowest ultimate failure load would be the most susceptible to injury. Thus, in each age group except for the youngest, the lower cervical spine C7-T1 would be the most susceptible to injury. For the 3-year-old age group, there was an indistinguishable difference in failure load between the highest (Oc-C2) and lowest (C7-T1) level, suggesting an equivalent risk for tensile failure. These tensile results are consistent with the compression experiments as well as previously reported injury data. Together the tension and compression spinal level tolerance data may help to explain upper cervical spine injures in the younger pediatric age range.[123] To date though level based tolerance criteria is not available or utilized in modeling efforts to minimize injury.

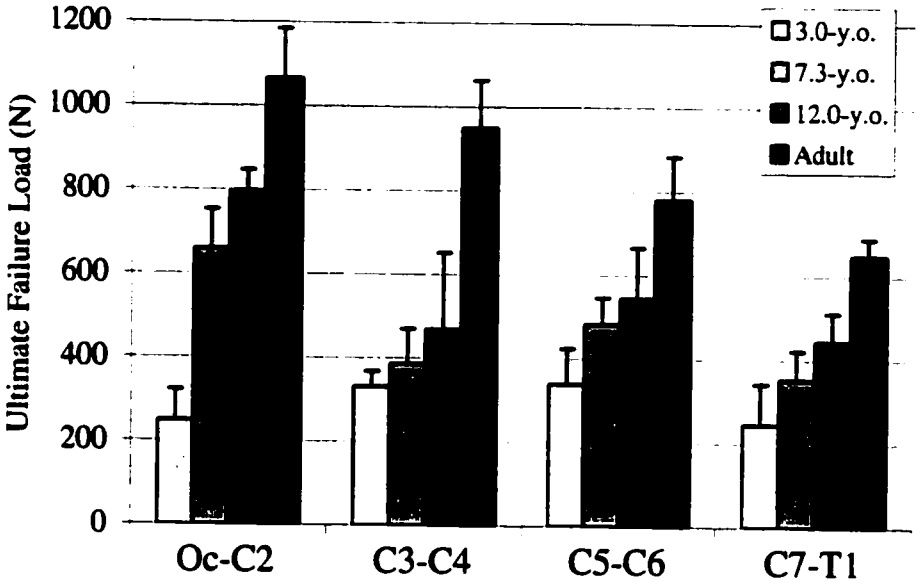

Figure 55. *FSU Tensile Ultimate Failure Load by Age and Spinal Level. These data are grouped to demonstrate level-related changes in development. Each bar is the mean of 4 specimens except the 12.0-y.o. bars contain 5 samples.*

4.4.1. COMPRESSION AND TENSION SCALING RELATIONSHIPS

The tolerance data collected herein was scaled to the adult values so that the human pediatric tolerance may be predicted from human adult data. These scaling factors are again based upon the second order fit equations explaining each property (***Table 11***). These scaling factors compare well with those generated for FSUs in tension by Pintar et al.[169], however they do not compare with the previous 6-year old automotive biomechanical data. For tension, the tolerance of the adult spine is 3,300-N and scaling the pediatric values give scaling factors of 0.91 for the 6-year old and 0.30 for the 3-year old. Our tensile factor is similar for the 3-year old; however, our data suggests a factor of 0.44 for the 6-year old. These data provide a multi-axis loading tissue, and property means of scaling the adult spine to model and understand the tolerance of the pediatric spine.

Table 11. *Scaling Values for Tolerance of the Pediatric Spine. These scaling values were generated from 2nd order polynomial fits of the data and represent the factor by which human adult data should be scaled to give child tolerance criteria.*

	Vertebral Compression		2-FSU Compression		FSU Tension	
Age	Ult. Load	Strength	Ult. Load	Strength	Ult. Load	Strength
1	.25	.52	.27	.53	.22	.49
3	.33	.57	.32	.58	.30	.56
6	.44	.64	.40	.64	.37	.60
9	.55	.71	.47	.70	.46	.65
12	.64	.77	.55	.76	.55	.71
15	.73	.84	.62	.81	.64	.76
Adult	1.00	1.00	1.00	1.00	1.00	1.00

4.4.2. SUMMARY

These data provide load and displacement criteria for the failure tolerance of the pediatric spine. Current use of child anthropomorphic test dummies lacks definitive end points where these dummies predict an injury. Thus, these data will be immediately applicable to the modeling of children in automotive injury scenarios. Further, sport and fall injuries may be able to be mitigated through an accurate understanding of the mechanical behavior from a tolerance or threshold perspective. The tolerance of the developing spine has been characterized throughout development; the load tolerance of the spine increases with maturity and loading rate and varies between genders and spinal levels.

CHAPTER 5:
FAILURE CHARACTERISTICS OF THE DEVELOPING SPINE

5.1. INTRODUCTION

Injuries to the developing spine can range from SCIWORA quadriplegia to a stable vertebral fracture without neurologic injury. Child spinal injuries are extremely difficult to diagnose and most often involve or origniate at the physis.[15, 23, 30, 109, 110, 115] The physis lies between the intervertebral disc (soft tissue) and vertebral body (hard tissue) and contains a number of cell layers which create vertebral bone. These cell layers (of the physis) proliferate cells, organize them and their extracellular matrix, and then calcify the matrix into primary spongiosa. This junction between a soft tissue and a very rigid tissue has been implicated in both tension and compression as the tissue locale most susceptible to injury. Injury to the growth plate may have no long-term effects at all or can cause complete arrest of the growth plate. Severe spinal injuries often include other structures in the spine but predominate through or at the physis.[4, 23, 109, 115] These injuries in children are often treated by spinal fusion which limits growth and range of motion. Identification of a less deleterious surgery would be advantageous for those cases where the growth plate may heal. Thus, it is one of the goals of this research to identify all of the structures involved in compression and tension failures in the hope that this might aid in the development of alternative, more beneficial, management procedures.

5.1.1. PHYSIS MATURATION MORPHOLOGY

The region between the intervertebral disc and the vertebral body begins first as a dense cellular mass, changing next into an organized growth plate, and finally into a cartilaginous endplate. These changes occur with natural spinal maturation and have a

distinct morphology. The changes in this region are paramount to variations in the functional biomechanics of the spine and are implicated to be most susceptible to injury—having the lowest tolerance. This section will discuss the developmental course of the growth region (physis) morphologically to aid the understanding of subsequent failure analyses.

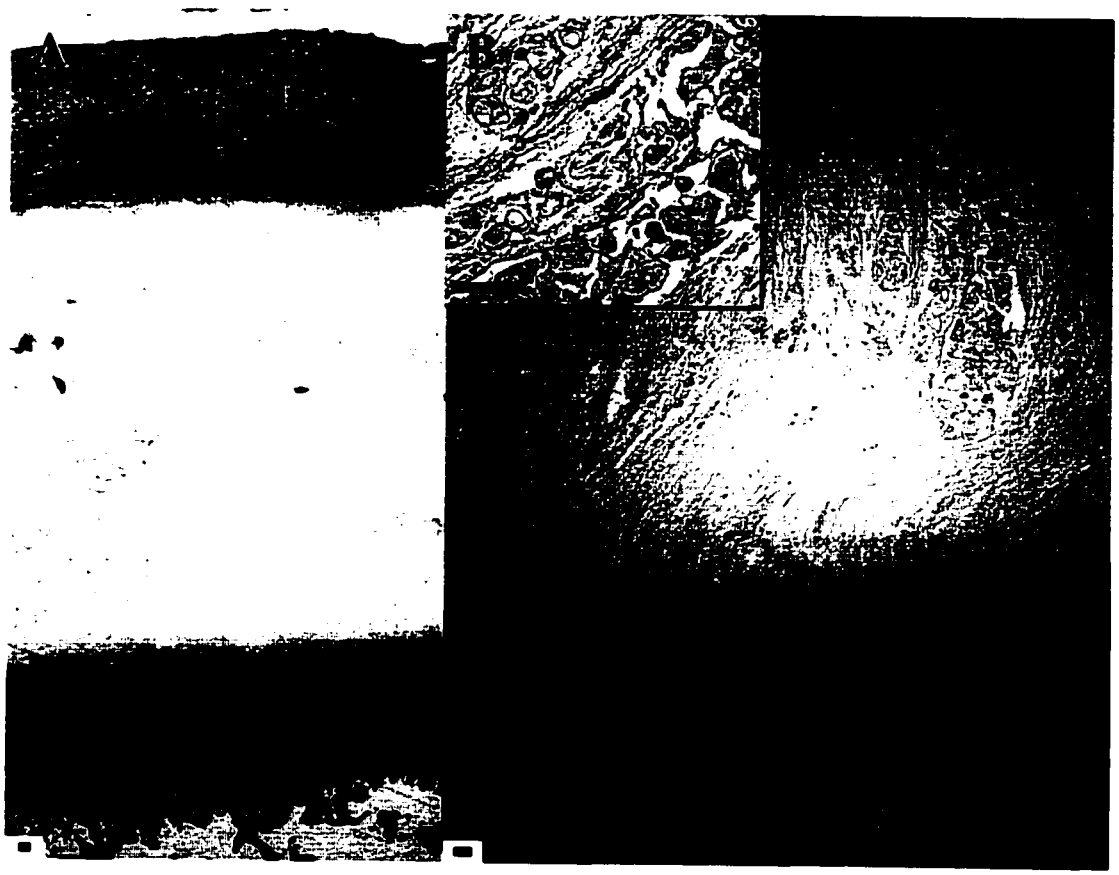

Figure 56. *Developmental Morphology of the Physis. (A) Five-year old baboon C3-4 intervertebral disc and growth regions. H&E preparation demonstrating the intervertebral disc (near its periphery) and the massing of cellular tissue organizing to form the physis. (B) Section of the same tissue at the center of the disc demonstrating the cellular nature of the nucleus pulposus. Unlike the adult disc's acellular nature, the developing nucleus pulposus and annulus fibrosis contain numerous cells. Scale bar = 10.0-μm.*

A dense cellular mass forms between the intervertebral disc and the vertebral body in utero and this mass begins to organize by three-years of age (***Figure 56***). These cells organize into distinct columnar arrangements which facilitate the production of extracellular matrix and bone cells. These organized cells form the physis on either side of the vertebral body (***Figure 57***). This organized growth plate exists from around six years of age until 18-years; at which point this layer flattens into a layer of cartilage known as the vertebral end plate.

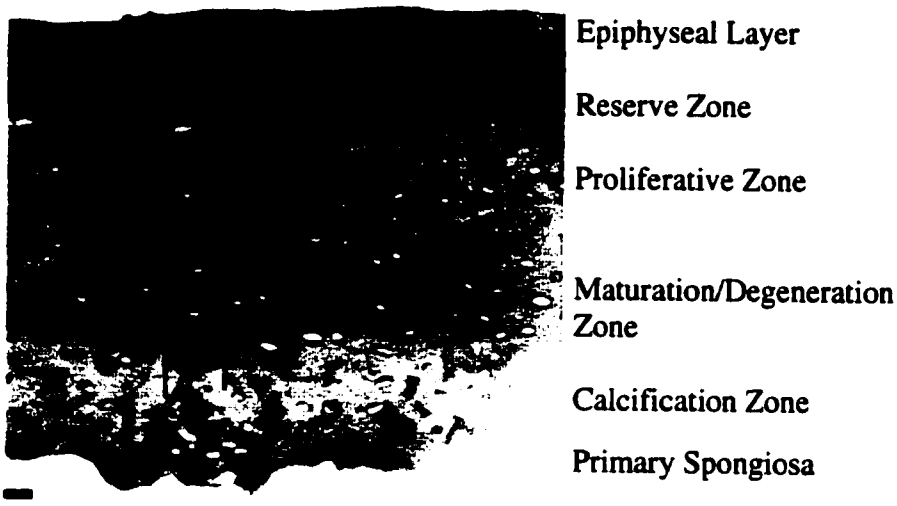

Figure 57. *Histological Section of Baboon Vertebral Physis. A high contrast section of the inferior C6 vertebral physis of a 12-year old, demonstrating the specific zones of the physis and loosely showing the cellular columns. Scale bar = 10.0-μm.*

This discussion of the developing physis represents the first look at the baboon physis morphology and shows that it compares well with published human long bone morphological studies of the physis.[15, 84, 86] The vertebral physis appears to have a much less substantial epiphysis region than that found in long bones; leading a number of authors to deem it a ring apophysis.[99, 156] Other than a diminished epiphyseal region, the baboon spinal physis appears morphologically similar to human long bone growth plates.

5.1.2. PHYSIS INJURY AND TREATMENT

Undiagnosed fractures and displacements of the vertebral physis have been suggested to contribute to SCIWORA, while diagnosed cases remain difficult to treat. Many physis failure patterns have been described in the literature.[4, 52, 53, 77] These 'limbus' fractures have been categorized into four types.[52, 53, 184] Type I lesions are pure avulsions of the posterior cortical vertebra (cartilaginous injury). Type II are defined as having larger central fractures that include the cortical or cancellous bone. Type III fractures are lateral-posterior bony avulsions (similar to teardrop fractures) and type IV fractures extend beyond the disc margins to push bone and cartilage into the spinal canal. These physis fractures can occur independently or in concert with other vertebral fractures such as burst, teardrop, or chance fractures.

Treatment of these fractures is not that dissimilar from treatment of the same fractures in adults. However, children have growth potential that enhances bone remodeling and subsequent healing. Reduction, fusion, and decompression are surgical options for the most severe spinal fractures. Fusion of a spinal level involves removing the intervertebral disc and fusing together adjacent vertebral bodies. This can easily lead to kyphotic deformity if the alignment is not rigidly maintained. Thus, spinal instrumentation may be used, but must be monitored since the child continues to grow. Casting and immobilization are indicated for stable compression fractures with less than 50% body height loss and for tension injuries. These non-operative approaches have had satisfactory results; however, it has been suggested that fractures involving the growth plate treated non-operatively often progress to deformity.[83]

5.2. METHODS

5.2.1. EXPERIMENTAL DESIGN

The primary goal of this experimental effort was to examine patterns in the tissue failures created experimentally in compression and tension. The effects of loading on different tissues were analyzed across development, so the involvement of the growth plate and adjacent tissues was specifically ascertained. This study investigated the tissues tested

previously (Chapter 4) for their mechanical tolerance. These include isolated T9 vertebrae (compression), cervical functional spinal units (tension), and 2-FSU constructs (compression). These baboon tissues were qualitatively examined using plane radiographs, computed tomography scans, and dissection methods. Subsequent to this analysis, the injured physis was examined more closely to determine the zone or tissue where the failure occurred. The specific hypotheses tested by this study were:

1. *Compression injuries to isolated vertebral bodies involve the failure of the physis predominating into and disrupting the cancellous structure.*

2. *Compressive failures in 2-FSU constructs involve a fracture that predominates through the physis.*

3. *Tension failures of maturing lower cervical functional spinal units occur at the zone of calcification in the physis and do not include intervertebral disc disruptions. Mature functional spinal units fail at the endplate-vertebra junction and also do not involve the intervertebral disc.*

4. *Tensile injuries to the upper cervical spine (Oc-C2) appear as dens fractures. The specific type is dependant upon the maturity of the tissues.*

5. *Dynamic tensile loading generates different tissue failure patterns compared with quasi-static tensile loading.*

5.2.2. SPECIMEN IMAGING

After tolerance testing, each specimen had anterior/posterior and lateral radiographs taken for analysis purposes (HP Faxitron - 43855A, Hewlett Packard, McMinnville, OR). If these radiographs were sufficient to establish injury, the specimen was dissected to further delineate the failures. When x-ray did not provide the resolution necessary to identify injury, a computed tomography scan was performed on a GE Light Speed CT Scanner (GE Medical Systems, Milwaukee, WI). A GE Analysis Pack (GE Medical Systems, Milwaukee, WI) was used to manipulate the CT images, elucidating the injured tissues. For injuries in question, a musculoskeletal radiologist was consulted. These techniques enabled the determination of fractures, dislocations, and avulsions. Ligamentous damage was visualized upon dissection of the tissues.

5.2.1. TISSUE PREPARATION

The specimens failed in tension were then grossly dissected using a high-speed cutting tool (Midas Rex, Fort Worth, TX). Tissue sections from the C3-C4, C5-C6 and C7-T1 functional spinal units were alternately cut into coronal and sagittal plane sections for histological analysis. Each tissue block was fixed for light microscopy using ambient light in 10% formaldehyde. After 18 to 24-hours in the fixative, the tissue was rinsed with distilled water and dehydrated with increasing concentrations of alcohol. Finally, the tissue was placed in propylene oxide, and infiltrated with and embedded in Epon-Araldite for sectioning. The embedded tissue was sectioned at the University of Washington Pathology Laboratory where serial 1-μm sections were cut using glass knives and a Sorvall MT2-B ultramicrotome (Dupont-Sorvall, Newtown, CT). For light microscopy, the sections were stained with Hematoxylin and Eosin to elucidate nuclei (blue), cytoplasm (pink), and connective tissue (purple). These sections were then evaluated by light microscopy using a BHTU Olympus (Olympus Optical Co. Ltd., Tokyo, Japan) microscope.

5.2.3. INJURY ASSESSMENT AND ANALYSIS

Injury is defined as a tissue damage or loss of structure resulting from a mechanical input. Each specimen's specific injury was documented to be the sum of the individual tissues affected. The vertebral body compression injuries were visible on plane radiograph and annotated as a binary value of involvement for the cancellous bone, cortical bone, and vertebral growth plate (end plate in adults). Evaluation of the 2-FSU compression failures was accomplished via the use of computed tomography scans and dissection techniques. The clinical fracture was noted for each of these specimens along with each of the involved spinal tissues. Finally, the single FSU tension injuries were immediately discernable by location. Subsequent to this visual inspection, the specific tissues injured were noted from histological analyses of the intervertebral disc and growth plate (end plate) regions. These data will enable the qualitative evaluation of each of the stated hypotheses.

5.3. RESULTS

The qualitative results presented herein were obtained by the author with as much objectivity as possible and, where necessary, a consultation was requested to identify specific injuries. The injuries were separated into compressive and tensile tissue failures which were based on the mode of tissue loading and not necessarily the mechanism of tissue injury.

5.3.1. COMPRESSION TISSUE FAILURES

Vertebral body compressive failures were found to include all three of the tissue regions in the vertebra (cortical bone, cancellous bone, and growth plate). In these specimens, the cancellous bone is crushed as is evidenced upon radiograph and the cortical bone and growth plate exhibit splits in their tissues (***Figure 58***). The 0.5-to-2.0-mm crevasses in the surface of the growth plate are easily visualized after the compressive loading to failure (***Figure 59***). These crevasses extend beyond the cellular layer of the physis and include a split in the cortical shell as well. The splits were not specific to either the inferior or superior growth plate and they predominated in various directions. The most common injuries were two parallel splits running anterior / posterior in the physis.

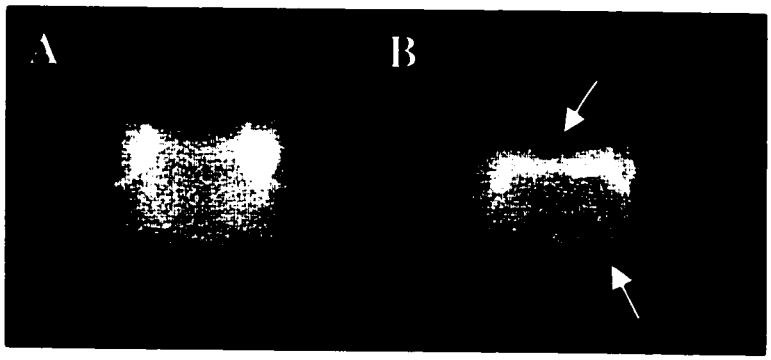

Figure 58. *Vertebral Body Compression Experiment Radiographs. (A) Pre-test radiograph anterior/posterior demonstrating normal cancellous structure. (B) Post-crush radiograph anterior/posterior with vertebral growth plate and cortical disruption as well as disorganized cancellous structure. These radiographs are from a 15-year old male specimen.*

Figure 59. *Post Compression Vertebral Body Photographs. These specimens demonstrate the crevasses in the physis and cortical shell which result from compression loading. (A) 2-year old, (B) 6-year old, and (C) 18-year old vertebral body preparations.*

The 2-FSU constructs, also subjected to compression loading, had very different tissue injuries. These injuries were related to both age and spinal level (***Figure 60***). The upper cervical spine (Oc-C2) demonstrated very consistent C1 vertebral burst fractures. These burst fractures occurred at the physes or growth regions for the maturing specimens. Further, a few of these upper cervical injuries involved an avulsion of the tip of the dens (type II fracture) which protruded into the canal space. Injuries to the lower cervical spine C3-C5 and C6-T1 demonstrated a similar pattern to each other showing growth region (synchondroses) fractures in the young and burst and complex fractures in adolescence and adulthood (***Figure 60***). The very young specimens (< 6-years) failed at the cartilaginous region adjacent to the vertebra which connects to the posterior neural arch. Specimens less than 6-years of age demonstrated failures of this type and also exhibited disc protrusions posteriorly. Adolescent and adult specimens demonstrated burst fracture patterns which were classical and also included fractures of the lateral masses and spinous process (***Figure 61***). The burst fracture portion of these injuries predominated through the physis and often included intervertebral disc protrusion into the body. Finally, a few of the specimens demonstrated intervertebral disc protrusion anteriorly with a shearing of the physis off of the vertebral surface.

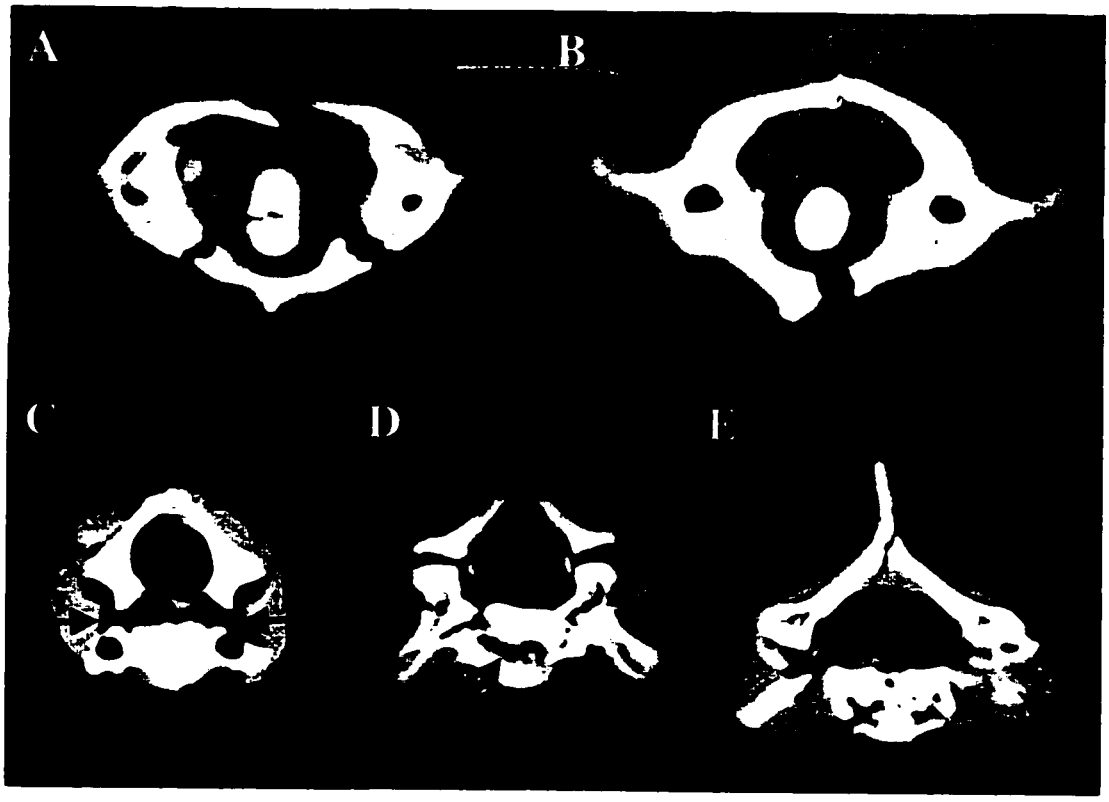

Figure 60. *Computed Tomography of Injured 2-FSU Compression Specimens. (A) 6-year old C1 burst fracture where the anterior fractures occur at growth regions. (B) 15-year old C1 burst fracture. (C) 5-year old C4 synchrondroses failure at each margin separating the anterior body from the posterior neural arch. (D) 10-year old C4 burst fracture including lateral mass involvement. (E) 16-year old C7 burst fracture with spinous process fracture.*

Figure 61. *Sagittal Sections of 2-FSU Compression Failure Specimens. (A) 5-year old C4 burst fracture with physis involvement both superiorly and inferiorly and intervertebral disc protrusion into the body. (B) Lateral radiograph of specimen A demonstrating the burst fracture as well. (C) 10-year old C4 burst fracture demonstrating physis failure and disc protrusion into C4 and a wedge fracture of C5. (D) 15-year old C6-C7 intervertebral disc protrusion anteriorly with bony avulsion of C7, severing of the physis (arrow).*

5.3.2. TENSION TISSUE FAILURES

Tensile loading of single cervical functional spinal units demonstrated very similar results across developmental age and by level. The lower cervical spine C3-C4, C5-C6, and C7-T1 most often failed in tension as a physis lesion separating the physis from the vertebral body. The Oc-C2 spinal level exhibited differing failure patterns in the child and adult. Each injury is listed in ***Table 12*** and represents the visual inspection, and radiograph and CT analyses of these tissues. Histological examination will more clearly determine the tissues (cellular regions) injured.

Table 12. *Injuries from Tensile FSU Experimentation Based upon Inspection, Radiographs, and CTs. Key: LIG=ligamentous failure, DNS=dens fracture-type, SKL=basilar skull fracture, LAM=laminar fracture, IP=inferior physis failure, SP=superior physis failure, B=both physes injured, SV=superior vertebral fracture, and PTG=concomitant potting failure.*

Age	OC-C2	C3-C4	C5-C6	C7-T1
1	DNS-3	IP	IP	IP
2	DNS-1	SP	PTG	IP
2	DNS-1	IP	IP	IP
3	SKL/PTG	PTG/LAM(C4)	IP	IP
5	SKL	IP	PTG	PTG
6	DNS-1	IP	IP	IP
7	LIG/PTG	SP/B	IP	IP
7	LIG(1-2)	IP	SP	IP
9	LIG(1-2)	IP	SP	IP
10	LIG(0-1)	IP	IP	IP
11	DNS-1	IP	IP	IP
11	PTG/LIG(0-1)	IP	IP/SV	SP
13	LIG(1-2)	IP	IP	IP
15	LIG(1-2)	IP	IP	IP
16	DNS-2	IP	SP	IP
18	LIG(1-2)	SP	IP/B	IP
18	DNS-2	SP	IP	SP
26	DNS-2	IP	IP	IP

A detailed analysis of each of the failed physes revealed two different types of failures: young tissues (16-years or less) demonstrated physis failure at the zone of calcification which connects the cartilaginous physis to the vertebral bone (***Figure 62***), and adult tissues (18-year +) exhibited failures of the interface between the end plate and the intervertebral disc (***Figure 63***). None of the young tissue failures included intervertebral disc involvement and all of the adult tissues did include rupture of the annular fibers attaching the disc to the end plate.

Figure 62. *Physis of 13-Year Old C5-C6 Prepared After Tensile Injury. (A) C6 superior physis intact showing bony interdigitation with the zone of calcification. (B) C5 inferior physis implicating the calcification zone (missing) as the zone of physis failure. Scale bar = 10.0-•m.*

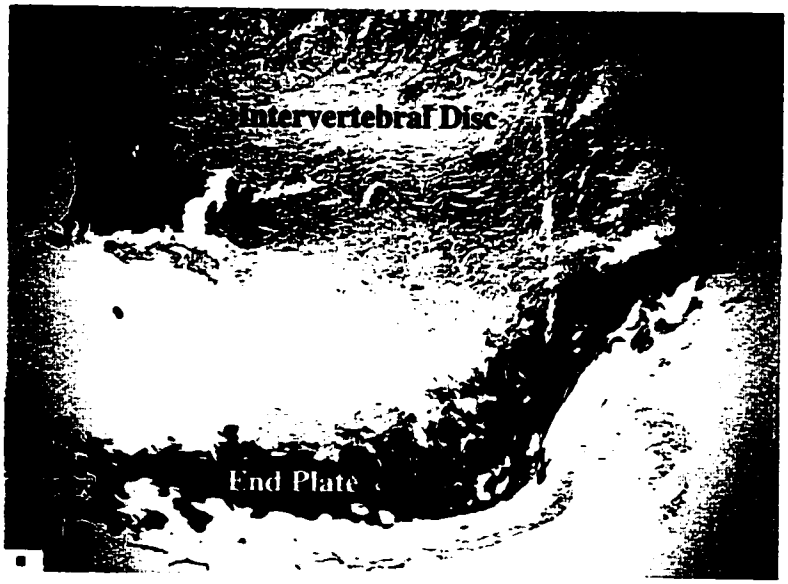

Figure 63. *Adult (18-year old) C7 End Plate Failure as a Result of Tensile Loading. The vertebral end plate ruptures the intervertebral disc upon failure. Scale bar = 10.0-•m.*

Finally, the single functional spinal units failed at various rates did not exhibit any different failure patterns; all eight specimens (10-year old) had physis failures at the zone

of calcification (C3-C4, C5-C6, C7-T1) and ligamentous failure between C1 and C2 (Oc-C2). Most of the growth plate injuries were to the inferior physis, but three specimens did have failures at both the inferior and superior physis.

5.4. DISCUSSION

Examining how developing spinal tissues fail provides insight on the susceptibility of various tissues and indications for clinical management. The physis has been implicated as highly susceptible to injury; unfortunately, assessment via radiographic films has found detection of these injuries difficult. The data collected herein may provide an understanding of the tissues associated with spinal injuries in children for both assessment and management purposes. Comparison of the experimentally created injuries with those presenting in the clinic may demonstrate relationships of age and involved tissues which would suggest a specific injury and subsequent course of action. Compression and tension injuries both have shown physis involvement even though they are extremely different otherwise. This discussion will examine each of the tested hypotheses and then the implications for this research will be evaluated.

Hypothesis 1. Compression injuries to isolated vertebral bodies involve the failure of the physis predominating into and disrupting the cancellous structure. Since all (100%) of the vertebral compressive tests resulted in physis and cancellous disruptions, the null hypothesis is rejected. Thus, vertebral body compressive failures involve injury to the physis and cortical shell as well as cancellous disruption.

Hypothesis 2. Compressive failures in 2-FSU constructs involve a fracture that predominates through the physis. The null hypothesis is rejected because every 2-FSU segment included a fracture, schmorls node, or disc herniation which disrupted the physis. In this way, the physis was compromised for all (100%) of the two functional spinal unit experiments regardless of level and age (except the adult specimens where the physis is fused).

Hypothesis 3. Tension failures of maturing lower cervical functional spinal units occur at the zone of calcification in the physis and do not include intervertebral disc disruptions. Mature functional spinal units fail at the endplate-vertebra junction and also do not involve the intervertebral disc. The first part of this hypothesis involving the developing lower cervical spine was demonstrated through dissection and histological analysis in all specimens, so the null hypothesis is rejected. This hypothesis' second part dealing with the mature spine leads to an acceptance of the null hypothesis. The null hypothesis states that the mature FSU does not fail at the endplate-vertebra junction, but rather injury predominates at the intervertebral disc-endplate boundary. Since all but one adult specimen exhibited this pattern, the stated hypothesis is rejected.

Hypothesis 4. Tensile injuries to the upper cervical spine (Oc-C2) appear as dens fractures. The specific type is dependent upon the maturity of the tissues. The null hypothesis is rejected for this study even though many ligamentous failures occurred. The very young demonstrated mostly type I dens fractures while the adults demonstrated type II dens fractures in tension. Thus, the alternate hypothesis as stated above is accepted.

Hypothesis 5. Dynamic tensile loading generates different tissue failure patterns compared with quasi-static tensile loading. Since the high-rate tensile failures were not dissimilar from the low-rate failures, the effects of loading rate do not appear to affect the tissue injury pattern. Thus, the null hypothesis is accepted.

5.4.1. PHYSIS PATHO-MECHANICS

The patho-mechanics of the spine can be examined using the known loading inputs and the resulting tissue injury mechanisms. Compression loading to the young spine (< 6-years) results in failures through the growth regions (synchrondroses) in both the upper and lower cervical spine. The injuries in the lower cervical spine can result in SCIWORA due to the lack of bone present where the failures occur. Vertebral compressive fractures in the very young also predominate through the growth region (physis) on the superior and inferior boundaries of the vertebral body. In tension, these

young baboons experience physis failures in the lower cervical spine where the disc and growth plate pull off of the vertebral body. This too might be difficult to recognize on plane radiographs and can have severe destabilizing consequences. The very young upper cervical spine (Oc-C2) is the most susceptible cervical level to failure and these injuries include type-I dens fractures and basilar skull fractures. If identified, all of these injuries in young children can heal relatively easily since the young spine has a high growth potential.

Juvenile (ages 7-to-12-years) injury patterns are a bit different from the very young. In compression, these young baboons experience burst fractures that are associated with other fractures such as lateral mass or spinous process fractures. These have been characterized as 'limbus' type-II fractures involving central fractures and disruptions of the growth plates by the intervertebral disc. Vertebral fractures at this age go through the physis and disrupt the cancellous bone. Tension injuries to this age group are ligamentous in the upper cervical spine; however the most susceptible levels for injury are the lower cervical spine where physis failures are most common. These physis failures tear the zone of calcification away from the vertebral body, but do not disrupt the intervertebral disc. Tensile injuries that result in an unstable spine for this age group appear to be good candidates for non-operative treatment. Given that the disc is not disturbed and it is still highly cellular, it appears that this motion segment can be retained whether or not the growth plate arrests.

Adolescent (13-to-18-years) injuries move closer to approximating the adult patterns. In compression, the adolescent lower cervical spine is most susceptible to injuries such as burst fractures or tear-drop fractures affecting the physis. Disc herniation or tear-drop fractures appear to force the intervertebral disc away from its centroid and shear the growth plate from its vertebral surface. These compression-induced injuries can have vertebral physis injuries which also affect the trabecular bone. Examining the adolescent spine for tension induced injuries finds that the most susceptible level has clearly shifted to the lower cervical spine resulting in physis failures at the zone of calcification. Since

this is the most active period for the vertebral physis, adolescent injuries should also heal with a high degree of success.

The thinning and calcification of the growth plate into the vertebral endplate change the injury response of the spine as adulthood approaches. Compression injuries involve the endplate and demonstrate primarily burst fractures in the adult. The lower cervical spine has the lowest tolerance to injury and demonstrates physis failures in tension. However, when injuries occur in the upper cervical spine (Oc-C2) they include principally type-II dens fractures. The tensile endplate failures in adults appear to disrupt the intervertebral disc as has been seen by others.[206, 207] This coupled with the decreased growth/healing potential, can be an indication for spinal fusion to stabilize the spine and limit further injury.

5.4.2. SUMMARY

This chapter aimed to understand the injuries created in the developing spine from a patho-mechanics perspective with attention to the specific tissues injured. In this way, a mode of loading can predict an injury mechanism and all of the affected tissues and vice versa. This information may provide patterns to aid clinical assessment and management to most positively aid the injured child.

CHAPTER 6:
MODELING THE DEVELOPING SPINE

6.1. INTRODUCTION

The experimental mechanical data collected, while inherently novel and exciting, will not reach its full potential unless its applicability extends to the development of injury prevention schemes. These injury prevention designs will most certainly utilize computational or physical modeling of the developing spine. Therefore, the data collection in the experimental section was designed to facilitate the development and validation of computational models, generate failure criteria, and validate physical dummy models. The first step in these modeling procedures is the development of viscoelastic rigid body model constitutive equations. All of the data collected herein is adequate to completely model the non-linear viscoelastic response of the developing spine. The scope of this part of my project includes the development of these modeling approaches and the evaluation of the sample relationships created. Comprehensive modeling of the developing spine is beyond the scope of this project; however this research will provide the framework for future, thorough modeling of the maturing spine.

6.1.1. CONSTITUTIVE NONLINEAR VISCOELASTIC MODELING

The most accurate and effective modeling strategies have reviewed the factors with the highest sensitivity on model performance and have focused their attention on obtaining the best data to satisfy those factors. This review will discuss modeling efforts and techniques that will be seminal to the effective modeling of the developing spine.

Early modeling efforts assumed tissues to be isotropic and linearly elastic. These models described the mechanical behavior well in a very specific domain; they were accurate over a small range of strains and lacked any time dependent characteristics. Since the stress-strain relationships discovered in developing spinal tissues are nonlinear and exhibit stress-relaxation, perhaps a more sophisticated modeling approach is necessary. Kelvin-Voigt, Maxwell, and Standard Linear Solid mechanical models have been utilized to describe biologic tissues with nonlinear and viscoelastic responses. These models will be discussed in light of the model requirements for the developing spine

The most important degree of complexity in a constitutive model of any soft tissue is nonlinear elasticity.[62] Most soft tissues exhibit a nonlinear stress response to strains which contains a toe region of low modulus, an inflection point where the tissue 'stiffens', and a functional range where the modulus is linear. A model containing only linear material properties will not accurately cover any range of strains beyond a few percent.[62] Thus, nonlinear elastic tissue responses are preferable even though they may affect the speed of the simulation.

Another factor common to current constitutive relationships is that of viscoelasticity. The stress-strain relationship is typically affected by strain rate; as the strain rate increases, the elastic stiffness increases. Although viscoelasticity has considerable effects on the functional response of soft tissues, it may be able to be neglected for high or very slow strain rates. High strain rates, similar to those seen in impact injury events, do not have enough time for viscous relaxation to occur. Therefore, these events can be approximated by the nonlinear elastic tissue response. Similarly for the very slow strain rates, the tissues are fully relaxed throughout the entire test and these tissues can be approximated by the nonlinear elastic tissue response multiplied by a 'relaxation' scalar. Unfortunately though, without a viscous modeling component, the strain-rate dependence of the stiffness cannot be accurately modeled. Thus, a purely elastic model must be tuned (for stiffness / modulus) to the rate at which it will be utilized. Therefore, while injury prevention modeling may be initially approximated using a nonlinear elastic tissue response, an ideal model would include nonlinear viscoelastic tissue responses.

Nonlinear viscoelastic modeling may be accomplished via a number of different techniques. The mechanical response of biologic materials are often defined by series and parallel combinations of Kelvin-Voigt, Maxwell, or Standard Linear Solid Elements containing springs and dashpots. These models may be linear, non-linear, elastic or viscoelastic depending on the definition of the specific spring and dashpot elements. Further, biologic data may be used to tune physical relationships already known to exist or it may be empirically applied through curve fitting algorithms. Thus, there are many ways in which the biomechanical response of spinal tissues may be modeled. Choosing the method which most accurately represents the real biomechanical response of the spine and is computationally feasible requires difficult decisions.

The response of biologic tissues has been modeled by many investigators using customized analyses of the Kelvin-Voigt Model with non-linear spring and non-linear dashpot components.[62, 87, 107, 141] These modeling endeavors have chosen Kelvin-Voigt Model parameters because of their accuracy in modeling rate-dependence and their computational ease. All of these efforts though have used different parameters (coefficients) to explain the model response.

Many modeling efforts have utilized a nonlinear viscoelastic approach using a customized version of the quasi-linear viscoelastic theory developed by Fung.[61] This analysis has been tailored to best model specific tissues or loading rates. The quasi-linear viscoelastic theory as originally proposed was strain rate independent which lead Iatridis et al.[87] to modify their methods to include strain rate dependence at the expense of a linear viscoelastic response. This method was used to model nucleus pulposus and very closely approximated its transient and dynamic shear response. The quasi-linear viscoelastic theory also utilizes only the stress relaxation response of a tissue to identify the complete response of the tissue. This has led to under estimation of the elastic mechanics. Subsequently, the theory has been tuned to include a nonlinear exponential form of the elastic response.[107, 198] A nonlinear exponential was used to define the elastic response and the viscous component was defined using the reduced relaxation equation. This reduced relaxation function, however, has been shown to be rather invariant between

tissues and specimens.[62, 141] Unfortunately, a limitation of these quasi-linear viscoelastic approaches is the inability to directly apply the coefficients to an element in a lumped parameter model. Further, in all of these analyses, a number of coefficients have been derived from one or two experimental tests producing a non-unique solution.

In summary, there are many modeling approaches which may be used to approximate the mechanical response of the developing spine. It is clear, though, that nonlinear viscoelastic modeling appears best justified by the experimental data and the biomechanical literature. A Kelvin-Voigt Model estimation using nonlinear springs and nonlinear dashpots should provide a good first approximation of spinal mechanics. This model deforms over time with an instantaneous application of force similarly to the response of biologic tissues. Also, Kelvin-Voigt Model parameters are easily applied to a lumped parameter element. The nonlinear estimation of the elastic response using an exponential formula has been shown to be successful in biologic tissue modeling and seems proper for this application. Finally, the nonlinear estimation of the damping has been proposed to encompass rate dependence in the Kelvin-Voigt Model and should enable the accurate representation of the viscous mechanics of the spine.

6.2. METHODS

6.2.1. EXPERIMENTAL DESIGN

This computational effort utilized the data collected on the functional biomechanical response of the spine (Chapter 3) to develop a methodology for explaining the biomechanical behavior of pediatric spinal tissues. A nonlinear viscoelastic modeling approach using a Kelvin-Voigt Model was employed to determine material coefficients describing the behavior of the developing spine in tension. This computational exercise resulted in viscoelastic model parameters defined by nonlinear methods enabling the evaluation of the developmental changes in spinal soft tissues for injury prevention.

The computational time and effort required to curve-fit and obtain parameters for each specimen in all loading directions was beyond the scope of this research project. This modeling effort focused on the methodology to characterize the nonlinear viscoelastic

response of tissues across developmental ages. Specifically, comparisons were performed by age to appreciate its affect on the shape of the stress-strain relationship and modeling coefficients. Each tissue's viscoelastic response was characterized using a Kelvin-Voigt model of a spring and a dashpot in parallel. The spring is defined by an exponential approximation of the stress-strain relationship and the strain rate dependant dashpot is approximated by a nonlinear damping coefficient derived from the hysteresis energy at various loading rates.

6.2.2. RIGID BODY MODEL PARAMETERS

This analysis is based upon a theoretical Kelvin-Voigt Model which examines spring and dashpot element properties for application into a rigid body model. This theoretical construct of a spring and dashpot in parallel represents a first order approximation of the mechanical response of a single functional spinal unit. The theory uses four coefficients to explain the non-linear mechanics of the spine (A, B, c_1, and, c_2). These coefficients were found using equations which approximate the stress-strain relationship for spring coefficients A and B (***Equation 4***), and then used the hysteresis energy developed from constant velocity tests to obtain a dashpot coefficient. The dashpot coefficient is specific to loading rate so a curve fit of the coefficients 'c' by velocity gave a nonlinear equation defining the dashpot characteristics (***Equation 4***). The curve fitting was performed using Igor Pro 4.0 (WaveMetrics, Inc., Lake Oswego, OR) and custom equations for both the spring and dashpot analysis.

Equation 4. *Axial Tension and Compression Constitutive Element Equations. These spring and dashpot coefficients are the first effort to model developing spinal tissues.*

$$\sigma = A\left(e^{B\varepsilon} - 1\right) \qquad c = \frac{HE}{2vx_{max}}, \qquad c(v) = c_1 x^{C_2} \quad \text{or} \quad c(v) = c_1 x + c_2$$

A, B, c_1, and c_2 are the material coefficients of interest while HE is hysteresis energy resulting from a triangular wave displacement input at a constant velocity, v.[22] These spring and dashpot coefficients describe the stress profile for a given strain input.

These coefficients were obtained for four representative specimens across the developmental spectrum at the C3-C4 spinal level. After generating the coefficients, they were compared with the experimental stress-strain relationships to determine if the modeling approach is appropriate. This computational work lays the foundation for the generation of full rigid body modeling constitutive equations for the developing spine.

6.3. RESULTS

The results for this computational modeling effort clearly direct an approach for future constitutive modeling, but moreover provide a very unique look into the mechanical response of developing tissues. First, the nonlinear viscoelastic coefficients were obtained using curve fits of the experimental stress-strain and constant loading rate experiments (***Table 13***). The coefficients A and B were obtained using the loading curve for these experimental data. The A coefficient decreases with increasing maturity and the B coefficient increases with advanced maturity. The curve fits for these data were quite different as a function of age (***Figure 64***). The goodness of fit for each exponential worsens with increasing age suggesting that the exponential model becomes less appropriate with increasing development.

Table 13. *Nonlinear Viscoelastic Tensile Parameters for the Developing C3-C4 Functional Spinal Unit of one Specimen at each Age. The goodness of fit chi^2 and R^2 values indicate the strength of the constituent function for the given data set.*

Age	A	B	Chi^2	C_1	C_2	R^2
3-y.o.	0.6021	1.989	1.043	272.6	-0.097	0.980
6-y.o.	0.3656	3.532	4.926	383.9	-0.052	0.998
12-y.o.	0.2417	5.630	11.110	404.5	-0.054	0.897
Adult	0.2353	6.826	13.579	438.7	-0.098	0.967

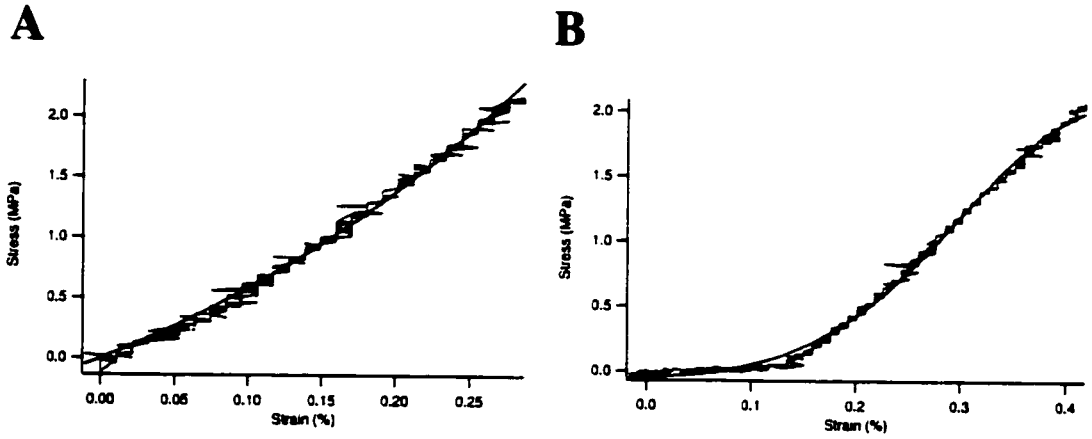

Figure 64. *Experimental Data Fit for the Nonlinear Elastic Approximation of the Stress-Strain Data. (A) 6-year old male tensile stress-strain curve with exponential fit. (B) Adult male stress-strain relationship and curve fit. Note the approximation of the inflection point between the toe region and the linear functional region.*

These elastic responses may be directly used in modeling efforts since they represent normalized data and also depict the shape of the nonlinear response. The parallel arm to this elastic spring in Kelvin-Voigt model is a dashpot. The damping coefficients measured from the hysteresis energy (***Figure 65***) of constant loading rate experiments appear to provide a power relationship between the damping coefficient and loading rate. These damping coefficients (***Figure 66***) decrease with increasing loading rate and demonstrate a good power fit. The coefficients dictate the damping in the system and are good over the loading ranges from 0.05-mm/sec to 5.0-mm/sec.

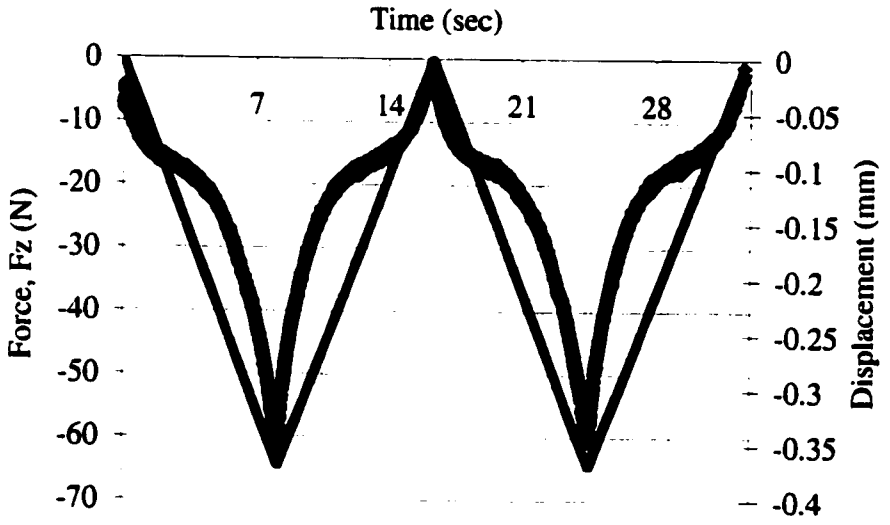

Figure 65. *Force and Displacement Time Histories for a Constant Velocity Triangular Wave Displacement Input. These curves were used to measure the hysteresis energy (the energy lost in the system) at various loading rates.*

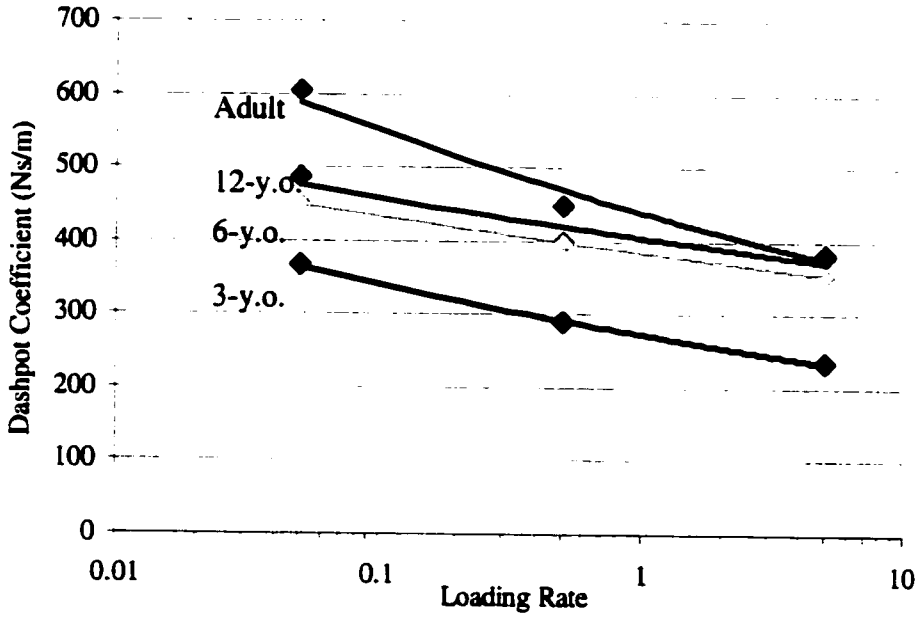

Figure 66. *Dashpot Coefficients for the Developing C3-C4 Functional Spinal Unit in Tension. These dashpots are nonlinear in time, varying with loading rate.*

The stress-strain relationships of the C3-C4 functional spinal unit in tension were determined across developmental age. The mean of three specimens in each age group was taken given a similar initial load reference (100-N). Then seven time points from the normalized load reference were selected from these data to approximate the stress-strain relationship. These stress-strain curves provide an appreciation for the developmental changes in both the toe region and linear region of these tissue's responses (***Figure 67***). The model curves overlay the mean and first standard deviation of the experimental data quite well (***Figure 68***) giving confidence in these modeling methods.

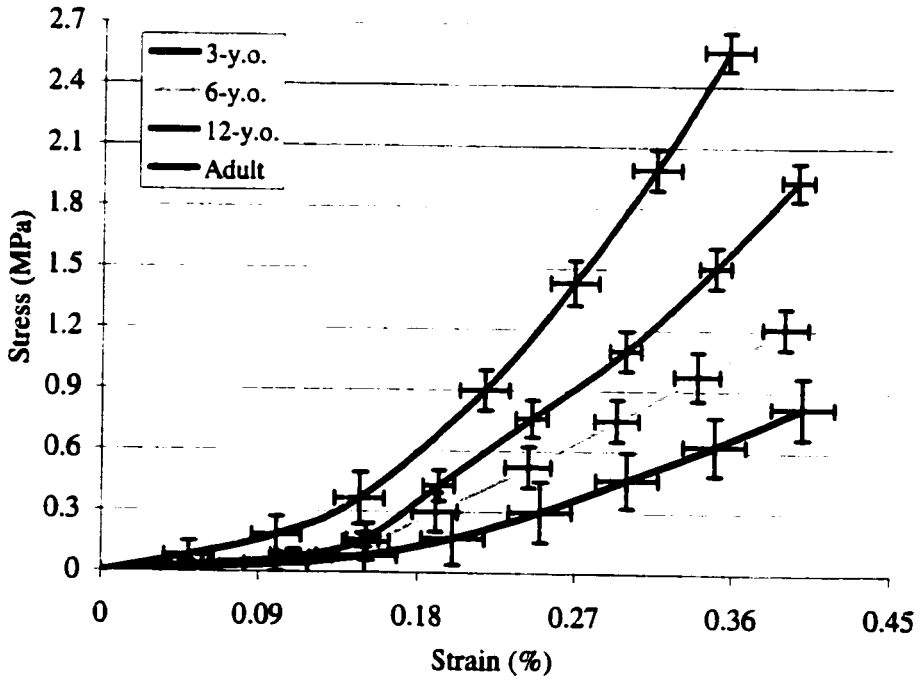

Figure 67. *Stress-Strain Relationships of Developing Spinal Tissues. These curves for the C3-C4 functional spinal unit in tension reveal the true shape of the nonlinear elastic response.*

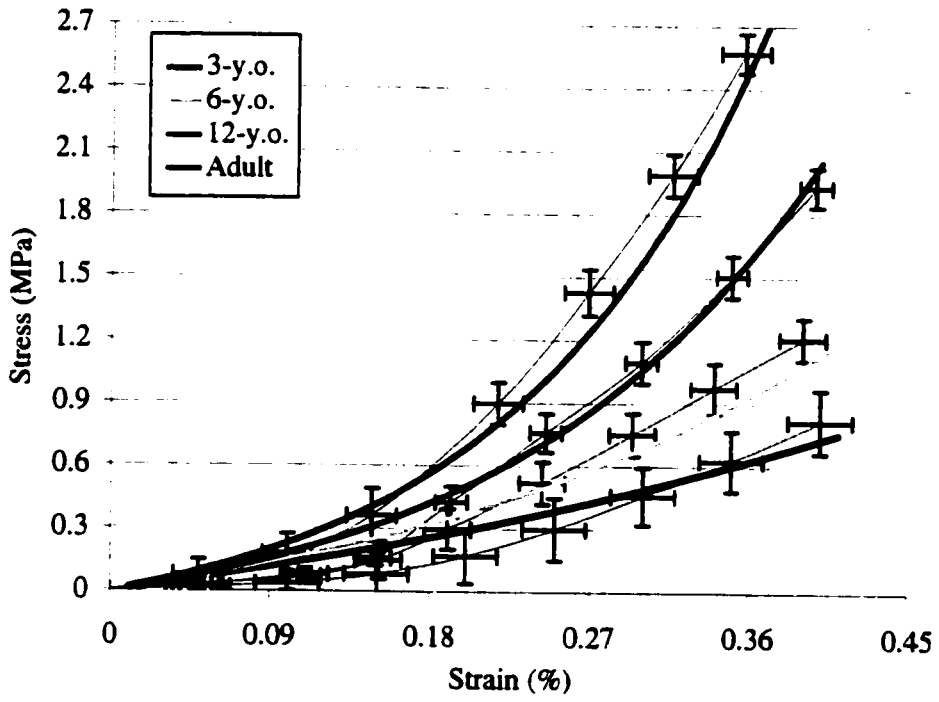

Figure 68. *Model Validation of Stress-Strain Relationships with Experimental Data. The mean and standard deviation for 3 specimens at each age shown with the model fits (lines) of each developmental group. The model falls within one standard deviation of the experimental data indicating the appropriateness of the methodology.*

6.4. DISCUSSION

The goal of this computational effort was to determine if the data collected could be explained using standard nonlinear viscoelastic theory. In general, the nonlinear elastic response of the tissues could be modeled effectively as well as the nonlinear damping coefficients. Future modeling efforts can build on this data set and follow similar methods for successful nonlinear elastic modeling of the tissues. These methods have generated four coefficients defining the Kelvin-Voigt Solid spring and dashpot parameters and did so using three distinct data sets for the dashpot parameter generation and one data set defining the elastic response. While this represents a non-unique solution, the use of independent data sets to define the model parameters enhances the specific applicability of this model compared with classical quasi-linear viscoelastic theory which uses only stress-relaxation data.

6.4.1. MODEL EVALUATION

The data presented herein represent the first time developing spinal tissues have been modeled; therefore a critical examination of these modeling efforts should be performed. The curve fit of the stress-relaxation data demonstrated chi square values which inceased with age. This suggests that the tensile mechanics of the spine can be approximated by this exponential only at the younger ages. As the spine develops, its stress-strain relationship changes and achieves a less than optimal fit to the exponential. The quasi-linear viscoelastic model as defined by Fung has been shown to have poor elastic fidelity in spite of the seminal role of the elastic response.[107] Therefore, it appears as though the nonlinear exponential modeling effort best approximates across the developmental spectrum, but age specific nonlinear modeling may be necessary. In this way, specific and appropriate nonlinear elastic stress-strain relationships can be determined and imported into a rigid body model.

To my knowledge, no other work has published nonlinear dashpot coefficients for viscoelastic materials. The coefficients developed herein are comparable with reported linear dashpots. De Jager et al.[37] reported spinal ligament dashpots of 300-N-s/m and utilized these in computational efforts. Also, the hysteresis energy method was used by Camacho [21] in determining dashpot coefficients of 515-N-s/m. for a cervical spine rigid body model. Camacho further performed a sensitivity analysis on these dashpot coefficients in head impact events. He found that the spine failure load was approximated within 7% for changes in the dashpot coefficient from 50% to 150%. This suggests that the dashpot coefficients may not be the most sensitive feature in a dynamic computational model.

The nonlinear dashpot coefficients determined herein, increase with increasing tissue development. This indicates that spinal tissues exhibit an increased rate sensitive component with increasing maturation. Also, the dashpot coefficients decrease with increasing loading rate. Given that the resultant stress from a dashpot is equivalent to the coefficient multiplied by the loading rate, the overall resultant stress increases with

loading rate. This computational result is supported by the loading rate experiments where increased stress is observed at higher displacement rates.

Finally, the Kelvin-Voigt model of nonlinear viscoelasticity represents a very simplified model to understand the bulk mechanics of the cervical spine. More complex formulations may be developed which better explain the mechanical behavior of the spine throughout development. For example, Kelvin-Voigt models may be placed in parallel with each other or in series with another spring to enhance the applicability, fidelity, and sensitivity of the model's response.

Limitations of this modeling approach include the use of a single Kelvin-Voigt model where more or other models may more accurately represent the response of the developing functional spinal unit. Further, the experimental data may limit the applicability of the modeling approach due to the definition of the damping coefficient. The calculation of hysteresis energy assumes that the experimental test displaced the tissue at high rates in 'perfect' triangular waves; this is not experimentally feasible. Also, the dashpot coefficients are not defined for highly dynamic loading rates unless we can assume that the same power relationship holds to high-rate events. Even with these limitations, this methodology for developing a constitutive model of maturing spinal tissues should produce more accurate predictions than previously possible.

6.4.2. SUMMARY

A formulation of nonlinear viscoelastic theory has been utilized to describe the mechanical response of developing spinal tissues. These constitutive relationships describe the response of the tissues using a nonlinear Kelvin-Voigt model. Use of these constitutive equations in rigid body modeling does, however, require substantial validation. The data collected in this experimental effort provide a first step in validation and further analysis of these data will advance its applicability. However, the experimental testing of human pediatric tissues will engender superior validation data. Sensitivity analyses need to be performed to determine those characteristics of the tissues' mechanical response that are most important to specific modeling situations. While these

first order equations provide a good approximation of the spinal mechanics, a thorough analysis of these tissues in tension, compression, by gender, and by level is required for the most accurate model predictions and the best chances for the advancement of injury prevention schemes.

CHAPTER 7:
NEW INSIGHT ON THE DEVELOPING SPINE

A contemporary review of the developmental biomechanics literature revealed very little data concerning the spine, its injury prevention, or management. Thus, this research program was initiated to understand the developmental course of the spine from a biomechanical perspective. The main effect of skeletal maturity (development) was correlated with material and structural properties in the functional range and at failure. The secondary effects of gender, spinal level, and loading rate were examined for their role in spinal developmental mechanics. The sum of these experiments has significantly altered the view of the developmental biomechanics of the spine, the failure patterns of pediatric spinal tissues, and the basic understanding of mechanical property development.

This chapter will examine the general findings of this research project as well as discoveries within and between each of the previous four chapters that warrant discussion. These sections will include: (i) spinal maturation from a mechanical perspective, (ii) age, size, gender, and spinal level as predictors of spinal mechanics, (iii) tolerance and indicators of severe spinal injury, (iv) scaling and modeling of the human pediatric spine, and (v) experimental and computational limitations.

7.1. SPINAL MATURATION FROM A MECHANICAL PERSPECTIVE

As the spine develops from cartilaginous tissue, it begins to develop its mechanical functionality immediately. The very young baboon spine exhibits approximately one third of the stiffness of the adult spine and it is about one quarter of its adult size.

Interestingly, though, the tissue comprising this very young spine has material properties that are 45% of their adult value. This suggests that the tissue consists of constituents and possibly organization that closely approximate their mature makeup; therefore the mechanical development of the immature spine appears to be dictated by an increase in the amount of tissue (size) and not the intrinsic mechanics of that tissue.

The spine develops its functional mechanical characteristics and its tolerance mechanical characteristics at different time courses (***Figure 69***). The functional mechanical properties (stiffness) develop earlier in skeletal maturation than the tolerance (ultimate failure load) characteristics. As a juvenile, the functional characteristics of the spine are of primary importance for posture and movement. During these years of growth, the spine is more ductile and flexible than it is as an adult. As the tissues mature, its tolerance characteristics catch up at the same time the spine begins to be subjected to potentially higher loads. Thus, it is my contention that the functional characteristics develop earlier by necessity of posture and motion while the tolerance characteristics develop later when the spine may need to be able to withstand higher loads.

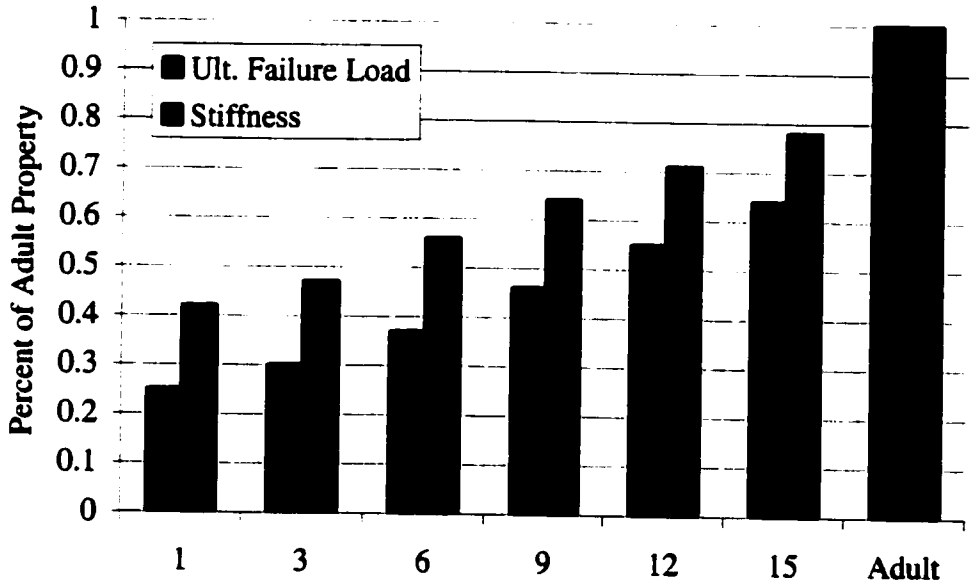

Figure 69. *Scaling Relationships of Functional and Tolerance Characteristics. The scaling relationships for the tensile FSU data are presented to demonstrate the % of stiffness compared with the % of ultimate load developed for the very young.*

7.2. PREDICTORS OF DEVELOPING SPINE MECHANICS

The functional biomechanics of developing spinal tissues demonstrated a strong correlation between skeletal maturity and the development of both structural and material properties. In fact, the structural properties (stiffness, ultimate load) exhibited a stronger correlation with development than the material properties (modulus, strength). This suggests that the size of a spinal tissue is the primary dictator of its developmental properties and that the tissues' material properties confer a smaller portion of its mechanics. However, this is not to say that size explains the entire mechanical response of the tissues; the modulus of elasticity and ultimate strength increased significantly with maturation.

A look at the developing vertebra specifically revealed gender differences which indicated that female vertebrae are stronger (higher ultimate strength) than similar age male vertebrae. Male vertebrae failed at a slightly higher ultimate load than the same aged female vertebrae; however, female vertebrae were smaller, ranging only up to half the size of their male age-matched counterparts. This suggests that while their skeletal maturity appears similar, the material properties comprising these female bones are stronger. The enhanced strength of the female vertebrae earlier in life may have hormonal roots which could also affect earlier osteoporotic onset in females. It is important to note that this model (baboon) has a high degree of sexual dimorphism. Thus, we must be very careful applying these results directly to the developing female human spine. While the gender effects associated with human spinal development are likely similar to those discovered here, these data should be viewed with an understanding of the model limitations.

The mechanics of the various cervical spine levels were investigated with age, and the structural properties (stiffness and ultimate failure load) appeared to motivate differences between the levels. Thus, the size of each level likely dictates its mechanical response between levels. The material properties (elastic modulus and strength) were distinct between a few levels but not with a high degree of certainty. Therefore, given the

mechanics of one spinal level based on age and gender, size will have the greatest predictive ability to explain the mechanics of the other cervical levels.

In summary, the size of a spinal tissue appears to be the primary dictator of its developmental properties; however the tissues' material properties confer a portion of its developmental mechanics. Gender based differences in spinal tolerance are dictated by the material properties since size between genders cannot predict vertebral tolerance accurately. Finally, the structural properties not constituent properties of individual functional spinal units have emerged the primary indicator of their mechanics. These relationships define the mechanical response of the developing spine and may be incorporated into statistical and computational modeling efforts.

7.3. PREDICTORS OF SPINAL INJURY

The data collected in this research effort will aid in spinal injury prediction through enhanced tolerance values for modeling and anthropomorphic test dummies as well as aid in the assessment of spinal injuries through an analysis of specific mechanisms. Therefore, these predictive tools, based on baboon biomechanical data, may have applications in child injury prevention and management.

Previous tolerance values for the developing spine (***Table 2***) included a 3,000-N load in compression and tension for the 6-year old and a 1,000-N load in tension for the 3-year old. The most recent formulation of the automotive standard FMVSS 208 was developed using some of the tensile data collected herein and represents a significant improvement in injury reference values for children. These new standards match quite closely with the experimental scaling from this research (***Table 14***). The FMVSS 208 peak tolerance values underestimate in tension, but overestimate the compressive thresholds as measured in this work. It is important to note that the tensile testing in this study was performed quasi-statically. Thus, the absolute tolerance values reported are likely conservative given the results of the high rate tensile experiments. The scaling values though, should be independent of rate if the effect of rate is consistent across the developmental spectrum. Further, since the pediatric data are scaled from the adult human tolerance

values, the child tolerances are only as accurate and rate-applicable as the adult human values. Even with these limitations, the injury reference values discovered herein may be applied to anthropomorphic test dummy assessment. In this way, these tolerance values provide an injury prediction tool for automotive crash scenarios involving pediatric occupants.

Table 14. *Neck Injury Thresholds Revisited. The 'New' tolerance values are those generated from the scaling data of this research project and have basis in experimental biomechanics experimentation. The FMVSS tolerance data are those currently mandated by NHTSA for crash-test compliance and are based on a number of scaling factors including experimental data. Finally, the 'Old' tolerance values were those representing the previous standard without the support of biomechanical data.*

Age	**Tension**			**Compression**		
	New	FMVSS	Old	New	FMVSS	Old
Adult	4,170-N	4,170-N	3,300-N	4,000-N	4,000-N	4,000-N
12-y.o.	2,293-N			2,200-N		
6-y.o.	1,543-N	1,490-N	3,000-N	1,600-N	1,820-N	3,000-N
3-y.o.	1,251-N	1,130-N	1,000-N	1,280-N	1,380-N	
1-y.o.	1,042-N			1,080-N		

Loading rate was found to alter the failure mechanics of 10-year old human equivalent baboon tissues significantly. The failure load was found to be up to 4-times greater at higher loading rates (5-m/sec) than for the quasi-static failure experiments. Others have demonstrated loading rate effects in adult tissues,[151, 196, 199] but this research provides a relationship which enables loading rate scaling of pediatric spinal tolerance. Unfortunately, as yet, we do not know the relationship between loading rate and the development of spinal tissues. Perhaps this relationship is constant since the viscous response of the spine (time constant) exhibits little age dependence. Loading rate significantly affects the mechanical response of the developing spine and thus should be incorporated into any predictive model of spinal mechanics.

The mechanical predictive tool enables the assessment of injurious loads in the pediatric spine; however, when the child exceeds these loads, injury occurs which requires management. The tissue failure characteristics uncovered in this research provide another predictive tool which may guide management in the clinic. The most susceptible spinal level to injury (the lowest ultimate failure load) was found to correspond to the epidemiology literature quite well. The lower cervical spine was the most susceptible level to injury in compression and tension for each age except that of the very young (<5-years). Here the tolerance of the upper cervical spine was very similar to that of the lower cervical spine. Thus, the load path may dictate which level is injured for this young age group. In general though, this suggests regions where special attention should be taken to attempt to determine if a spinal injury exists. Since radiographic assessment is difficult, perhaps this work will enable the clinical focus to be directed to a specific region of the spine based upon the age of the child and the suspected mode of loading.

Each of the compression and tension experiments revealed distinct tissue injuries which can be categorized mechanistically. A common thread between all of the pediatric injuries was the involvement of the physis. The tensile series demonstrated physis failures that were predominantly of the inferior physis, revealing the relative strength of the superior growth plate. No distinguishable patterns were present between developing or adult tissues of the lower cervical spine. The Oc-C2 level exhibited differing tissue failures with age suggesting a relative weakness of the dens in early childhood and adulthood with respect to the surrounding ligamentous tissues. Tissue structural analyses revealed that the pediatric tensile physis failures occurred through the zone of calcification and did not include damage to the intervertebral disc. On the contrary, adult tensile injuries involved lesions of the endplate associated with intervertebral disc structural damage.

The compressive mechanisms involved injuries to the physis, vertebra, and intervertebral disc tissues. These compression tissue failures were quite severe and had symptoms suggesting instability. Compression injuries always involved the growth plate whether the associated injury was disc herniation or burst fracture. Indications for these

compression injuries are that they have severely disrupted the growth region of the spine and therefore, fusion for stabilization purposes is preferable. Injuries involving tensile mechanisms may not require fusion if a growth plate is injured since the disc will likely be intact. Non-operative strategies may benefit the child in these cases where the growth potential is high and they are not dangerously unstable.

7.4. SCALING AND MODELING OF THE HUMAN CHILD SPINE

The primary model investigated in this research was the cadaveric baboon. It represented the best model for understanding developing tissues and provided an excellent anatomical comparison with the human spine. The adult baboon spine is approximately 3/4 the size of the human adult spine. Therefore, the direct application of structural mechanical properties will be in error. The material properties generated herein represent the best data set for application to the human in computational, statistical, or physical models. This model assumes that the constituent mechanics of spinal tissues and their rate of development with skeletal maturation are similar across species. There are no indications that this is untrue, so the effects of small changes in the material property development rate should be nearly insignificant. As previously stated, the differences between the sexes in *papio anubis* are quite pronounced, and when comparing anatomy, more disparate than in humans. Gender based predictions of spinal mechanics should therefore be cautiously utilized. Another difference between the baboon and human cervical spine is at the cervical-thoracic junction. The baboon spine naturally bends in extension up to approximately 20-degrees across three spinal levels (T1-3). The human spine bends approximately 4-degrees across these same levels. Therefore, any segment involving the first thoracic vertebra may be susceptible to natural extension due to the spinal ligament and disc anatomy. This angulation is beneath the C7-T1 functional spinal unit, but may affect it. In all though, the baboon spine represents an excellent model for the evaluation of spinal biomechanics as they are related to skeletal maturity or development.

Validation of this model is necessary for its applicability to be accepted. Therefore, a comparison of the adult data collected herein and the human adult spine literature should

provide a good first validation of the cadaver baboon model. A comparison of the vertebral body compression testing revealed adult modulus (275-MPa) and strength (19-MPa) to overlap human vertebral body and isolated trabecular bone material properties.[80, 91, 136, 139] Comparison of the adult baboon functional spinal unit was more difficult due to the lack of data in the literature. The single FSU tensile modulus was found in this study for adult baboons to be 12.0-MPa (C3-C4), 10.1-MPa (C5-C6), and 9.8-MPa (C7-T1). These values compare quite well with data from Yoganandan et al.[205] reporting adult values of 12.75-MPa (C3-C4), 11.8-MPa (C5-C6), and 11.1-MPa (C7-T1) for the human spine. These mechanical associations provide a good degree of confidence in the baboon model as a predictor for human spine material properties. Further validation of this model is necessary using human pediatric tissues; however, in light of the complete dearth of developmental biomechanics data on the spine, this model provides substantial functional and tolerance criteria.

The computational modeling of the developing spine is a precursor to the development of injury prevention schemes for children. The first model of the developing spine bestowed nonlinear elastic responses to these tissues with success. An examination of the stress-relaxation time constants reveals that the viscous component of the developing spine is relatively insensitive to maturation. The time constants are not significantly correlated with age when you separate out the spinal levels. Thus, they appear to remain constant even though the tissue enhances its constituent makeup and organization. This leads me to believe that the viscous component of viscoelasticity is not directly related to the elastic function of the tissue since they do not develop together. Further research is needed to more completely understand this relationship; however, the development of constituent equations should remain a goal for this data due to their broad applicability in modeling.

7.5. LIMITATIONS

Limitations of this research include the use of an animal model which, although the baboon anatomically and mechanically compares well with humans, is only

approximately 3/4 the size. Further, these data were collected on osteoligamentous specimens and the absence of musculature may influence the functional biomechanics. A uniform quasi-static loading rate was used for all of these experiments to define their functional characteristics and that rate might not approximate the rates at which certain events occur. However, this low loading rate offers a first step from which increasing rates of loading can be investigated. The failure tests on the vertebral bodies and single functional spinal units were performed at quasi-static loading rates, so their failure loads are likely conservative. This limitation is further manifest in the assessment of the injuries to these tissues. For the tension series though, there was no difference between the quasi-static tissue failures and the dynamic tissue failures. The loads were, however, very different. Finally, the use of the disc cross-sectional area and height for normalization purposes may lead to experimental inaccuracies. These tissues were normalized using only the disc while the other structures of the spine were intact and carrying load. Thus, the material properties should be applicable to the functional spinal units as a whole but not representative of disc properties. In this respect the material properties represent a bulk modulus and strength for the entire functional spinal unit. This limitation should not affect the results significantly; however it was necessary to normalize the developmental mechanics for broad application.

Another limitation is the observation and review of the failed tissues. All radiographs and CTs were viewed and annotated by at least two observers; however, the dissected 2-FSU compression failures and physis histological sections were only examined by myself. Also, the computational modeling involved a number of assumptions which limit its applicability and predictive strength. First, the Kelvin-Voigt model alone may not completely describe the complex mechanics of spinal viscoelastic tissues and a more complicated system of springs and dashpots is required. Further, the nonlinear curve fits of the experimental data did not perfectly approximate the experimental data leading to inaccuracies. While the estimation of damping using the hysteresis energy has sound basis, it assumes perfect triangular waves at high rates which were unable to be produced experimentally. All of these limitations aside, this research provides a glimpse into the

functional and tolerance biomechanics of the developing spine which has not previously been known.

CHAPTER 8:
CONCLUSION

The developmental morphology of the human cervical spine reveals a highly dynamic and interdependent system within which the tissue morphology and mechanics are coupled. The paucity of data pertaining to the basic functional morphology and biomechanics of the developing neck has been manifest in numerous spinal injuries to the pediatric populace with catastrophic outcomes. Prevention of these injuries has been attempted using unvalidated models with neck injury thresholds established in the absence of experimental data. Further, a lack of understanding of the progression of these injuries and the tissues at risk obviates the development of clinical management procedures. Therefore, this research effort has included experimental and computational investigations into the biomechanical response of the developing spine. The measurement of the maturing spine's functional biomechanics enables 'physiologic' computational modeling and physical modeling with biofidelic responses. The tolerance measurements provide thresholds for injury in these models. And the failures generated in these developing spinal tissues provide an enhanced understanding of the maturing physis and its injury. Together, these data support the clinical management of injuries to children and facilitate the modeling of injury situations, providing realistic predictions to aid in the generation of enhanced injury prevention schemes.

CHAPTER 9:
FUTURE RESEARCH

This research project is just the beginning of what could become a career defining the maturation of connective tissues. The first step following this research involves the complete quasi-linear viscoelastic modeling of each functional spinal unit in compression and tension. This will facilitate the development of a rigid body dynamic model to aid in understanding the developmental biomechanical response of the spine. This model will enable parametric analyses and simple tests to motivate further experimental work without wasting precious tissues. This model will need to be validated and so that will be the next experimental endeavor of this project. Human pediatric tissues will be tested non-destructively in various loading directions and then failed in different modes at the various levels. In this way, a few human pediatric tissues will facilitate the validation of the model in a number of loading directions. Basic science questions will also be addressed as they relate to the maturation of tissues. The investigation of material properties versus structural properties throughout development remains intriguing. Further, the gender differences identified in this model suggest the further characterization of these tissues for their bone mineral density, hormone/cytokine levels, or microstructure. Also, it would be interesting to examine the differences between the intervertebral disk tissue and the supporting ligaments. This would mean an examination of the various spinal tissues individually for their contribution to the mechanics of the functional spinal unit. This would enhance modeling efforts and basic understanding of the maturation of specific connective tissues. Complete comprehension of these

developmental changes in spinal tissues may have broad-reaching applications as well as spawn other research projects.

GLOSSARY

Anisotropic – A tissue containing material properties that vary with direction.

Avulsion – A tearing away or forcible separation of the bone by its ligamentous attachment.

Biofidelic – Containing properties enabling a structure to match the biologic tissue response for a given loading input.

Burst Fracture – Produced by axial compression at high loading rates resulting in the fragmentation of the vertebral body in the transverse plane and a loss of vertebral body height.

Cancellous Bone – Bone with lattice-like or spongy structure.

Cortical Bone – A superficial thin layer of compact bone.

Creep – Progressive deformation of soft tissues due to a constant load over an extended period of time.

Dens – The superior bony projection of C2 (axis) upward to within the C1 (atlas) vertebral ring. This bony prominence enables much of the axial rotation of the cervical spine (≈40-degrees) and is the source of fractures with sever consequences. Type I dens fractures are oblique fracture through the upper part of the dens, type II dens fractures occur through the junction of the dens with the body of C2 and type III dens fractures occur through the body of the axis. Also called the Odontoid.

Ductile – The quality whereby a material exhibits extensive deformation before failure.

Elasticity – Property of a material that allows it to return to its original shape and size after being deformed.

Elastic Zone – The zone of spinal motion whereby the load-deformation curve is linear (elastic).

FSO – Full Scale Output. Is used to refer to a quality of a device based on its full scale output.

Functional Spinal Unit – A single functional spinal unit includes two vertebrae with the intervening disc and soft tissues. One spinal motion segment.

Haversine – An inverted cosine wave offset by half its amplitude. If continuous, it appears as a sine wave with an offset.

Injury Assessment Values – Thresholds of biological tissue failure that are used in conjunction with anthropomorphic test dummy outputs to define protection reference values of safety.

Latitudinal – In reference to spinal growth it is the circumferential growth of the vertebral body outward laterally in the transverse plane.

Longitudinal – In reference to spinal growth it is the height growth of the vertebral body out of the transverse plane.

Material Properties - Mechanical properties of modulus of elasticity and strength which are normalized by the geometry of the structure tested so that these properties define any volume of the material.

Meninges – Ligamentous attachments along the length of the spinal canal which attach to the spinal cord and hold it in place.

Modulus of Elasticity – The ratio of the stress to strain at any point in the elastic region of a load-deformation curve, yielding a value for stiffness.

Neutral Zone – The zone of spinal motion which exists when very small loads are applied to the spine and ends when the soft tissues of the spine start becoming taut.

Patho-Mechanics – Condition of tissues related to the mechanics (effects of forces) on the tissues. Refers to the injured or functional tissue response from a mechanical standpoint following a mechanical event.

Patho-Morphology – Condition of tissues related to the morphology of the tissues. Refers to the injured or intact morphological appearance (organization and position) of tissues following a mechanical event.

Physis (Physeal) – The primary longitudinal growth region in the bones of the skeleton. The physis contains morphologically distinct cellular zones which transform a cartilaginous analog into bone.

PIDF – Proportional, Integral, Differential, and Feedforward feedback control provide different control parameters. The proportional gain establishes the correct magnitude and shape of the waveform, integral control adjusts the steady state response, differential control can be used to remove overshoot and tune the dynamic event and feedforward control will stabilize a dynamic waveform.

Primary Spongiosa – Initially calcified spongy bone lying adjacent to the physis.

Protection Reference Value – Data which defines safe limits of anthropomorphic test dummy outputs to specific loading conditions.

Secondary Spongiosa – Spongy bone that has been transformed by osteoclast/osteoblast remodeling into stronger cancellous bone than the primary spongiosa.

Sexual Dimorphism – The occurrence of distinct anatomical structure, size, etc. between the genders of the same species.

Spinal Anatomy – The lumbar vertebra below serves as a review of relevant spinal anatomy.

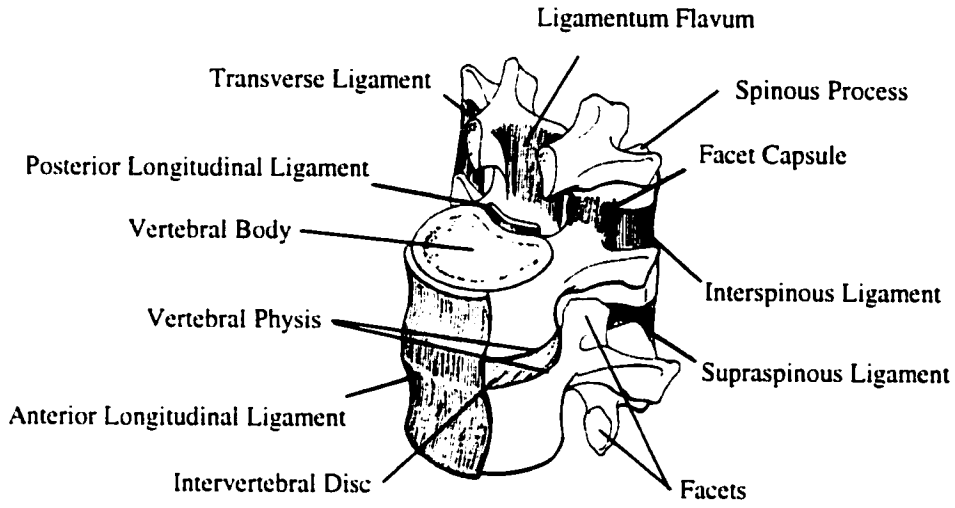

Stiffness – Defines the load–deformation relationship of a tissue. The slope of the linear region of the load-displacement profile is the measure of stiffness.

Stress-Relaxation – decrease in the stress in a tissue with time after a material has been deformed to a constant length.

Structural Properties - Properties of stiffness and ultimate failure load which are specific to the geometry of the material tested. These properties are applicable only to the material tested with similar geometry and size.

Teardrop Fracture – Produced by axial compression of the neutral and minimally flexed cervical spine resulting in a sagittal fracture plane that runs horizontally near the anterior endplate/growth plate.

Viscoelasticity – Property whereby a material exhibits a change of stress or deformation over time when under constant deformation (stress relaxation) or under constant load (creep).

Wedge Compression Fracture – Produced by axial compression at no more than 1-cm anterior to neutral position resulting in a wedging of the anterior vertebral body.

LIST OF ABBREVIATIONS

ABL - Applied Biomechanics Laboratory

AIS - Abbreviated Injury Score

CFC - Channel Frequency Class

DAC - Data Acquisition Card

FMVSS - Federal Motor Vehicle Safety Standard

FSU - Functional Spinal Unit

LVDT - Linear Variable Differential Transformer

MTS - Materials Testing System

NHTSA – National Highway Traffic Safety Administration

PIDF - Proportional, Integral, Differential, and Feedforward

PMMA - Poly-Methylmethacrylate

SAE - Society of Automotive Engineers

SCIWORA - Spinal Cord Injury WithOut Radiographic Anomaly

BIBLIOGRAPHY

1. National Center for Statistics and Analysis. Fatality Analysis Reporting System. 1997.
2. AHMANN, PA, SMITH, SA, SCHWARTZ, JF and CLARK, DB. Spinal cord infarction due to minor trauma in children. Neurology 1975;25:301-7.
3. ALLEN, BL, JR., FERGUSON, RL, LEHMANN, TR and O'BRIEN, RP. A mechanistic classification of closed, indirect fractures and dislocations of the lower cervical spine. Spine 1982;7:1-27.
4. AUFDERMAUR, M. Spinal injuries in juveniles. Necropsy findings in twelve cases. J-Bone-Joint-Surg-Br 1974;56B:513-9.
5. BACKAITIS, S and MERTZ, H. Hybrid III: The First Human-Like Crash Test Dummy. Warrendale: Society of Automotive Engineers, Inc., 1994.
6. BAILEY, DK. The Normal Cervical Spine in Infants and Children. Radiology 1952;59:712-19.
7. BANK, RA, BAYLISS, MT, LAFEBER, FP, MAROUDAS, A and TEKOPPELE, JM. Ageing and zonal variation in post-translational modification of collagen in normal human articular cartilage. The age-related increase in non-enzymatic glycation affects biomechanical properties of cartilage. Biochem J 1998;330:345-51.
8. BARTLEY JR., M, ARNOLD, J, HASLAM, R and JEE, W. The relationship of bone strength and bone quality in health, disease, and aging. J Gerontol 1966;21:517-21.
9. BELL, G, DUNBAR, O, BECK, J and GIBB, A. Variations in strength of vertebrae with age and their relation to osteoporosis. Calcif Tissue Res 1967;1:75-86.
10. BELYTSCHKO, T, SCHWER, L and PRIVITZER, E. Theory and application of a three-dimensional model of the human spine. Aviation Space and Environmental Medicine 1978;9:158.
11. BICK, E and COPEL, J. The Ring Apophysis of the Human Vertebra. J Bone and Joint Surgery 1951;33-A:783-7.
12. BOLING, EP. Gender and osteoporosis: similarities and sex-specific differences. J Gend Specif Med 2001;4:36-43.
13. BONNEL, F, DIMEGLIO, A, BALDET, P and RABISCHONG, P. Biomechanical activity of the growth plate. Clinical incidences. Anat Clin 1984;6:53-61.
14. BREIG, A. Biomechanics of the Central Nervous System. Stockholm: Almquist and Wiksell, 1960.
15. BRIGHT, R. Physeal Injuries. In: Fractures in Children. ed. Rockwood, C, Wilkins, K and King, R. Philadelphia: J.B. Lippincott Co., 1991.
16. BRIGHTON, CT. Structure and function of the growth plate. Clin Orthop 1978;22-32.
17. BRIGHTON, CT. Morphology and biochemistry of the growth plate. Rheum Dis Clin North Am 1987;13:75-100.

18. BRYCE, R, ASPDEN, R and WYTCH, R. Stiffening effects of cortical bone on vertebral cancellous bone in situ. Spine 1995;20:999-1003.

19. BUCKLEY, SL, GOTSCHALL, C, ROBERTSON, W, JR., STURM, P, TOSI, L, THOMAS, M and EICHELBERGER, M. The relationships of skeletal injuries with trauma score, injury severity score, length of hospital stay, hospital charges, and mortality in children admitted to a regional pediatric trauma center. J-Pediatr-Orthop 1994;14:449-53.

20. CAIN, CC and FRASER, RD. Bony and vascular anatomy of the normal cervical spine in the sheep. Spine 1995;20:759-65.

21. CAMACHO, D. Dynamic Response of the Head and Cervical Spine to Near-Vertex Head Impact: An Experimental and Computational Study. Department of Biomedical Engineering,Duke University. 1998.

22. CAMACHO, D, NIGHTINGALE, R, ROBINETTE, J, VANGURI, S, COATES, D and MYERS, B. Experimental Flexibility Measurements for the Development of a Computational Head-Neck Model Validated for Near-Vertex Head Impact. Proceedings of STAPP 1997;41st Annual Meeting:473-86.

23. CANALE, S. Physeal Injuries. In: Skeletal Tramua in Children. ed. Green, N and Swiontkowski, M. Philadelphia: WB Saunders Co., 1998.

24. CARTER, JW. Compressive Cervical Spine Injury: The Effect of Injury Mechanism on Structural Injury Pattern and Neurologic Injury Potential. Department of Bioengineering,University of Washington. 2002.

25. CARTER, JW, MIRZA, SK, TENCER, AF and CHING, RP. Canal geometry changes associated with axial compressive cervical spine fracture. Spine 2000;25:46-54.

26. CATTELL, H and FILTZER, D. Pseudosubluxation and other normal variations in the cervical spine in children. A study of one hundred and sixty children. J. Bone Joint Surg (Am) 1965;47:1295-309.

27. CHESHIRE, DJ. The paediatric syndrome of traumatic myelopathy without demonstrable vertebral injury. Paraplegia. 1977;15:74-85.

28. CHOI, JU, HOFFMAN, HJ, HENDRICK, EB, HUMPHREYS, RP and KEITH, WS. Traumatic infarction of the spinal cord in children. J-Neurosurg 1986;65:608-10.

29. CLAUSEN, J, GOEL, V, TRAYNELIS, V and SCIFERT, J. Uncinate processes and Luschka joints influence the biomechanics of the cervical spine: Quantification using a finite element model of the C5-C6 segment. J Orthop Res 1997; 15:342-7.

30. COHEN, B, CHORNEY, GS, PHILLIPS, DP, DICK, HM, BUCKWALTER, JA, RATCLIFFE, A and MOW, VC. The microstructural tensile properties and biochemical composition of the bovine distal femoral growth plate. J Orthop Res 1992;10:263-75.

31. CRAWFORD, AH. Operative treatment of spine fractures in children. Orthop-Clin-North-Am 1990;21:325-39.

32. CURREY, J and BUTLER, G. The mechanical properties of bone tissue in children. J Bone Joint Surg 1975;57-A:810-4.

33. CURREY, JD. Changes in the Impact Energy Absorption of Bone with Age. Journal of Biomechanics 1979;12:459-69.

34. CUSICK, JF, MYKLEBUST, J, ZYVOLOSKI, M, SANCES, A, JR., HOUTERMAN, C and LARSON, SJ. Effects of vertebral column distraction in the monkey. J Neurosurg 1982;57:651-9.

35. DANTO, MI and WOO, SL. The mechanical properties of skeletally mature rabbit anterior cruciate ligament and patellar tendon over a range of strain rates. J Orthop Res 1993;11:58-67.

36. DAUVILLIERS, F, BENDJELLAL, F, WEISS, M, LAVASTE, F and TARRIERE, C. Development of a finite element model of the neck. Proc 38th Stapp Car Crash Conference 1994;#942210:77-91.

37. DE JAGER, M, SAUREN, A, THUNNISSEN, J and WISMANS, J. A three-dimensional head-neck model: validation for frontal and lateral impacts. Proc 38th Stapp Car Crash Conference 1994;#942211:93-109.

38. DE JAGER, M, SAUREN, A, THUNNISSEN, J and WISMANS, J. A global and detailed mathematical model for head-neck dynamics. Proc 40th Stapp Car Crash Conference 1996;#962430:269-81.

39. DENG, Y and GOLDSMITH, W. Response of a human head/neck/upper-torso replica to dynamic loading – II. Analytical/numerical model. J Biomech 1987;20:487-97.

40. DESANTIS KLINICH, K, SAUL, R, AUGUSTE, G, BACKAITIS, S and KLEINBERGER, M. Techniques for developing child dummy protection reference values. NHTSA Event Report: Child Injury Protection Team. 1996.

41. DICKMAN, CA, CRAWFORD, NR, TOMINAGA, T, BRANTLEY, AG, COONS, S and SONNTAG, VK. Morphology and kinematics of the baboon upper cervical spine. A model of the atlantoaxial complex. Spine 1994;19:2518-23.

42. DICKMAN, CA, ZABRAMSKI, JM, HADLEY, MN, REKATE, HL and SONNTAG, VK. Pediatric spinal cord injury without radiographic abnormalities: report of 26 cases and review of the literature. J Spinal Disord 1991;4:296-305.

43. DIETRICH, AM, GINN, P-ME, BARTKOWSKI, HM and KING, DR. Pediatric cervical spine fractures: predominantly subtle presentation. J-Pediatr-Surg 1991;26:995-9; discussion 9- 1000.

44. DOSKOCIL, M, VALOUCH, P and PAZDERKA, V. On vertebral body growth. Funct Dev Morphol 1993;3:149-55.

45. DVORAK, J, ANTINNES, JA, PANJABI, M, LOUSTALOT, D and BONOMO, M. Age and gender related normal motion of the cervical spine. Spine 1992;17:S393-8.

46. DVORAK, J, PANJABI, MM, NOVOTNY, JE and ANTINNES, JA. In vivo flexion/extension of the normal cervical spine. J Orthop Res 1991;9:828-34.

47. EBBESEN, EN, THOMSEN, JS, BECK-NIELSEN, H, NEPPER-RASMUSSEN, HJ and MOSEKILDE, L. Lumbar vertebral body compressive strength evaluated by dual-energy X-ray absorptiometry, quantitative computed tomography, and ashing. Bone 1999;25:713-24.

48. EDMONDSTON, SJ, SINGER, KP, DAY, RE, PRICE, RI and BREIDAHL, PD. Ex vivo estimation of thoracolumbar vertebral body compressive strength: the relative contributions of bone densitometry and vertebral morphometry. Osteoporos Int 1997;7:142-8.

49. EDWARDS, W. Principles of cervical spine biomechanical testing. In: Frontiers in head and neck trauma. ed. N. Yoganandan, E A. Washington, D.C.: IOS Press, 1998.

50. ELERAKY, MA, THEODORE, N, ADAMS, M, REKATE, HL and SONNTAG, VK. Pediatric cervical spine injuries: report of 102 cases and review of the literature. J Neurosurg 2000;92:12-7.

51. EPPINGER, R, SUN, E, BANDAK, F, HAFFNER, M, KHAEWPONG, N and MALTESE, M. Development of improved injury criteria for the assessment of advanced automotive restraint systems - II. National Highway Traffic Safety Administration. Washington D.C. 1999.

52. EPSTEIN, NE and EPSTEIN, JA. Limbus lumbar vertebral fractures in 27 adolescents and adults. Spine 1991;16:962-6.

53. EPSTEIN, NE, EPSTEIN, JA and MAURI, T. Treatment of fractures of the vertebral limbus and spinal stenosis in five adolescents and five adults. Neurosurgery 1989;24:595-604.

54. EVANS, DL and BETHEM, D. Cervical spine injuries in children. J-Pediatr-Orthop 1989;9:563-8.

55. FESMIRE, FM and LUTEN, RC. The pediatric cervical spine: developmental anatomy and clinical aspects. J-Emerg-Med 1989;7:133-42.

56. FISHER, L and VAN BELLE, G. Biostatistics : a methodology for the health sciences. New York: J. Wiley, 1993.

57. FISHMAN, L. Chronological versus skeletal age, an evaluation of craniofacial growth. Angle Orthod 1979;49:181-9.

58. FISHMAN, L. Radiographic evaluation of skeletal maturation; a clinically oriented method based on hand wrist films. Angle Orthod 1982;52:88-112.

59. FISHMAN, L. Maturation patterns and prediction during adolescence. Angle Orthod 1987;57:178-93.

60. FRISCHHOLZ, R and SPINNLER, K. Class of Algorighms for Realtime Subpixel Registration. Fraunhofer Institute for Integrated Circuits IIS. Erlangen, Germany. 2000.

61. FUNG, Y. Biomechanics: Mechanical Properties of Living Tissues. New York: Springer-Verlag, 1993.

62. FUNK, JR, HALL, GW, CRANDALL, JR and PILKEY, WD. Linear and quasi-linear viscoelastic characterization of ankle ligaments. J Biomech Eng 2000;122:15-22.

63. FYHRIE, DP and SCHAFFLER, MB. Failure mechanisms in human vertebral cancellous bone. Bone 1994;15:105-9.

64. GARC'IA, F-P, TORRE, H, FLORES, L and REA, J. The cervical vertebrae as maturational indicators. J-Clin-Orthod 1998;32:221-5.

65. GAUFIN, L and GOODMAN, S. Cervical Spine Injuries in Infants: Problems in Management. J of Neurosurgery 1975;42:179-84.

66. GILAD, I and NISSAN, M. A study of vertebra and disc geometric relations of the human cervical and lumbar spine. Spine 1986;11:154-7.

67. GILSANZ, V, BOECHAT, MI, GILSANZ, R, LORO, ML, ROE, TF and GOODMAN, WG. Gender differences in vertebral sizes in adults: biomechanical implications. Radiology 1994;190:678-82.

68. GILSANZ, V, BOECHAT, MI, ROE, TF, LORO, ML, SAYRE, JW and GOODMAN, WG. Gender differences in vertebral body sizes in children and adolescents. Radiology 1994;190:673-7.

69. GOEL, V and CLAUSEN, J. Prediction of load sharing among spinal components of a C5-C6 motion segment using the finite element approach. Spine 1998;23:684-91.

70. GRAUER, J, PANJABI, M, CHOLEWICKI, J, NIBU, K and DVORAK, J. Whiplash Produces an S-Shaped Curvature of the Neck with Hyperextension at Lower Levels. Spine 1997;22:2489-94.

71. GRECO, F, DE PALMA, L, SPECCHIA, N and MANNARINI, M. Growth-plate cartilage metabolic response to mechanical stress. J. Pediatric Orthopaedics 1989;9:520-4.

72. GUSE, RJ, CONNOLLY, JF, ALBERTS, R and LIPPIELLO, L. Effect of aging on tensile mechanical properties of the rabbit distal femoral growth plate. J Orthop Res 1989;7:667-73.

73. HADLEY, MN, ZABRAMSKI, JM, BROWNER, CM, REKATE, H, SONNTAG, V and K. Pediatric spinal trauma. Review of 122 cases of spinal cord and vertebral column injuries. J-Neurosurg 1988;68:18-24.

74. HALL, B. Immobilization and cartilage transformation into bone in the embryonic chick. Anat. Rec 1972;173:391-404.

75. HAMILTON, MG and MYLES, ST. Pediatric spinal injury: review of 174 hospital admissions. Journal Of Neurosurgery 1992;77:700-4.

76. HAMILTON, MG and MYLES, ST. Pediatric spinal injury: review of 61 deaths. J-Neurosurg 1992;77:705-8.

77. HANDEL, SF, TWIFORD, TW, JR., REIGEL, DH and KAUFMAN, HH. Posterior lumbar apophyseal fractures. Radiology 1979;130:629-33.

78. HANSSON, T. Work and back injuries. Sem Spine Surg. 1992;2-15.

79. HASSEL, B and FARMAN, AG. Skeletal maturation evaluation using cervical vertebrae [published erratum appears in Am J Orthod Dentofacial Orthop 1995 Jun;107(6):19A]. Am-J-Orthod-Dentofacial-Orthop 1995;107:58-66.

80. HAYES, WC, PIAZZA, SJ and ZYSSET, PK. Biomechanics of fracture risk prediction of the hip and spine by quantitative computed tomography. Radiol Clin North Am 1991;29:1-18.

81. HENRYS, P, LYNE, ED, LIFTON, C and SALCICCIOLI, G. Clinical review of cervical spine injuries in children. Clin-Orthop 1977;172-6.

82. HILL, S, MILLER, C, KOSNIK, E and HUNT, W. Pediatric Neck Injuries: A Clinical Study. J of Neurosurgery 1984;60:700-6.

83. HUBBARD, D. Injuries of the Spine in Children and Adolescents. Clinical Orthopaedics and Related Research 1974;100:56-65.

84. HUNZIKER, EB. Growth plate structure and function. Pathol Immunopathol Res 1988;7:9-13.

85. HUNZIKER, EB. Mechanism of longitudinal bone growth and its regulation by growth plate chondrocytes. Microsc Res Tech 1994;28:505-19.

86. IANNOTTI, JP. Growth plate physiology and pathology. Orthop Clin North Am 1990;21:1-17.

87. IATRIDIS, JC, SETTON, LA, WEIDENBAUM, M and MOW, VC. The viscoelastic behavior of the non-degenerate human lumbar nucleus pulposus in shear. J Biomech 1997;30:1005-13.

88. KAIGLE, A, EKSTROM, L, ROSTEDT, M, HOLM, S and HANSSON, T. Minimum Thawing Time of Frozen Spinal Specimens used for in-vitro Biomechanical Testing. XVIIth ISBCongress. Calgary, Canada:1999;

89. KANEOKA, K, ONO, K, INAMI, S and HAYASHI, K. Possible Zygapophyseal Joint Injury Mechanism During Whiplash Loading. Proceedings of the Orthopaedic Research Society 1998;44th Annual Meeting:

90. KASAI, T, IKATA, T, KATOH, S, MIYAKE, R and TSUBO, M. Growth of the cervical spine with special reference to its lordosis and mobility. Spine 1996;21:2067-73.

91. KELLER, T. Predicting the compressive mechanical behavior of bone. J Biomech 1994;27:1159-68.

92. KELLER, T, HANSSON, T, ABRAM, A, SPENGLER, D and PANJABI, M. Regional variations in the compressive properties of lumbar vertebral trabeculae. Effects of disc degeneration. Spine 1989;14:1012-9.

93. KELLER, T, ZIV, I, MOELJANTO, E and SPENGLER, D. Interdependence of lumbar disc and subdiscal bone properties: a report of the normal and degenerated spine. Journal of Spinal Disorders 1993;6:106-13.

94. KEWALRAMANI, LS and TORI, JA. Spinal cord trauma in children. Neurologic patterns, radiologic features, and pathomechanics of injury. Spine 1980;5:11-8.

95. KIRKISH, S. Comparison of the NHTSA & Hybrid III Child Dummies. attachment I to minutes of the Hybrid III Dummy Family Task Group 1995;October 18, 1995.

96. KLEINBERGER, M. Application of finite element techniques to the study of cervical spine mechanics. Proc 37th Stapp Car Crash Conference 1993;#933131:261-72.

97. KLEINBERGER, M and SUMMERS, L. Mechanisms of injuries for adults and children resulting from airbag interactions. Association for the Advancement of Automotive Medicine. Orlando, FL:1997;405-20.

98. KLEINBERGER, M, SUN, E, EPPINGER, R, KUPPA, S and SAUL, R. Development of Improved Injury Criteria for the Assessment of Advanced Automotive Restraint Systems. NHTSA. 1998.

99. KNUTSSON, F. Growth and Differentiation of the Postnatal Vertebra. Acta Radiologica 1961;55:401-8.

100. KOELLER, G, S, M, MEIER, W and HARTMANN, F. Biomechanical properties of human intervertebral discs subjected to axial dynamic compression- influence of age and degeneration. J Biomech 1986;19:807-16.

101. KOTANI, Y, CUNNINGHAM, BW, CAPPUCCINO, A, KANEDA, K and MCAFEE, PC. The role of spinal instrumentation in augmenting lumbar posterolateral fusion. Spine 1996;21:278-87.

102. KRISS, VM and KRISS, TC. SCIWORA (spinal cord injury without radiographic abnormality) in infants and children. Clin-Pediatr-Phila 1996;35:119-24.

103. KUDLACEK, S, SCHNEIDER, B, RESCH, H, FREUDENTHALER, O and WILLVONSEDER, R. Gender differences in fracture risk and bone mineral density. Maturitas 2000;36:173-80.

104. KUMARESAN, S, YOGANANDAN, N and PINTAR, F. Finite element analysis of anterior cervical spine interbody fusion. Biomed Mater Eng 1997;7:221-30.

105. KUMARESAN, S, YOGANANDAN, N and PINTAR, FA. Age-Specific Pediatric Cervical Spine Biomechanical Responses: Three-Dimensional Nonlinear Finite Element Models. Proceedings of STAPP 1997;41st Annual Meeting:31-61.

106. KWAN, KM, PANG, MK, ZHOU, S, COWAN, SK, KONG, RY, PFORDTE, T, OLSEN, BR, SILLENCE, DO, TAM, PP and CHEAH, KS. Abnormal compartmentalization of cartilage matrix components in mice lacking collagen X: implications for function. J Cell Biol 1997;136:459-71.

107. KWAN, MK, LIN, TH and WOO, SL. On the viscoelastic properties of the anteromedial bundle of the anterior cruciate ligament. J Biomech 1993;26:447-52.

108. LAING, N. Abnormal development of vertebrae in paralyzed chick embryos. J Morphol 1982;173:179-84.

109. LAWSON, JP, OGDEN, JA, BUCHOLZ, RW and HUGHES, SA. Physeal injuries of the cervical spine. J-Pediatr-Orthop 1987;7:428-35.

110. LEE, FY, RHO, JY, HARTEN, R, JR., PARSONS, JR and BEHRENS, FF. Micromechanical properties of epiphyseal trabecular bone and primary spongiosa around the physis: an in situ nanoindentation study. J Pediatr Orthop 1998;18:582-5.

111. LENOX, JB, STALNAKER, RL, WHITE, CD, MOORE, GT, ANDERSON, OM, SCHLEICHER, RR, PEEL, HH, MARTIN, SS and DRISCOLL, GD. Development of Neck Injury Tolerance Criteria in Human Surrogates. I. Static Tensile Loading in the Baboon Neck: Preliminary Observations. Experimental Safety Vehicles 1982;Technical Session #5:279-86.

112. LEVENTHAL, H. Birth Injuries of the Spinal Cord. J of Pediatrics 1960;56:447-53.

113. LIND, B, SIHLBOM, H, NORDWALL, A and MALCHAU, H. Normal range of motion of the cervical spine. Arch Phys Med Rehabil 1989;70:692-5.

114. LINSENMAYER, TF, EAVEY, RD and SCHMID, TM. Type X collagen: a hypertrophic cartilage-specific molecule. Pathol Immunopathol Res 1988;7:14-9.

115. LUNDIN, O, EKSTROM, L, HELLSTROM, M, HOLM, S and SWARD, L. Injuries in the adolescent porcine spine exposed to mechanical compression. Spine 1998;23:2574-9.

116. LYSELL, E. Motion in the cervical spine. An experimental study on autopsy specimens. Acta Orthop Scand 1969;:Suppl:1+.

117. MANKIN, KP and ZALESKE, DJ. Response of physeal cartilage to low-level compression and tension in organ culture. J Pediatr Orthop 1998;18:145-8.

118. MARTINEZ, JB, OLOYEDE, VO and BROOM, ND. Biomechanics of load-bearing of the intervertebral disc: an experimental and finite element model. Med-Eng-Phys 1997;19:145-56.

119. MAUREL, N, LAVASTE, F and SKALLI, W. A three-dimensional parametrized finite element model of the lower cervical spine. Study of the influence of the posterior articular facets. J Biomech 1997;30:921-31.

120. MAZESS, RB. On aging bone loss. Clin Orthop 1982;239-52.

121. MCELHANEY, J. Biomechanical analysis of swimming pool neck injuries. Transactions of the SAE 1979;88:494-500.

122. MCELHANEY, JH, PAVER, JG, MCCRACKIN, HJ and MAXWELL, GM. Cervical spine compression responses. Proceedings of the 27th Stapp Car Crash Conference 1983;163-77.

123. MCGRORY, BJ, KLASSEN, RA, CHAO, EY, STAEHELI, JW and WEAVER, AL. Acute fractures and dislocations of the cervical spine in children and adolescents. J-Bone-Joint-Surg-Am 1993;75:988-95.

124. MCPHEE, IB. Spinal fractures and dislocations in children and adolescents. Spine 1981;6:533-7.

125. MELVIN, J. Injury Assessment Reference Values for the CRABI 6-month Infant Dummy in a Rear-Facing Infant Restraint with Air Bag Deployment. SAE International Congress and Exposition 1995;Paper #950872:

126. MENEZES, A. Traumatic lesions of the craniovertebral junction. In: Textbook of Craniovertebral Junction Abnormalities. ed. Vangilder, J, Menezes, A and Dolan, K. Mount Kisco: Futura Publishing, 1987.

127. MERTZ, H. An assessment of compressive neck loads under injury-producing conditions. Physician and Sports Medicine 1978;6:95-106.

128. MERTZ, H. Anthropomorphic Test Devices. In: Hybrid III: The First Human-Like Crash Test Dummy. ed. Backaitis, S and Mertz, H. Warrnedale, PA: Society of Automotive Engineers, Inc., 1994.

129. MERTZ, H, DRISCOLL, J, LENOX, J, NYQUIST, G and WEBER, D. Responses of animals exposed to deployment of various passenger inflatable restraint systems concepts for a variety of collision severities and animal positions. SAE Transactions 1982;Paper # 826047:

130. MERTZ, H and PATRICK, L. Strength and Response of the Human Neck. SAE Transactions 1971;80:Paper #710855.

131. MERTZ, H and WEBER, D. Interpretations of the impact responses of a three-year-old child dummy relative to child injury potential. SAE Transactions 1982;Paper #826048:

132. MERTZ, HJ. Injury assessment values used to evaluate Hybrid III response measurements. In: Hybrid III: The first human-like crash test dummy. ed. Backaitis, S and Mertz, H. Warrendale, PA: Society of Automotive Engineers, Inc., 1994.

133. MERTZ, HJ, PRASAD, P and IRWIN, AL. Injury Risk Curves for Children and Adults in Frontal and Rear Collisions. Proceedings of STAPP 1997;41st Annual Meeting:13-9.

134. MILLER, J and SKOGLAND, L. Musculoskeletal interactions in the adolescent spine. A study of the effect of some geometric and material property changes in a three-dimensional mathematical model. In: On the importance of growth in idopathic scoliosis. A biochemical, radiological and biomechanical study. University of Oslo. 1982.

135. MORA, S, GOODMAN, W, LORO, M, ROE, T, SAYRE, J and GILSANZ, V. Age-related changes in cortical and cancellous vertebral bone density in girls: assessment with quantitative CT. Am J Roentgenol 1994;162:405-9.

136. MOSEKILDE, L. Age-related changes in vertebral trabecular bone architecture-assessed by a new method. Bone 1988;9:247-50.

137. MOSEKILDE, L. Sex differences in age-related changes in vertebral body size, density and biomechanical competence in normal individuals. Bone 1990;11:67-73.

138. MOSEKILDE, L. Vertebral structure and strength in vivo and in vitro. Calcif Tissue Int 1993;53:S121-5: discussion S5-6.

139. MOSEKILDE, L and MOSEKILDE, L. Normal vertebral body size and compressive strength: relations to age and to vertebral and iliac trabecular bone compressive strength. Bone 1986;7:207-12.

140. MYERS, B. Failure tolerance of the adult cervical spine, Personal Communication, February 6, 2002. Washington, D.C.

141. MYERS, BS, McELHANEY, JH and DOHERTY, BJ. The viscoelastic responses of the human cervical spine in torsion: experimental limitations of quasi-linear theory, and a method for reducing these effects. J Biomech 1991;24:811-7.

142. MYERS, BS and WINKELSTEIN, BA. Epidemiology, classification, mechanism, and tolerance of human cervical spine injuries. Crit Rev Biomed Eng 1995;23:307-409.

143. MYKLEBUST, JB, PINTAR, F, YOGANANDAN, N, CUSICK, JF, MAIMAN, D, MYERS, TJ and SANCES, A, JR. Tensile strength of spinal ligaments. Spine 1988;13:526-31.

144. NEUMANN, P, EKSTROM, LA, KELLER, TS, PERRY, L and HANSSON, TH. Aging, vertebral density, and disc degeneration alter the tensile stress-strain characteristics of the human anterior longitudinal ligament. J-Orthop-Res 1994;12:103-12.

145. NEUMANN, P, KELLER, T, EKSTROM, L, HULT, E and HANSSON, T. Structural properties of the anterior longitudinal ligament. Correlation with lumbar bone mineral content. Spine 1993;18:637-45.

146. NEUMANN, P, KELLER, TS, EKSTROM, L and HANSSON, T. Effect of strain rate and bone mineral on the structural properties of the human anterior longitudinal ligament. Spine 1994;19:205-11.

147. NICHOLSON, P, CHENG, X, LOWET, G, BOONEN, S, DAVIE, M, DEQUEKER, J and VAN DER PERE, G. Structural and material mechanical properties of human vertebral cancellous bone. Med Eng Phys 1997;19:729-37.

148. NIGHTINGALE, R, MCELHANEY, J, CAMACHO, D, KLEINBERGER, M, WINKELSTEIN, B and MYERS, B. The Dynamic Responses of the Cervical Spine:

Buckling, End Conditions, and Tolerance in Compressive Impacts. Stapp Car Crash Conference 1997;41st Annual Meeting:451-71.

149. NITECKI, S and MOIR, CR. Predictive factors of the outcome of traumatic cervical spine fracture in children. J-Pediatr-Surg 1994;29:1409-11.

150. NOYES, F and GROOD, E. The strength of the anterior cruciate ligament in humans and rhesus monkeys: age-related and species-related changes. J. Bone Joint Surg 1976;58 A:1074-82.

151. NOYES, FR, DELUCAS, JL and TORVIK, PJ. Biomechanics of anterior cruciate ligament failure: an analysis of strain-rate sensitivity and mechanisms of failure in primates. J Bone Joint Surg Am 1974;56:236-53.

152. NYQUIST, G. Correlation of field injuries and GM Hybrid III dummy responses for lap-shoulder belt restraint. J. of Biomedical Engineering 1980;102:487-93.

153. OGDEN, J. Radiology of postnatal skeletal development. XI. The first cervical vertebra. Skeletal Radiol 1984;12:12-20.

154. OGDEN, J. Radiology of postnatal skeletal development. XII. The second cervical vertebra. Skeletal Radiol 1984;12:1169-77.

155. OGDEN, J, GANEY, T, SASSE, J, NEAME, P and HILBELINK, D. Development and Maturation of the Axial Skeleton. In: The Pediatric Spine: Principles and Practice. ed. Weinstein, S. New York: Raven Press, 1994.

156. OGDEN, J and GROGAN, D. Postnatal skeletal development and growth of the musculoskeletal system. In: The scientific basis of orthopaedics. ed. Albright, J and Ra, B. New York: Appleton & Lange, 1987.

157. OSENBACH, RK and MENEZES, AH. Spinal cord injury without radiographic abnormality in children. Pediatr Neurosci 1989;15:168-74.

158. PANG, D and POLLACK, IF. Spinal cord injury without radiographic abnormality in children--the SCIWORA syndrome. J-Trauma 1989;29:654-64.

159. PANG, D and WILBERGER, JE. Spinal cord injury without radiographic abnormality in children. Journal of Neurosurgery 1982;57:114-29.

160. PANJABI, MM, CRISCO, JJ, VASAVADA, A, ODA, T, CHOLEWICKI, J, NIBU, K and SHIN, E. Mechanical properties of the human cervical spine as shown by three- dimensional load-displacement curves. Spine 2001;26:2692-700.

161. PANJABI, MM, DURANCEAU, J, GOEL, V, OXLAND, T and TAKATA, K. Cervical human vertebrae. Quantitative three-dimensional anatomy of the middle and lower regions. Spine 1991;16:861-9.

162. PANJABI, MM, DURANCEAU, JS, OXLAND, TR and BOWEN, CE. Multidirectional instabilities of traumatic cervical spine injuries in a porcine model. Spine 1989;14:1111-5.

163. PANJABI, MM, KRAG, M, SUMMERS, D and VIDEMAN, T. Biomechanical time-tolerance of fresh cadaveric human spine specimens. J Orthop Res 1985;3:292-300.

164. PANJABI, MM, KRAG, MH and CHUNG, TQ. Effects of disc injury on mechanical behavior of the human spine. Spine 1984;9:707-13.

165. PANJABI, MM, WHITE, AAD, KELLER, D, SOUTHWICK, WO and FRIEDLAENDER, G. Stability of the cervical spine under tension. J Biomech 1978;11:189-97.

166. PENNING, L and WILMINK, JT. Rotation of the cervical spine. A CT study in normal subjects. Spine 1987;12:732-8.

167. PETERSON, RH, GOMEZ, MA and WOO, SL. The effects of strain rate on the biomechanical properties of the medial collateral ligament: A study of immature and mature rabbits. Trans Orthop Res Soc. 1987;127.

168. PETERSON, RH and WOO, SL. A new Methodology to Determine the Mechanical Properties of Ligaments at High Strain Rates. J. Biomechanical Engineering 1986;108:365-7.

169. PINTAR, F, MAYER, R, YOGANANDAN, N and SUN, E. Child Neck Strength Characteristics Using an Animal Model. Stapp Car Crash Journal 2000;44:

170. PINTAR, FA, YOGANANDAN, N, PESIGAN, M, REINARTZ, J, SANCES, A, JR. and CUSICK, JF. Cervical vertebral strain measurements under axial and eccentric loading. J Biomech Eng 1995;117:474-8.

171. PLANATH, I, RYGAARD, C and NILSSON, S. Synthesis of Data Towards Neck Protection Criteria for Children. IRCOB1. 1992;155-65.

172. POKHARNA, HK and PHILLIPS, FM. Collagen crosslinks in human lumbar intervertebral disc aging [see comments]. Spine 1998;23:1645-8.

173. POLLACK, IF, PANG, D and SCLABASSI, R. Recurrent spinal cord injury without radiographic abnormalities in children. J-Neurosurg 1988;69:177-82.

174. PRASAD, P and DANIEL, RP. A Biomechanical Analysis of Head, Neck, and Torso Injuries to Child Surrogates Due to Sudden Torso Acceleration. ASME Paper # 841656 1984;25-40.

175. PRASAD, P and KING, A. An experimentally validated dynamic model of the spine. Journal of Applied Mechanics 1974;41:546.

176. REBER, J and GOLDSMITH, W. Analysis of large head-neck motions. J Biomech 1979;12:211-22.

177. ROCKOFF, S, SWEET, E and BLEUSTEIN, J. The relative contribution of trabecular and cortical bone to the strenght of human lumbar vertebrae. Calcif Tissue Res 1969;3:163-75.

178. ROSNER, B. Fundamentals of biostatistics. New York: Duxbury Press, 1995.

179. SAITO, T, YAMAMURO, T, SHIKATA, J, OKA, M and TSUTSUMI, S. Analysis and prevention of spinal column deformity following cervical laminectomy I. Pathogenetic analysis of post-laminectomy deformities. Spine 1991;16:494-502.

180. SCHER, AT. Trauma of the spinal cord in children. S-Afr-Med-J 1976;50:2023-5.

181. SCOTT, JE, BOSWORTH, TR, CRIBB, AM and TAYLOR, JR. The chemical morphology of age-related changes in human intervertebral disc glycosaminoglycans from cervical, thoracic and lumbar nucleus pulposus and annulus fibrosus. J-Anat 1994;184:73-82.

182. SULLIVAN, CR, BRUWER, AJ and HARRIS, LE. Hypermobility of the Cervical Spine in Children: A Pitfall in the Diagnosis of Cervical Dislocation. American Journal of Surgery 1958;95:636-40.

183. SWINDLER, DR and WOOD, CD. An atlas of primate gross anatomy: baboon, chimpanzee, and man. Seattle, WA: Seattle, University of Washington Press, 1973.

184. TAKATA, K, INOUE, S, TAKAHASHI, K and OHTSUKA, Y. Fracture of the posterior margin of a lumbar vertebral body. J Bone Joint Surg Am 1988;70:589-94.

185. TOMINAGA, T, DICKMAN, CA, SONNTAG, VK and COONS, S. Comparative anatomy of the baboon and the human cervical spine. Spine 1995;20:131-7.

186. TOWNSEND, EJ and ROWE, M. Mobility of the upper cervical spine in health and disease. Pediatrics 1952;10:567-74.

187. TRELSTAD, R. Mesenchymal cell polarity and morphogenesis of chick cartilage. Dev Biology 1977;59:153-63.

188. URBAN, J and ROBERTS, S. Development and degeneration of the intervertebral discs. Mol Med Today 1995;1:329-35.

189. VOGEL, HG. Species differences of elastic and collagenous tissue--influence of maturation and age. Mech Ageing Dev 1991;57:15-24.

190. VOO, L, KUMARESAN, S, YOGANANDAN, N and PINTAR, F. Finite element analysis of cervical facetectomy. Spine 1997;22:964-9.

191. VOO, L and LIU, Y. Buckling analysis: a modal method of estimating cervical spine injury potential. In: Head and Neck Injuries in Sports. ed. Ef, H. Philadelphia: American Society of Testing and Materials, 1994.

192. WALSH, JW, STEVENS, DB and YOUNG, AB. Traumatic paraplegia in children without contiguous spinal fracture or dislocation. Neurosurgery 1983;12:439-45.

193. WENG, MS and HAYNES, RJ. Flexion and extension cervical MRI in a pediatric population. J-Pediatr-Orthop 1996;16:359-63.

194. WHITE, AA and PANJABI, MM. Clinical Biomechanics of the Spine. New York: Lippincott, 1990.

195. WILLIAMS, J and BELYTSCHKO, T. A three-dimensional model of the human cervical spine for impact simulation. Journal of Biomechanical Engineering 1983;105:321-31.

196. WOO, S, LIVESAY, G, RUNCO, T and YOUNG, E. Structure and function of tendons and ligaments. In: Basic Orthopaedic Biomechanics. ed. Mow, V and Hayes, W. Philadelphia: Lippincott - Raven, 1997.

197. WOO, S, ORLANDO, C, GOMEZ, M, FRANK, C and AKESON, W. Tensile properties of the medial collateral ligament as a function of age. J Orthop Res 1986;4:133-41.

198. WOO, SL, GOMEZ, MA and AKESON, WH. The time and history-dependent viscoelastic properties of the canine medical collateral ligament. J Biomech Eng 1981;103:293-8.

199. WOO, SL, PETERSON, RH, OHLAND, KJ, SITES, TJ and DANTO, MI. The effects of strain rate on the properties of the medial collateral ligament in skeletally immature and mature rabbits: a biomechanical and histological study. J Orthop Res 1990;8:712-21.

200. YAMADA, H. Ratios for age changes in the mechanical properties of human organs and tissues. In: Strength of Biological Materials. ed. Fg, E. Huntington, NY: Robert E. Krieger Publishing Co., 1973.

201. YERBY, SA, BAY, BK, TOH, E, MCLAIN, RF and DREWS, MJ. The effect of boundary conditions on experimentally measured trabecular strain in the thoracic spine. J Biomech 1998;31:891-7.

202. YINGLING, VR, CALLAGHAN, JP and MCGILL, SM. Dynamic loading affects the mechanical properties and failure site of porcine spines. Clin Biomech (Bristol, Avon) 1997;12:301-5.

203. YNGVE, DA, HARRIS, WP, HERNDON, WA, SULLIVAN, JA and GROSS, RH. Spinal cord injury without osseous spine fracture. J-Pediatr-Orthop 1988;8:153-9.

204. YOGANANDAN, N, KUMARESAN, S and PINTAR, FA. Geometric and mechanical properties of human cervical spine ligaments. J Biomech Eng 2000;122:623-9.

205. YOGANANDAN, N, KUMARESAN, S and PINTAR, FA. Biomechanics of the cervical spine Part 2. Cervical spine soft tissue responses and biomechanical modeling. Clin Biomech (Bristol, Avon) 2001;16:1-27.

206. YOGANANDAN, N, LARSON, SJ, PINTAR, FA, GALLAGHER, M, REINARTZ, J and DROESE, K. Intravertebral pressure changes caused by spinal microtrauma. Neurosurgery 1994;35:415-21; discussion 21.

207. YOGANANDAN, N, MAIMAN, DJ, PINTAR, F, RAY, G, MYKLEBUST, JB, SANCES, A, JR. and LARSON, SJ. Microtrauma in the lumbar spine: a cause of low back pain. Neurosurgery 1988;23:162-8.

208. YOGANANDAN, N and PINTAR, F. Epidemiology and Injury biomechanics of motor vehicle related trauma to the human spine. Stapp Car Crash Conference 1989;33:

209. YOGANANDAN, N and PINTAR, F. Inertial loading of the human cervical spine. J. Biomechanical Engineering 1997;119:237-40.

210. YOGANANDAN, N, PINTAR, F, BUTLER, J, REINARTZ, J, SANCES, A, JR. and LARSON, SJ. Dynamic response of human cervical spine ligaments. Spine 1989;14:1102-10.

211. YOGANANDAN, N, PINTAR, FA, MAIMAN, DJ, CUSICK, JF, SANCES, A, , J and WALSH, PR. Human head-neck biomechanics under axial tension. Med-Eng-Phys 1996;18:289-94.

212. YU, S, HAUGHTON, V, HO, P, SETHER, L, WAGNER, M and HO, K. Progressive and regressive changes in the nucleus pulposus. Part II. THe adult. Radiology 1988;169:93-7.

213. ZHU, Q, OUYANG, J, LU, W, LU, H, LI, Z, GUO, X and ZHONG, S. Traumatic instabilities of the cervical spine caused by high-speed axial compression in a human model. An in vitro biomechanical study. Spine 1999;24:440-4.

APPENDIX A: VERTEBRA SKELETAL MATURATION INDEX

This vertebra skeletal maturation index was developed using the book by Kuhns et al. under the supervision of musculoskeletal radiologist Frederick Mann, M.D. This index includes a number of views of each of the first three vertebra which were used to determine the human equivalent age of the baboon tissues tested in this project. CT images were manipulated to categorized each specimen into one of the skeletal maturation groups. A sample figure below demonstrates the features of each of the 18 images corresponding to one year of spinal development.

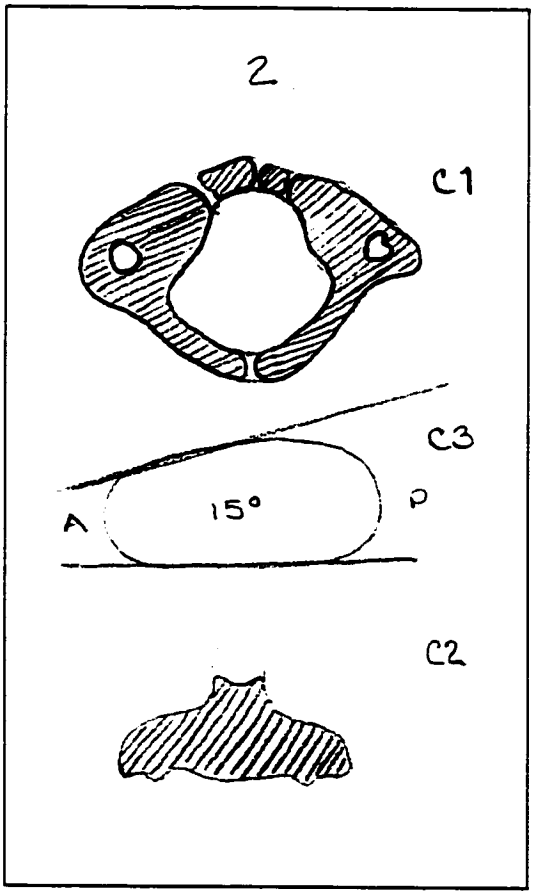

Figure A1. *Representative skeletal maturity index entry. The index features the human equivalent age at top (2-years) followed below by images of the C1, C2, and C3 vertebrae from different plane. The C1 (top) is from a transverse view and is used to denote fusion of that vertebra throughout age. The C2 vertebra (bottom) demonstrates the frontal plane vertebral section showing the maturation of the dens. Finally, the C3 (middle) illustrates the sagittal plane view of vertebral body development.*

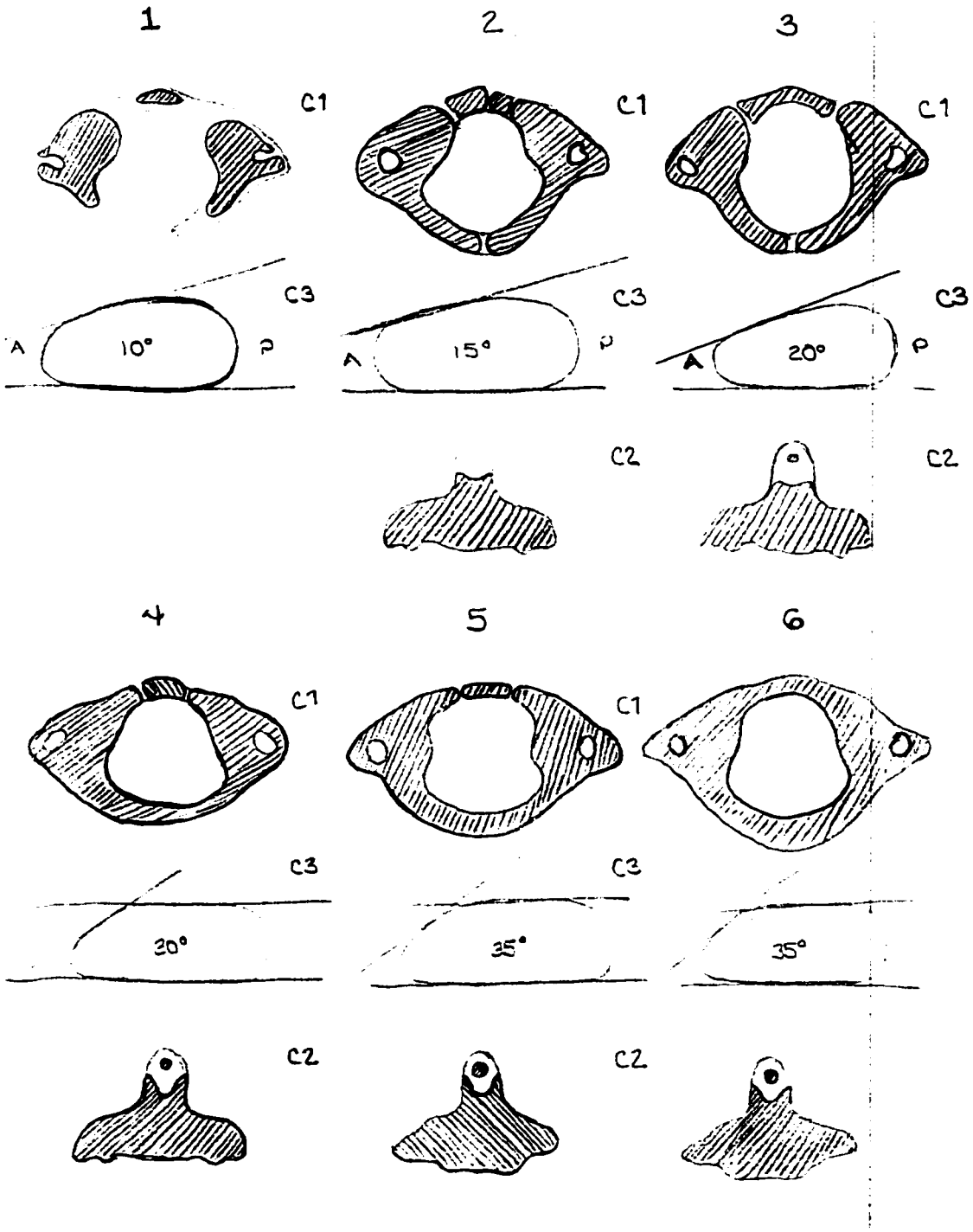
1
C1
C3
A
10°
P
C2
2
C1
C3
A
15°
P
C2
3
C1
C3
A
20°
P
C2
4
C1
C3
30°
C2
5
C1
C3
35°
C2
6
C1
35°
C2

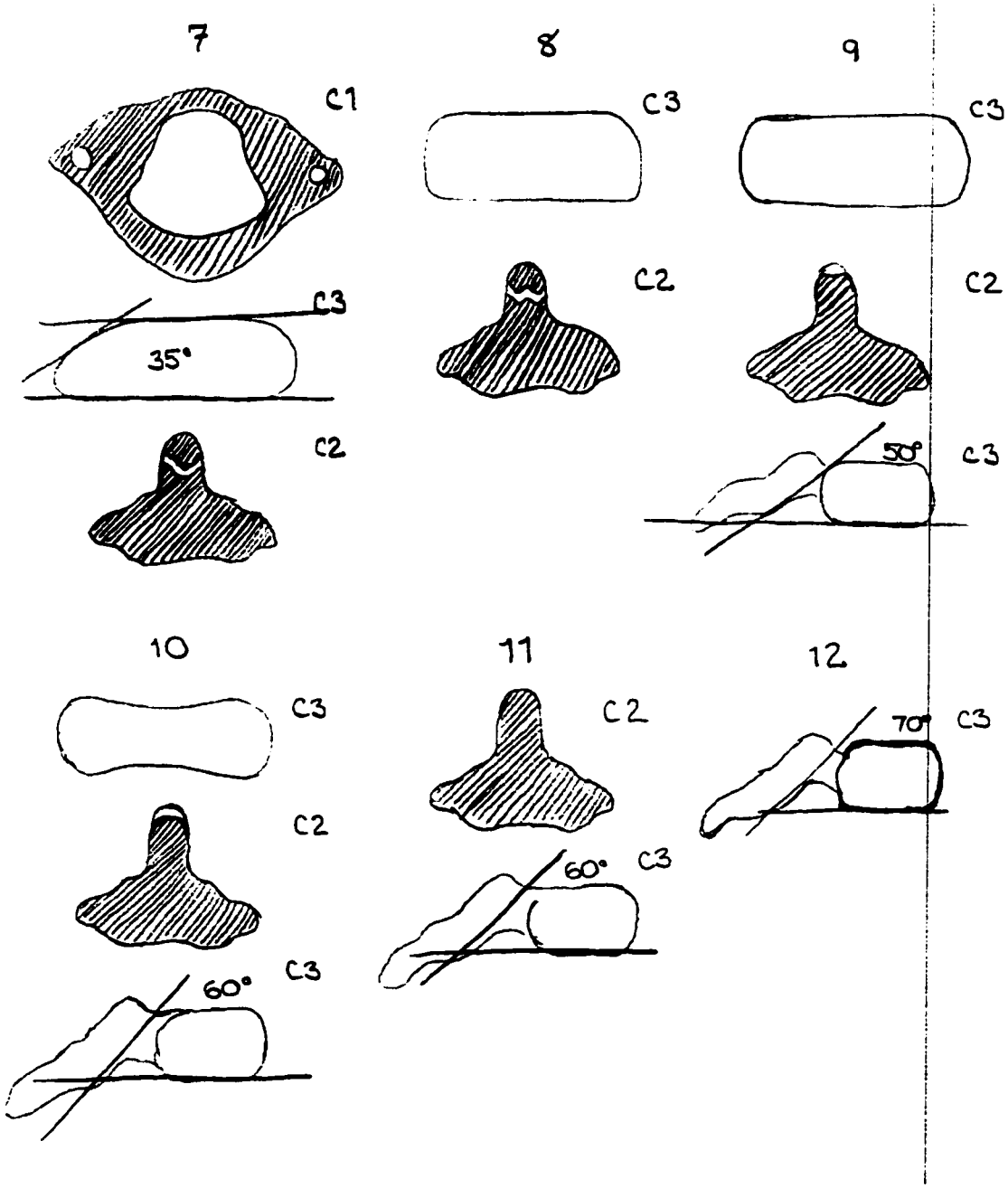
7
C1
C3
35°
C2
8
C3
C2
9
C3
C2
50°
C3
10
C3
C2
C3
60°
11
C2
60°
C3
12
70°
C3

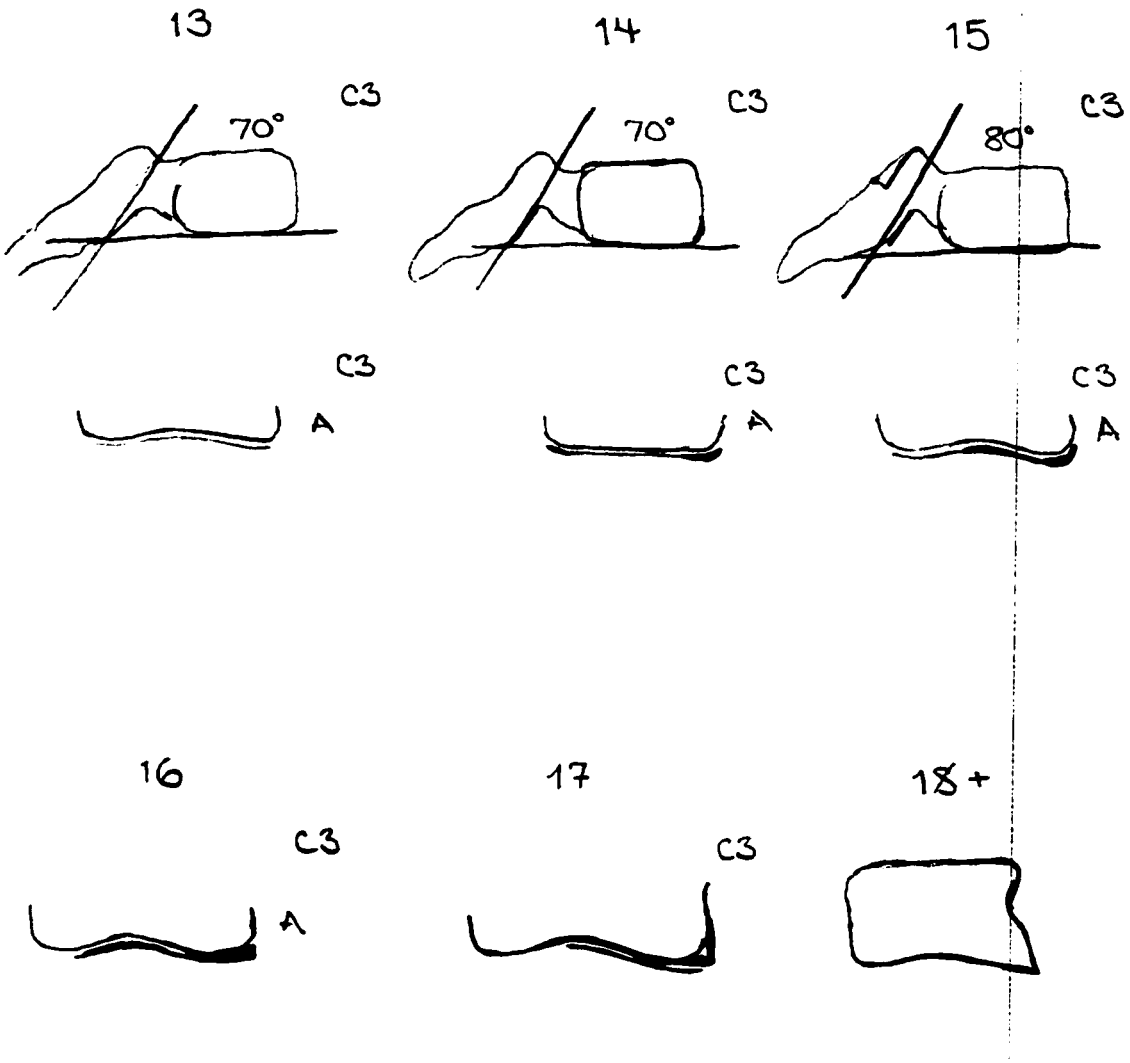
13
70°
C3
C3
A
14
70°
C3
C3
A
15
80°
C3
C3
A
16
C3
A
17
C3
18+

APPENDIX B: DEVELOPING SPINE ANATOMICAL MEASUREMENTS

Anatomical measurements were made on each specimen for comparison and normalization purposes. These involved the tracing on plane radiographs to determine the bony landmarks and make measurements. The following protocol was used to trace and measure each specimen.

General Tracing Guidelines:

- Begin by tracing the outer borders of the potting cups. The borders will be used as reference points in order to properly realign the tracing paper to the x-ray. If the outer borders of the potting cups are not clearly seen through the tracing paper, darken the borders directly on the x-ray with pencil.

- The superior and posterior sides of the cups tend to appear as ellipses. Locate the edges of the ellipses and draw a line from one edge to the other. The lateral sides of the cups should be perpendicular to the corresponding lines drawn from the superior and posterior sides of the cup. If the borders are not perpendicular, use the lines drawn from the superior and posterior sides of the cup as reference lines and draw the lateral sidelines perpendicular to the reference lines.

- For additional reference guidelines, trace the wiring inside the potting cups.

Lateral View Tracing:

- When tracing C3, C5, and C7, the areas of interest is the inferior half of the vertebral body and the facets. In many cases, the x-ray images are hard to see through the tracing paper. Therefore, to maintain accuracy, frequent comparison of the actual x-ray with the tracings is highly recommended. Taping one side of the tracing paper to the x-ray helps this function as this allows the paper to be turned over without concerns of realigning the tracings with the x-ray.

- Another technique in maintaining accurate tracings is darkening the area of interest directly onto the x-ray with a pencil. This will enhance the area of interest under the

light box and will aid in producing accurate tracings.

- Apply these techniques with other tracings as well. The level of clarity in the tracings is directly related to the accuracy of the obtained measurements. Therefore, a higher degree of clarity reflects better measurements.

- When tracing C4, C6, and T1, the areas of interest are the vertebral body and the facets.

- When tracing C2, the inferior half of the vertebral body, facets, and dens are the areas of interest. It is important that the lateral sides of the dens, the superior tip of the dens, and the inferior half of the vertebral body are clear.

- If any parts mentioned above are not clear on the x-rays, then observe the x-rays with the anterior view of the same specimen and determine if the corresponding parts are clear. If they are, then obtain the distances from the bottoms or tops of the cups to the relative reference points of the indeterminable part. The obtained distance should be the same distance on the lateral viewing x-rays. The measurement can roughly estimate the location of the specific part on the lateral view x-ray.

Anterior View Tracing:

- When tracing C3, C5, and C7, the area of interest is the inferior half of the vertebral body. When tracing C4, C6, and T1, the area of interest is the vertebral body. When tracing C2, the entire vertebral body and the dens are the areas of interest.

Lateral Measurements

- Draw lines 1, 2, and 8 in alignment with the vertebral bodies. Try to make these lines parallel as possible.

- Draw lines 3 and 4 in alignment with the anterior and posterior sides of the vertebral body. Try to make lines 3 & 4 perpendicular to lines 1 & 2.

- Use the rectangle formed from lines 1-4 as a guideline in developing the centroid.

- Inside the rectangle, the centroid should be .5 of lines 3 & 4 and .75 of lines 1 & 2 starting from the anterior side of the vertebral body (Figure B1).

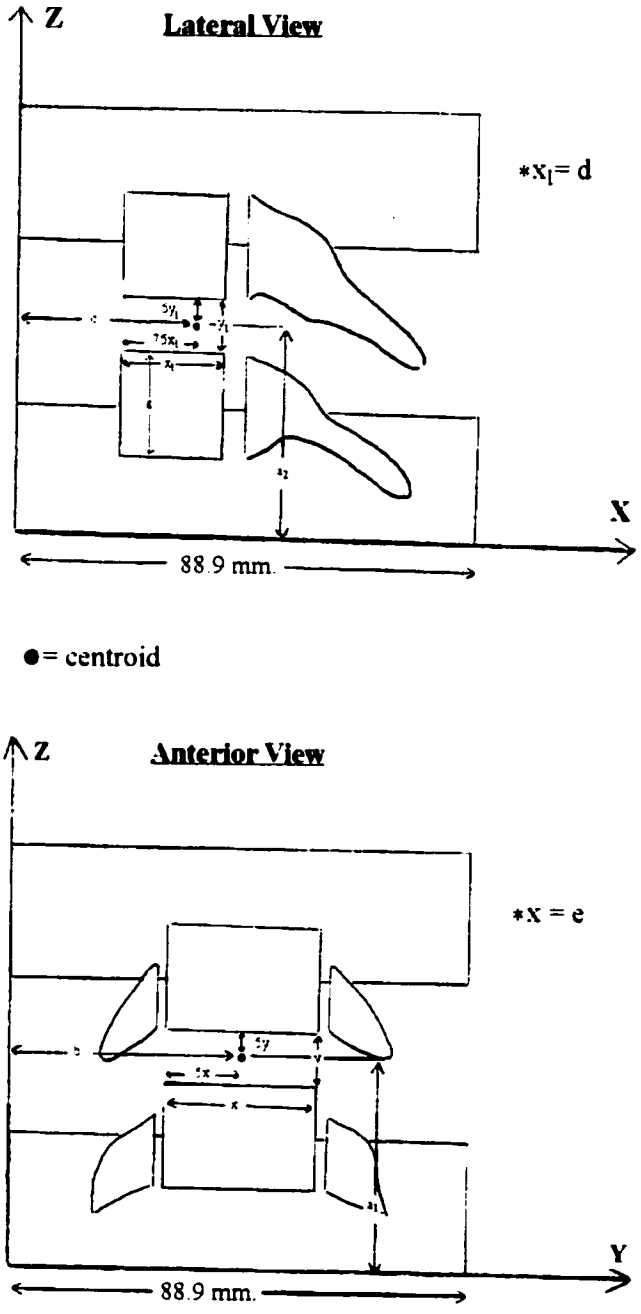

Figure B1 and Figure B2. *These depict the selection of the centroid of the disc and the measurements taken from that centroid.*

- Once the centroid is established, a measurement for a_2 is acquired by obtaining the distance from the centroid to the bottom of the cup (Figure B1).
- A measurement for c is acquired by obtaining the distance from the centroid to the anterior side of the cup (Figure B1).
- Measure the distance of the vertebral bodies of C4, C6, or T1 from the anterior side to the posterior side. This measurement is d (Figure B2).
- Draw line 5 in alignment with the superior half of C4, C6, or T1 facet.
- Draw lines 6 & 7 in alignment with the anterior and posterior sides of the C4, C6, or T1 facet. Try to make lines 6 & 7 perpendicular with line 5.
- The distance of the segment of line 5 that is in between lines 6 & 7 is the measurement f (Figure B3).

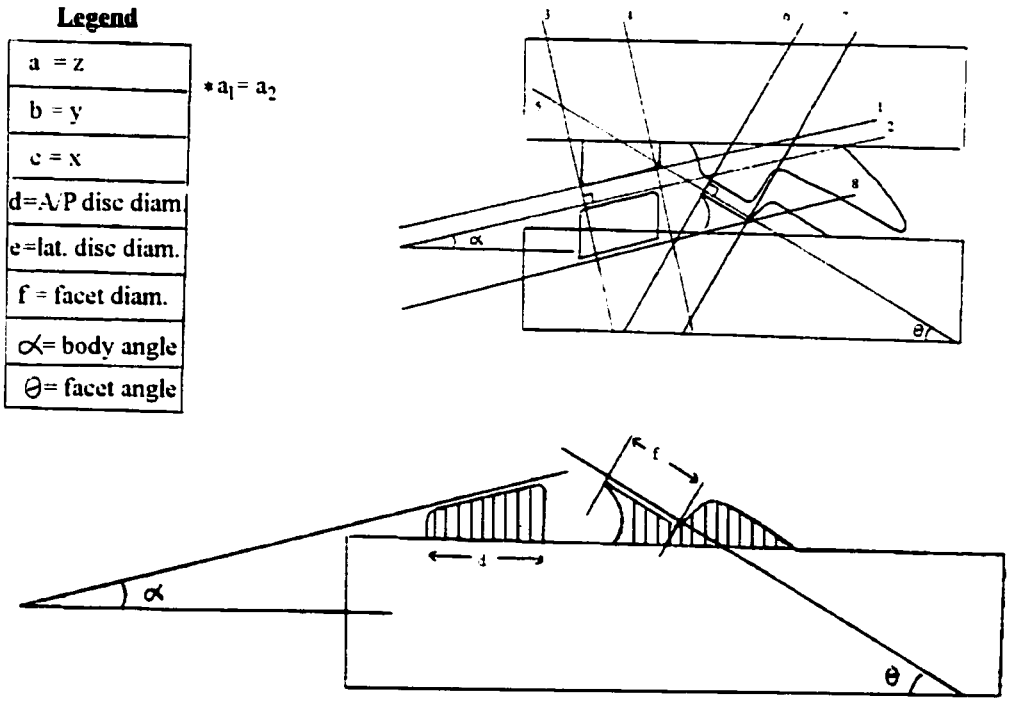

Figure B3. *Lateral view (sagittal plane) of bottom potting cup with inferior vertebra. This view enables the measurement of the vertebral body and intervertebral disc dimensions.*

- The distance between lines 2 & 8 is the measurement g.
- α & θ are obtained by measuring the angle of lines 2 & 5 and with the bottom of the cup as the reference line (Figure B3).
- On the lateral view of C2, the centroid is determined by measuring the midpoint from the tip of the dens to the bottom of the vertebral body. Once the midpoint is determined, shift the point to the far posterior side of the dens. This is your centroid.
- Once the centroid is determined for lateral C2, follow the directions given above in obtaining a_2 & c.
- Determine f & θ by following the directions above. Note: for lateral C2, d, g, and α cannot be determined.

Anterior Measurements

- Draw lines 1 & 2 in alignment with the vertebral bodies. Try to make these lines parallel as possible (Figure B4).
- Draw lines 3 & 4 in alignment with the lateral sides of the vertebral body. Try to make lines 3 & 4 perpendicular to lines 1 & 2.
- Use the rectangle formed from lines 1-4 as a guideline in developing the centroid.

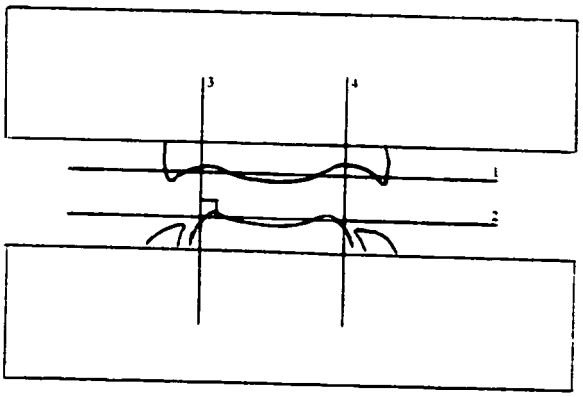

Figure B4. *Anterior view of a single FSU for measurement of the intervertebral disc dimensions.*

- Inside the rectangle, the centroid should be .5 of lines 3 & 4 and .5 of lines 1 & 2 (Figure B2).

- Once the centroid is established, a measurement for a_1 is acquired by obtaining the distance from the centroid to the bottom of the cup.

- A measurement for b is acquired by obtaining the distance from the centroid to the specimen right lateral side of the cup.

- Measure the distance of the vertebral bodies of C4, C6, or T1 from the lateral sides. This measurement is e.

- On the anterior view of C2, the centroid is determined by measuring the center point of the vertebral body. The measurement parameters are from the superior tip of the dens to the inferior edge of the vertebral body. The lateral parameters are from the far left of the vertebral body to the far right.

- Once the centroid is determined for anterior C2, follow the directions given above in obtain a_1, b, & e.

APPENDIX C: SPECIMEN DEMOGRAPHICS

Specimen #	Tissue	Species	Age [yrs]	Sex	Weight [kg]	Experiments
02-101-97	C-Spine&Head	P.c.anubis	5	M	10.1	Vert / FSU
02-102-97	C-Spine&Head	P.c.anubis	10	M	11	FSU
02-103-97	C-Spine&Head	P.c.anubis	18	M	15.6	Vert / FSU
02-104-97	C-Spine&Head	P.c.anubis	30	F	18.5	Vert
02-107-97	C-Spine&Head	P.c.anubis	18	M	15.9	Vert / FSU
02-108-97	C-Spine&Head	P.c.anubis	13	M	19	FSU
02-109-97	C-Spine&Head	P.c.anubis	11	M	18.6	FSU
02-110-97	C-Spine&Head	P.c.anubis	13	M	15.6	Vert
02-111-98	C-Spine&Head	P.c.anubis	10	M	8.4	FSU HR
02-112-98	C-Spine&Head	P.c.anubis	7	M	8.4	FSU
02-113-98	C-Spine&Head	P.c.anubis	15	M	6.7	Vert / FSU
02-114-98	C-Spine&Head	P.c.anubis	6	F	4.6	Vert
02-116-98	C-Spine&Head	P.c.anubis	11	F	9	Vert
02-117-98	C-Spine&Head	P.c.anubis	10	F	7	Vert
02-118-98	C-Spine&Head	P.c.anubis	8	M	7.8	Vert
02-119-98	C-Spine&Head	P.c.anubis	6	M	11.5	Vert
02-120-98	C-Spine&Head	P.c.anubis	10	M	10.6	FSU HR
02-121-98	C-Spine&Head	P.c.anubis	10	M	9.4	FSU HR
02-122-98	C-Spine&Head	P.c.anubis	10	M	10.2	FSU HR
02-123-98	C-Spine&Head	P.c.anubis	14	F	9.2	Vert
02-124-98	C-Spine&Head	P.c.anubis	16	M	7.67	FSU
02-125-98	C-Spine&Head	P.c.anubis	3	M	4.9	Vert / FSU
02-126-98	C-Spine&Head	P.c.anubis	2	M	3.96	Vert / 2FSU
02-127-99	C-Spine&Head	P.c.anubis	9	M	10	2FSU
02-128-98	C-Spine&Head	P.c.anubis	5	F	8.3	Vert
02-129-98	C-Spine&Head	P.c.anubis	9	M	12.3	FSU
02-130-98	C-Spine&Head	P.c.anubis	11	M	9.7	FSU HR
02-131-98	C-Spine&Head	P.c.anubis	23	F	12.9	Vert
02-132-98	C-Spine&Head	P.c.anubis	10	M	11.5	2FSU
02-133-98	C-Spine&Head	P.c.anubis	6	M	9.2	2FSU
02-135-99	C-Spine&Head	P.c.anubis	9	M	9	FSU HR
02-136-99	C-Spine&Head	P.c.anubis	6	M	6.6	Vert / FSU
02-138-99	C-Spine&Head	P.c.anubis	11	M	12	FSU HR
02-141-99	C-Spine&Head	P.c.anubis	7	M	8.3	2FSU
02-142-99	C-Spine&Head	P.c.anubis	2	M	3.9	Vert / FSU
02-144-99	C-Spine&Head	P.c.anubis	9	M	12	FSU HR
02-145-99	C-Spine&Head	P.c.anubis	16	F	10.5	Vert
02-150-99	C-Spine&Head	P.c.anubis	7	M	7.8	2FSU
02-151-99	C-Spine&Head	P.c.anubis	15	F	7.8	Vert
02-152-99	C-Spine&Head	P.c.anubis	2	M	7	FSU
02-153-99	C-Spine&Head	P.c.anubis	17	M	11.3	2FSU
02-154-99	C-Spine&Head	P.c.anubis	7	M	8.7	FSU
02-155-99	C-Spine&Head	P.c.anubis	8	M	8.5	2FSU
02-156-99	C-Spine&Head	P.c.anubis	11	M	8.24	FSU
02-164-00	C-Spine&Head	P.c.anubis	9	M	10	2FSU
02-165-00	C-Spine&Head	P.c.anubis	5	M	6.3	2FSU
02-171-00	C-Spine&Head	P.c.anubis	4	M	6	2FSU
02-177-00	C-Spine&Head	P.c.anubis	6	M	9.2	2FSU
02-178-00	C-Spine&Head	P.c.anubis	11	M	8.9	2FSU
02-181-00	C-Spine&Head	P.c.anubis	8	M	9.8	2FSU
02-185-00	C-Spine&Head	P.c.anubis	12	M	9.8	2FSU
02-192-01	C-Spine&Head	P.c.anubis	14	M	10.8	2FSU
02-195-01	C-Spine&Head	P.c.anubis	16	M	9.4	2FSU
02-198-01	C-Spine&Head	P.c.anubis	11	M	9.3	2FSU
02-200-01	C-Spine&Head	P.c.anubis	26	M	29.2	Vert / FSU
02-201-01	C-Spine&Head	P.c.anubis	0	M	_	2FSU
02-203-01	C-Spine&Head	P.c.anubis	1	M	2.25	Vert / FSU
02-205-01	C-Spine&Head	P.c.anubis	23	M	37.44	2FSU
02-206-01	C-Spine&Head	P.c.anubis	26	M	36.78	2FSU
02-207-01	C-Spine&Head	P.c.anubis	22	M	30.96	2FSU

APPENDIX D: STATISTICAL TABLES AND RESULTS

This section includes the analysis of variance tables generated in the statistical testing of these hypotheses. These were performed on SPSS statistical software and represented the bulk of the secondary effects evaluations. Tukey honest significant difference tables of post-test contrasts are also presented displaying the significance of each factor individually.

Vertebral Body Compression Functional Mechanics

Tests of Between-Subjects Effects

Dependent Variable: Stiffness

Source	Type III Sum of Squares	df	Mean Square	F	Sig.
Corrected Model	504174.023[a]	1	504174.023	.969	.337
Intercept	97997089	1	97997089	188.418	.000
GENDER	504174.023	1	504174.023	.969	.337
Error	10402100	20	520104.998		
Total	1.10E+08	22			
Corrected Total	10906274	21			

a. R Squared = .046 (Adjusted R Squared = -.001)

Tests of Between-Subjects Effects

Dependent Variable: Modulus

Source	Type III Sum of Squares	df	Mean Square	F	Sig.
Corrected Model	34253.801[a]	1	34253.801	11.710	.003
Intercept	673127.675	1	673127.675	230.125	.000
GENDER	34253.801	1	34253.801	11.710	.003
Error	58501.051	20	2925.053		
Total	732962.062	22			
Corrected Total	92754.851	21			

a. R Squared = .369 (Adjusted R Squared = .338)

Functional Spinal Unit Compression Functional Mechanics

Tests of Between-Subjects Effects

Dependent Variable: stiffness

Source	Type III Sum of Squares	df	Mean Square	F	Sig.
Corrected Model	406317.731[a]	55	7387.595	11.763	.000
Intercept	2233390.2	1	2233390.2	3556.109	.000
AGE	287435.943	13	22110.457	35.205	.000
LEVEL	71782.072	3	23927.357	38.098	.000
AGE * LEVEL	40559.304	39	1039.982	1.656	.139
Error	10048.691	16	628.043		
Total	2931461.0	72			
Corrected Total	416366.422	71			

a. R Squared = .976 (Adjusted R Squared = .893)

Multiple Comparisons

Dependent Variable: stiffness

Tukey HSD

(I) level	(J) level	Mean Difference (I-J)	Std. Error	Sig.	95% Confidence Interval	
					Lower Bound	Upper Bound
1.00	2.00	-77.6278*	8.354	.000	-101.5279	-53.7276
	3.00	-83.6167*	8.354	.000	-107.5168	-59.7165
	4.00	-53.9139*	8.354	.000	-77.8140	-30.0138
2.00	1.00	77.6278*	8.354	.000	53.7276	101.5279
	3.00	-5.9889	8.354	.889	-29.8890	17.9112
	4.00	23.7139	8.354	.052	-.1862	47.6140
3.00	1.00	83.6167*	8.354	.000	59.7165	107.5168
	2.00	5.9889	8.354	.889	-17.9112	29.8890
	4.00	29.7028*	8.354	.013	5.8026	53.6029
4.00	1.00	53.9139*	8.354	.000	30.0138	77.8140
	2.00	-23.7139	8.354	.052	-47.6140	.1862
	3.00	-29.7028*	8.354	.013	-53.6029	-5.8026

Based on observed means.

*. The mean difference is significant at the .05 level.

Tests of Between-Subjects Effects

Dependent Variable: modulus

Source	Type III Sum of Squares	df	Mean Square	F	Sig.
Corrected Model	249.059[a]	41	6.075	3.381	.013
Intercept	2727.925	1	2727.925	1518.254	.000
AGE	156.899	13	12.069	6.717	.001
LEVEL	28.029	2	14.015	7.800	.007
AGE * LEVEL	51.160	26	1.968	1.095	.452
Error	21.561	12	1.797		
Total	3328.428	54			
Corrected Total	270.620	53			

a. R Squared = .920 (Adjusted R Squared = .648)

Multiple Comparisons

Dependent Variable: modulus

Tukey HSD

(I) level	(J) level	Mean Difference (I-J)	Std. Error	Sig.	95% Confidence Interval	
					Lower Bound	Upper Bound
2.00	3.00	1.6474*	.447	.008	.4554	2.8395
	4.00	1.9990*	.447	.002	.8069	3.1910
3.00	2.00	-1.6474*	.447	.008	-2.8395	-.4554
	4.00	.3515	.447	.718	-.8405	1.5436
4.00	2.00	-1.9990*	.447	.002	-3.1910	-.8069
	3.00	-.3515	.447	.718	-1.5436	.8405

Based on observed means.

*. The mean difference is significant at the .05 level.

Tests of Between-Subjects Effects

Dependent Variable: taucomp

Source	Type III Sum of Squares	df	Mean Square	F	Sig.
Corrected Model	8750.818[a]	55	159.106	6.607	.000
Intercept	121068.668	1	121068.668	5027.435	.000
AGE	2289.781	13	176.137	7.314	.000
LEVEL	4501.167	3	1500.389	62.304	.000
AGE * LEVEL	1809.832	39	46.406	1.927	.079
Error	385.306	16	24.082		
Total	142342.492	72			
Corrected Total	9136.124	71			

a. R Squared = .958 (Adjusted R Squared = .813)

Functional Spinal Unit Tension Functional Mechanics

Tests of Between-Subjects Effects

Dependent Variable: Stiff

Source	Type III Sum of Squares	df	Mean Square	F	Sig.
Corrected Model	209955.782[a]	55	3817.378	5.913	.000
Intercept	1790056.3	1	1790056.3	2772.615	.000
AGE	125723.248	13	9671.019	14.979	.000
LEVEL	51521.788	3	17173.929	26.601	.000
AGE * LEVEL	24297.121	39	623.003	.965	.557
Error	10329.925	16	645.620		
Total	2168821.1	72			
Corrected Total	220285.708	71			

a. R Squared = .953 (Adjusted R Squared = .792)

Multiple Comparisons

Dependent Variable: Stiff

Tukey HSD

(I) level	(J) level	Mean Difference (I-J)	Std. Error	Sig.	95% Confidence Interval	
					Lower Bound	Upper Bound
1.00	2.00	-68.9111*	8.470	.000	-93.1434	-44.6788
	3.00	-51.1167*	8.470	.000	-75.3489	-26.8844
	4.00	-7.9611	8.470	.784	-32.1934	16.2712
2.00	1.00	68.9111*	8.470	.000	44.6788	93.1434
	3.00	17.7944	8.470	.195	-6.4378	42.0267
	4.00	60.9500*	8.470	.000	36.7177	85.1823
3.00	1.00	51.1167*	8.470	.000	26.8844	75.3489
	2.00	-17.7944	8.470	.195	-42.0267	6.4378
	4.00	43.1556*	8.470	.001	18.9233	67.3878
4.00	1.00	7.9611	8.470	.784	-16.2712	32.1934
	2.00	-60.9500*	8.470	.000	-85.1823	-36.7177
	3.00	-43.1556*	8.470	.001	-67.3878	-18.9233

Based on observed means.

*. The mean difference is significant at the .05 level.

Tests of Between-Subjects Effects

Dependent Variable: mod

Source	Type III Sum of Squares	df	Mean Square	F	Sig.
Corrected Model	212.470[a]	41	5.182	3.241	.016
Intercept	1844.027	1	1844.027	1153.346	.000
AGE	102.923	13	7.917	4.952	.005
LEVEL	42.375	2	21.188	13.252	.001
AGE * LEVEL	62.941	26	2.421	1.514	.228
Error	19.186	12	1.599		
Total	2233.397	54			
Corrected Total	231.656	53			

a. R Squared = .917 (Adjusted R Squared = .634)

Multiple Comparisons

Dependent Variable: mod

Tukey HSD

(I) level	(J) level	Mean Difference (I-J)	Std. Error	Sig.	95% Confidence Interval	
					Lower Bound	Upper Bound
2.00	3.00	1.2256*	.421	.033	.1011	2.3500
	4.00	2.2733*	.421	.000	1.1488	3.3978
3.00	2.00	-1.2256*	.421	.033	-2.3500	-.1011
	4.00	1.0477	.421	.069	-7.673E-02	2.1722
4.00	2.00	-2.2733*	.421	.000	-3.3978	-1.1488
	3.00	-1.0477	.421	.069	-2.1722	7.673E-02

Based on observed means.

*. The mean difference is significant at the .05 level.

Tests of Between-Subjects Effects

Dependent Variable: tautens

Source	Type III Sum of Squares	df	Mean Square	F	Sig.
Corrected Model	2897.281[a]	55	52.678	1.201	.356
Intercept	78430.566	1	78430.566	1787.853	.000
AGE	1129.560	13	86.889	1.981	.098
LEVEL	353.336	3	117.779	2.685	.082
AGE * LEVEL	1298.021	39	33.283	.759	.765
Error	701.897	16	43.869		
Total	90501.597	72			
Corrected Total	3599.178	71			

a. R Squared = .805 (Adjusted R Squared = .135)

Vertebral Body Compressive Tolerance

Tests of Between-Subjects Effects

Dependent Variable: yield

Source	Type III Sum of Squares	df	Mean Square	F	Sig.
Corrected Model	16672871[a]	18	926270.607	18.751	.017
Intercept	93739483	1	93739483	1897.665	.000
GENDER	589332.788	1	589332.788	11.930	.041
AGE	16545257	15	1103017.1	22.330	.013
GENDER * AGE	20203.628	2	10101.814	.205	.826
Error	148191.811	3	49397.270		
Total	1.16E+08	22			
Corrected Total	16821063	21			

a. R Squared = .991 (Adjusted R Squared = .938)

Tests of Between-Subjects Effects

Dependent Variable: Strength

Source	Type III Sum of Squares	df	Mean Square	F	Sig.
Corrected Model	255.978[a]	18	14.221	23.908	.012
Intercept	4141.086	1	4141.086	6961.905	.000
AGE	164.681	15	10.979	18.457	.017
SEX	7.205	1	7.205	12.113	.040
AGE * SEX	3.601	2	1.800	3.027	.191
Error	1.784	3	.595		
Total	4458.075	22			
Corrected Total	257.762	21			

a. R Squared = .993 (Adjusted R Squared = .952)

2 Functional Spinal Unit Compressive Tolerance

Tests of Between-Subjects Effects

Dependent Variable: load

Source	Type III Sum of Squares	df	Mean Square	F	Sig.
Corrected Model	70620713[a]	52	1358090.6	17.253	.000
Intercept	4.24E+08	1	4.24E+08	5386.753	.000
AGE	63293714	17	3723159.6	47.300	.000
LEVEL	3877634.1	2	1938817.0	24.631	.000
AGE * LEVEL	3845740.7	33	116537.596	1.481	.275
Error	708425.750	9	78713.972		
Total	5.07E+08	62			
Corrected Total	71329139	61			

a. R Squared = .990 (Adjusted R Squared = .933)

Multiple Comparisons

Dependent Variable: load

Tukey HSD

(I) level	(J) level	Mean Difference (I-J)	Std. Error	Sig.	95% Confidence Interval	
					Lower Bound	Upper Bound
1.00	2.00	-311.5714*	87.658	.015	-556.3155	-66.8273
	3.00	259.7857*	87.658	.038	15.0416	504.5298
2.00	1.00	311.5714*	87.658	.015	66.8273	556.3155
	3.00	571.3571*	86.583	.000	329.6161	813.0981
3.00	1.00	-259.7857*	87.658	.038	-504.5298	-15.0416
	2.00	-571.3571*	86.583	.000	-813.0981	-329.6161

Based on observed means.

*. The mean difference is significant at the .05 level.

Tests of Between-Subjects Effects

Dependent Variable: streng

Source	Type III Sum of Squares	df	Mean Square	F	Sig.
Corrected Model	2353.097[a]	35	67.231	5.424	.021
Intercept	28748.809	1	28748.809	2319.561	.000
AGE	1099.836	17	64.696	5.220	.025
LEVEL	1142.976	1	1142.976	92.220	.000
AGE * LEVEL	142.071	17	8.357	.674	.757
Error	74.364	6	12.394		
Total	31896.342	42			
Corrected Total	2427.462	41			

a. R Squared = .969 (Adjusted R Squared = .791)

Functional Spinal Unit Tension Tolerance

Tests of Between-Subjects Effects

Dependent Variable: Ult

Source	Type III Sum of Squares	df	Mean Square	F	Sig.
Corrected Model	6232883.9[a]	55	113325.161	7.320	.000
Intercept	19226211	1	19226211	1241.876	.000
AGE	4822224.6	13	370940.357	23.960	.000
LEVEL	717131.077	3	239043.692	15.441	.000
AGE * LEVEL	689136.020	39	17670.154	1.141	.401
Error	247705.345	16	15481.584		
Total	27000854	72			
Corrected Total	6480589.2	71			

a. R Squared = .962 (Adjusted R Squared = .830)

Multiple Comparisons

Dependent Variable: Ult

Tukey HSD

(I) level	(J) level	Mean Difference (I-J)	Std. Error	Sig.	95% Confidence Interval	
					Lower Bound	Upper Bound
1.00	2.00	175.7083*	41.475	.003	57.0459	294.3708
	3.00	162.6856*	41.475	.006	44.0231	281.3480
	4.00	279.7900*	41.475	.000	161.1276	398.4524
2.00	1.00	-175.7083*	41.475	.003	-294.3708	-57.0459
	3.00	-13.0228	41.475	.989	-131.6852	105.6396
	4.00	104.0817	41.475	.096	-14.5808	222.7441
3.00	1.00	-162.6856*	41.475	.006	-281.3480	-44.0231
	2.00	13.0228	41.475	.989	-105.6396	131.6852
	4.00	117.1044	41.475	.054	-1.5580	235.7669
4.00	1.00	-279.7900*	41.475	.000	-398.4524	-161.1276
	2.00	-104.0817	41.475	.096	-222.7441	14.5808
	3.00	-117.1044	41.475	.054	-235.7669	1.5580

Based on observed means.

*. The mean difference is significant at the .05 level.

Tests of Between-Subjects Effects

Dependent Variable: strength

Source	Type III Sum of Squares	df	Mean Square	F	Sig.
Corrected Model	84.225[a]	41	2.054	11.284	.000
Intercept	780.585	1	780.585	4287.848	.000
AGE	37.567	13	2.890	15.874	.000
LEVEL	31.459	2	15.729	86.404	.000
AGE * LEVEL	13.459	26	.518	2.844	.031
Error	2.185	12	.182		
Total	935.136	54			
Corrected Total	86.409	53			

a. R Squared = .975 (Adjusted R Squared = .888)

Multiple Comparisons

Dependent Variable: strength

Tukey HSD

(I) level	(J) level	Mean Difference (I-J)	Std. Error	Sig.	95% Confidence Interval	
					Lower Bound	Upper Bound
2.00	3.00	.9993*	.142	.000	.6198	1.3787
	4.00	1.9201*	.142	.000	1.5406	2.2995
3.00	2.00	-.9993*	.142	.000	-1.3787	-.6198
	4.00	.9208*	.142	.000	.5414	1.3002
4.00	2.00	-1.9201*	.142	.000	-2.2995	-1.5406
	3.00	-.9208*	.142	.000	-1.3002	-.5414

Based on observed means.

*. The mean difference is significant at the .05 level.

CURRICULUM VITAE

(3/2002)

DAVID JOHN NUCKLEY, PH.D.

UNIVERSITY OF WASHINGTON
DEPARTMENT OF BIOENGINEERING
Mailstop 359798
Seattle, Washington 98105
Telephone: 206.341.4000
Fax: 206.731.5752

Personal Data

Home Address	3109 NE 82nd Street Seattle, Washington 98115 206.522.6619 [Phone]
Electronic Address	dnuckley@u.washington.edu http://students.washington.edu/~dnuckley
Social Security Number	296.68.8154
Date/Place of Birth	April 12, 1973 Parma, Ohio, USA

Education

Undergraduate Education	Syracuse University Syracuse, New York B.S., Bioengineering, 1995 Syracuse Scholar, Cum Laude with Honors
Graduate Education	University of Washington Seattle, Washington Ph.D., Bioengineering, 2002 Biomechanics Pathway

Research Experience

Developmental Biomechanics of the Cervical Spine: Pediatric Injury Prevention and Management Through Experimental Biomechanics Research (1997-)

Applied Biomechanics Laboratory. University of Washington.
NHTSA and CDC funded research.

Assessing Neural-Space Integrity of the Cervical Spine: Enhancing the Sensitivity and Utility of Clinical Instability Assessemnt (1996-2001)

Applied Biomechanics Laboratory. University of Washington.
CSRS and OREF funded research.

Development of Neural Space Occlusion Transducers for Neural-Space Integrity Assessment (1995-1997)

Applied Biomechanics Laboratory. University of Washington.
CDC funded research.

Retinal Anatomy of a New Species of Bresiliid Shrimp From a Hydrothermal Vent Field on the Mid-Atlantic Ridge (1994-1995)

Institute for Sensory Research, Optical Laboratory. Syracuse University.
NSF and NIH funded research.

Teaching Experience

Course Instruction

BIOEN / EE 436 – Medical Instrumentation — University of Washington, 2002

As instructor, I lectured on signal transduction, biologic signals, and applications of instrumentation for clinical and research measurements of biological systems. This course also contains a laboratory experience and design project which supplement the coursework. This course is also giving me experience in designing a course sylabus, preparing laboratory experiments, and preparing and grading exams.

BIOEN 520 – Orthopaedic Biomechanics — University of Washington, 1999

As a co-instructor, I lectured on instrumentation for orthopaedic research, a review of soft-tissue biomechanics, and biomechanics of the spine. This course was team taught giving me experience in designing a course sylabus, preparing and grading exams, and class instruction.

BIOL 202 – Animal Biology — University of Washington, 1998

As a teaching assistant, I lectured and ran laboratory sections (2) for students over topics of basic animal biology from biological systems to development. I gained an appreciation for large class style teaching and the preparation necessary for laboratory driven courses.

BIOEN 599 – Laboratory Techniques in Biomechanics — University of Washington, 1997

I prepared hands-on experiments for students in this graduate level course designed to introduce students to many techniques in biomechanics. This teaching assistantship enabled me to share my expertise with peers in a small setting through lectures once a week and laboratory sessions.

BEN 306 - Engineering Analysis of Living Systems II Syracuse University, 1995

As a teaching assistant, I was responsible for holding office hours for students and grading their homework assignments. This undergraduate teaching experience introduced me to the rigors of preparing for a class and having a complete understanding of the material taught.

BEN 305 – Engineering Analysis of Living Systems I Syracuse University, 1994

My first teaching experience involved holding office hourse and annotating homework assignments for students. This teaching assistantship introduced me to means of effective teaching and the effort required.

Invited lectures

Cervical Spine Biomechanics: An Introduction - REHAB 445, Dr. Mark Guthrie, instructor; University of Washington, 2000, 2001, and 2002.

This lecture introduced physical therapy, occupational therapy, and prosthetic and orthotics students to the mechanics of the spine. I introduced the basic mechanics along with clinical and engineering perspectives on injury prevention and management.

Tensile Mechanics of the Developing Spine (2001), Developmental Biomechanics of the Spine (2002) – NHTSA / DOT Project Updates, Dr. Rolf Eppinger, chair; Biomechanics Research Division, 2001, and 2002.

These lectures provided updates to the research groups funded by NHTSA. These lectures not only served to report progress, but also were used to garner support and further funding in the NHTSA community.

Low-Speed Rear-End Whiplash Cervical Spine Injury Mechanisms (1996), Cervical Spine Injury Risk Assessment: Applied Statistics (1998), Clinical Instability of the Spine: Investigating Structural and Neural Instability (1999) – BIOEN 599, Biomechanics Seminar Series, Dr. Joan Sanders, instructor; University of Washington, 1996, 1998, and 1999.

These lectures to academic peers aimed to teach a new method as well as convey current research results. I presented results of most recent research and new analysis or presentation methods to get peer feedback.

Neural-Space Integrity of the Cervical Spine - Traveling Fellows Seminar, Dr. Sigmund Hansen, coordinator; University of Washington, 1999.

This presentation was an examination of present assessment of spinal injury in the clinic and research in our laboratory which may improve this assessment by including an understanding of neural space integrity. This presentation to traveling clinicians was clinical in nature and demonstrated research application.

Developmental Biomechanics of the Cervical Spine – Northwest Tissue Center, 1998.

This presentation introduced a non-technical audience to pediatric spinal injuries, the developmental changes in the spine, and introduced our research agenda aimed at understanding the biomechanics of this population.

Neural-Space Integrity of the Lower Cervcial Spine – Spine Conference, Dr. Sohail Mirza, coordinator; Harborview Medical Center, 1998.

I presented a biomechanical introduction and examination of spine integrity to clinicians in orthopaedics and neurosurgery. This lecture was a technical review of experimental methods and research leading to understanding neural space changes of the spine in various injury scenarios.

Cervical Spine Injuries: Whiplash. – Meeting of the Human Factors and Ergonomist Society, Seattle, WA, 1997.

This lecture was directed towards ergonomists interested in the biomechanics of whiplash injury. I presented a review of the clinical literature and a number of biomechanical approaches to investigating injuries sustained in automotive accidents.

Student Mentoring

Michael Eck, Joseph Van Nausdle, Patrick Medley, and Kit Tainter – University of Washington undergraduate student mentoring (1999 -). These students performed original research at the Applied Biomechanics Laboratory under my supervision. I taught them basic laboratory skills, took each of them through a unique project in the laboratory and each project culminated in an abstract to a major scientific meeting or research publication. These mentoring experiences have helped me become a better one-on-one teacher. Further, these experiences have enhanced my skills at managing a research project and identifying subsets for undergraduate education. I only hope that the students received as much as I did from these experiences.

Business Experience

Nuckley Companies, Inc. *Consultant* 8/93 to 8/95

Provided operations and management information. Supplied employee and customer advice. Observed and recommended operations strategies. Aided in transition of ownership for both customer and employee relationships.

Nuckley Packaging Co. Inc. *Chief Executive Officer* 8/91 to 8/93

Chief engineer and product manager. Conducted Sales and Purchasing. Supervised 18 employees, and governed total operation (8/91 to 8/93, after my father passed away). Prepared the company for sale and sold the company, summer 1993.

Manuscripts – Peer Reviewed

Nuckley, DJ, Carter, J, Eck, M, et al. Effects of Development and Gender on Vertebral Body Compressive Mechanics. Bone 2002; In Preparation.

Nuckley, D, Konodi, M, Raynak, G, et al. Neural Space Integrity of the Lower Cervical Spine: Effect of Anterior Lesions. Spine 2002; In Review.

Nuckley, D, Konodi, M, Raynak, G, et al. Neural Space Integrity of the Lower Cervical Spine: Effect of Normal Range of Motion. Spine 2002; 27 (6): 587-95.

Nuckley, DJ, Van Nausdle, J, Raynak, G, et al. Examining the Relationship Between Whiplash Kinematics and a Direct Neurologic Injury Mechanism. International Journal of Vehicle Design 2002: March Publication.

Ching, R, Nuckley, D, Hertsted, S, et al. Tensile Mechanics of the Developing Cervical Spine. Stapp Car Crash Journal 2001;45:329-36.

Raynak, GC, Nuckley, DJ, Tencer, AF, et al. Transducers for Dynamic Measurement of Spine Neural-Space Occlusions. Journal of Biomechanical Engineering 1998;120:787-91.

Nuckley, DJ, Jinks, RN, Battelle, B-A, et al. Retinal Anatomy of a New Species of Bresiliid Shrimp From a Hydrothermal Vent Field on the Mid-Atlantic Ridge. Biological Bulletin 1996;190:98-110.

Nuckley, D. The Visual Morphology of the Hydrothermal Vent Shrimp, Rimicaris (Snake Pit): A look at evolutionary adaptation. Syracuse University;Undergraduate Honors Thesis. 1995.

Manuscripts – Invited

Medley, P, Nuckley, D, Ledoux, W, et al. A Computational and Experimental Methodology to Measure Cervical Spine Shear Mechanics. Injury Biomechanics Research: 29th International Workshop. San Antonio, TX:2001;

Van Nausdle, J, Nuckley, D, Raynak, J, et al. Cervical Spine Whiplash Kinematics and Its Effect on Neural Space Integrity. Injury Biomechanics Research: 29th International Workshop. San Antonio, TX:2001;

Nuckley, D, Eck, M, Hertsted, S, et al. Tensile Mechanics of the Developing Baboon Cervical Spine. Injury Science Research: 28th International Workshop. Atlanta, GA:2000;85-90.

Ching, R, Hertsted, S and Nuckley, DJ. Age-Related Cervical Spine Mechanics and Injury Tolerance. Proceedings of the NCIPC Injury Prevention Through Biomechanics Workshop. Atlanta, GA:2000;

Nuckley, D, Carter, J, Eck, M, et al. Compressive Mechanics of the Developing Spine. Injury Biomechanics Research: 27th International Workshop. San Diego, CA:1999;101-4.

Ching, RP, Carter, JW, Raynak, GC, et al. Transient and Post-Traumatic Measurement of Cervical Spinal Canal and Neuroforaminal Deformation: Potential Mechanisms for Neurologic Injury. In: Frountiers in Head and Neck Trauma: Clinical and Biomechanical. ed. Yoganandan, N and Al., E. Washington, D.C.: IOS Press Ohmsha, 1998.

Nuckley, DJ, Raynak, GC, Mirza, SK, et al. Effects of Normal Ranges of Motion on the Dimensions of Cervical Spinal-Canal and Intervertebral-Foramen. Seventh Injury Prevention Through Biomechanics. Wayne State University, Detroit, MI:1997;131-6.

Raynak, GC, Nuckley, DJ, Mirza, SK, et al. Soft Tissue Strains and Neurologic Tissue Compression in Low Speed Cervical Spine Whiplash Injury: A Pilot Study. Sixth Injury Prevention Through Biomechanics. Wayne State University, Detroit, MI:1996;47-57.

Abstracts

Nuckley, DJ, Hertsted, S and Ching, R. Effect of Strain Rate on Cervical Spine Tensile Mechanics. World Congress of Biomechanics IV. Calgary, Alberta:2002; in review.

Nuckley, DJ, Hertsted, S, Tainter, C, et al. Compressive Biomechanics of Fracture and Neurologic Integrity in teh Pediatric Spine. World Congress of Biomechanics IV. Calgary, Alberta:2002; in review.

Nuckley, D, Hertsted, S, Carter, J, et al. Compressive Biomechanics of Developing Spinal

Tissues. Proceedings of the 25th Annual Meeting of the American Society of Biomechanics. San Diego, CA:2001;55-6.

Nuckley, DJ, Konodi, M, Ching, R, et al. Effect of Cervical Lesions on Neural Space Integrity. Proceedings of the 47th Annual Meeting of the Orthopaedic Research Society. San Francisco, CA:2001;945.

Nuckley, D, Hertsted, S, Eck, M, et al. Developmental Biomechanics of the Cervical Spine: Compression and Tension. University of Washington Biomechanics Symposium 2001. Seattle, WA:2001;

Nuckley, D, Eck, M and Ching, R. Tensile Characteristics of the Developing Cervical Spine. Annals of Biomedical Engineering 2000;28 Supplement 1:9, T1.56.

Nuckley, D, Carter, J, Eck, M, et al. Tissue Compressive Mechanics and Constituent Properties of the Developing Spine. Annals of Biomedical Engineering 2000;28 Supplement 1:6, T1.43.

Nuckley, DJ, Konodi, MA, Mirza, SK, et al. Spine Neural Space Integrity Associated with Anterior Cervical Lesions. Annals of Biomedical Engineering 2000;28 Supplement 1:9, T1.57.

Nuckley, D, Carter, J, Eck, M, et al. Compressive Mechanics of the Developing Spine. Proceedings of the 46th Annual Meeting of the Orthopaedic Research Society. Orlando, FL:2000;386.

Summa, C, Mirza, S, Konodi, M, et al. Cervical Spine Instability as Measured by Neural Space Occlusion: Series #2 Lateral Lesions. Proceedings of the 28th Annual Meeting of the Cervical Spine Research Society. Charleston, SC:2000;37-8.

Mirza, S, Raynak, J, Nuckley, D, et al. Pattern of Structural Failure and Neural Compression in Acceleration Injuries of the Cervical Spine. Proceedings of the 28th Annual Meeting of the Cervical Spine Research Society. Charleston, SC:2000;50-1.

Mirza, SK, Nuckley, DJ, Konodi, MA, et al. Cervical Spine Instability as Measured by Neural Space Occlusion. Proceedings of the 27th Annual Meeting of the Cervical Spine Research Society. Seattle, WA:1999;

Nuckley, DJ, Raynak, GC, Ching, RP, et al. Neural Instability of the Lower Cervical Spine. Proceedings of the 26th Annual Meeting of the Cervical Spine Research Society. Atlanta, GA:1998;169-71.

Raynak, GC, Nuckley, DJ, Mirza, SK, et al. Neuroforaminal Space Stenosis Associated with Sub-injury Cervical Spine Position. Proceedings of the 44th Annual Meeting of the Orthopaedic Research Society. New Orleans, LA:1998;256.

Nuckley, DJ, Raynak, GC, Mirza, SK, et al. Cervical Spine Intervertebral Foramen Stenosis Resulting From Quasi-Static Normal Ranges of Motion. Proceedings of the 25th Annual Meeting of the Cervical Spine Research Society. Rancho Mirage, CA:1997;93-5.

Raynak, GC, Nuckley, DJ, Ching, RP, et al. A Transducer for the Dynamic Measurement of Neural-Space Occlusions in the Spine. 1997 ASME International Mechanical Engineering Congress and Exposition. Dallas, TX:1997;33-4.

Chamberlain, SC, Lakin, RC, Wharton, DN, et al. Vision in Hydrothermal Vent Shrimp: Unusual structures for seeing in an unusual environment. Annals of Biomedical Engineering 1994;22 Supplement 1:56.

Chamberlain, SC, Lakin, RC, Wharton, DN, et al. Retinal Structure in Hydrothermal Vent Shrimp from the Mid-Atlantic Ridge. Society for Neuroscience. Miami Beach, FL:1994;132.

Grant Proposals

Ching, R, Song, K, Mann, F, Caler, W, Nuckley, D, Carter, J. Age-Related Cervical Spine Mechanics and Injury Tolerance. Centers for Disease Control, 1999. Funded. (Co-Author)

Ching, R, Mirza, S, Camacho, D, Tencer, A, Song, K, Mann, F, Harruff, R, Harrington, R, Caler, W, Nuckley, D, Carter, J. Neck Mechanics and Injury Tolerance as a Function of Developmental Age. National Highway Traffic Safety Administration:Cooperative Agreement Program # NRD-01-8-07346, 1998. Funded. (Co-Author)

Ching, R, Mirza, S, Nuckley, D. The Potential for Spinal Cord Injury in the Pediatric Cervical Spine. Royalty Research Fund:RRF Scholar Application -1, 1998. (Co-Author)

Ching, R, Mirza, S, Tencer, A, Nuckley, D. Age-Dependent Properties of the Spine at Harborview Medical Center. National Highway Traffic Safety Administration:Cooperative Agreement, 1998. Funded. (Co-Author)

Mirza, S, Ching, R, Chapman, J, Gradey, S, Nuckley, D. Cervical Spine Instability as Measured by Neural Space Occlusion. Cervical Spine Research Society:1998. Funded. (Primary Author)

Mirza, S, Ching, R, Tencer, A, Chapman, J, Nuckley, D, Raynak, G. Neural Instability of the Cervical Spine. Orthopaedic Research and Education Fund:1998. Funded. (Primary Author)

Ching, R, Nuckley, D. Spinal Cord Injury in the Pediatric Cervical Spine: Assessing the Role of Developmental Hypermobility. Howard Hughs Memorial Institution:University of Washington, 1997. (Co-Author)

Memberships and Honors

Sigma Xi, 1995-present

BioMedical Engineering Society (student chapter president at UW, 1996) 1994-present

GAANN Fellow, 1996-1998

Tau Beta Pi, National Engineering Honor Society, 1993-present

Syracuse Scholar, University Valedictorian (1 of 10 students), 1995

Syracuse University Varsity Gymnastics Team, 1991-1995

Syracuse University Remembrance Scholar, 1994

Golden Key National Honor Society, 1993- present

Phi Kappa Alpha, Honor Fraternity, 1994

Newman Association 1991-1998